Effect of soil structure on temporal and spatial dynamics of bacteria

A thesis submitted in partial fulfilment of the requirements of the Abertay University for the degree of Doctor of Philosophy

by

Archana Juyal,

BSc, MSc

Abertay University

School of Science, Engineering and Technology

August 2015

I certify that this thesis is the true and accurate version of the thesis approved by examiners.

Signed…… …. Date……

(Director of Studies)

Declaration

I hereby declare that this thesis has been composed by myself and that it has not been accepted in any previous applications for the degree. The work of which it is a record, is my own, unless otherwise stated. All verbatims have been distinguished by quotation marks and sources of information specifically acknowledged by means of references.

Archana Juyal

Acknowledgments

I am very grateful to my supervisors, Prof. Wilfred Otten and Dr Ruth Falconer for their professional support, encouragement and guidance throughout the course of my PhD. Both my supervisors were very approachable and helpful in every possible way. Thanks for always guiding me and ensuring I am on the right track of my research.

I would also like to extend my sincere thanks to Dr Thilo Eickhorst for his support and guidance throughout my research. I thank him for his patient listening and advice whenever I had difficulties in my research. I would also like to thank all the members and technicians from Dr Eickhorst's lab who always assisted me in laboratory requirements and for their help in conducting some basic soil analysis experiments.

I would also like to thank Prof Philippe Baveye for his support and kindness to allow me to come to his Lab and carry out my research work.

I would also like to thank Dr Andrew Spiers for sharing his knowledge on microbiology and guiding me in ME lab in Abertay.

Thanks to Dr Simona Hapca for her guidance and help with statistics.

The financial support from the Scottish Overseas Research Student Award Scheme (SORSAS) and German Academic Exchange Service (DAAD) for carrying out this research is greatly acknowledged.

I would also like to thank Dr Sonja Schmidt for her help and guidance in CT lab and proofreading my thesis. Thanks for always listening to my problems patiently and encouraging me all the time.

Thanks to my colleagues and friends Roshni, Nde and Sylvie for healthy discussions, spontaneous coffee breaks and emotional support, making my time in Abertay memorable.

Finally I would like to specially thank my family who have provided a source of support and encouragement, throughout the journey of this PhD, but also for everything I do in life.

Abstract

Soil is a complex heterogeneous system comprising of highly variable and dynamic micro-habitats that have significant impacts on the growth and activity of resident microbiota. A question addressed in this research is how soil structure affects the temporal dynamics and spatial distribution of bacteria. Using repacked microcosms, the effect of bulk-density, aggregate sizes and water content on growth and distribution of introduced *Pseudomonas fluorescens* and *Bacillus subtilis* bacteria was determined. Soil bulk-density and aggregate sizes were altered to manipulate the characteristics of the pore volume where bacteria reside and through which distribution of solutes and nutrients is controlled. X-ray CT was used to characterise the pore geometry of repacked soil microcosms. Soil porosity, connectivity and soil-pore interface area declined with increasing bulk-density. In samples that differ in pore geometry, its effect on growth and extent of spread of introduced bacteria was investigated. The growth rate of bacteria reduced with increasing bulk-density, consistent with a significant difference in pore geometry. To measure the ability of bacteria to spread thorough soil, placement experiments were developed. Bacteria were capable of spreading several cm's through soil. The extent of spread of bacteria was faster and further in soil with larger and better connected pore volumes. To study the spatial distribution in detail, a methodology was developed where a combination of X-ray microtopography, to characterize the soil structure, and fluorescence microscopy, to visualize and quantify bacteria in soil sections was used. The influence of pore characteristics on distribution of bacteria was analysed at macro- and microscales. Soil porosity, connectivity and soil-pore interface influenced bacterial distribution only at the macroscale. The method developed was applied to investigate the effect of soil pore characteristics on the extent of spread of bacteria introduced locally towards a C source in soil. Soil-pore interface influenced spread of bacteria and colonization, therefore higher bacterial densities were found in soil with higher pore volumes. Therefore the results in this showed that pore geometry affects the growth and spread of bacteria in soil. The method developed showed showed how thin sectioning technique can be combined with 3D X-ray CT to visualize bacterial colonization of a 3D pore volume. This novel combination of methods is a significant step towards a full mechanistic understanding of microbial dynamics in structured soils.

Table of Contents

List of Figures

List of Tables

1 Introduction

1.1 Soil

Soil forms a thin layer at the Earth's surface and acts as an interface between the atmosphere and lithosphere. It is a growth medium for plants and microorganisms and consists of minerals, water, gases and organic matter. Soil provides both a habitat and a source of energy for life, including plant roots, animals and microorganisms. In return, these contribute to soil formation and influence the soil's physical and chemical properties and the vegetation that grows in it (Young et al., 2005; Voroney & Heck, 2015). Soils are formed by the physical and chemical weathering of the rocks and minerals. The weathering processes convert the minerals and rocks into secondary minerals and fine particles with a large surface area and also provides nutrient for plants and animals (Young et al., 2005).

Soils contribute to all four different dimensions of ecosystem services classified by millennium ecosystem assessment into those associated with the provision of goods (e.g., food, fibre, fuel, fresh water), those that support life on the planet (e.g., soil formation, nutrient cycling, flood control, pollination), those derived from benefits of regulation of ecosystem processes (e.g., climate regulation, disease control, detoxification) and those cultural services that are not associated with material benefits (e.g., recreation, aesthetic and cultural uses) (Barrios, 2007).

1.1.1 Soil structure

The mineral component of soil is composed of particles of sand, silt and clay. Based on the proportion of these particles the soil is classified into textural

classes such as sandy loam, silt clay and clay loam (Lavelle, 2012). These mineral particles are bound together with organic matter and inorganic cements to form aggregates arranged spatially in various sizes and shapes. This arrangement of particles into aggregates and the distribution of pore spaces both within and between these aggregates are referred to as soil structure (Rowell, 1994). Microaggregates are formed by binding of organic molecules (OM) attached to clay (Cl) particles and polyvalent (P) cations (Al^{3+},Fe^{3+},Ca^{2+} and Mg^{2+}) to form compound particles (Cl-P-OM) (Edwards and Bremner, 1967). Macroaggregates are formed by physically binding of microaggregates together by fungal hyphae, networks of plants roots and roots hairs or chemically with fibrous organic matter (Bossuyt et al., 2001).

The importance of binding agents to maintain the stability of soil structure was highlighted by Tisdall and Oades (1982). They classified organic binding agents into three broad classes; persistent, transient and temporary. Persistent binding agents include the humic materials associated with polyvalent cations; transient binding agents are polysaccharides derived from plant and microbes and the temporary binding agents include roots, root hairs and fungal hyphae (Tisdall and Oades, 1982; Cambardella, 2006). Therefore, all these three binding agents act together to form stable aggregates in soil. Aggregates of different sizes have different stability and resistance to various environmental stress i.e. micro and mesoaggregates are more stable than macroaggregates. For example, macroaggregates are readily disrupted by rewetting of dry soil, freezing or thawing or from the gentle agitation whereas micro- and mesoaggregates are more resistant unless intense agitation is enforced (Bronick & Lal, 2005).

The aggregation process defines a network of pores of different sizes and shapes which affects the distribution of air, water and nutrients in soil. It is important to note here that aggregates are formed after soil is broken into smaller pieces due to a force. This can be a mechanical force, by which we measure the aggregate size distribution, but it is to some extent arguably an arbitrary measure. More recently methods have become available that assess soil structure without the requirement of such a disruption. This non-invasive method includes X-ray CT and is described in more detail later in this chapter.

The pore space is defined as the percentage of the total soil volume occupied by pores.

$$Pore\ space\ (\%) = \frac{pore\ volume}{soil\ volume} \times 100 \qquad \text{Equation 1.1}$$

Often it is also described as porosity, in which case reference is often made to the volume fraction rather than the percentage. The porosity of soil and the density at which soil particles are packed are inversely related. Soil bulk-density (g of soil per volume) and soil particle density (g of solid particles per volume) are used to determine the pore volume of soil according to the following formulas

$$\varepsilon = 1 - (\rho b / \gamma s) \qquad \text{Equation 1.2}$$

Where, ρ_b = bulk-density of sample (g cm^{-3}), γ_s = soil particle density (g cm^{-3}),

ε = porosity

Total pore space can be categorized into classes according to the sizes and shape of pores as macropores (>100 µm), mesopores (30-100 µm) or micropores (<30 µm) (Koorevaar, Menelik and Dirksen 1983). However, Voroney & Heck, 2015 classified the pores into macropores (>10 µm), and micropores (<10-µm) showing that a uniformly accepted definition is lacking.

The pores are classified according to their sizes, their ability to retain water and the forces applied to extract water molecules held by surface tension forces. The classification of pores is arbitrary and the actual pore sizes range from nanoscale to cm's. In macropores rapid diffusion of air and infiltration of water occurs. Macropores are created by physical processes like wetting and drying or freeze-thaw cycles which can lead to formation of cracks, or by biological processes like root growth and burrowing activities of earthworms, termites and ants (Bronick & Lal, 2005; Lavelle, 2012; Voroney & Heck, 2015). Micropores retain water for plants and provide aqueous habitats where microorganisms live. The complex geometry of macropore pathways determines the distribution of water, gas, solutes and microbes in soil (Young and Crawford, 2004). Pore network characteristics such as porosity, number of pores, pore length, pores size distribution, connectivity and tortuosity are considered as factors that influence the transport of solute and water flow through soil (Luo et al., 2010).

The pore network provides various habitats for microbes that vary in their physical, chemical and biological characteristics, resulting in heterogeneous distribution of microbes in soil. Depending on the moisture content, 45-60 % of the total soil volume consists of pores that are either air or water filled. The heterogeneity of pore networks affects the relative proportion of air- versus water-filled pores, thus regulating water and nutrient availability, gas diffusion and biotic interactions (Frey, 2015).

In soil, water acts physically as an agent for transport by mass flow and as a solvent and reactant in chemical and biological reactions. Soil water influences the soil aeration, osmotic pressure, pH of the solution and the moisture

available to microbes in soil (Frey, 2015). In soil, water content can be measured as the mass of water in soil (gravimetric water content) or water per unit volume in soil (volumetric water content). Soil water is also described in terms of its potential energy. The water potential is defined as the potential energy of water per unit mass of water in the system relative to free water and can be described by the sum of gravitational, matric, osmotic and pressure potentials. The adhesion force of water to the surface of soil matrix is attributed as the matric potential (matric forces). When soil is thoroughly saturated by heavy rainfall or irrigation and after a period drainage, the water held by soil available for plant use is in equilibrium with gravitational suction, the soil is said to be at its field capacity where no more water drains from soil (Cassel and Nielsen, 1986). At field capacity, the gravitational forces that drags the water downward is counterbalanced by osmotic and matric forces that hold water (Voroney & Heck, 2015). When the water is being absorbed by plants and not replenished a point is reached where plants can no longer extract water adhered to soil particles and the soil is said to be at its permanent wilting point. Soil is said to be at its water holding capacity when the amount water held is between the field capacity and the permanent wilting point and hence an indication of the amount potentially available to plants (Bardgett, 2005). The water retention curve is used to determine the volume and distribution of water in soil as it describes the hydraulic and gaseous pathway in soil. This curve describes the relationship between the moisture content and the matric potential energy. An impact of this curve on various soil functions is summarized in Figure 1.1 (Young and Ritz, 2005). In Figure 1.1 it can be seen that a higher level of aerobic microbial activity occurs when pores are air and water filled.

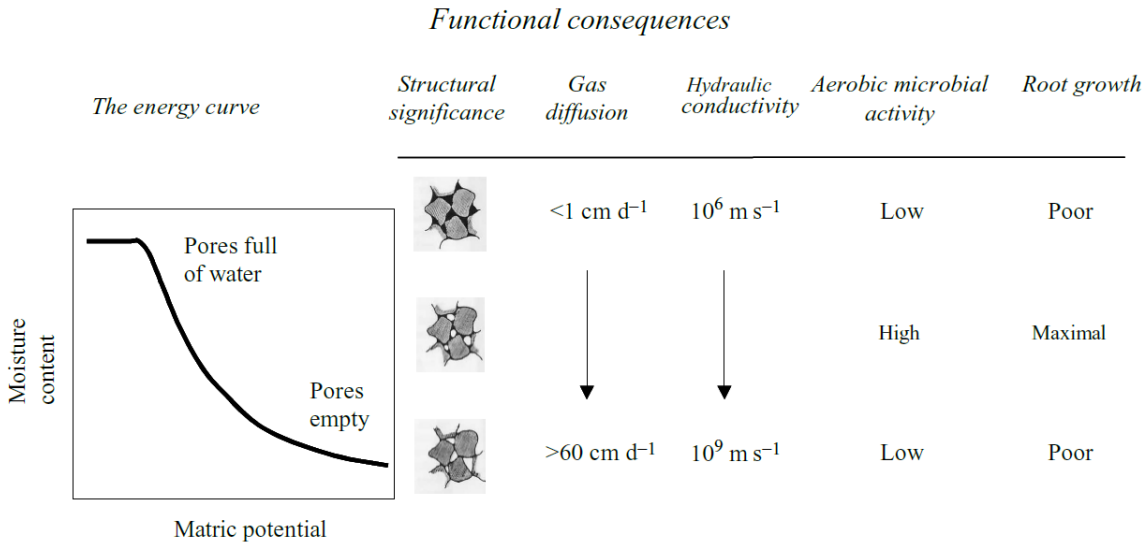

Figure 1.1: Summary of water retention curve on different soil functions (from, Young & Ritz 2005).

1.1.2 Methods to quantify soil structure

To assess soil structure, various direct and indirect methods have been used over the years. A review article by Dıaz-Zorita et al.(2002) describes various destructive procedures to assess the structure of soil. Measurements such as soil bulk-density, aggregate stability, water repellency, water retention and hydraulic conductivity are used to assess the structure or used as indirect measures of how structure affects functioning of soil. The methods, however, are all indirect and either requires assumption relating pore size to water retention, or require soil to be destructively sampled (aggregate size distribution). Image analysis of soil thin sections prepared form resin impregnated soil samples is another method that has been used to measure size, shape, and distribution of pores and aggregates and allows these measurements to be made without destroying the distribution of solid and pores. Various studies have used thin sections to determine soil structure (FitzPatrick et al., 1986); pore architecture (Moran et al., 1988; Drees et al.,

1994, Harris et al., 2003, Pagliai, Vignozzi and Pellegrini, 2004); pore size distributions (Tippkotter et al., 2009); soil organic matter distribution (Faldme et al. 2014) and root-soil contacts (Kooistra et al., 1992). This method is, however, limited to 2D and to assess the pore architecture in 3D this method requires stacking up of images acquired at high resolution which is very time consuming. Blair et al. (2007) developed a methodology to simulate three-dimensional structure from the two-dimensional sections of soil. But this did not work well for soils with large cracks. Recent development in technology allows the use of techniques like X-ray computed tomography to attain the third dimension. X-ray CT allows for visualisation and quantification of soil structure in three dimensions without disrupting the samples. Thus it also allows repeated measurements of the same samples overtime which is very helpful in research work related to studying for example the response of biotic characteristics to changing conditions in soil (Helliwell et al., 2013).

Nuclear Magnetic Resonance (NMR) or Magnetic Resonance Imaging (MRI) is another potential non-destructive technique to analyse the soil environment. Pohlmeier et al. (2010) used MRI to investigate root water uptake in natural sand. Nakashima et al. (2011) used time-domain low-field NMR to detect heavy oil contaminated portion in undisturbed sandy soil samples from a real site contaminated with heavy oil. These techniques are, however, somewhat limited as equipment is not readily available and Fe content in soil can interfere with the imaging. In this study X-ray tomography was used to quantify soil structure, therefore a brief description of this technique is given in the following section.

1.2 X-ray Computed Tomography

X-ray Computed Tomography (CT) is a non-destructive and non-invasive technique which applies the principal of attenuation of an electromagnetic wave to visualise and quantify the internal structure of an object in 2D and 3D. The application of X-ray CT began in the early 80's; Petrovic et al. (1982) were the first to use this technique in a geological study. They demonstrated the potential for studies of the physical soil environment by observing the relationship between soil bulk-density and X-ray attenuation.

1.2.1 Principle of X-ray tomography

The theory of X-ray CT has been covered in detail in numerous reviews (Ketchman & Carlson, 2001; Mees et al., 2003; Cnudde et al., 2006; Taina et al., 2008; Piers et al., 2010; Mooney et al., 2012; Helliwell et al., 2013). Briefly, X-ray are emitted that intersect the sample and produce a series of radiograph images of samples acquired at incremental angular positions (Taina et al., 2008; Helliwell et al., 2013). A laboratory based X-ray CT scanner in general is typically made of three parts, a X-ray source, a rotating sample stage and a detector (Figure 1.2). The X-ray source is a highly evacuated tube that consists of two electrodes: an anode and a cathode. A high voltage is applied across the electrodes; the cathode then accelerates electrons and produce X-rays as they strike the anode (Wildenschild et al., 2002). The X-rays emitted from the source pass through the sample and a portion of the X-ray beam is either absorbed or scattered because the sample itself becomes a secondary source of X-rays and electrons through atomic interactions (Mooney et al., 2012). This process of reduction in intensity of X-rays as they are absorbed or scattered while passing

through the object is called attenuation The attenuation coefficient characterises how easily a material can be penetrated by an X-ray beam, and is related to the density of the sample, the energy of radiation and the electron density of the voxel of interest (Helliwell et al., 2013). The X-ray passing through an object is projected onto a detector where a radiograph image is generated. For reconstruction, the values of linear integration of the X-ray attenuation coefficient of the radiographic images are used. The most common technique for reconstruction is the filter back-projection algorithm through which cross-sectional 2D image slices are generated from the radiograph images. Each image (slice) describes the X-ray attenuation coefficient of the voxel (volume elements) in 3D expressed in Hounsfield unit (HU) or greyscale value (i.e. 0 to 255 for an 8-bit image). In general, pore spaces are associated with low densities, whereas mineral materials are of higher density and would have a higher value (Taina et al., 2008; Mooney et al., 2012). The greyscale values captured by the detector (X-ray CT used in this thesis) can be converted to HU, where a value of 0 HU would represent distilled water and -1000 HU represents air (at standard temperature and pressure), by calibrating with a flask of water before scanning each sample (Mooney et al., 2012; Houston et al., 2013). Over the years three different types of scanners have been used for environmental research, namely benchtop, medical and synchrotron (Figure 1.2). In principle, the methodology used for scanning is the same in both benchtop and medical systems. However in medical CT scanners the sample is static and both the source and detector rotate around the object (Figure 1.2b), whereas in benchtop CT scanners it is the sample that rotates between a fixed X-ray energy source and a detector (Figure 1.2a) (Mooney et al., 2012). The

advantage of industrial scanner over medical ones is that smaller objects can be scanned as the object can be moved closer to the X-ray source due to the reduced focal spot size. This allows the object to be moved closer to the narrower section of the X-ray beam, generating primary magnification and higher resolution through improved detection; therefore a wider range of scales can be covered (Ketcham & Carlson, 2001). In the case of a medical scanner the resolution image quality is limited, so from a soil perspective to classify microscopic pore characteristics and finer root systems an industrial X-ray CT or synchrotron scanner is more preferred (Mooney et al., 2012). Compared to industrial scanners, synchrotron scanners use a monochromatic beam instead of a polychromatic beam (used in industrial scanners) (Figure 1.2c). This enables better distinction of materials, enabling for example K-edge scanning. K-edge is the binding energy of the electrons of atoms in the K shell with a sudden increase in attenuation of photons just above the binding energy of the K shell electron. Such techniques can be used to identify specific compounds in composite materials. Another advantage of synchrotron over industrial scanners is the speed of scan (typical scan <15 minutes) and the acquisition of low-noise data with fewer artefacts. But access to synchrotron scanners is restricted and the size of sample is usually small (Wildenschild et al., 2002).

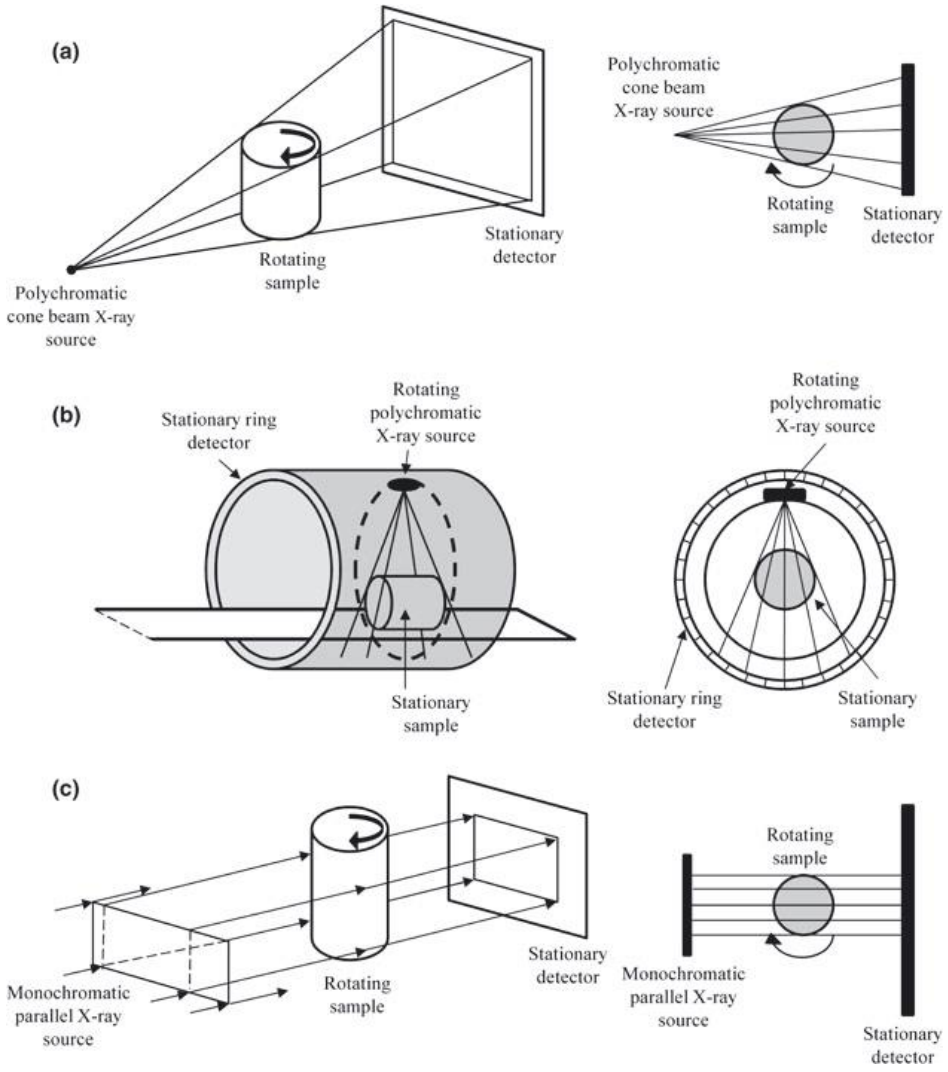

Figure 1.2: Example of different types of CT systems a) industrial system, b) medical system and c) synchrotron system (Helliwell et al., 2013).

1.2.2 Image segmentation

X-ray CT produces grey scale images whose grey scale values area ordered relate to the attenuation coefficient. The X-ray CT images of soil samples comprise of three phase's i.e. mineral grains, water and air filled pore space and the organic materials. Among these three phases, the soil minerals have the highest attenuation and in grey scales this corresponds to bright voxels and the pore space have darker voxels (Helliwell et al., 2013). To quantify specific features in soil samples, image segmentation techniques are used to convert

the greyscale CT image into a binary image for quantitative analysis. Over the years, different segmentation methods have been applied on soil images to identify the solid and pore phases. However no standard thresholding method has been adopted due to substantial challenges faced in segmenting soil data related to the heterogeneity of soil material (Iassonov et al., 2009; Baveye et al., 2010, Wang et al., 2011, Hapca et al., 2013). Iassonov et al. (2009) reviewed fourteen different segmentation methods ranging from global methods to locally adaptive methods that have been applied to porous media. The local thresholding methods showed more stable results compare to global ones. Among all the methods, the best segmentation results were shown by Oh and Lindquist's (1999) indicator kriging method and Bayesian segmentation algorithm (Berthod et al.1996). However, the limitation of these two methods was that they required supervision by knowledgeable operators and they were computationally demanding (Iassonov et al., 2009). In another study by Wang et al. (2011), indicator kriging method showed better performance on simulated soil images compared to four other thresholding methods. However, a study by Baveye et al. (2010) showed how operators bias the selection of thresholding methods, yielding variable results from the same soil images using the same thresholding method. To overcome the computational demand and the required expert knowledge, Houston et al. (2013) developed an improved version of an indicator-kriging algorithm. The improved method allowed varying the size of the kriging window according to the conditions within the soil image. The advantage of this method was that it allowed better segmentation for images containing imbalanced proportion of material phases or higher degree of spatial heterogeneity (Houston et al., 2013). In addition, the method is fully automated

and does not require the operator defined parameters of the previous kriging methods needed.

After image segmentation various characteristics of soil such as porosity, pore connectivity, pore size distribution and surface area are obtained. Various software packages (proprietary + bespoke) are available to quantify some of these pore characteristics e.g. Volume Graphic studio Max (Schmidt et al., 2012; Tracy et al., 2012), ImgTools (Falconer et al., 2012); SCAMP (Crawford et al., 2011) and 3DMA-Rock-software (Kravchenko et al., 2011; Wang et al., 2013; Negassa et al., 2015).

1.2.3 Limitation of X-ray tomography

The industrial X-ray CT scanner also has certain limitations, like beam hardening and ring artefacts which cause problems in phase identification during image analysis. Beam hardening is caused due to absorption of low energy photons as they are emitted faster than the higher energy photons. As the beam of the industrial systems is polychromatic, comprising of low and higher energy levels the X-rays change as they go through a sample. This causes higher attenuation at the boundaries of samples. Therefore, the edges appear brighter than the centre of the sample. This effect is more prevalent in higher density materials. Beam hardening can be minimized by using thin sheets of filters (aluminium, copper, tin) in the path of X-ray beam to remove lower-energy photons. Ring artefacts are caused by defects in the detector which cause recording of incorrect or high beam intensities, appearing as rings in the reconstructed images (Wildenschild et al., 2002). Nowadays, most of the

CT scanners have inbuilt image processing tools that can minimize beam hardening and ring artefacts both pre and post scanning (Mooney et al., 2012).

1.2.4 Applications in soil science

Over the years X-ray tomography has been applied in soil science to characterize soil properties like minerals (Kalukin et al., 2000; Ketcham et al., 2005), organic matter (Sleutel et al., 2008, Quinton et al., 2009), pore-space geometry (Heijs et al., 1995; Perret et al., 1999; Anderson et al., 2003; Elliot et al., 2010), water content (Heijis et al., 1995; Rogasik et al., 1999; Mooney, 2002) and roots (Gregory et al., 2003, Perret et al., 2007; Tracey et al., 2012; Schmidt et al., 2012). X-ray CT has allowed determination of various properties of the soil pore network non-destructively, including pore diameter, pore connectivity, tortuosity, pore circularity and pore size distribution (Helliwell et al., 2013). For example, Perret et al. (1999) determined pore tortuosity, numerical density, and hydraulic radius in undisturbed cores. The role of macropore networks in determining preferential flow patterns was reported by Heijes, Ritsema and Dekker (1996). (Baveye et al. 2002) examined dependence of macroscopic soil parameters including soil bulk-density, volumetric water content, volumetric air content and gravimetric water content on size, shape and positioning of soil samples. They reported that some measurements in small size samples exhibited erratic fluctuations which stabilized with increasing sample volume (Baveye et al., 2002). X-ray CT has been used to determine the effect of soil compaction on soil macropore geometry. For example, Kim et al. (2010) characterized the effect of compaction on macropore geometry in field cores. The studies revealed a decrease in CT-measured porosity,

macroporosity, number of macro- (69 %) and mesopore (75 %). X-ray CT has also been used to examine the effect of different management practices on soil structure and stability. Papadopoulos et al. (2009) used X-ray CT to examine the effect of different management practices on aggregate structure and stability. They compared soil stability in stable and unstable aggregate fractions from organically and conventional managed soils and showed that intra-aggregate porosity did not affect soil stability (Papadopoulos et al., 2009). Some recent studies have shown differences in intra-aggregate pore structures in soil with contrasting land use and management practices (Kravchenko et al., 2011; Wang et al., 2012). For example, Kravchenko et al. (2011) characterized the pore structure of soil aggregates with different land use and management practices, namely, conventional tillage (chisel plow) (CT), no-till (NT), and native succession vegetation (NS). They observed a heterogeneous distribution of pores with a greater number of large pores in CT management soil aggregates than NT and NS (Kravchenko et al., 2011).

Other applications of X-ray CT involve characterization of the root system (Gregory et al., 2003; Heeraman et al., 1997; Kaestner et al., 2006; Lontoc–Roy et al., 2006; Perret et al., 2007, Tracy et al., 2012). For example, Gregory et al. (2003) measured the length and diameter of wheat and rapeseed roots. The current state of the art in relation to X-ray CT to visualise roots in soil was recently documented in a review by Mooney et al. 2012.

Studies have also been undertaken to quantify invertebrate burrows in soil (Joschko et al., 1993; Capoweiz et al., 1998). Capoweiz et al. (1998) reported how the burrowing behaviour of earthworms varied with seasons. The effect of

soil compaction on earthworm burrowing was reported in a study by Jegou et al. (2002); Langmaack et al. (2002) & Schrader et al. (2007). The use of X-ray CT in studies of earthworm behaviour in soil is well documented in a review by Taina et al. (2008). For example, Langmaack et al. (2002) measured soil pore volume, length, tortuosity and connectivity of burrowing systems in soil with different tillage treatments and concluded that intrinsic soil processes had a bigger impact on soil rehabilitation than tillage operations.

To date, bacteria cannot be visualised using X-ray systems due to low attenuation of X-rays and similarities with the soil-water complex (O'Donnell et al., 2007). However, X-ray CT allows assessment of the habitat in which these microorganisms live. In the past 3-4 years, X-ray tomography has been used in combination with other culture based or molecular techniques to study the distribution and function of microbial populations in their habitat (Kravchenko et al., 2013; Kravchenko et al., 2014). These studies are described in detail in section 1.6 of this chapter.

1.3 Life in soil

A large proportion of Earth's biodiversity resides in soil (Ettema & Wardle, 2002). This large biodiversity contributes to the majority of ecosystem services. According to Pimentel et al. (1997) the estimated economic profit from soil biodiversity is 1546 billon dollars annually. A vast range of microbes and animals can reside in soil because of its high physical and chemical heterogeneity which develops and maintains a large number of niches (Barrios, 2007). As shown in Figure 1.3 soil organisms can be classified into groups according to their body size such as microflora (1–100 μm, e.g. bacteria and

fungi), microfauna (5–120 µm, e.g. protozoa and nematodes), mesofauna (80 µm–2 mm, e.g. microarthopods and enchytraeids) and macrofauna (500 µm–50 mm, e.g. earthworms, termites and millipedes) (Swift et al., 1979). Among this soil community the most diverse and numerous members are the microbes, dominating with literally thousands of species present in soil. The microflora group includes bacteria, fungi, actinomyctes and algae, with bacteria and fungi the most abundant ones. In terms of biomass, fungi dominate by representing a significant portion of the ecosystem nutrient pool. however in terms of total numbers and diversity, bacteria form the largest proportion of the soil microbial community (Young et al., 2005). It is evident that a single gram of soil may harbour from 10^8 (bulk soil) up to 10^{11} (rhizosphere) prokaryotic cells (Torsvik et al., 1990,Portillo et al., 2013) and an estimated species diversity of 4×10^3 (Torsvik et al., 1990) to 8×10^6 species (Gans et al., 2005). The soil microbial community has immense metabolic and physiological heterogeneity which enables them to live, adapt and proliferate in a broad range and changes of environmental conditions (Madigan et al., 2010). With such high bacterial diversity within the soil environment, the importance of the functions these organisms perform within the soil ecosystems such as plant growth, nutrient cycling, soil structure and maintenance of soil productivity is well established. The functioning of these organisms is controlled by interactions such as mutualism, commensalism, antagonism, competition, parasitism/predation and neutralism with each other (Van Veen et al., 1997).The diversity of soil biota is important for sustaining soils and particularly within the agricultural system, since microorganisms perform diverse ecological services including supplying nutrients to plant, stimulate plant growth through production of growth

hormones, control or inhibit the activity of plant pathogens, maintenance of soil structure, microbial leaching of inorganics and mineralization of organic pollutants (Burd et al., 2000; Zhuang et al., 2007; Zaidi et al., 2008; Hayat et al., 2010). Microbial diversity and biomass are highest in the top 10 cm of soil and it declines with depth. For example, in a montane forest in Colorado bacterial diversity decreased by 20-40% in deeper horizons compared to surface soil (Eilers et al., 2012).

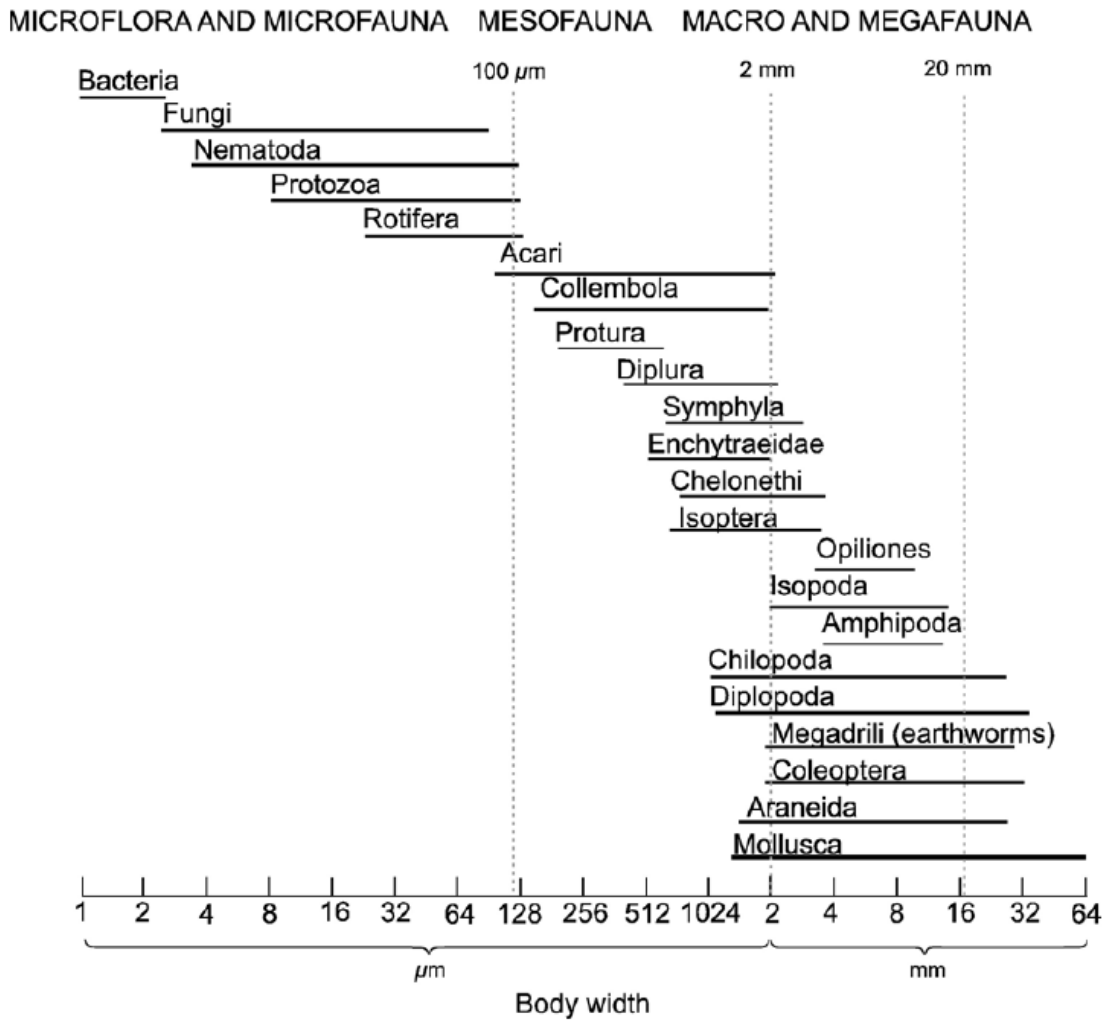

Figure 1.3: Classification of soil organisms according to the width of their body size (from Swift et al., 1979).

1.3.1 Bacteria used in this thesis

Plant growth promoting bacteria (PGPB) are being used for enhanced crop production due to their adaptability in a wide variety of environments, faster growth rate and biochemical versatility to metabolize a wide range of natural and xenobiotic compounds (Bhattacharyya & Jha 2012). A variety of bacteria belonging to genera Agrobacterium, *Arthrobacter, Azotobacter, Azospirillum, Bacillus, Burkholderia, Caulobacter, Chromobacterium, Erwinia, Flavobacterium, Micrococcous, Pseudomonas and Serratia* are used as inoculants in soil to enhance nutrient availability (Gray and Smith, 2005). These bacteria may exist in the rhizosphere, on the rhizoplane or in the spaces between the cells of root cortex (Hayat et al., 2010). In this study bacteria belonging to genera *Pseudomonas fluorescens* and *Bacillus subtilis* are used. Both this strains are capable of controlling plant diseases. *Pseudomonas fluorescens* are gram-negative, motile, rod shaped bacteria that are found in soil, water and on plant surfaces (http://www.ncbi.nlm.nih.gov/genome/150). The average length of *P. fluorescens* SBW25 is 3.1± 0.8 µm and the diameter is 0.9± 0.1 µm (Ping et al., 2013). *Bacillus subtilis* are gram-positive, motile, rod shaped bacteria that inhabit soil (http://www.ncbi.nlm.nih.gov/genome/665). *Bacillus subtilis* are 3-5 µm long with a width of about 1 µm. *Pseudomonas* belongs to the proteobacteria genera and *Bacillus* belongs to the firmicutes. *Pseudomonas fluorescens* produces growth regulators like siderophores, and indole-3-acetic acid whilst *Bacillus subitlis* produces indole-3-acetic acid. There are numerous studies reviewed in Hayat et al. (2010) and Sivashakthi et al. (2014) which have used *Pseudomonas* and *Bacillus* species as model organisms to either promote plant growth or control diseases. Both these

bacterial groups are selected as they are equally abundant in the rhizosphere and in the bulk soil environment (Kravchenko et al., 2013). Despite this, still very little knowledge is available on how the growth or spread (movement) is affected by soil physical conditions, such as pore geometry or moisture content. Therefore, factors affecting survival spread and root-colonising ability of these species in soil environment needs to be understood.

1.4 Distribution of bacteria in soil

Bacteria depend on water filled pore networks or pore spaces that are covered with water films for their growth and activity (Vos et al., 2013). Bacteria are located in both small and large pores, but the bacterial population is found more consistently in smaller pores. This is because, small pores retain water longer in drying soil condition and also bacteria are protected from predators which cannot enter such pores. Therefore the bacterial population distribution is highly variable in large pores where they are more prone to predators consumption (Foster, 1988; Frey, 2015). Direct observation of microbial cells *in situ* has revealed the uneven distribution of microbes in soil. Bacteria are mostly found as isolated cells or in form of microcolonies and biofilms in soil. The number of cells per microcolony observed in microscopic studies was very low (Kilbertus, 1980; Foster, 1988; Nunan et al., 2001). The oligotrophic status of the soil habitat and the limited number of hydrated microsites in unsaturated soil are some of the factors that were thought to restrict the development of large microcolonies (Or et al., 2007). The small microbial colonies tend to aggregate and form microbial hotspots in zones where nutrient availability is high such as areas with accumulated particulate organic matter, animal manure and the

rhizosphere (Nannipieri et al. 2003). The colonization of bacteria in such areas occur either due to active movement of the bacteria towards them or due to passive transport by water flow or large burrowing animals. In air-filled pores bacteria migrates through the fungal hyphae networks (Young et al., 2008). According to Time et al. (1988) the mechanism of bacterial movement in soil can be categorised into physical, geochemical and biological processes. In physical processes, bacteria movement is through the water flow in soil pore networks whereas in geochemical processes like filtration, adsorption/desorption and sedimentation delays their movement through pores in soil. In biological processes, the intrinsic characteristics like the size of bacteria, growth or death rate and the motility mechanisms influence their transport through soil (Abu-ashour et al., 1994). Therefore, the movement of bacteria through various mechanisms leads to their heterogeneous distribution in soil.

Bacteria have a range of motility mechanisms broadly categorised into: swimming, swarming, gliding, twitching and sliding (Figure 1.4). Bacteria require flagella for swimming and swarming motility, type IV pili for twitching motility or they do some form of gliding or sliding as a form of passive translocation (Harshey, 2003). In swimming, individual bacterial cells moves through liquid environments by rotating flagella whereas in swarming bacteria spread through the surface in groups by flagella motion (Kearns, 2010). Gliding is the active surface movement that occurs along the long axis of cell. Gliding is defined as a smooth movement of cells, generally along the long axis of the cell. Twitching motility is the movement of bacteria by the extension and retraction of type IV pili. And lastly, sliding is a passive form that relies on growing culture in

combination with reduced surface tension between cell and surface. Sliding relies on production of surfactants to reduce surface tension between bacteria and surface and enable a bacterial colony to spread away from the origin driven by the outward pressure of cell growth (Harshey, 2003; Kearns, 2010). The most common motility mechanism is the swimming motility, where flagella propelled bacteria follow chemical gradients by chemotaxis (Young et al., 2008). Chemotaxis is the movement of bacteria towards or away from a higher chemical concentration (Abu-ashour et al., 1994). The non-motile cells rely on passive mechanisms like diffusion or transport with water flow through soil. Thus the movement of motile or non-motile bacteria through the water-filled pore network results in non-random distribution in soil. The motility mechanism of the bacteria used in this thesis was swimming, swarming and twitching in the case of *Pseudomonas* sp. and swimming, swarming, gliding and spreading in the case of *Bacillus* sp. (Harshey, 2003).

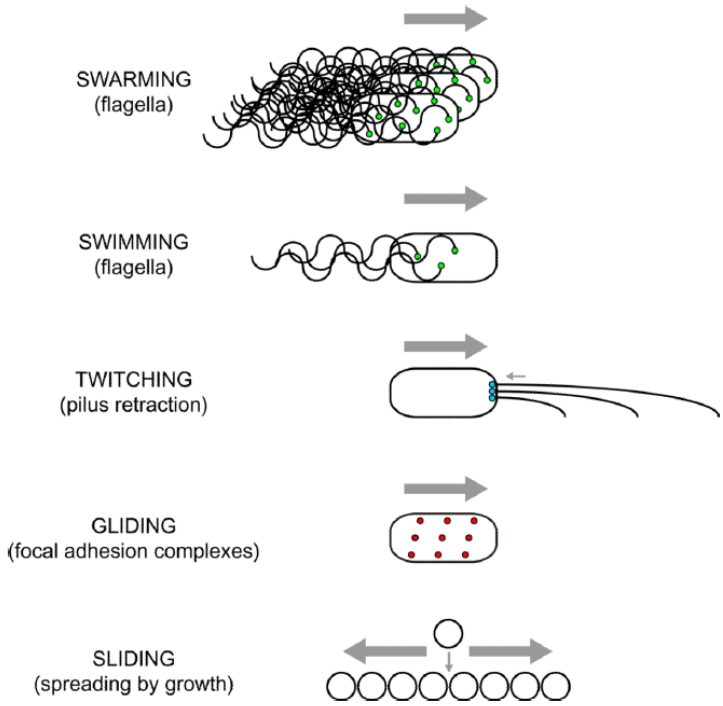

Figure 1.4: Diagrammatic representation of different bacteria motility mechanism. The grey arrows indicate the direction of bacterial cell movement and the coloured circles indicated the type of motors that power the movement of bacteria (Kearns 2010).

The habitat of microbes depends on the size of the organisms, which ranges from a µm for bacteria to larger than 100 µm for fungi (Coleman et al., 2001). Due to the complexity of aggregate matrix the localization of bacteria is restricted to very small microhabitats which means the majority of the soil surface area is devoid of bacteria (Vos et al., 2013). According to Young and Crawford (2004), microbes cover only 10^{-6}% of the total soil surface area. This demonstrates that the spatial arrangement of microorganisms in soil has a huge impact on their access to C and on the way they compete and interact (Nannipieri et al., 2003). Parkin (1933) categorized the spatial patterns of microbes into four scales: microscale, plot scale, landscape scale, and regional scale. Few studies have researched spatial patterns at all these scales (Lauber et al., 2008; Wu et al., 2009; Fierer et al., 2009, Nunan et al., 2003).

1.5 Methods to quantify microscale distribution of bacteria in soil

Over the years different experimental and modelling approaches have been used to investigate and quantify the distribution and activity of microbes in soil. The approaches can be categorized broadly into a) Imaging techniques b) Non-imaging techniques and c) Modelling techniques.

1.5.1 Imaging techniques

Microscopy techniques are used to observe bacteria in their natural environment. Since soil is a complex medium, studying the distribution of bacteria has been challenging owing to visualization and sampling difficulties caused by the complex structure and opacity of soil. Early studies using microscopic techniques indicated that bacteria are unevenly distributed in soil. Resin embedding techniques were used to study in situ spatial distribution of bacteria in soil. In 1955, Alexander and Jackson were the first to introduce the soil thin sectioning technique to study the micro-organisms in natural soil. Nunan et al. (2007) has described the history of how the technique has emerged and modified from a qualitative to a quantitative analysis. Briefly, Jones and Griffiths (1964) modified this method to map spatial distribution of bacterial colonies in soil aggregates. Then in 1973, Foster et al. (1973) produced images of soil bacteria and fungi at the ultra-structural scales (nanometre and kilometre scales). Thin sectioning techniques involve four main steps which are fixation, staining, dehydration and resin impregnation (Li et al., 2003). In this method the samples are taken from undisturbed soil cores and fixation is done to preserve the soil structure and the spatial pattern of the microbes with the soil matrix. The samples are then impregnated in resin and

thin sections approximately 25 μm are prepared from the block after polymerization of resin and used to observe bacteria under a microscope. Tippkotter (1996) performed an experiment where different types of resins were tested for soil thin sections and concluded that a polyester resin crystic and palatal resin were the most suitable ones. A couple of studies have used polyester resin to embedding soil samples to examine the *in situ* spatial distribution of archaea and bacteria in soil (Li et al., 2004; Eickhorst & Tippkötter, 2008). Thin sections have been used to visualize inoculated bacteria and rhizobia in soil at high cell densities (White et al., 1994; Li et al., 2004). These techniques, however, have several limitations; it is hard to assign a particular function to a specific group of bacteria as no distinction can be made between the active and non-active cells. Autofluorescence produced by the resin and soil particles interferes with the visualization of stained cells. However the fluorescence caused by resin was reported to decrease if thin sections were thinner. Hence the ideal thin sections are reported to be of thickness ≤ 15 μm. The measurements made by this technique were two dimensional whereas soil is a 3-D medium. This limitation can be overcome to some degree by using confocal laser scanning microscopy which produces 3-D images of samples by using the graph processing software (Li et al., 2003; Nunan et al., 2007).

To visualise bacteria in soil thin sections, different types of fluorochromes like acridine orange, ethidium bromide, 4',6-diamidino-2-phenylindole (DAPI),magnesium salt of 8-anilino-1-napthalene, Thiazine red R have been used (Li et al., 2003). These fluorochromes stain specific components of the organism like nucleic acids, proteins, lipids, cell membranes (Li et al., 2004; Nunan et al., 2007). Reporter gene like GFP markers are widely used to study

plant- microbe interactions (Tombolini & Jansson, 1998; Zhang et al. 2010; Zhang et al. 2011). The major advantages of GFP is it can be analysed in living cells without any need for exogenous substrate and its stability (Zhang & Xing, 2010). Tombolini et al. (1998) used GFP markers for spatial localization of bacteria (*Rhizobium meliloti*) on roots in soil .They concluded that the GFP protein was stable for more than 150 hours under starved conditions similar to the soil environment. Zhang et al. (2011) used GFP as a marker to study colonization of the natural biocontrol agent *Bacillus subtilis* N11 on banana roots.

In situ hybridization technique like FISH (Fluorescent in situ hybridization) is another upcoming technique which is used to quantify bacteria in soil. FISH is a nucleic acid technique that uses 16S rRNA specific oligonucleotide probes which are fluorescently labelled to target cells in a complex environment (Eickhorst & Tippkötter, 2008). This technique is useful in detecting bacteria belonging to a specific group or determine a particular functional gene (Dechesne et al., 2007). FISH methods have been used to study soil-plant-microbes interactions in rhizosphere and rhizoplane (O'Donnell et al., 2007). In context to the localization of bacterial colonies in a complex 3-dimensional structure of soil, FISH techniques were combined with the thin section method to detect organisms in undisturbed soil samples (Eickhorst & Tippkötter 2008). This technique, however, had limitations like the autofluorescence of soil minerals and organic materials which interfered with the signal intensities. Also accessibility of the probes to some areas of inner aggregate pores was problematic. This limitation was overcome by using a CARD-FISH (Catalyzed reporter deposition-fluorescent in situ hybridization) technique which used

oligonucleotides probes labelled with horseradish peroxidase enzyme that produce high signal intensity of tyramides (Eickhorst & Tippkötter, 2008). By combining this CARD-FISH technique with the experimental technique and modelling methods investigation of a particular species and its interactions with other species can be determined in the soil microhabitats.

1.5.2 Non-Imaging techniques

Since microbes reside in soil pores, the distribution of microbes is related to the structure and composition of aggregates. Hattori (1988) proposed a fractionation method in which microbial analysis was conducted on washed fractions of soil aggregates. The extracted microbes from soil were then quantified either by direct plate counting or by molecular method for which DNA was extracted from soil.

Microsampling is another technique which is used to measure the spatial distribution of specific bacteria present and its volume at different scales. The strategy is to randomly sample large numbers of soil microsamples with defined volumes and then detect the presence or absence of a particular targeted bacterial group. These data were then compared with the theoretical spatial distribution results (Grundmann et al., 2001). NH^{+}_{4} oxidisers were the first to be analysed at microhabitat scales using these methods. NO^{-}_{2} oxidisers were found to more evenly spread as compared to oxidisers of NH^{+}_{4}. The theoretical distribution investigated by computer simulations was limited owing to the time requirement to run the simulation. Dechense et al. (2003) developed a statistical data analytical method to replace the former one. This method was used to study the spatial distribution of two different bacterial types, NH^{+}_{4} oxidizers and

2, 4 -D degraders, in soil columns. Pallud et al. (2004) analysed the spatial distribution of 2, 4-degrader which remained unaffected as compare to addition of 2, 4-D substrate. An increase in colonized patches of size more than 0.5 mm in diameter at higher densities was observed after 2, 4-D addition (Pallud et al., 2004). Since the results obtained from this method on the relationship between spatial patterns of microbes and the soil structure is not quantifiable, it is difficult to study the effect of structure on spatial pattern of microbes (Nunan et al., 2007).

1.5.3 Modelling technique

Mathematical models are used to study the impact of microbial distribution on the ecological function. These models help in designing experiments which will provide more information about a specific aspect to be measured at a given scale.

Some models like fractal-based or network models have been used for many years to simulate the complex structure of soil. In 2001 a fractal-based model was used to link the soil function with the geometry of soil structure (Young et al., 2001). The effect of soil structure on the activities of soil biota was also analysed. However, these models used a simplified version of soil structure, and hence were incapable of representing variation in microhabitat heterogeneity (Nunan et al., 2007). In the early 1990's the knowledge of specific location of bacterial population in relation to the physiochemical microenvironment was limited. The models were developed based on the assumption that bacteria were randomly or uniformly distributed. For e.g.

random distribution of microbes and substrates were assumed to examine the effect of extracellular enzyme use on soil microbe's habitat. Later in 2004, a Markov chain model was introduced to simulate the three-dimensional soil structure at microhabitat scale. In this model the voxels can take either the pore or solid state. It can be used to study the microbial cells in soil by increasing the number of states that can be assigned to a pixel. Crawford et al. (2006) developed the same kind of model (i.e. using voxels to define a particular state) using the 2-dimensional images obtained from X-ray tomography to predict the three dimensional soil structures (Feeney et al., 2006). Individual based modelling is another method which can be used to study the effect of microbial communities on soil function. In this model individual elements are considered to analyse it effect on the whole system. Ginovart et al. (2005) was the first one to use this model to study the mineralization of C, N and nitrification process in soil. The Lattice Boltzmann method is another model which can be used to study the microbial function in soil. This method basically tracks the movement of individual particles and in the complex porous media (O'Donnell et al., 2007). However, a methodology needs to be developed where the images obtained from the biological thin sections of soil can be integrated with modelling methods to study the distribution and activity of microbes in soil system.

1.6 Current state: what do we know about the effect of soil structure on microbial distribution and activity at microscale

The distribution of microbes and their activity in soil is spatially correlated at scales ranging from microns to centimetres (Nunan et al., 2002; Dechesne et al., 2003; Dechesne et al., 2007). It has been recognized that the spatial pattern

of microbial distribution is related to the location and characteristics of soil pores (Grundmann et al., 2001; Nunan et al., 2003; Pallud et al., 2004; Ruamps et al., 2011). This is because soil pores at the microscale control the water, air and nutrient fluxes which then influence the micro-environmental conditions for microbial growth and functioning (Negassa et al., 2015). In recent years, advancements in technology have permitted analyses of the factors that promote diversity and activity of microbes in soil. In particular, the use of X-ray tomography has permitted obtaining the exact information of the pore structure of the soil matrix at micron resolutions (Nunan et al., 2006; Kravchenko et al., 2011; Mooney et al., 2012; Wang et al., 2012; Helliwell et al., 2013). This has opened opportunities to assess the effect of different characteristics of soil pores on microbial processes at microscale. In the last 3-4 years there have been studies that have used combinations of methods to quantify the pore characteristics with simultaneous assessment of microbial distribution and activity at microscale (Ruamps et al., 2011; Ruamps et al., 2013; Bouckaert et al., 2013; Negassa et al., 2015; Kravchenko et al., 2014; Wang et al., 2013; Kravchenko et al., 2013; Juarez et al., 2013). As per my knowledge, the combination of methods to quantify bacterial distribution in soil was first evaluated by Kravchenko et al. (2013) who studied the effect of intra-aggregate pore structure on the distribution of introduced bacteria (*E.coli*) in soil aggregates from contrasting managements. In their study, they used X-ray CT to quantify the pore structure of aggregates and a membrane filter method to evaluate the number of CFU of *E.coli* in aggregates. Their results showed that *E.coli* were abundantly distributed in medium sized pores (30-60 um) of the aggregates exteriors. They also showed a difference in *E.coli* distribution in

aggregates from different management practices. *E.coli* was more homogenously distributed in aggregates of highly disturbed soil and heterogeneously distributed in undisturbed soils. This difference was observed because in aggregates of disturbed soils, medium size pores were more abundant and uniformly spread throughout the aggregates compared to aggregates of undisturbed soils which had more larger pores (> 100 µm) and fewer medium sized pores (Kravchenko et al., 2013). The influence of pore characteristics on the composition of microbial community has been noted in some recent studies (Ruamps et al., 2011; Kravchenko et al., 2014). For example, Kravchenko et al. (2014) demonstrated that the composition of bacterial community was influenced by the intra-aggregate pore characteristics in macroaggregates. In this study, the relationship between intra-aggregate pore characteristics and composition of bacterial community in macro-aggregates from two contrasting agricultural management practices was assessed. A pyro-sequencing method was used to analyse the bacterial community and the intra-aggregate pore characteristics were obtained from X-ray CT. The results showed that the bacterial community composition was different between aggregates from contrasting agricultural management practices. Actinobacteria, Proteobacteria, Firmicutes and Gemmatimonadetes were the common bacterial communities present in aggregates from long-term organic management with cover crops (OF) and Acidobacteria in aggregates from the conventional management (CF). This difference in the community composition was related to the difference in the pore-size distribution and intra-aggregate pore variability in aggregates from contrasting management. The greater presence of large size pores (>100 µm) was positively related to the

relative abundance of Actinobacteria, Proteobacteria and Firmicutes in the OF aggregates. This is because in large pores the availability of nutrients would have been high due to nutrient influx via water flow in large pores or from root exudates. However, in aggregates from both treatments, the relative abundance of large number of different bacteria groups were found in medium size pores (32-84 µm).

Fewer studies have recognized the relationship between soil pores and soil C process (Bouckaert et al., 2013; Juarez et al., 2013; Ruamps et al., 2013; Negassa et al. 2015). For example, Bouckaert et al. (2013) used a combination of X-ray tomography and a kinetic model to study the relationship between C (carbon) mineralisation and the pore volumes in the undisturbed soil cores.

A combination of research methods is a first step towards a full mechanistic understanding of microbial dynamics in structured soils. However, there is still a lack of understanding of specific bacterial community distributions and functioning in soil. Since the bacterial community is so vast in soil may be useful to study the spatial distribution of introduced bacterial communities in soil to generate empirical data on which to base predictive models for better soil management. So far, only a few studies have looked at the spatial distribution of specific bacteria (White et al., 1994; Dechesne et al., 2005; Enwall et al., 2010; Kravchenko et al., 2013; Wang et al., 2013) at microscale and the information about the effect of pore structure on this distribution is rare.

1.7 Aim and objectives

From above it is clear that soil structure influences all processes in soil including microbial activity yet how this regulation precisely occurs is still unclear. The overall aim of this thesis is therefore to quantify the effect of soil structure on the growth and distribution of bacteria in microcosm systems of varying complexity.

The objectives to achieve this aim are

1) To quantify pore characteristics of soil in microcosm packed with different aggregate sizes and bulk-densities to determine how the pore geometry can be manipulated in experimental systems (Chapter 3).
2) To quantify growth of selected bacterial strains in soil packed with different aggregate size and bulk-densities to investigate how geometry of pores in different structure affects the growth of bacteria soil (Chapter 3).
3) To quantify the extent of spread of selected bacterial strains in soil microcosms packed with different aggregate sizes, bulk-densities and water content (Chapter 4).
4) Develop a method to quantify the spatial distribution of bacteria in soil by combining for the first time the physical technique to quantify pore geometry in soil in 3D (X-ray CT) , with biological techniques for *in situ* visualisation of bacteria (thin sections) (Chapter 5).
5) To use this novel combination of techniques to quantify the spatial distribution of selected bacterial strains towards a carbon source in soil (Chapter 6).

2 Development of materials and methods

2.1 Introduction

This chapter describes the protocols developed to build soil microcosms for enumeration of bacteria in soil. This is followed by the different staining methods used to visualise bacteria to enable counting in disturbed and undisturbed soil samples. Lastly, the method used to quantify soil structure throughout this study is outlined. All the chemicals and reagents used in this study were purchased from Sigma Aldrich UK unless otherwise stated.

2.2 Bacterial strains and general inoculum preparation

2.2.1 Bacterial strains used in this work

The bacterial strains used in this work were *Pseudomonas fluorescens* and *Bacillus subtilis* strains. As discussed in chapter 1 both these strains occur naturally in soil and are known to promote plant growth and control plant diseases (Krid et al., 2011). Some of the morphological and physiological characteristics of *Pseudomonas* and *Bacillus* bacteria that could affect their growth and functioning in soil are listed in Table 2.1. The two strains differ in their ability to grow under anaerobic conditions and motility which may affect their response to wetness in soil. Their difference in ability to form spores will affect survival and mobility with water flow, but these are not considered in this thesis.

Table 2.1: Some morphological and physiological characteristics of *Pseudomonas fluorescens* and *Bacillus subtilis* strains used in this study that may impact on the way they respond to soil physical conditions (Harshey, 2003; Ping et al., 2013; Sivasakthi et al., 2014).

Characteristics	*Pseudomonas fluorescens*	*Bacillus subtilis*
Size of bacteria	3-4 µm x0.1 µm	3-5 µm x 0.1 µm
Respiration	Obligate aerobe	Aerobic and facultative anaerobe
Motility	Swimming, swarming and twitching	Swimming, gliding and spreading
Spore formation	-	Endospores

The wild and mutant types of these strains and their sources are listed in Table 2.2. Mutants of both bacterial strains were tagged with GFP marker (details in table 2.2).

The strains were maintained on specific culture media plates. *Pseudomonas* were grown on King's media (KB) (10 g Glycerol, 1.5 g K_2HPO_4, 1.5 g $MgSO_4.7H_2O$, 20 g Proteose peptone No.3 (Becton, Dickinson & company, UK), 15 g technical agar (1.5 %) per litre) (Kings et al., 1954) and *Bacillus* were grown on Luria- Bertani medium (LB) (10 g NaCl, 10 g Tryptone, 10 g Yeast extract 15 g technical agar (1.5 %) per litre) (Sambrook et al., 1989). Antibiotics were added to the culture media for GFP-tagged strains. They were added in the following concentration: Kanamycin-50 µg ml^{-1} for *Pseudomonas* and Gentamycin-50 µg ml^{-1} for the *Bacillus* strain. The antibiotics were sterilised by filtering with 0.2 µm GD/Xfilter (Whatman, UK). For long term use and storage, strains were maintained at -80°C in KB and LB with 50 % (v/v) glycerol solution.

When needed, the strains were recovered from the -80°C stocks by streaking them onto appropriate selective media plates before use.

Table 2.2: Bacterial strains used in this study. Type and source of *Pseudomonas* and *Bacillus* strains are listed here.

Type of bacteria	Type of strain	Genotype/Description	Source
Pseudomonas fluorescens	SBW25	Isolated from the phyllosphere of sugar beet (Rainey & Bailey, 1996).	A. Spiers, Abertay University
	SBW25-GFP	SBW25::mini-Tn*7*(Gm)$_{PrrnB\ P}$ GFPASVa, Gm^R(unpublished, A. Spiers; mini-Tn7 cassette from Lambersten et al., 2004)	A. Spiers, Abertay University
Bacillus subtilis	NRS1473-GFP	(NRS1473) NCIB3610 *sacA*::$P_{hy\text{-}spank}$-GFPmut2,Km^R (Hobley et al., 2013)	N. Stanley-Wall, University of Dundee
	NCIB3610	also known as DSM10, probably derived from a soil isolate (Nakamura et al., 1999; Zeigler et al., 2008)	DSMZ, Germany

Table footnotes: DSMZ, Leibniz Institute DSMZ-German Collection of Microorganisms and Cell Cultures; Gm^R, Gentamycin resistance; Km^R, Kanamycin resistance; NCBI, National Collection of Industrial Bacteria, UK (now the NCIMB).

The growth rate of both bacterial strains was studied in pure media using spectrophotometry. Briefly, 1 ml of overnight culture was transferred into 50 ml liquid broth in a conical flask. The culture was incubated in a rotating shaker (200 rpm) at 28°C. Every 30 minutes 1 ml of the culture was transferred into plastic cuvettes (10 mm size) for OD_{600} reading using a spectrophotometer (Thermo Fisher Scientific, UK). The OD reading was first adjusted to zero by taking the pure liquid medium as a blank before a reading of the sample was taken. Results showed an increase in cell numbers overtime for both strains as

shown in Figure 2.1. Doubling time for *Pseudomonas* cells was estimated to be 110 minutes and 50 minutes for *Bacillus* strain in pure media from the exponential phase of the growth curve shown in Figure 2.1. Among the two strains, *Bacillus* showed a faster growth rate compare to *Pseudomonas* in pure media.

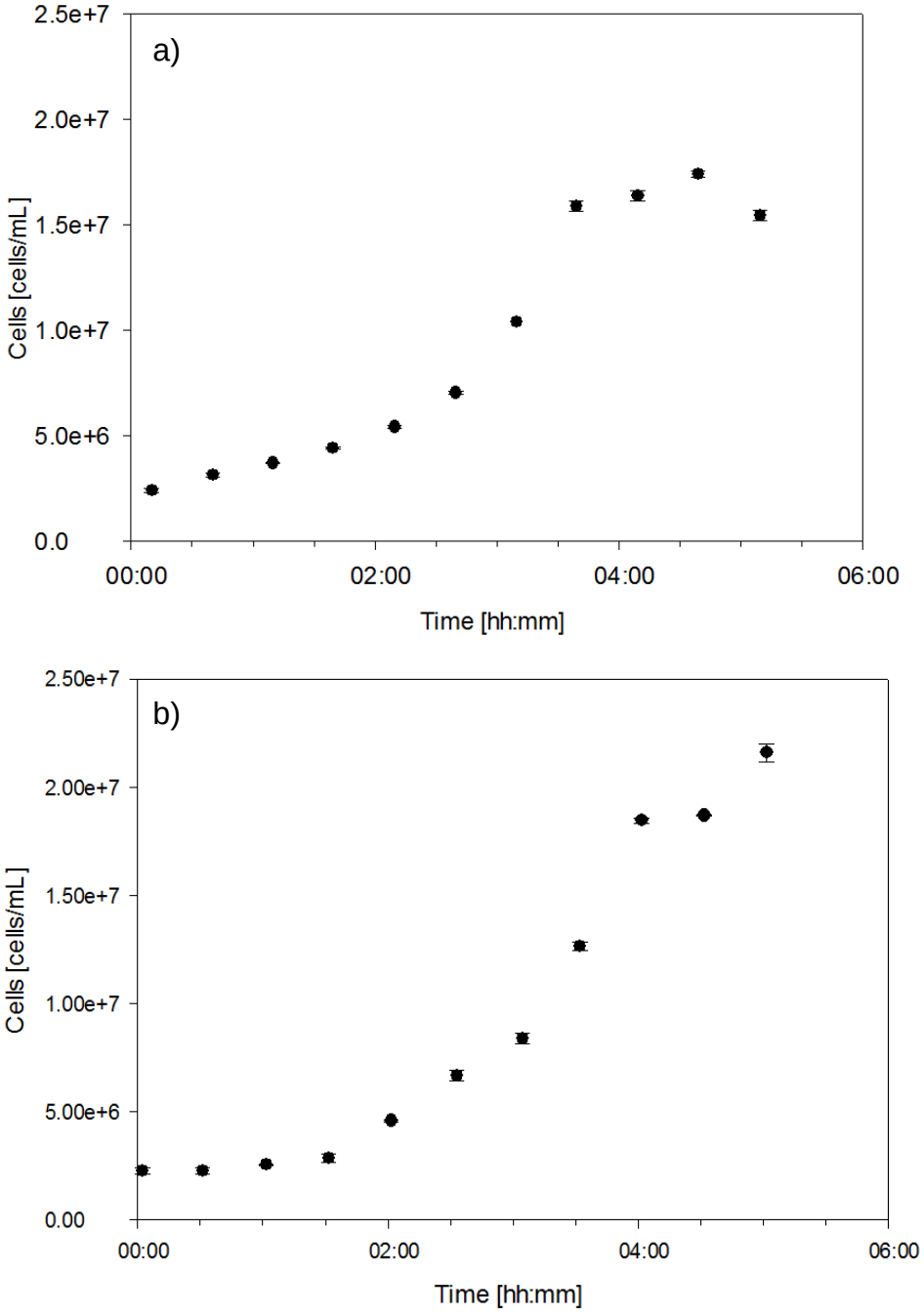

Figure 2.1: Growth curve of *Pseudomonas* (a) and *Bacillus* (b) grown in pure media at 28°C. Data are means ±SE (n=2).

2.2.2 Cell harvesting for inoculation in soil

For inoculation in soil, an overnight culture was prepared by transferring one colony grown on a media plate into 10 ml of sterile broth and incubated at 28°C on a shaker at 200 rpm 24 hr. The cells were harvested by centrifugation (4000 x g) for 5 minutes at 4°C. After washing the cells twice in a sterile phosphate buffer saline (PBS) solution, they were again suspended in small volume of PBS solution. The cell density of the cell suspension was measured using a spectrophotometer (Thermo Fisher Scientific, UK) reading at 600 nm. The cell density of *Pseudomonas* was 6.46E+07 cells ml^{-1} and 7.85E+07cells ml^{-1} for *Bacillus* strain.

2.3 Collection of soil and preparation of soil microcosms

2.3.1 Soil collection and processing

The soil used in this project was a sandy loam soil (Pajor et al., 2010; Schmidt et al., 2012). It was collected from the Bullion field of the James Hutton Institute in 2011. Upon collection, the soil was air-dried in the greenhouse, sieved down to different size aggregates (0.5-1 mm, 1-2 mm, 2-4 mm) and stored at room temperature. The soil characteristics, quantified for the 1-2 mm aggregate size fraction are as follows: Sand, 55.7 %; Silt 31.0 %; Clay, 13.3 %; C_{total}, 3.2 %; N_{total}, 0.19 %; C/N ratio, 17.1; Organic matter, 5.5 %. In all experiments in this thesis sterilised soil was used. The sieved soil was sterilized by autoclaving (moist heat) in glass bottles at 121°C at 100 kPa for 20-30 minutes. The sterilization procedure was repeated again with a 24hr interval time to ensure the autoclaving procedure was successful (Trevors, 1996).

2.3.2 Soil microcosms preparation

Throughout this project, repacked soil microcosms were used as it is possible to exert control over physical and chemical properties of soil in laboratory based studies. This helps in obtaining representative samples that can be replicated to compare different treatments. In this study, factors such as bulk-density, aggregate size and water content were controlled.

2.3.2.1 Packing of soil microcosms

The procedure of packing microcosms was adapted from the research work done by Pajor (2012). In all experiments, sterilised sieved soil was packed in polyethylene (PE) cylinders of size 3.40 cm^3 (1.7 cm diameter and 1.5 cm height) unless otherwise stated. After sterilisation, the moisture content equivalent to a desired water filled pore volume was adjusted. To adjust the water filled pore volume, firstly the amount of water already present in soil was determined by a gravimetric method using the following equation (Page et al., 1982).

$$\boldsymbol{Amount\ of\ water\ present\ in\ soil} = \frac{\boldsymbol{W_w - W_d}}{\boldsymbol{W_d}} \qquad \text{Equation 2.1}$$

Where, W_w = Wet weight of soil, W_d = Oven dried weight of soil

Using the equation, the amount of water present per gram of air-dried soil obtained was 0.0277 g/g. Then, the amount of water required in addition to that already present in soil was calculated by volumetric method using the calculation steps shown below (Equation 2.2-2.7):

$$V_{samples} = \pi r^2 h \qquad \text{Equation 2.2}$$

$$\rho_s = \frac{M_{solids}}{V_{samples}} = M_{solids} = \rho_s \times V_{samples}$$ Equation 2.3

$$\gamma = \frac{M_{solids}}{V_{solids}} = \mathrm{V_{solids}} = \frac{M_{solids}}{\gamma}$$ Equation 2.4

$$\mathrm{V_{pores}} = \mathrm{V_{sample}} - \mathrm{V_{solids}}$$ Equation 2.5

$$Water\ per\ gram\ of soil = \frac{V_{water}}{M_{solids}}$$ Equation 2.6

$$V_a = V_b - V_c$$ Equation 2.7

Where, ρ_s = soil bulk-density(g cm^{-3}); $V_{samples}$ = volume of PE ring (cm^3); r = radius of ring (cm), h = height of ring (cm); M_{solids} = weight of soil (g); γ = soil particle density; V_{solids} = volume of solids (cm^3), V_{pores} = volume of pores (cm^3), V_a = amount of water need to be added in soil (cm^3 g); V_b = amount of water present per gram of soil (cm^3 g); V_c = amount of water already present in soil (cm^3).

To adjust the water filled pore volume, sterilised distilled water (dH_20) was added to air-dry soil and left for 48 hrs to equilibrate (Kieft et al., 1987; Harris et al., 2003). Thus the water content of air-dried soil was adjusted according to the desired bulk-density (Table 2.2). The amount of soil required to pack at a specific bulk-density per cylinder was weighed and poured in two halves into the cylinder. The first halve was added into the cylinder and compressed with a piston. The top surface was loosened a bit with a scalpel before the other half was added and compressed with a steel piston. Scraping of the soil surface was done to roughen the surface as it prevented a layering effect as observed in the research performed by Pajor (2012). This piston passed through the ring easily thus reducing the differences in the compaction near the edges of the cylinders.

2.3.2.2 Soil microcosm inoculation

Bacteria were introduced in soil either as suspension (chapter 3 & 5) or as point source (chapter 4 & 6) based on the research question. For inoculation as suspension, 500 µl of the cell suspension (sterile PBS solution for control samples) per cylinder was added to the soil in a weighing boat. The suspension was mixed well with a sterile pipette tip. The mixture was then divided into halves and packed in similar way as described above (Figure 2.2).

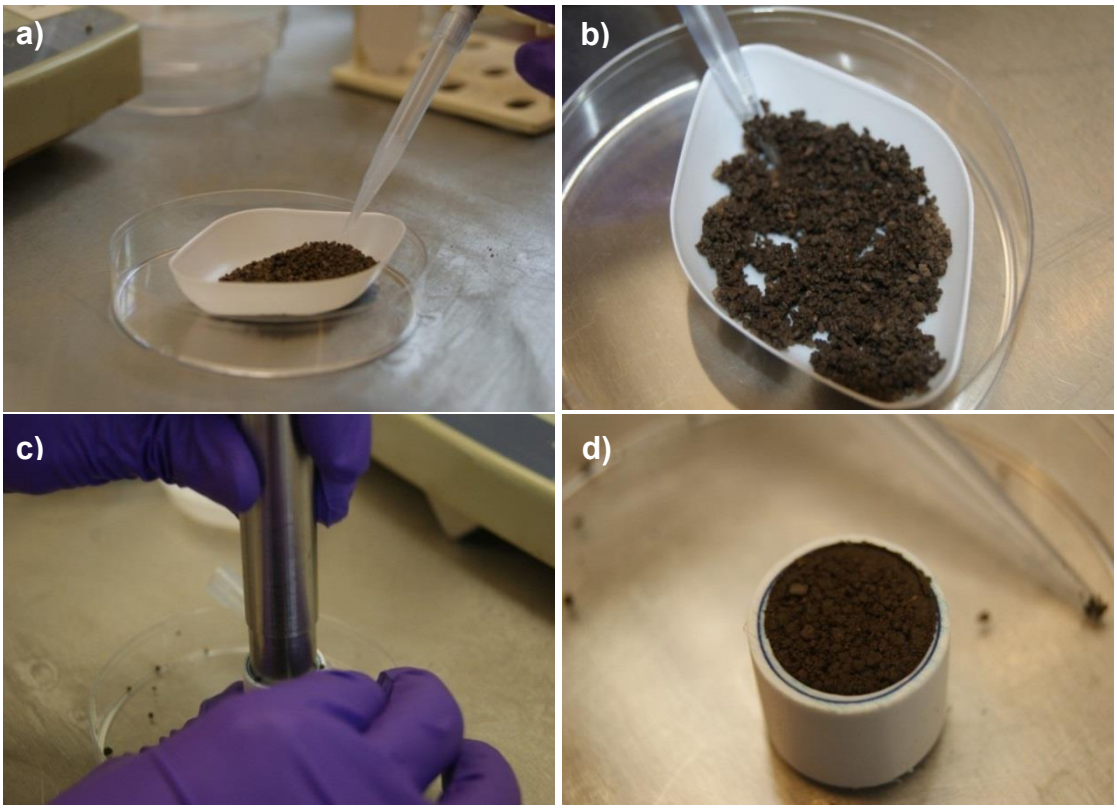

Figure 2.2: Inoculation and packing of soil microcosms. Steps involved are a) addition of bacteria inoculum in soil, b) Mixing of soil with bacteria inoculum, c) packing of soil in ring with a steel piston and d) packed soil microcosms

In case of inoculation with a pellet, the cell suspension was mixed with low point melting agarose (Fisher bio-reagents, UK) to prepare an inoculation bead (henceforth referred as agarose pellet). A low melting point agarose (Fisher bioregaents, UK) was selected as it can remain in a melted state at 35°C, which

serves as an advantage as bacterial cells can survive at this temperature. To prepare an agarose pellet, 1000 µl inoculum of cell suspension prepared above was mixed with 30 ml of LMP agarose solution in a centrifuge tube. The mixture was poured into a petridish which was left under the laminar flow at room temperature to cool down and solidify. The solidified agarose was then cut down into small circular pellets using the circular end of a 1000 µl pipette tip. A single agarose pellet was of size 2.5 mm in diameter and 5 mm in height. One inoculum pellet per sample was taken. For control samples all the above treatments were prepared in a similar way except for agarose beads where 1000 µl of sterile dH_20 was used instead of bacteria inoculum. The method of introducing the agarose pellet in the soil is described in the respective chapters as it was different for each experiment.

2.3.2.3 Optimization of water content and bacteria inoculum volume in soil

Moisture content influences the growth and activity of bacteria as they live in water filled pore space or water films in soil (Uhlířová et al., 2005; Wolf et al., 2013). Microbial activity is reported to be maximal when water-filled pores space is between 30 % - 70 % depending on the soil type and organic matter content (Haney & Haney 2010). At lower moisture content the diffusion of substrate decreases whereas at higher moisture content, the rate of oxygen supply decreases (Stres et al., 2008; Carson et al., 2010). Therefore in this thesis, water content of soil was adjusted to promote growth of introduced bacteria in soil.

As bacteria were introduced in soil in liquid form (as cell suspension) in some chapters, its addition could increase the total water content of soil by 20-40 %. As most of the soil pores are water filled at higher water content, the diffusion of oxygen declines into micropores causing the development of anaerobic conditions in soil. Therefore, a preliminary experiment was carried out to optimize the total water content, including the inoculum volume to enhance growth conditions for introduced bacteria in soil. In this experiment, four treatments with different volumes of water filled pores including the bacteria inoculum volume were tested for promoting growth of bacteria. The water content including the inoculum volume of each treatment ranges between 57 % - 84 % as detailed in Table 2.2. The soil was wetted to the desired water content for each treatment and packed at a bulk-density of 1.3 g cm^{-3} in PE rings as described in section 2.3.2.1. Three replicates per treatment were prepared. The soil was incubated for 7 days. On sampling day, the soil rings were emptied in 10 ml sterile PBS solution. The tubes were shaken for 15 minutes on a shaker at room temperature. Bacteria were enumerated by plate counting method (Page et al., 1982). Briefly, the soil suspension was serially diluted up to 10^{-7} in PBS solution, and 0.1 ml of aliquots of last three dilutions was spread on selective agar media plates. Plates were incubated at 28°C for 48 hrs. Plates of dilution 10^{-6} were selected for counting colonies as it had an appropriate number of colonies for all treatments (Page et al., 1982). The plates were counted under UV excitation light as GFP signal illuminated green colour under UV light (Figure 2.3). Using the CFU formula (equation 2.8), the colonies were then extrapolated to CFU per gram of soil.

$$Colony\ forming\ units\ per\ g\ of\ soil = \frac{Number\ of\ colonies}{Final\ dilution\ used\ X\ diltuon\ factor} \qquad \text{Equation 2.8}$$

In samples with the same percentage of water filled pores but different inoculum volume, bacteria CFU counts were higher in samples inoculated with 500 µl of bacterial suspension compare to samples inoculated with 250 µl of bacterial suspension. Whereas, in case of samples with the same inoculum volume but different percentage of water filled pores bacteria CFU counts were higher in samples with 40 % water filled pores. Among all the treatments highest number [1.24E+08 (s.e 5.81E+06) CFU/g soil] of CFU counts was observed in treatment with 75 % of water filled pores (Figure 2.4). Therefore, for all further experiments the total water content was adjusted to 75 % pores filled with water.

Table 2.3: Treatments set up with different total water content packed at bulk-density1.3 g cm^{-3} in PE rings of size 3.40 cm^3. Water filled pores and inoculum volume used in each treatment is detailed.

Treatments	Water filled pores [%]	Inoculum volume [µl]	Total water-filled pore space [%]
1	50	500	84
2	50	250	67
3	40	500	75
4	40	250	57

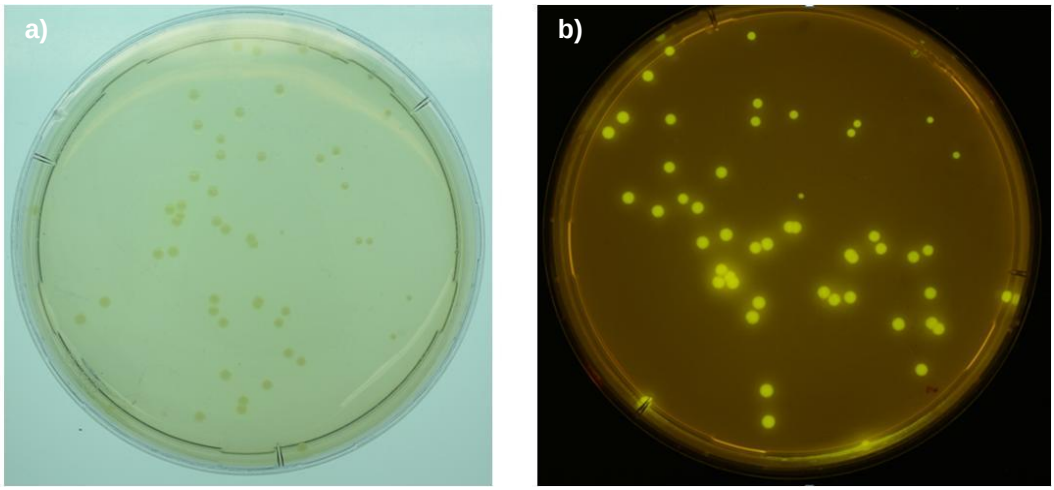

Figure 2.3: Visualization of GFP-tagged cell colonies a) under white/visible light b) UV light in agar plates isolated from soil samples by serial dilution method

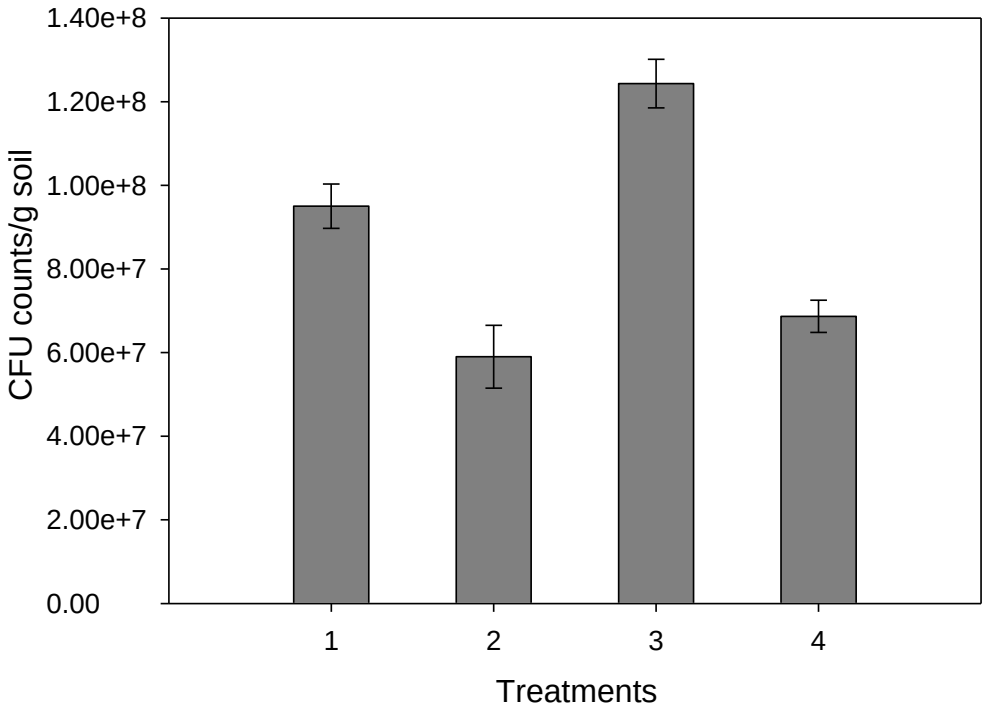

Figure 2.4: Average CFU counts of *Pseudomonas* bacteria inoculated in soil with different water content. Treatments were 1) 50 % water filled pores with 500 µl inoculum volume 2) 50 % water filled pores with 250 µl inoculum volume 3) 40 % water filled pores with 500 µl inoculum volume and 4) 40 % water filled pores with 250 µl inoculum volume. Data are means ±SE (n=3)

2.3.3 Growth pattern of *Pseudomonas* and *Bacillus* in soil

After optimizing the total water content a growth study of GFP-tagged *Pseudomonas* and *Bacillus* cells was undertaken to monitor the survival and growth rate of both selected strains in soil. For this experiment, both GFP-tagged bacterial strains were inoculated in soil and packed in PE rings as described in above sections. Three replicates per strain per sampling day were prepared. The rings were sealed in the plastic bags and incubated at 23°C for 15 days. Soil rings were sampled every alternate day. Both bacterial strains were enumerated by plate counting method as described in the above section. For counting cells, plates of dilution 10^{-5} for *Pseudomonas* and 10^{-3} for *Bacillus* were selected. A fluctuation in the growth pattern of both bacterial strains was observed as shown in Figure 2.5. Both strains showed a decrease in CFU counts on day 1 compare to day 0. For example, *Pseudomonas* CFU counts were 5.17E+07 (s.e 7.51E+06) CFU/g soil on day 0 and 2.33E+06 (s.e 3.33E+05) CFU/g soil on day 1. The reason could be a sudden shock of nutrient starved conditions in soil compared to that of the nutrient rich media. Overall the growth pattern of both *Pseudomonas* and *Bacillus* did not show much increase in cell counts. This might have been due to lack of nutrients as no external nutrient source was added to soil. Among the two strains, *Pseudomonas* showed higher growth rate compare to *Bacillus* in soil which is opposite to that seen in pure media (section 2.2.1). For example on day 5, *Pseudomonas* counts was 3.70E+07 (s.e 1.44E+07) CFU g^{-1} soil and *Bacillus* counts was 9.67E+05 (s.e 1.17E+05) CFU g^{-1} soil. Therefore, from this experiment it was concluded that both introduced bacterial strains survived but doesn't necessarily grow in soil.

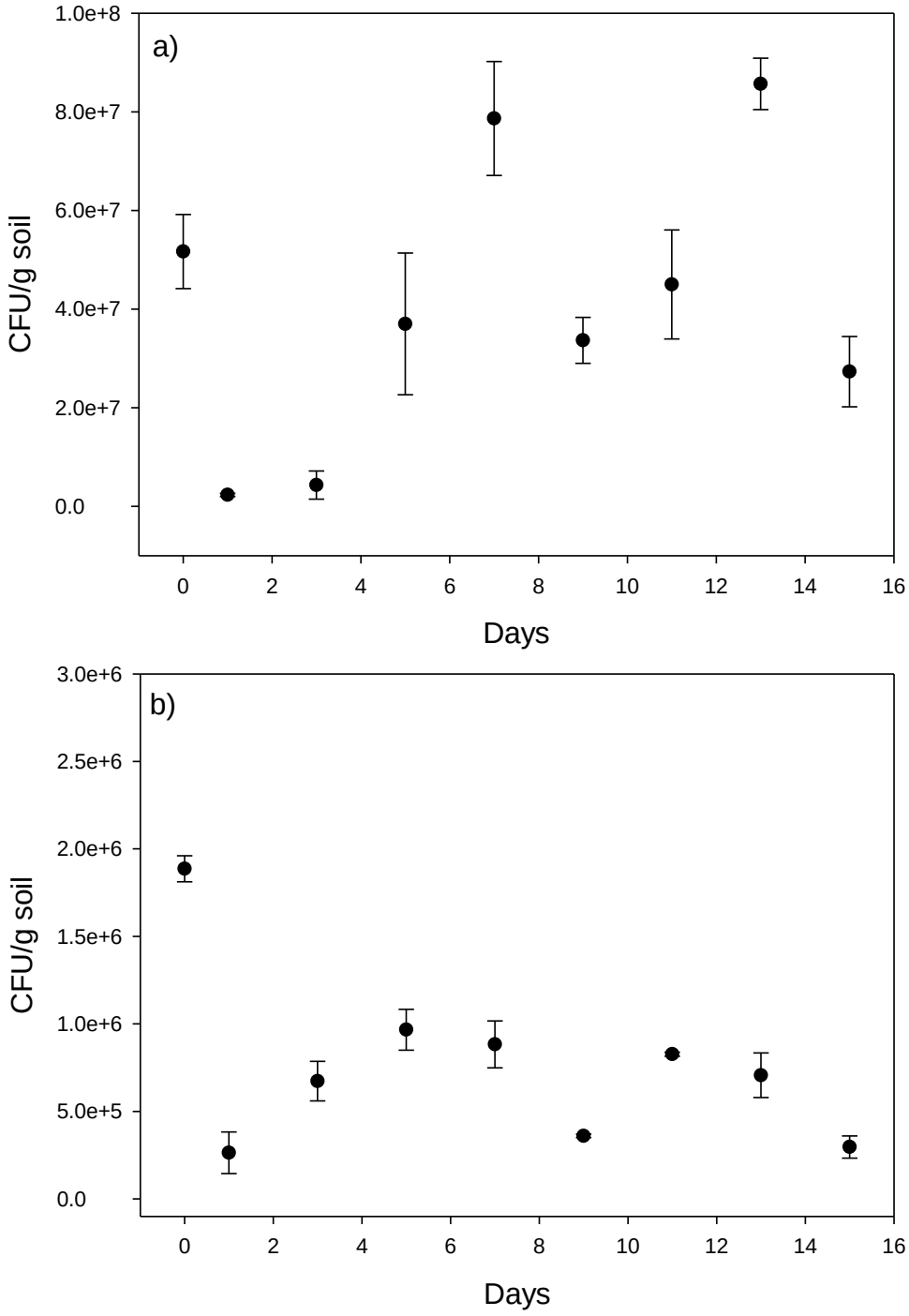

Figure 2.5: Growth curve of *Pseudomonas* (a) and *Bacillus* (b) grown in soil at 23°C. Data are means ±SE (n=3).

2.4 Analysis of soil structure using X-ray tomography

Throughout this project, X-ray computed tomography was used to quantify soil structure non-destructively. The Metris X–Tek HMX 225 scanner (Nikon Metrology) at the SIMBIOS centre in Abertay University was used to scan soil microcosms. The highest achievable resolution of this scanner is 5 µm and it can generate X-rays up to 225 KEV, with a current between 0-2000 µA.

2.4.1 Image acquisition

A standard protocol was used to set up the scan. The energy settings scan resolution and scanning time varied between experiments but the procedure to set up a scan was as described here. To set up scanning, X-Tek InspectX v2.2 software (Nikon Metrology X-Tek Systems Ltd, Tring, UK) was used. There were several steps in this software to set up a scan. The first one was to adjust the position of sample to ensure that the sample is in the field of view throughout scanning. The resolution of the scan is related to the position of sample. The closer the sample was to the X-ray gun (source) the higher was the scan resolution. Throughout this project the resolution of the scan varied between 10 µm and 24 µm depending on the size of the soil microcosms. The second step was to optimize the X-ray settings by changing the current and voltage settings. The X-ray setting was optimized by observing the changes in the histogram of the samples during live imaging, with the optimal set up maximising separation of peaks corresponding to pore and solid phase. A molybdenum target (except for Chapter 6 where Tungsten was used) with a 0.25 mm aluminium filter was applied to minimize beam hardening. A Metris software CT Pro v2.1 (Nikon Metrology X-Tek Systems Ltd, Tring, UK) was

used to reconstruct the radiographs produced by X-ray CT of samples into a three dimensional volume.

Volume Graphics Studiomax (VGStudio MAX) v2.2 software (Volume graphics, Heidelberg, Germany) was used to check the quality of scan and then convert the 3D volumes of the scanned samples into voxel thick image stacks for further processing. To convert the images from 32-bit to unsigned 8-bit format the image contrast of scan images was changed. This was done by defining upper and lower interval in the histogram of the scan image. The images stacks were then exported as unsigned 8-bit size BMP file format for further processing.

2.4.2 Image analysis

To analyse the soil pore characteristics, a region of interest was selected from the image stacks. To select a region of interest, Image J software was used. Grey scale image stacks (*bmp format) were imported in Image J v1.47 (http://rsbweb.nih.gov/ij/) and a region of interest was cropped for quantification of samples. The size of the region of interest (ROI) varied in each chapter depending on the area analysed in the samples but the largest ROI possible was always selected. The selected ROI was then segmented using, Indicator kriging thresholding method (Houston et al., 2013; Hapca et al., 2011). This method produces binary images where solid material was represented as white and the pores were classified as black as shown in Figure 2.6. The segmented images were then evaluated by in house developed software (Houston et al., 2013). The software was used to quantify the pore volume (porosity), fraction of visible pore space (limited to the resolution of scan), connectivity of pore volume and soil-pore interface of the pore volume (surface area) as shown in Figure

2.7. The figure illustrates the pore characteristics like porosity, highest connected pores and the soil-pore interface that can be analysed from 3D segmented images of selected region of interest using the in house developed software. These characteristics of pore geometry were chosen as size of pores defines the habitat for bacteria, connectivity of pores influences distribution of nutrient sources and movement of bacteria and the soil-pore interface is the surface where bacteria are usually attached. An alteration in these characteristics of pores can influence the function of microorganisms in soil, which is the topic of investigation in this thesis

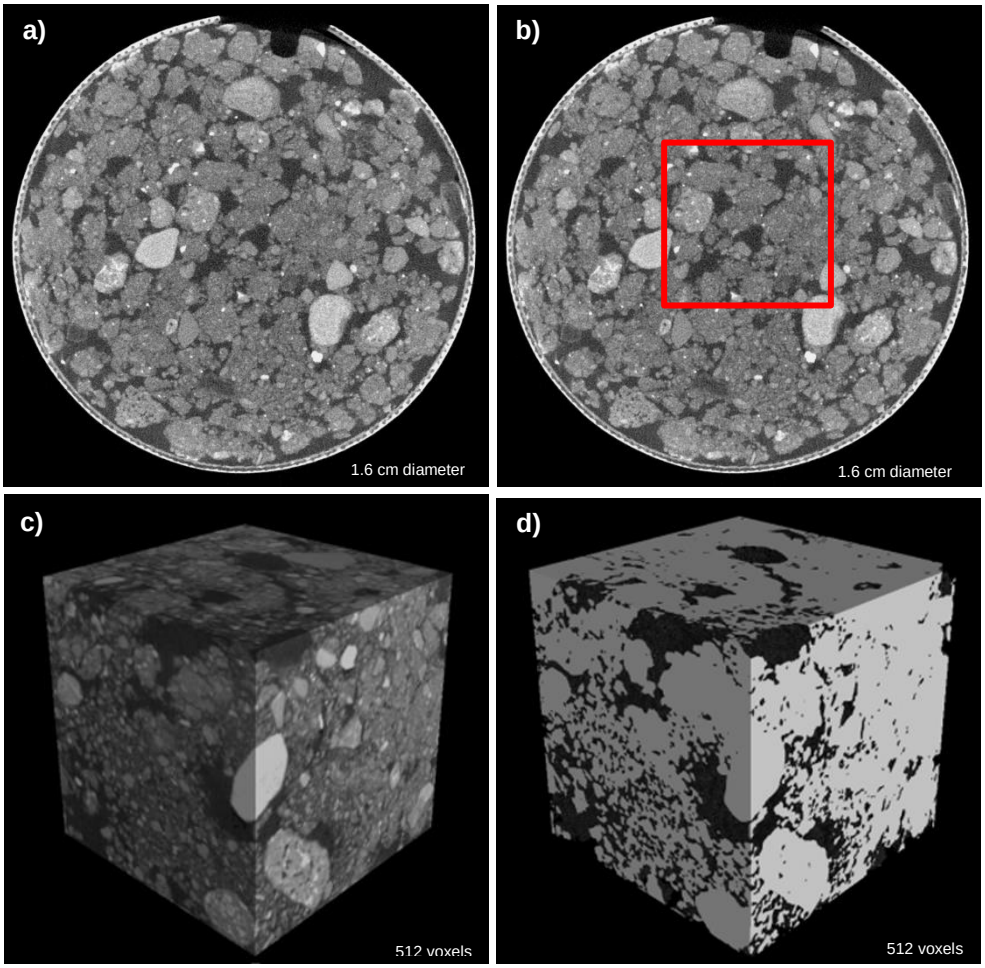

Figure 2.6: Stages of image analysis for quantification of soil pore characteristics. a) Original CT scan volume, b) selection of region of interest (red frame), c) 3D view of selected region of interest and d) 3D segmented volume of selected region of interest.

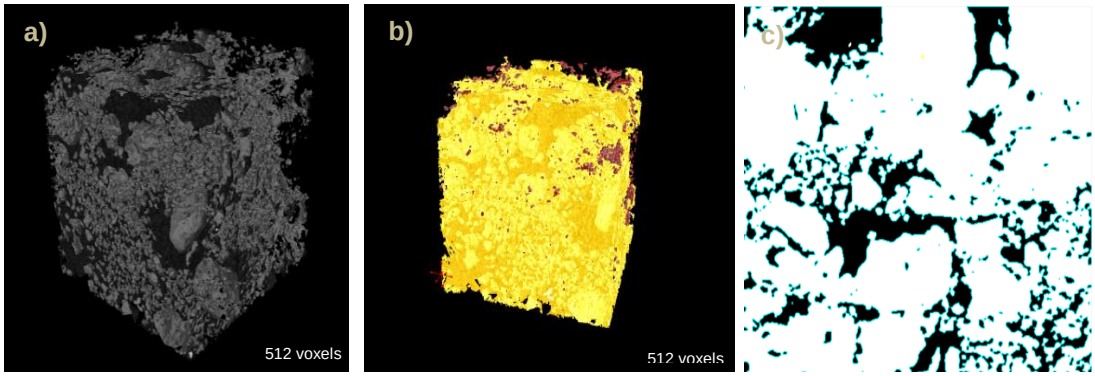

Figure 2.7: Extracted segmented volume for soil pore analysis. a) Pore volume for porosity analysis, b) Connectivity of pores (yellow signifies largest connected pore) and c) soil-pore interface area of pore analysis

2.5 Enumeration of bacteria in soil

Direct counting using fluorescent dyes and epifluorescent microscopy was used to enumerate bacteria in soil. Green fluorescent protein (GFP) marker was used to visualise and quantify bacteria in soil. A VectaShield H-1200 medium containing DAPI (4', 6-diamino-2-phenylindole) was used as a counterstain to test the consistency of the GFP signal. A ZEISS Axioskop 2 microscope equipped with a HBO 100 W Hg vapour lamp was used for evaluating the bacteria in soil samples. The GFP signals were examined under double excitation filter (no. 24, Carl Zeiss, Oberkochen, Germany) and total cells were enumerated under UV excitation (F46-000, AHF, Tübingen, Germany) set. Bacterial cells were observed under 63x (except for chapter 6 where 100x) objective lens and enumerated using a counting grid (10 x 10, 1.25 mm^2, Carl Zeiss) integrated in the ocular (eyepiece) of the microscope. The cells were counted at random or fixed (as described in individual chapters) microscopic fields of views on the filter sections and extrapolated to 1 g of soil using following equation (Page et al., 1982)

$$N_g = \frac{N_f \times A \times D}{W_s \times a_m \times V_f \times v_s}$$ Equation 2.9

Where, N_a = number of bacteria per g of soil; N_f = average number of bacteria per grid; A = area of filter (314 mm^2); D = dilution factor (10^2), W_s = weight of soil; a_m = area of counting grid; V_f = volume used for filtration.

2.6 Summary

In this chapter the common materials and methods used in this thesis plus some short experiments to establish growth conditions were presented. The method of harvesting bacterial cells for inoculating in soil is described. Methods used to introduce bacteria in soil and the procedures of preparing soil microcosms are also presented. The water content of soil microcosm inoculated with bacteria was set to 75 % water-filled pore space, as this optimizes growth of bacteria. Growth rate of both *Pseudomonas* and *Bacillus* strain was quantified in pure media and in soil. The results showed how the growth rate of these strain differs between nutrient medium. Also, the standard protocol used throughout this thesis to quantify soils structure by X-ray tomography is also described.

3 Effect of soil structure on growth of bacteria

3.1 Introduction

Bacteria have been introduced in soil to enhance crop productivity by providing nutrients to plants and controlling plant pathogens (Elsas et al., 1986; Heijnen, 1991; van Veen et al., 1997; Adesemoye et al., 2009; Bhattacharyya & Jha, 2012; Pereg & McMillan, 2015). A large number of bacteria are used as commercialised plant growth promoting bacteria (PGPB) strains for agricultural practice (Lucy et al., 2005; Banerjee et al., 2006). Some of the commercialized PGPB strains are *Pseudomonas* spp., *Bacillus* spp., Streptomyces spp. and various Rhizobia spp. (Glick, 2012). Among these strains, *Pseudomonas* and *Bacillus* are the most frequently studied for plant grow promotion and disease control (Krid et al., 2011; Sivasakthi et al., 2014). For example, *Pseudomonas fluorescens* has been used to suppress plant pathogens and stimulate plant growth hormones for enhanced crop production (Santoyo et al., 2012). Both these species are also well known for their capability to promote plant growth activity by colonizing the plant root area (Hayat et al., 2010). Glick (2012) and Ahemad & Kibret (2014) have reviewed several studies that have been successful in introducing bacteria into soil. The survival of introduced bacteria was affected by the biotic and abiotic factors in soil. Soil texture, structure, temperature, moisture level, pH, nutrient availability, grazing by predators and antagonism are some of the factors which alter the properties of soil which in turn affect the functionality of the microbial activity in soil (Trevors et al., 1994; van Veen et al., 1997). Li et al. (2002) investigated the effect of increasing bulk-density on soil microbial populations and enzyme activities in sandy loam soil. They found a decline in the microbial population by 26-39 % with increasing bulk-density from 1.0 to 1.6 g cm^{-3}. For forest soils, microbial biomass and the

total amount of carbon mineralization and net nitrification rates all declined with increasing bulk-density (Tan & Chang 2007).

Soil aggregation is another property of soil that might affect the growth and activity of bacteria as the aggregate composition determines the intra and inter aggregate porosity, which controls movement of water and gas in soil. Fernazed et al. (2010) reported that the accumulation of carbon differs according to the size of the soil aggregates. This can result in different rates of emission of CO_2 from soil varying in aggregate sizes (Strong et al., 2004; Drury et al., 2004; Sey et al., 2008). For example, soils with aggregates of size <0.25 mm showed increased CO_2 emission compared to soils packed with macro aggregates of a size >0.25 mm (Sey et al., 2008). The reasons could be due to (i) differences in organic matter quantity and quality; (ii) differences in microbial populations and distributions inside aggregates; and (iii) different physical conditions, such as diffusion and pore size distribution for different aggregate sizes. Therefore, it is important to investigate the effect of different aggregate sizes on growth of bacteria in combination with more data on physical properties.

To investigate the impact of soil properties on bacterial communities, an experiment was designed where soil parameters can be manipulated. Repacked microcosms are an experimental method, which allow for some control over soil structural parameters that are replicable at macroscopic scales. It allows the study of different factors by manipulating parameters such as pore characteristics, moisture content and soil texture (Vos et al., 2013). Different types of microcosms, such as sieved soil (sterilised or unsterilized), artificial soil, intact soil cores and transparent soil are being used to study activity of

indigenous or introduced bacteria (Vos et al., 2013, Downie et al., 2012, Otten et al., 2012). However one drawback of such systems is that they do not represent the exact field situation, which is far more complex in nature. But in order to predict the behaviour of microorganisms with changing environmental conditions it is essential to first understand the behaviour in a simple system.

To date no systematic study of the impact of soil bulk-density and aggregate sizes on soil pore network characteristics and their effect on subsequent growth of bacteria has been done. In fact, the majority of studies have a limited description of soil physical conditions e.g. texture. An alteration in the geometry of soil pores like porosity, connectivity and tortuosity affects functions like water infiltration, hydraulic conductivity, air permeability and mobility of nutrients. This in turn affects the activity of microorganisms, which influences the bioavailability of nutrients needed for plant growth (Beylich et al., 2010; Mangalassery et al., 2013). X-ray tomography is the rapidly advancing technique in soil science that is been successfully used to study pore characteristics of soil at finer resolution (see section 1.4 for detailed application).

Thus the aim of this chapter is to construct different microcosms with different soil bulk-density and aggregate sizes and quantify the effect on pore geometry and its influence on the growth rate of *Pseudomonas* and *Bacillus* bacteria in soil.

3.1.1 Hypotheses

1) Increasing bulk-density decreases total porosity, connectivity and soil-pore interface area of pores.
2) An increase in the soil aggregate sizes does not affect porosity but decreases the soil-pore interface of pores.
3) Increasing bulk-density decreases the growth rate of *Pseudomonas* and *Bacillus* in soil.
4) Increasing aggregate size classes influence the growth rate of *Pseudomonas* and *Bacillus* in soil.
5) The growth rate of *Pseudomonas* and *Bacillus* will respond differently to the pore geometry of soil.

3.2 Materials and methods

3.2.1 Bacteria inoculum preparation

GFP-tagged *Pseudomonas fluorescens* SBW25 and *Bacillus subtilis* NRS1473 cell were used as bacterial inoculum. Growth and harvesting conditions of both strains are described in detail in section 2.2.1. Briefly, *Pseudomonas* and *Bacillus* cells were grown overnight in their respective liquid cultures on a rotary shaker (200 rpm) at 28°C. Cells were harvested by centrifugation (5000 x g) and washed with and resuspended in sterile PBS solution. The initial cell density of *Pseudomonas* was 6.46E+08 cells ml^{-1} of soil and *Bacillus* was 7.85E+08 cells ml^{-1}.

3.2.2 Preparation of soil microcosms

Sterilised sieved soil was used. Details of the soil type and sterilization are given in 2.3.1. Soil microcosms were prepared in PE rings of size 3.40 cm^3 (diameter 1.5 cm and height 1.7 cm). The moisture content of sterilised soil was bought to 40 % water filled pores using sterile distilled water. Two experiments were conducted, one looking at the effect of bulk-density, and the second one looking at the effect of aggregate size. In the first experiment, sterilised sieved soil of 1-2 mm size aggregates was used. The amount of water added to acquire 40 % water filled pores for each bulk-density is detailed in table 3.1. The amount of soil required to obtain each bulk-density was then inoculated with 500 µl of the bacterial suspension, mixed well and packed in PE rings using a push rod. Soil was packed to different bulk-densities (1.2, 1.3, 1.4, 1.5 and 1.6 g cm^{-3}). Control samples were packed in a similar manner except that 500 µl sterile dH_20 was used instead of a cell suspension. Soil microcosms were sampled at four times. Three replicates per treatment for each sampling day were prepared. Therefore in total 120 microcosms were prepared. In the second experiment, sieved soil of aggregate sizes 1-2 mm and 2-4 mm was used. Soil was wetted to same moisture content as above and packed in a similar way in PE rings at a bulk-density of 1.3 g cm^{-3}. Here in total 48 microcosms were prepared. All the microcosms were sealed in plastic bags to avoid drying and incubated at 23°C in the dark to allow bacteria to grow in soil. The plastic bags were opened and closed every day to allow for air exchange under a sterile bench. Soil microcosms were sampled on days 1, 5, 9 and 13.

To quantify the effect of different bulk-densities and aggregate sizes on soil structure, separate soil samples were used. For the different bulk-densities experiment, soil was packed in PE rings (4 cm height and 3.7 cm diameter). For different aggregate sizes experiment, samples preparation is described (details in section 5.2.1).

Table 3.1: The amount of water added in dry soil per ring to attain moisture content with 40 % water filled pores and the amount of soil added per ring to pack at a particular density is listed.

Bulk-density ($g\ cm^{-3}$)	Water added/ring (ml)	Soil added/ring (g)
1.2	0.62	4.81
1.3	0.55	5.09
1.4	0.49	5.38
1.5	0.42	5.66
1.6	0.36	5.95

3.2.3 Preparation of soil samples for CARD-FISH

On each sampling day the soil microcosm were emptied into 50 ml centrifuge tubes containing 10 ml of a sterile PBS solution. The tubes were then shaken for 15 minutes at room temperature. The preparation of soil samples for CARD-FISH was carried out according to the protocol by Eickhorst & Tippkötter(2008) Briefly, 500 µl of soil suspension prepared above was fixed in 4 % formaldehyde solution (216 µl of 37 % formaldehyde and 2 x 642 µl 1 X PBS). Samples were shaken in the incubator at 4°C for 2.5 hr. The fixed samples were then washed thrice with 1 X PBS solution and centrifuged at 10,000 g for 5 min at 4°C between each washing step. 100 µl of these fixed samples were diluted in 900 µl PBS/EtOH solution in 2ml eppendorf tubes. These samples were then

sonicated (Sonopuls HD2200, Bandelin, Berlin, Germany) twice at 10% power for 30 s with a pause of 30 s in between.

For filtration, 50 µl of the sonicated sample was diluted in 10 ml MQ water. The mixture was filtered on a polycarbonate filter (0.2 µm pores, 25 mm diameter; Sartorious, Germany). The filters were placed on a glass holder (Sartorius, Germany) for filtration and a vacuum of 800 mbar was applied. The filters were then dipped in 0.2% low melting point agarose (Invitrogen Life Technologies) and dried at 46°C.

For permeabilization of cells, filters were incubated with 85 µl of lysozyme solution at 37°C for 60 min in a sealed petri dish. The filters were then washed in H_2O_{MQ} and EtOH and air dried. Three small filters sections of every sample were cut from the whole filter and used for different staining. The remaining filter was stored at -20°C until further use.

3.2.4 In-situ hybridization and catalysed reporter deposition

For CARD-FISH staining, one of the filter sections was placed in 0.5 ml Eppendorf tube for the hybridization procedure. In the tubes containing filter sections, 400 µl of Hybridization buffer [100 mg ml^{-1} dextran sulfate (Sigma-Aldrich), 5M NaCl, 1M Tris-HCl (v/v), 35 % Formamide (Fluka), 10 % (v/v) SDS, blocking reagent (Roche, Germany) and H_2O_{MQ}] and 1.5 µl of 50 ng $µl^{-1}$ horseradish peroxidase-labelled oligonucleotide probe working solution was added. The tube was incubated for 2 h in a rotating incubator at 35°C.

After the hybridization step, the filter sections were successively washed in three steps. Firstly in a pre-warmed washing buffer (1M Tris-HCl, 0.5M EDTA,

10 % SDS, 5M NaCl and H_2O_{MQ}) for 5 min at 37°C followed H_2O_{MQ} for 2 min at RT. Lastly, with TXP [Triton-X 100 (Bio-Rad) , 1 X PBS) for 5 min at RT. The next step was to amplify the tyramide signal. For this the filter sections were incubated with the amplification buffer [100 mg ml^{-1} dextran sulfate (Sigma-Aldrich), blocking reagent , 5M NaCl , 1 X PBS] along with 0.15 % H_2O_2 solution and 1 µl of fluorescein- labelled tyramide solution for 20 min in a rotating incubator at 35°C. After incubation the samples were then washed in TXP and H_20 for 5 min each at RT. The filter sections were then left at RT to dry.

3.2.5 Enumeration of bacteria

Filter sections treated with CARD-FISH were then placed on a glass slide and mounted with VectaShield H-1200 containing DAPI (4', 6-diamino-2-phenylindole) stain. The filter sections were then covered with coverslips size 24 × 32 mm (Menzel Glaser, Germany). A ZEISS Axioskop 2 microscope equipped with a HBO 100 W Hg vapour lamp was used for evaluating the filter sections. The tyramide signal was examined under a double excitation filter (no. 24, Carl Zeiss, Oberkochen, Germany) and total cells were enumerated under a DAPI filter set (F46-000, AHF, Tübingen, Germany). Bacterial cells were counted under a 63× objective lens using a counting grid (10 × 10, 1.25 mm^2 Carl Zeiss, Germany) integrated in the ocular (eyepiece) of the microscope. The cells were counted at 15 selected microscopic fields of views on the filter sections. Cell counts were converted to cells per gram of soil.

3.2.6 X-ray computed tomography (CT)

Soil samples were scanned using a Metris X–Tek HMX CT scanner. Soil samples packed with different bulk-densities were scanned at 24 µm resolution with energy settings of 105 keV and 96 µA and 2000 angular projections. Soil samples packed with different aggregate size were scanned at 13 µm resolution with energy settings of 145 keV and 35 µA and 2000 angular projections. To minimize beam hardening a molybdenum target with a 0.50 mm aluminium filter was applied. Reconstruction of radiographs into three dimensional volumes was done using Metris X-Tek software CT Pro v2.1 (NIKON metrology, Tring, UK). VGStudioMAX V2.2 (Volume graphics, Heidelberg, Germany) was used to enhance the contrast of the reconstructed volumes and export it into 8- bit grey scale image stacks (*bmp format) for further processing. For structural analysis of different aggregate size treatment, the image stacks of soil samples used in chapter 5 were taken (details in section 5.3).

Image stacks were imported in ImageJ and a region of interest (ROI) of size 12.28 x 12.28 x 12.28 mm (512 x 512 x 512 voxels) was cropped. The ROI were cropped from the centre of the image stacks to exclude pores close to the edges of the ring core to avoid beam hardening and soil ring effects. The selected ROI was then segmented using Indicator kriging software to obtain binary images. In-house developed software ImgTools was used to quantify soil porosity, connectivity and soil-pore interface (Houston et al. 2013).

3.2.7 Statistical analysis

Statistical analysis was performed using SPSS software version 21. An independent t–test with 95 % confidence interval was used to investigate structural difference in mean porosity, connectivity and surface area across different bulk-density and aggregate size treatments. A generalised mixed effect Poisson model with log link function was used to investigate significant difference in cell numbers between sampling days with day as fixed factor. In different treatments, the significant difference between sampling days was investigated with treatments and days as fixed factor.

3.3 Results

3.3.1 Effect of bulk-density and aggregate size on the pore geometry of soil

Only pores larger than 13.4 µm for the experiment considering the impact of aggregate size and 24 µm for the experiment considering the impact of bulk-density could be seen with the resolution used in this experiment.

For pores larger than this resolution, a significant impact of bulk-density on the geometry of soil pores was detected. With increasing bulk-density the overall porosity and connectivity of pores was significantly reduced ($P<0.05$). Soil packed at a bulk-density of 1.2 g cm^{-3} had the highest porosity of 20 (s.e 1.6) % and this declined with the increasing bulk-density to a porosity of 9 (s.e 0.9) % for soil packed with a bulk-density of 1.6 g cm^{-3} (Table 3.2). The 2-D slices obtained from 3D volumetric images also showed a decline in the pores of soil with increasing bulk-density (Figure 3.1). The 3D-connectivity of pores also

reduced from 98 (s.e 0.5) % for loosely packed soil (1.2 g cm^{-3}) to 58 (s.e 6.1) % for densely packed soil (1.6 g cm^{-3}). Although, the mean surface area of soil pores declined with increasing bulk-density from 43 (s.e 1.7) cm^2 for 1.2 g cm^{-3} to 35 (s.e 5.1) cm^2 for 1.6 g cm^{-3} bulk-density this effect was not significant (Figure 3.2).

Table 3.2: Mean porosity, connectivity and surface area of pores packed at bulk-densities of 1.2 g cm^{-3}, 1.3 g cm^{-3}, 1.4 g cm^{-3}, 1.5 g cm^{-3}, 1.6 g cm^{-3}. Mean cell counts ±SE are presented (n=3).

Pore characteristics of soil			
Bulk-density (g cm^{-3})	**Porosity (%)**	**Connectivity (%)**	**Surface area (cm^2/ cm^3)**
1.2	20.0 ±1.6	98.2 ±0.5	43.2 ±1.7
1.3	17.3 ±0.9	96.5 ±0.5	43.8±1.5
1.4	12.5 ±0.6	83.6 ±3.0	41.1±1.6
1.5	9.4 ±1.0	66.8 ±4.0	34.3±3.9
1.6	8.7 ±0.9	57.5±6.1	35.0±5.1

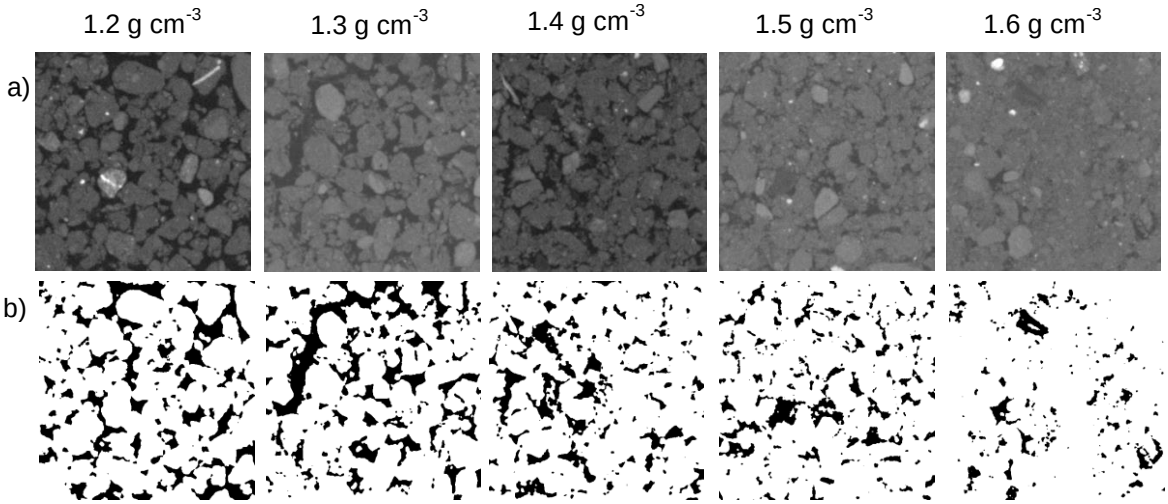

Figure 3.1: Selected two dimensional segmented (a) grey scale images (b) and their binary images (512 x 512 x 512 voxels) of soil packed at different bulk-densities. In binary images black area represents pores and white area represents the solid structure of soil.

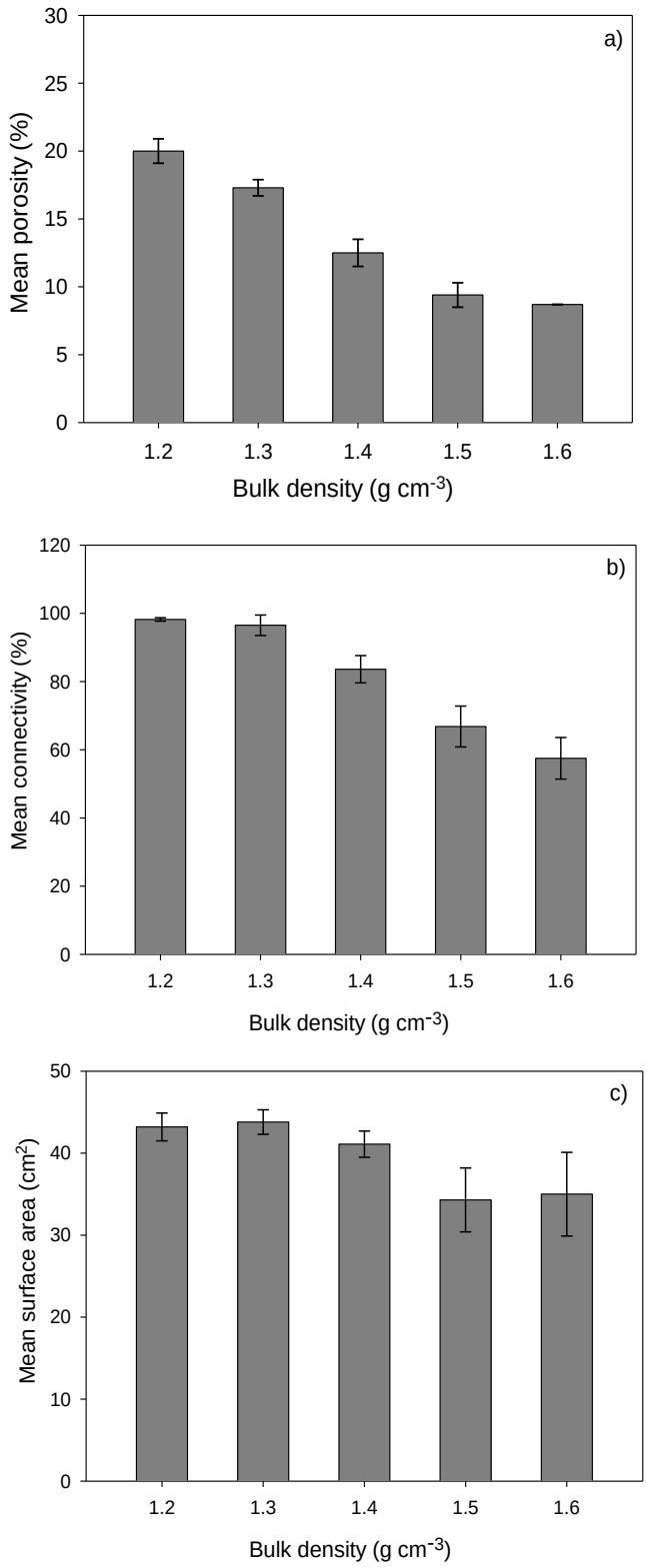

Figure 3.2: Mean porosity (a), connectivity (b) and surface area (c) of samples packed at different bulk-density as measured by X-ray tomography. Data shown are mean ±SE (n=3).

For soil packed with different aggregate sizes a clearly distinguishable difference in soil pores was evident by visual inspection of the 2D sliced images derived from microcosms (Figure 3.3). An increase in the size of pores with increasing diameter of aggregates was clearly visible. The visual difference was, however, not apparent in the quantitative measure we use to summarise the pore geometry. As expected, there was no significant ($P>0.05$) difference in porosity with an average porosity of 24 (s.e 1.3) % for larger size (2-4 mm) aggregates and 23 (s.e 1.1) % for smaller size aggregates (1-2 mm) (Figure 3.4). The connectivity of pores was also not significantly ($P>0.05$) different for both aggregate sizes. As the aggregate size decreased, the surface area of pores slightly increased from 11 (s.e 0.7) cm^2 for 2-4 mm size aggregates to 12 (s.e 0.2) cm^2 for 1-2 mm size aggregates (Table 3.3) but the difference was not significant.

Table 3.3: Mean porosity, connectivity and surface area of pores in soil of aggregate sizes 1-2 mm and 2-4 mm. Mean cell counts ±SE are presented (n=3)

Pore characteristics of soil			
Aggregate size (mm)	**Porosity (%)**	**Connectivity (%)**	**Surface area (cm^2/ cm^3)**
1-2	22.5 ±1.1	97.5 ±0.5	11.6 ±0.2
2-4	24.2 ±1.3	96.9 ±0.4	11.1 ±0.7

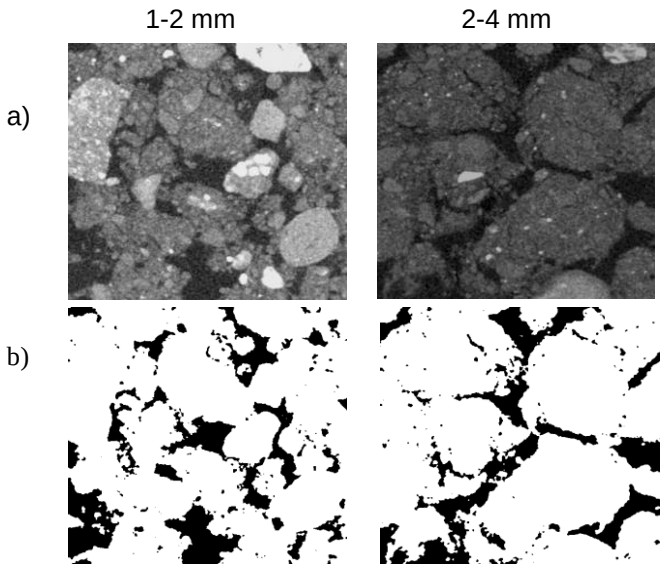

Figure 3.3: Selected two dimensional segmented (a) grey scale images and their corresponding (b) binary images (512 x 512 x 512 voxels) of soil packed with aggregate sizes 1-2 mm and 2-4 mm.

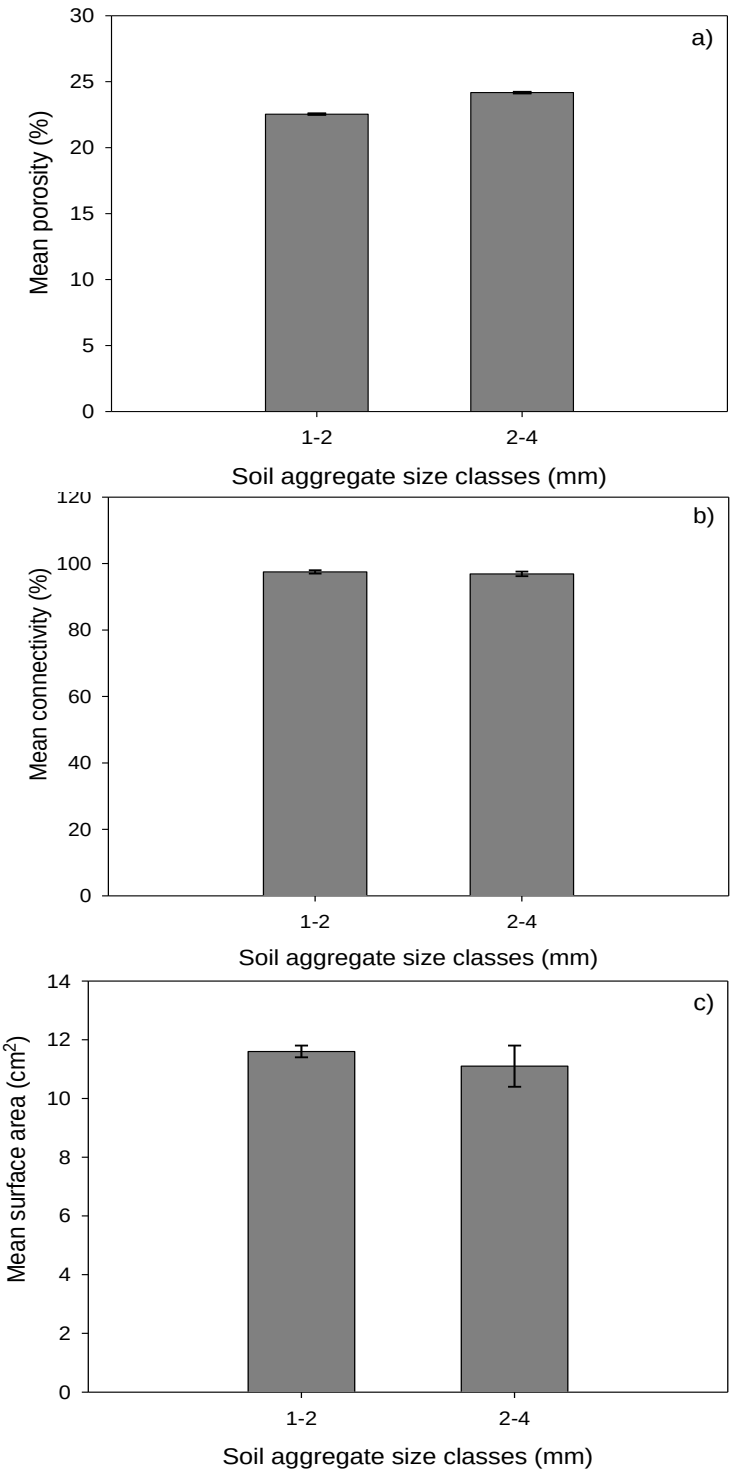

Figure 3.4: Mean porosity (a), connectivity (b) and surface area (c) of samples packed with different aggregate size classes as measured by X-ray tomography. Data shown are mean ±SE (n=3).

3.3.2 Visualization and enumeration of bacteria in soil

The expression of GFP signals was first tested to ensure whether the signals were high enough to count cells on filter sections. GFP signals were detected against brown colour soil background under double excitation filter (465-505 and 564-892 nm). However, the intensity of signals was much weaker and on counterstaining with DAPI it showed that not all GFP-tagged cells were detected.

Another polycarbonate filter section of the same samples used for GFP cell counting was taken and CARD-FISH was applied on them. The intensity of CARD-FISH signals was much greater than the GFP-signals under double excitation (Figure 3.5).To determine the growth of cell counts overtime, selected soil samples containing *Bacillus* cells were taken and counted for both GFP and CARD-FISH signals. In GFP cell counts, no increase in number of cell counts overtime was observed whereas from CARD-FISH counts an increase in number cell counts overtime was observed. Also, CARD-FISH treated bacteria showed a higher number of cell counts per gram of soil for all selected bulk-densities compared to the GFP-tagged cells counts (Figure 3.6).

Therefore, hereafter CARD-FISH was used as a staining and counting method for all samples.

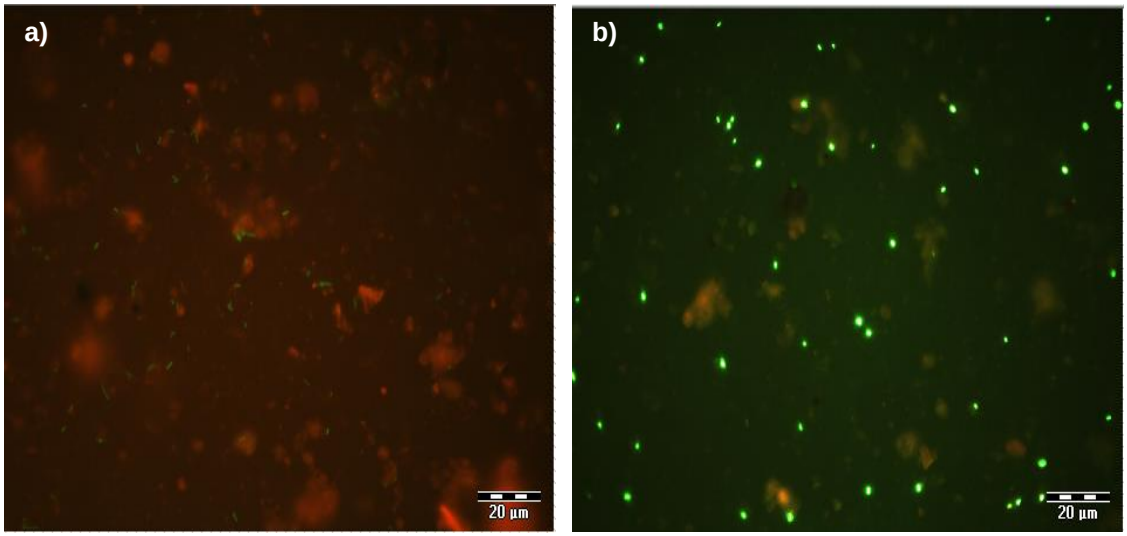

Figure 3.5: GFP-tagged (a) and CARD-FISH stained (b) *Bacillus subtilis* cells in soil filter sections under double excitation filter (465-505 and 564-892 nm). Scale bar 20 µm.

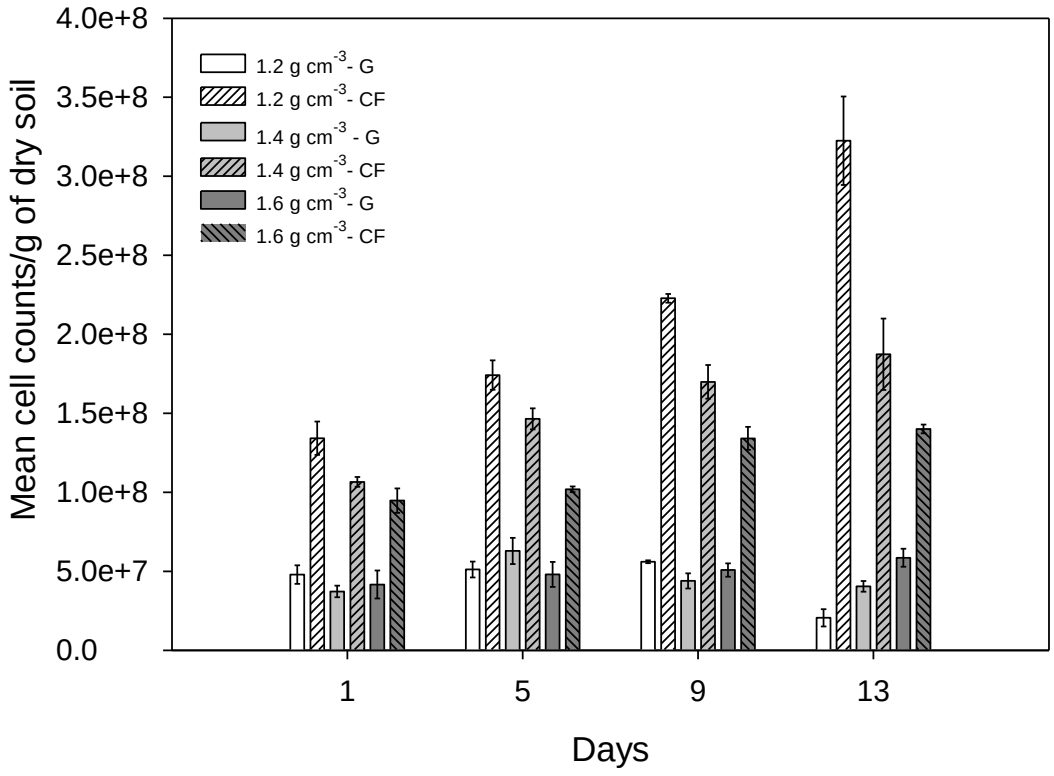

Figure 3.6: Average number of GFP-tagged (blank) and CARD-FISH stained (stripes) *Bacillus* cells per gram of soil at different sampling times in soil samples packed at bulk-densities 1.2 g cm^{-3} (white), 1.4 g cm^{-3}(grey) and 1.6 g cm^{-3}(dark grey). Data are means ±SE (n=3).

3.3.3 Effect of bulk-density and aggregate size on the growth rate of bacteria in soil microcosms

Different bulk-densities of soil significantly affected the growth rates of *Pseudomonas* and *Bacillus* in soil (Table 3.4), with cell counts increasing for both types of bacteria over time (Figure 3.7). For example, from day 1 to day 13 at a bulk-density of 1.3 g cm^{-3} cell counts increased 3.56 times for *Pseudomonas* and 5 times for *Bacillus* with cell densities of 9.37E+08 (s.e 2.80E+07) cells g^{-1} soil, and 5.12E+08 (s.e 2.61E+07) cells g^{-1} soil for *Pseudomonas* and *Bacillus* at day 13 and 2.66E+08 (s.e 1.42E+07) cells g^{-1}(*Pseudomonas*), and 1.01E+08 (s.e 5.65E+06) cells g^{-1} soil (*Bacillus*) at day 1. This trend was expected due to the growth of bacteria in soil. For all bulk-densities and at all sampling times, the number of cell counts for *Pseudomonas* cells was significantly higher than *Bacillus* cells ($P<0.05$, Figure 3.6). As the bulk-density increased, the number of cell counts decreased for both bacterial species ($P<0.05$) at all sampling times, except for soil packed at bulk-density of 1.2 g cm^{-3} where the average cell counts was lower than for soil packed at 1.3 g cm^{-3}. For example, at a bulk-density 1.6 g cm^{-3} the average numbers of *Pseudomonas* cells was 63 % lower compared to those at bulk-density 1.3 g cm^{-3}. A similar trend was observed for *Bacillus* cells where the number of cell counts was 66 % lower at bulk-density 1.6 g cm^{-3} ($P<0.05$, Table 3.3). Note that as all cell densities are expressed per gram that these are reductions beyond those one might expect (81 %) form an increase in bulk-density alone.

Table 3.4: Average cell counts per sampling day of CARD-FISH stained *Bacillus* and *Pseudomonas* strains in soil packed at bulk-densities of 1.2 g cm^{-3}, 1.3 g cm^{-3}, 1.4 g cm^{-3}, 1.5 g cm^{-3}, 1.6 g cm^{-3}. Averaged cell counts ±SE are presented (n=3).

Average number of *Bacillus subtilis* cell counts in soil (cells g^{-1} dry soil)					
Days	**1.2 g cm^{-3}**	**1.3 g cm^{-3}**	**1.4 g cm^{-3}**	**1.5 g cm^{-3}**	**1.6 g cm^{-3}**
1	1.34E+08 ±1.06E+07	1.01E+08 ±5.65E+06	1.07E+08 ±3.10E+06	9.62E+07 ±2.16E+06	9.48E+07 ±7.74E+06
5	1.74E+08 ±9.31E+06	3.41E+08 ±5.61E+06	1.46E+08 ±6.68E+06	1.14E+08 ±3.25E+06	1.02E+08 ±1.80E+06
9	2.23E+08 ±2.81E+06	4.44E+08 ±1.36E+07	1.70E+08 ±1.06E+07	1.48E+08 ±2.35E+05	1.34E+08 ±7.31E+06
13	3.22E+08 ±1.06E+07	5.12E+08 ±2.61E+07	1.87E+08 ±2.26E+07	1.79E+08 ±3.29E+06	1.40E+08 ±2.74E+06
Average number of *Pseudomonas fluorescens* cell counts in soil (cells g^{-1} dry soil)					
Days	**1.2 g cm^{-3}**	**1.3 g cm^{-3}**	**1.4 g cm^{-3}**	**1.5 g cm^{-3}**	**1.6 g cm^{-3}**
1	2.65E+08 ±1.74E+07	2.66E+08 ±1.42E+07	2.77E+08 ±2.25E+07	1.07E+08 ±2.19E+06	1.69E+08 ±7.54E+06
5	4.90E+08 ±1.65E+07	5.66E+08 ±4.51E+07	3.46E+08 ±1.61E+07	2.36E+08 ±7.68E+06	2.31E+08 ±9.13E+06
9	6.67E+08 ±2.02E+07	8.20E+08 ±3.64E+07	5.92E+08 ±8.96E+06	3.23E+08 ±1.14E+07	2.52E+08 ±1.34E+07
13	8.14E+08 ±2.07E+07	9.37E+08 ±2.80E+07	5.66E+08 ±1.60E+07	3.87E+08 ±1.18E+07	2.96E+08 ±1.68E+07

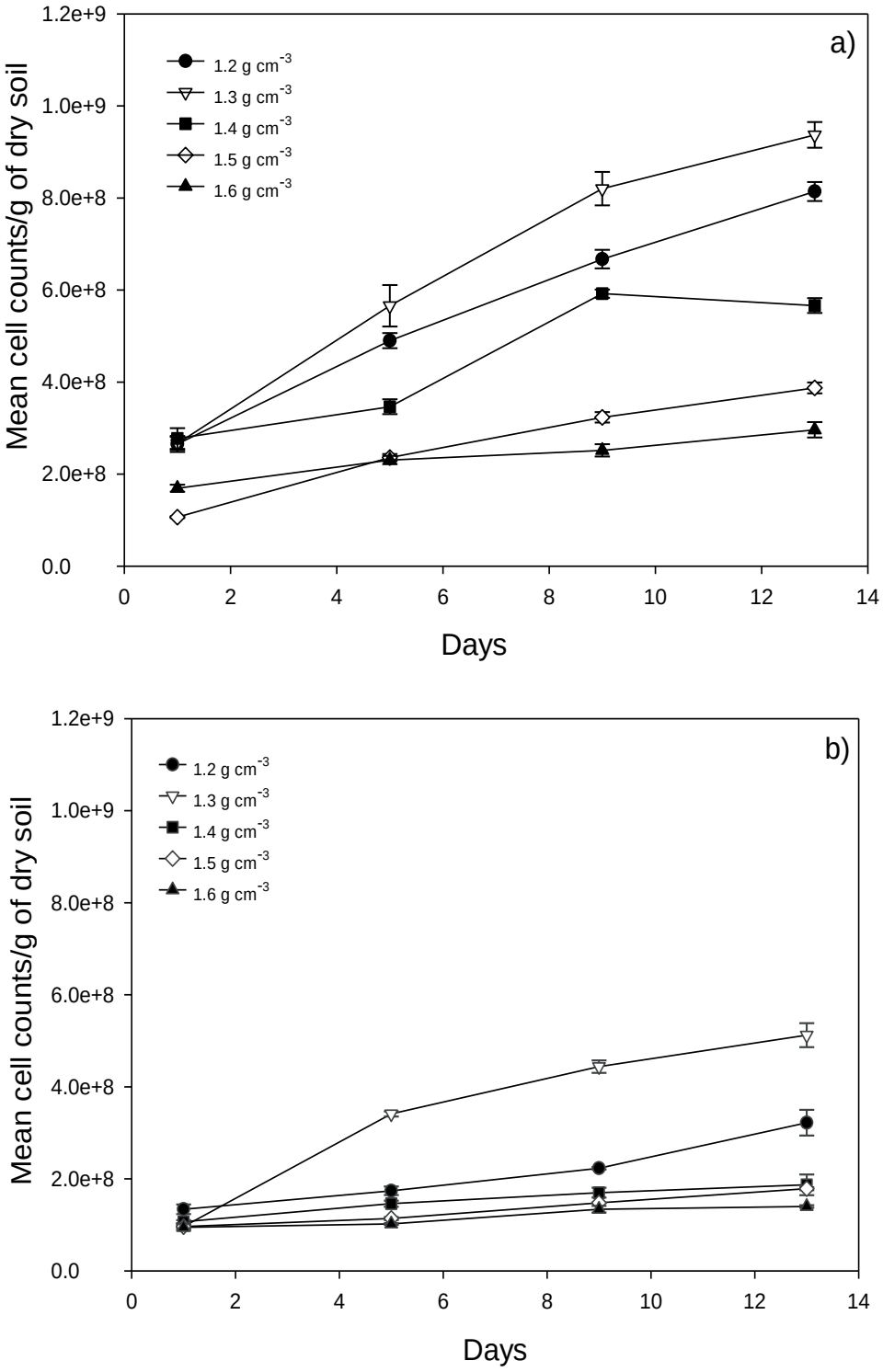

Figure 3.7: Average number of (a) *Pseudomonas* and (b) *Bacillus* cell counts per gram of soil detected at different sampling times in soil packed at bulk-densities 1.2 g cm^{-3}, 1.3 g cm^{-3}, 1.4 g cm^{-3}, 1.5 g cm^{-3} and 1.6 g cm^{-3}. Data are means ±SE (n=3).

Growth rate of both species was also found to be significantly affected by aggregate sizes of soil (Figure 3.8). The number of *Pseudomonas* and *Bacillus* cell counts significantly increased ($P<0.05$) in both aggregate size classes (Table 3.5). For example, from day 1 to day 13 in aggregate size 2-4 mm cell counts increased 3.3 times for *Pseudomonas* and 3.0 times for *Bacillus* with cell densities of 9.17E+08 (s.e 4.77E+07) cells g^{-1} soil and 3.71E+08 (s.e 9.55E+06) cells g^{-1} soil for *Pseudomonas* and *Bacillus* at day 13 and 2.73E+08 (s.e 2.32E+07) cells g^{-1} soil (*Pseudomonas*), and 1.23E+08 (s.e 1.98E+07) cells g^{-1} soil (*Bacillus*) at day 1. Overall in both aggregate sizes, the number of cell counts of *Pseudomonas* was significantly higher than of *Bacillus* on all sampling days (Figure 3.8).

Table 3.5: Average cell counts per sampling day of CARD-FISH-stained *B.subtilis* and *P. fluorescens* strains in soil aggregate sizes 1-2 mm and 2-4 mm. Averaged cell values ±SE are presented (n=3).

Average number of *Bacillus subtilis* cell counts in soil (cells g^{-1} dry soil)		
Days	**1-2 mm**	**2-4 mm**
1	1.01E+08 ±5.65E+06	1.23E+08 ±1.98E+07
5	3.41E+08 ±5.61E+06	2.10E+08 ±1.21E+07
9	4.44E+08 ±1.36E+07	3.07E+08 ±2.11E+07
13	5.12E+08 ±2.61E+07	3.71E+08 ±9.55E+06

Average number of *Pseudomonas fluorescens* cell counts in soil (cells g^{-1} dry soil)		
Days	**1-2 mm**	**2-4 mm**
1	2.66E+08 ±1.42E+07	2.73E+08 ±2.32E+07
5	5.66E+08±4.51E+07	4.54E+08 ±1.62E+07
9	8.20E+08 ±3.64E+07	8.74E+08 ±5.24E+06
13	9.37E+08 ±2.80E+07	9.17E+08 ±4.77E+07

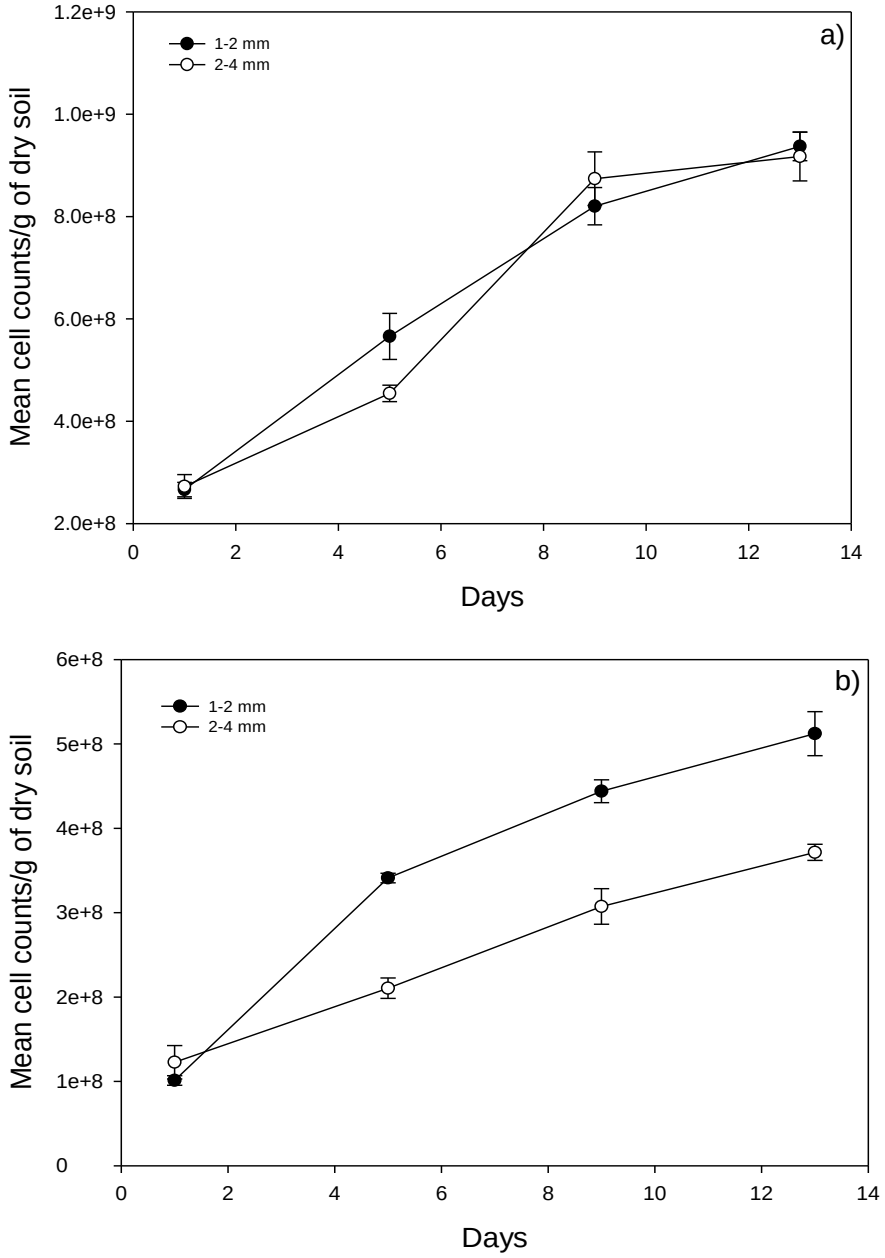

Figure 3.8: Average number of (a) *Pseudomonas* and (b) *Bacillus* cell counts per gram of soil detected at different sampling times in soil of aggregate size classes 1-2 mm and 2-4 mm. Data are means ±SE (n=3).

Between different aggregate size treatments, the number of cell counts of both *Pseudomonas* and *Bacillus* was higher in 1-2 mm size aggregates class compared to 2-4 mm size aggregates (Table 3.5). For example, on day 13 cell counts in smaller aggregates (1-2 mm) was 1.0 times (*Pseudomonas*) and 1.4 times (*Bacillus*) higher than in larger aggregates (2-4 mm), with cell densities of

Pseudomonas 9.37E+08 (s.e 2.80E+07) cells g^{-1} soil and 5.12E+08 (s.e 2.61E+07) cells g^{-1} soil for *Pseudomonas* and *Bacillus* in smaller aggregates (1-2 mm), and 9.17E+08 (s.e 4.77E+07) cells g^{-1} soil (*P. fluorescens*), and 3.71E+08 (s.e 9.55E+06) cells g^{-1} soil (*Bacillus*) in larger aggregates (2-4 mm).

3.4 Discussion

3.4.1 Effect of bulk-density and aggregate size on the pore geometry of soil

The effect of bulk-density and aggregate size on pore geometry was investigated as alteration in structure (Pupin et al., 2009; Nawaz et al., 2012). It is difficult to study the effect on activities of microorganisms in undisturbed samples as each replicate would be different and introduce more variability in the results. Therefore, repacked soil microcosms were used in this study. Here, the pore geometry was manipulated by altering some of the soil physical characteristics such as bulk-density and aggregate size which can be experimentally controlled. The effect of this preparation was subsequently quantified using X-ray CT.

Image analysis of 3D volumetric images of soil packed with different bulk-density confirmed and quantified the variation in the pores characteristics of the soil microcosms. A reduction in the total porosity and connectivity of pores with increasing bulk-density was observed. This can reduce soil functions like water infiltration, hydraulic conductivity, air permeability and mobility of nutrients, thus, influencing the micro-environmental conditions for microbial activity (Beylich et al., 2010; Wolf et al., 2013). These results are consistent with some previous

reports that showed influence of bulk-density on geometry of soil pores (Frey et al., 2009; Kim et al., 2010; Nawaz et al., 2012). Frey et al. (2009) reported a 17 % reduction in total porosity in severely compacted soil. Kim et al. (2010) studied the effect of compaction on 3D macropore geometry in undisturbed soil cores. The X-ray CT data indicated that the CT measured number of pores decreased by 71 % in compacted soil. The study also revealed a decrease in number of macro- (69 %) and mesopore (75 %).

For soil with different aggregate size classes packed at the same bulk-density, it was speculated that the total porosity and connectivity of pores would be the same and the soil-pore interface of pores would reduce with increasing aggregate size classes. This hypothesis is however formulated assuming the total pore volume is observed, yet in X-ray CT only the larger pores are observed. The percent of pores >13 µm was found to be not significantly different between different aggregate size classes. However, out of the total porosity (48 %), the percent of large pores observed in X-ray CT was 24 %. In case of surface area of pores the difference was also not significant. A plausible explanation for this is either the difference between the two selected aggregate size classes was not sufficient enough to show a difference or it could be the scan resolution (13.4 µm) where small pores (<13.4 µm) could not be detected. This result is opposite to the findings of Mangalassery et al (2013) who found a significant increase in porosity and surface area of pores with increasing aggregate size in sandy loam soil. They used aggregates sizes ranging from <0.5 mm to 2-4 mm and packed them at bulk-density 1.2 g cm^{-3}. They scanned soil cores at a resolution of 28.75 µm. Another reason for the difference may be

the scan resolution (pores >28.75 µm) and the size of the region of interest analysed for soil pore characteristics. They used a region of interest of size 27.92 mm x 27.92 mm whereas in this study the region of interest was 6.86 mm x 6.86 mm and, therefore, less representatives for the soil sample given the size of the aggregates we used. The size was, however, computationally constrained.

3.4.2 Effect of bulk-density and aggregate size on growth of bacteria in soil

The hypothesis that increasing bulk-density affects the growth of bacteria was validated; with the number of bacteria decreasing with increasing bulk-density. The results obtained in this study are consistent with several other studies which reported a reduction in the microbial community and its activity at higher bulk-density compared to the soil packed at lower bulk-density (Li et al., 2002; Frey et al., 2009; Pupin et al., 2009; Dick et al., 1988; Smeltzer et al., 1986; Tan and Chang, 2007, Tan et al., 2008). For example, Pupin et al. (2009) reported a reduction of 22-30 % in the number of bacteria at 1.7 g cm^{-3} bulk-density compared to the control (1.3 g cm^{-3}). Li et al. (2001) also reported a negative relationship of microbial numbers with the bulk-density of soil. A reduction in the microbial biomass carbon and nitrogen was reported due to 13-36 % decrease in air filled porosity caused by compaction of soil. The most probable justification for these results is that due to increased compaction of soil there are alterations in some of the soil factors which determine the living condition of microorganisms in soil. Mainly, an increase in the bulk-density of soil reduces the number of large pores and also the connectivity between the pores. This

results in reduced accessibility of organic substances, water movement and gas exchange. A reduction in O_2 diffusion through soil changes the soil environment into an anaerobic state, thus inhibiting the growth of aerobic microorganisms and its activity (Beylich et al., 2010, Torbet et al., 1992). In this study, both *Pseudomonas* and *Bacillus* sp. are aerobic microorganisms and they were both shown to be negatively affected by the increase in bulk-density of soil. We tried to mitigate this effect by choosing a wetness equivalent to 75 % of the pore space filled with water (and hence 25 % with air). Other factors, however, are also altered. For example, as more soil is packed in a microcosm at a higher bulk-density, and the number of cells at inoculation is constant per volume, it means that the cell count expressed per g soil is lower in soil with a higher density. We noted, however, that the differences we found were larger than this simply dilution effect. On the other hand, soil with a higher bulk-density will have larger organic matter content per volume soil. So each microcosm contained more organic matter at a higher bulk-density. This may also have affected the growth. This highlights the complex web of interactions that take place between physical space and other conditions. It is critical therefore that we do not just consider the growth but also the spread of bacteria, which is addressed in the next chapter.

In the second part of the experiment, an effect of aggregate size on growth of bacteria was investigated. A significant effect of aggregate size on the growth rate was observed only for *Bacillus* inoculated samples. The numbers of *Bacillus* cells counts were higher in smaller aggregates of 1-2 mm in size. The possibility of active growth in smaller size aggregates could be due to the

availability of more nutrients in smaller size aggregates. A non-significant effect of aggregate size on *Pseudomonas* cells counts was observed. This result agrees with the finding of Drazkiewuz, (1994) who found that soil type had more influence on the number of *Pseudomonas* than the aggregate size.

3.5 Conclusion

In this chapter physical properties of soil were manipulated by changing bulk-density and aggregate sizes to investigate the factors of soil structure that affect bacterial dynamics in soil. Cell counts of both the bacterial strains selected for this study showed a significant influence of bulk-density and aggregate sizes on their growth rate in soil. The characterization of soil pore geometry helped in understanding this effect. Higher number of bacterial cells was found in loosely packed soil where the porosity of soil was higher and well connected. The aggregate size was also found to influence the growth of bacteria with higher number found in small size aggregates. This study thus suggests that field management practices, such as compaction of soil through the use of heavy machinery and tillage practice can affect the growth of bacteria and thus on their activity. Future work could also investigate the effect of different range of aggregate size classes on growth rate of bacteria in soil. Also, further research is required to study the complete effect of compaction on the microbial processes in soil for good crop productivity and better soil management.

4 Effect of soil structure on spread of bacteria

4.1 Introduction

Bioremediation is a technique of introducing bacteria to the site of contamination to degrade harmful chemicals or pollutants. To stimulate bioremediation process wild-type or genetically modified bacteria are introduced in soil (Natsch et al., 1996). For a successful remediation process, bacteria have to reach the contaminant site from the point of inoculation. Therefore, it is essential to understand the factors that are involved in transport (spread) of bacteria in porous media (Natsch et al., 1996; Tan et al., 1991; Gannon et al., 1991). Soil is a complex porous media where several physical, chemical and biological factors affect transport of bacteria in soil (Abu-ashour et al., 1994; Shein & Devin, 2007; Wang et al., 2013). Some of these factors which are known to influence movement of bacteria are summarised in Table 4.1. Influence of some of these factors on transport of microorganisms have been investigated on intact and repacked soil columns (Abu-ashour et al., 1994; Bradford et al., 2006; Mailloux et al., 2003).

Table 4.1: Summary of the studies that investigated the effect of different soil factors affecting movement of bacteria through soil.

Factors		Reference (Author and year)
Soil physical factors	Bulk-density	Elsas et al. ,1991 Huysman et al.,1992
	Water content	Trevors et al., 1990 Elsas et al., 1991
	Pore size distribution	Natsch et al., 1996 Abu-Ashour et al., 1998
	Particle size distribution	Tan et al., 1991
	Texture	Smith et al., 1985 Hekman et al., 2005 Guimaraes et al., 1997 Lahlou et al., 2000 Singh et al., 2002 Banks et al., 2003
	Soil water and water flow	Elsas et al., 1991
Soil chemical factors	pH	Kinoshtia et al., 1993
	Ionic strength	Redman et al., 2004 Kim et al., 2009
Microbial factors	Cell size and shape	Gannon et al., 1991 Fontes et al., 1991 Weiss et al., 1995 Devin et al., 2003
	Motility	Gannon et al., 1991 Singh et al., 2002 Turnbull et al., 2002

Among the physical factors, water flow (a process called advection where bacteria move along with the water flow) is one of the main factor which influences transport of bacteria in soil. Influence of preferential flow channels on transport of introduced bacteria in deeper soil layer was reported by Natsch et al. (1996). Another study by Trevors et al. (1990) showed the influence of water movement on transport of genetically engineered *Pseudomonas fluorescens* C5t strain in vertical soil microcosms. The results showed that transport of cells was dependant on the rate of water flow and number of times the microcosms were flushed with groundwater. Pore shape and size is another factor that highly influences movement of bacteria, as pore sizes smaller than the average size of bacteria would prevent the passage of bacteria which would eventually result in blockage of pores (Shein & Devin, 2007). Presence of soil cracks and macropores could on the other hand lead to faster movement of bacteria. This might be the reason why in some studies which used intact and undisturbed soil columns there was a higher rate of translocation of bacteria compared to repacked soil columns; it was concluded that the presence of macropores resulted in more translocation of bacteria (Wang et al., 2013; Abu-ashour et al., 1994; Natsch et al., 1996).

In addition to the physical factors outlined above, alteration in some chemical properties like ionic strength and pH can also affect the movement of bacteria in soil. For example, an increase in ionic strength of the soil solution enhances sorption of bacteria to soil particles resulting in less movement of bacteria through soil (Gannon et al., 1991; Redman et al., 2004). This has been investigated by Redman et al (2004) who showed that an increase in ionic strength of the pore fluid resulted in increased attachment of *E.coli* strain to

quartz grains. Bacterial cell characteristics like size, shape and mode of motility were also reported as important factors influencing transport of bacteria through a soil column (Gannon et al., 1991, Fontes et al., 1991, Davis et al., 2003). For example, Gannon et al. (1991) reported a relationship between cell surface hydrophobicity, cell size and surface charge of 19 bacterial strains and their transport through soil. The results showed that transport of these strains was related to cell size, with bacteria less than 1 µm transported further through soil than bacteria that were >1 µm in size (Gannon et al., 1991) The combined influence of physico-chemical properties on movement of bacteria in porous media has also been studied in the past (Lahlou et al. 2000; Singh et al. 2002). For example, Singh et al (2002) investigated the role of bacterial motility and cell hydrophobicity on the horizontal and vertical movement of bacteria under different soil conditions. The results indicated that physical properties such as texture and pore size of different soil types influenced vertical transport of *Pseudomonas fluorescens* strains in soil whereas motility of bacteria influenced horizontal and vertical transport only in the presence of certain chemical stimulus (Singh et al., 2002). Since a combination of more than one factor is shown to affect movement of bacteria through soil it is necessary to study the movement of specific bacterial strains in soil, as different effects of environmental conditions may be expected between bacterial strains.

In the studies referred to in table 4.1 that studied the transport of bacteria through soil, bacterial inoculum was added on top of the soil surface and the columns were then percolated with a defined amount of water depending on the experiment. To quantify the amount of bacteria transported through the soil columns under different conditions, effluent water passed through the column

was collected and the cell density of bacteria was determined by serial dilution plating. As a result of this method of study the transport of bacteria is expected to be dominated by water flow (advection process). In order to understand the effect of soil structure on movement of bacteria in soil, introduction of an external water flow has to be excluded and there is limited literature available for this context, where bacteria is added as a point source. Therefore in this chapter preliminary experiments were carried out to refine and optimize the experimental setup by minimising water flow and decreasing the amount of liquid bacterial suspension that will be introduced into soil. In the absence of water movement, the spread can be quantified using baiting methods as, for example, used by Otten et al. (2001; 2004) for the spread of fungal growth through soil. They studied the effect of soil structure on the colonization efficiency of *Rhizoctonia solani* in sandy loam soil samples as a measure of spread. To obtain the rate, as well as the extent of spread, they quantified the efficiency of *R. solani* to colonize new nutrient sources from a local source of inoculum. In this method inoculum is introduced on one side of a soil sample of pre-defined thickness and a bait is placed on the other side and observed daily for colonisation. By doing this for replicated samples they were able to construct a profile that characterised the probability of spread through a layer of soil in a similar way as dispersal kernels are used to characterise spread in ecology. For a thin layer of soil, the probability to colonise a bait is close to 100 %, and they showed that the probability declines sigmoidally with distance. Vice versa, for a given thickness of soil, the probability that a bait becomes colonised increased from 0 for short times to a maximum, again following a sigmoidal increase with time. This kind of experimental setup is an efficient way to investigate the

spread of microbes through heterogeneous soil environments. To date, this kind of set up has not been used in studying the effect of soil physical conditions on the transport of bacteria though soil.

In the previous chapter (chapter 3), it was shown that soil structure affected the temporal dynamics of bacteria. It is however possible that factors affecting growth do not necessarily affect spread. For example, for fungi Otten and Gilligan (1998) showed that some soil physical conditions had no effect on growth, but a substantial effect on spread of fungi. Such studies have not been undertaken for bacteria in soil. In this chapter, therefore, the influence of soil structure on the spatial dynamics i.e. spread of bacteria was determined. *Pseudomonas* and *Bacillus* strains were used to investigate spread of bacteria under different physical properties of soil. It is expected that the extent of spread will differ between the two selected strains in microcosms with the same soil properties due to intrinsic variation in cell characteristics between the strains. In addition to the properties investigated in Chapter 3 (bulk-density and aggregates sizes) moisture content was also manipulated as this is a key property governing spread of bacteria.

4.1.1 Hypotheses

1) Bacteria are able to spread several centimetres though soil in a 2-week time frame.
2) Extent of spread of bacteria will be faster in soil with higher moisture content.
3) Increasing bulk-density will decrease the extent of spread of bacteria in soil.

4) Increasing aggregate size will increase the spread of bacteria in soil.
5) The probability that bacteria spread a specified distance decreases sigmoidally with increasing distance.

4.2 Materials and methods

The spread of bacteria is quantified by the likelihood of colonisation of bait in relation to the site of inoculation. To optimize experimental design to quantify the spread of bacteria as affected by soil structure different combinations of soil moisture content and inoculum volume were first tested. As bacteria are introduced within a liquid volume, the size of the volume and the wetness of the soil can result in passive movement due to water flow, an effect I try to minimize. Also, different types of baits were tested. This led to an optimised set-up where movement due to active transport and attraction by a bait were minimised whilst maintaining an experimental design that would allow for processing of large number of replicated samples. Details of evolvement to get to this optimized experimental setup are summarized in appendix I.

4.2.1 Bacterial strains

Wild type *Pseudomonas fluorescens* SBW25 and *Bacillus subtilis* NCIB3610 subtilis bacterial strains were used in this experiment. Both strains were cultivated in their respective selective media (details in chapter 2.1). For addition in soil, an overnight culture of both strains was prepared in their respective media broth at 28°C. Both the cells were harvested by centrifugation at 4000 x g for 5 minutes at 4°C, washed twice in 10 ml sterile PBS solution. Washed cells were suspended in sterile PBS solution for inoculation in soil. An

agarose pellet was used to provide a reproducible source of inoculum to inoculate soil. An agarose pellet was prepared as described in appendix I. Briefly, 1000 µl inoculum of washed cells prepared as above was mixed with 30 ml of LMP agarose solution in a centrifuge tube. The mixture was poured into a petridish, which was left in a laminar flow cabinet at room temperature to cool down and solidify. The solidified agarose was then cut down into small circular pellets by using the circular end of a 1000 µl pipette tip. A single pellet (henceforth referred to as inoculum pellet) was of size 2.5 mm in diameter and 5 mm in height. One inoculum pellet per sample was taken. Control samples were prepared in a similar way except for the agarose pellet bead where 1000 µl of sterile dH_20 was used instead of bacteria inoculum.

4.2.2 Soil

Sterilised soil (sandy loam) was used in this study. Soil was sterilised by autoclaving twice at 121°C for 15 min with 48hr interval (details in section 2.2). Autoclaved distilled water was added to sieved soil to obtain desired moisture content. The details of this differed per experiment and are given below. After adding water the soil was left for 48hr at 23°C to equilibrate.

In this study, four individual experiments were conducted to investigate the influence of soil factors (water content, bulk-density and aggregate sizes) on the spread of bacteria in soil and test the hypotheses outlined above. In each experiment, soil was packed in PE rings of size 3.40 cm^3 and a height of 1.5 cm (except for experiment 4 where rings with various heights were considered). The height of the rings is critical as it equals the distance over which spread of bacteria is measured.

To test the effect of moisture content (exp 1) sterilised soil of 1-2 mm size aggregates was prepared with moisture content equivalent to 40 % or 60 % water filled pores and packed at a bulk-density of 1.3 g cm^{-3}. The amount of soil and water used in each treatment is described in Table 4.2.

To test the effect of bulk-density (exp 2), sterilised soil of 1-2 mm size aggregates with moisture content equivalent to 60% water filled pores was packed at bulk-densities 1.3 g cm^{-3} and 1.5 g cm^{-3}. The amount of soil and water used in each treatment is described in table 4.3.

To test the effect of aggregate size (exp 3) sterilised soil of 0.5-1, 1-2 and 2-4 mm sized aggregates with a 60% water filled pores, were packed at a bulk-density of 1.3 g cm^{-3}. The amount of soil and water used in each treatment is described in table 4.4.

To quantify how distance affects the probability of colonisation of a bait (exp. 4) sterilised soil of 1-2 mm sized aggregates with a 60% water filled pores was packed at a bulk-density1.3 g cm^{-3} in PE rings of diameter 1.7 cm and a height of 1.5, 2.0, 2.5, 3.0 and 4.0 cm. The amount of soil and water required in each soil ring is described in table 4.5.

Table 4.2: Physical characteristics of repacked soil microcosm prepared to quantify effect of moisture content on spread of *Pseudomonas* and *Bacillus* bacteria through soil.

Treatment	Water filled pores (%)	Bulk-density (g cm^{-3})	Aggregate size (mm)	Height of the ring (cm)	Water added/ring (ml)	Soil added/ring (g)
1	40	1.3	1-2	1.5	0.55	5.09
2	60	1.3	1-2	1.5	0.89	5.43

Table 4.3: Physical characteristics of repacked soil microcosm prepared to quantify effect of bulk-density on spread of *Pseudomonas* and *Bacillus* bacteria through soil

Treatment	Water filled pores (%)	Bulk-density (g cm^{-3})	Aggregate size (mm)	Height of the ring (cm)	Water added/ring (ml)	Soil added/ring (g)
1	60	1.3	1-2	1.5	0.89	5.43
2	60	1.5	1-2	1.5	0.59	5.83

Table 4.4: Physical characteristics of repacked soil microcosm prepared to quantify effect of aggregate size on spread of *Pseudomonas* and *Bacillus* bacteria through soil

Treatment	Water filled pores (%)	Bulk-density (g cm^{-3})	Aggregate sizes (mm)	Height of the ring (cm)	Water added/ring (ml)	Soil added/ring (g)
1	60	1.3	0.5-1	1.5	0.89	5.43
2	60	1.3	1-2	1.5	0.89	5.43
3	60	1.3	2-4	1.5	0.89	5.43

Table 4.5: Physical characteristics of repacked soil microcosm prepared to quantify effect of distance on spread of *Pseudomonas* and *Bacillus* bacteria through soil

Treatment	Water filled pores (%)	Bulk-density (g cm^{-3})	Aggregate sizes (mm)	Height of the ring (cm)	Water added/ring (ml)	Soil added/ring (g)
1	60	1.3	1-2	1.5	0.89	5.49
2	60	1.3	1-2	2.0	1.20	7.32
3	60	1.3	1-2	2.5	1.50	9.16
4	60	1.3	1-2	3.0	1.80	10.99
5	60	1.3	1-2	4.0	2.40	14.65

4.2.3 Preparation of soil microcosms

In each experiment, the soil (prepared as described above) was placed in the ring and a push rod was used to compress soil to reach a particular density. The inoculum pellet was placed in a dish (in this case a cap of a centrifuge tube) and a soil ring was placed on top of the pellet. One autoclaved 2-4 mm size aggregate was placed on top surface of the sample as the bait for colonisation of bacteria. Samples were then sealed by closing the centrifuge tube in upright position to prevent drying of soil and incubated at 23°C (Figure 4.1). For the control treatment, the samples were prepared in similar way except that an agarose pellet without inoculum was used. Ten replicates per treatment were prepared. Each day the bait was removed from the surface and tested for colonisation by the bacteria. Daily sampling was done until all the samples for each treatment showed positive results. On each sampling day, the bait was replaced with a fresh aggregate (bait).

Figure 4.1: Experiment setup to quantify bacterial spread in soil. An agarose bead prepared with bacterial inoculum and agarose solution was used as a source. It was placed at the bottom of the soil sample. A single 2-4 mm aggregate was used as a bait to quantify successful colonisation of the soil. The bait was placed on the top of the sample.

4.2.4 Detection of bacteria on the baits

The 2-4 mm size aggregate which was kept on top of the soil core as a bait was used to quantify the spread of bacteria in soil. If the aggregates had become colonised it means that bacteria had spread over a distance equal to the thickness of the sample. The aggregates were removed and placed on KB media plates for detection of *Pseudomonas* and LB media plates for *Bacillus*. The plates were incubated at 28°C for 48hrs. After 48hrs the plates were checked for the presence of bacteria around the baits (Figure 4.2) which was taken as evidence that the bacteria had spread the distance.

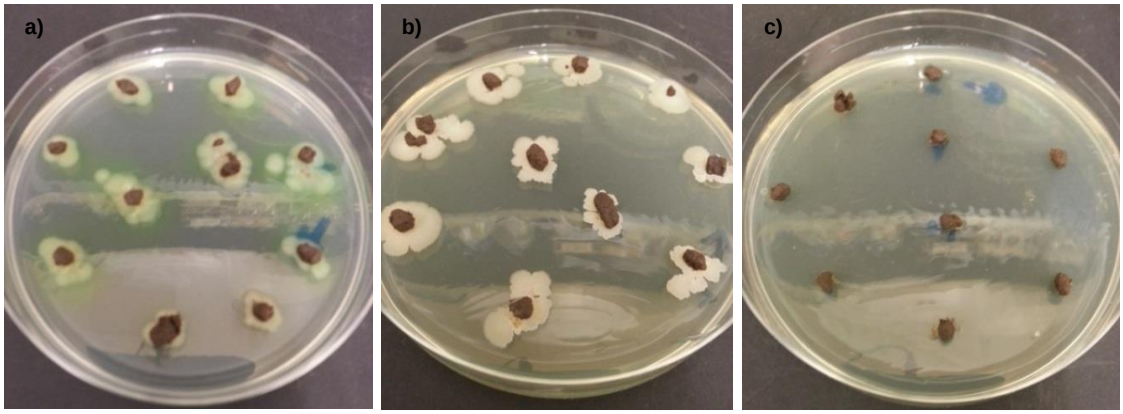

Figure 4.2: Examples of baits plated on selective media. Colonised baits showed growth of *Pseudomonas* (a) and *Bacillus* (b) on media plates after 48 hr of incubation at 28ºC. Baits from control samples showed no colonisation (c) of bacteria.

4.2.5 Analyses

Sigmoidal curves were fitted to the experimental data and used to characterise the spread of bacteria through soil similar to Otten et al. (2001), in order to study the effect of soil physical properties on the spread of bacteria through soil. Sigmoidal curves with 4 parameters were fitted to the experimental data collected for each treatment using Sigmaplot 11th Edition software. The sigmoid equation is

$$y = y_o + \frac{a}{1+ e^{-\left(\frac{x-x_0}{b}\right)}} \qquad \text{Equation 4.1}$$

Where, a is the maximum fraction of replicates with successful colonisation in all replicates (1.0) – measure of colonisation efficiency and hence successful spread through the microcosm, x_0 is the point of inflection (when the fraction of replicates with positive colonisation (and thus indicates spread through the microcosm) equals 0.5) and b is the steepness of curve and reflects the variation in the rate of spread.

For example, if spread occurs as a homogeneous sphere from the source of inoculation, then a steep colonisation front can be expected. If the spread is more heterogeneous, with areas within a colony of more rapid spread than

other areas, then a smoother progression towards the asymptote would be expected. During the fitting procedure the lower asymptote y_0 was fixed at 0 leaving 3 parameters to be estimated with the upper asymptote constrained to ≤1. For experiments 1-3 (details in section 4.2.2) the equation determines the number of days with successful spread in soil with different treatments. For experiment 4 the equation determines the distance covered by *Pseudomonas* cells overtime with successful spread in soil. The above means that the rate and efficiency of spread can be characterised by a small set of parameters and effects of soil treatments can be compared.

4.3 Results

For all treatments described below, the fraction of replicates with successful spread was plotted against sampling days. The parameters of the sigmoidal curves fitted are shown in Tables 4.6 - 4.8 for different experiments.

4.3.1 Influence of soil moisture content on spread of *Pseudomonas* and *Bacillus* in soil

Within 12 days, both bacteria species had spread at least 1.5 cm showing that bacteria spread substantial distances through soil even in the absence of flow. Increasing moisture content influenced the spread of both *Pseudomonas* and *Bacillus* bacteria in soil (Figure 4.3; Table 4.6). The value of the inflection point ($X_{0,}$ equivalent to days at which the fraction of replicates with positive spread equals to 0.5) was used to compare the effect of different treatments on the extent of spread of bacteria in soil. This is hereafter referred to as colonization day. The spread of bacteria was faster in wetter soil (moisture content with 60

% water filled pores) compared to drier soil (moisture content with 40 % water filled pores). In samples inoculated with *Bacillus*, colonization day (X_o) was 6.94 (s.e 0.18) for soil with 40 % water filled pores and 1.62 (s.e 0.09) for soil with 60 % water filled pores space. The colonization day (X_o) of *Pseudomonas* inoculated samples was 9.37 (s.e 0.20) in soil with 40 % moisture content and 3.00 (s.e 0.03) in soil with 60 % moisture content. From the steepness parameter it is evident that the number of replicates with successful colonization increased rapidly in soil with 60 % water filled pores [0.15 (s.e 0.07) for *Bacillus*; 0.25 (s.e 0.11) for *Pseudomonas*] compare to soil with 40 % water filled pores [0.60 (s.e 0.16) for *Bacillus*; 0.45 (s.e 0.15) for *Pseudomonas*] (Figure 4.3). Comparing the speed of spread between *Pseudomonas* and *Bacillus* strain for the given soil type, *Bacillus* moved faster than *Pseudomonas* in both treatments. For example, the colonization day was 1.62 (s.e 0.09) for *Bacillus* 3.00 (s.e 0.03) for *Pseudomonas* in soil with 60 % water filled pores space (Table 4.6). In both treatments no colonization was observed in any of the replicates of control samples.

Table 4.6: Estimated parameters of a sigmoidal curve fitted to data describing the relationship between the fraction of replicates with successful spread and sampling days for *Pseudomonas* and *Bacillus* inoculated in soil with 40 % or 60 % water filled pores space and packed to bulk-density of 1.3 g cm^{-3}.

Strains	Water filled pores	r^2	Parameter a	Parameter b	Parameter X_0
Bacillus	40%	0.988	1.0	0.60	6.94
	60%	0.991	1.0	0.15	1.62
Pseudomonas	40%	0.978	1.0	0.45	9.37
	60%	0.996	1.0	0.25	3.00

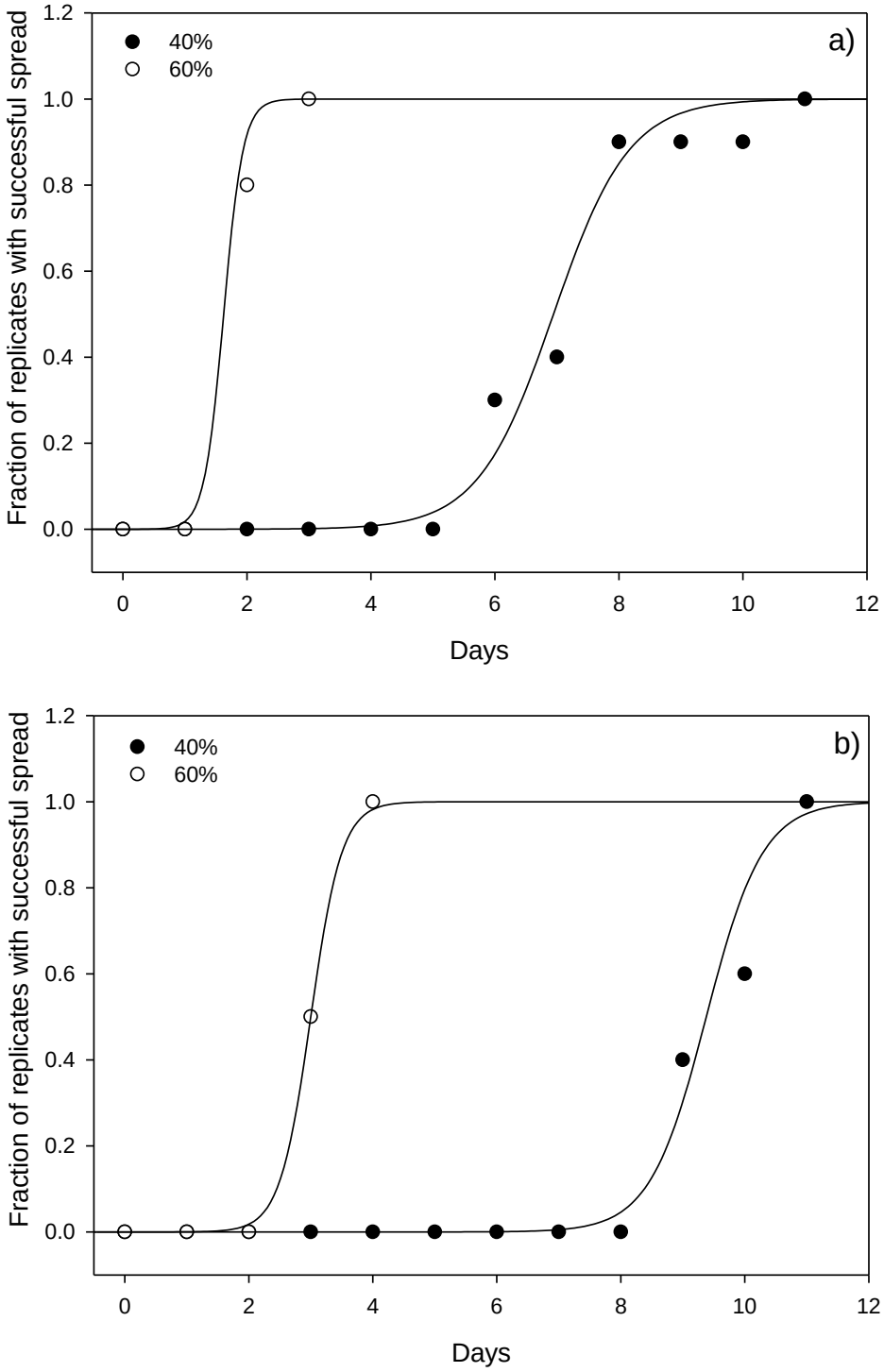

Figure 4.3: Number of positive replicates with successful spread of a distance of 1.5 cm through soil with 40 % (●) and 60 % (○) water filled pores packed at 1.3 g cm^{-3} for *Bacillus* (a) and *Pseudomonas* (b). The lines are sigmoidal curves. For both treatments successful colonisation was quantified as the number of successful colonisations of a bait placed at a distance from a source of inoculum.

4.3.2 Influence of bulk-density on spread of *Pseudomonas* and *Bacillus* in soil

In all replicates, all baits eventually became colonised irrespective of the bulk-density. However, the time it took for replicates to become colonised was affected by the bulk-density for both bacterial strains. Increasing bulk-density decreased the rate of spread of *Pseudomonas* and *Bacillus* in soil (Figure 4.4; Table 4.7). In *Bacillus* inoculated samples, the colonization day (X_o) was 1.62 for soil packed at lower bulk-density and 8.70 for soil packed at higher bulk-density. The colonization day (X_o) of *Pseudomonas* inoculated samples was 3.00 in soil packed at lower bulk-density, compare to soil packed at higher bulk-density where it was 9.22. The number of replicates with successful colonization declined with increasing bulk-density, as evident from the difference in the steepness parameter. The number of replicates with successful colonization at higher bulk-density was 0.33 (s.e 0.01) for *Bacillus* and 0.50 (s.e 0.27) for *Pseudomonas* inoculated samples. Whereas, at lower bulk-density the number of replicates with successful colonization was 1.62 for *Bacillus* and 0.25 (s.e 0.11) for *Pseudomonas* inoculated samples (Table 4.7). In both bulk-density treatments, the spread of *Bacillus* was slightly faster than *Pseudomonas* bacteria (Figure 4.4). In both treatments no colonization was observed in any of the replicates of control samples.

Table 4.7: Estimated parameters of a sigmoidal curve fitted to the data describing the relationship between the fraction of replicates with successful spread and sampling days for *Pseudomonas* and *Bacillus* inoculated in soil with 60 % water filled pores packed to bulk-densities 1.3 and 1.5 g cm^{-3}.

Strains	Bulk-density (g cm^{-3})	r^2	Parameter a	Parameter b	Parameter X_0
Bacillus	1.3	0.991	1.0	0.15	1.62
	1.5	0.999	1.0	0.33	8.70
Pseudomonas	1.3	0.999	1.0	0.25	3.0
	1.5	0.9436	1.0	0.50	9.22

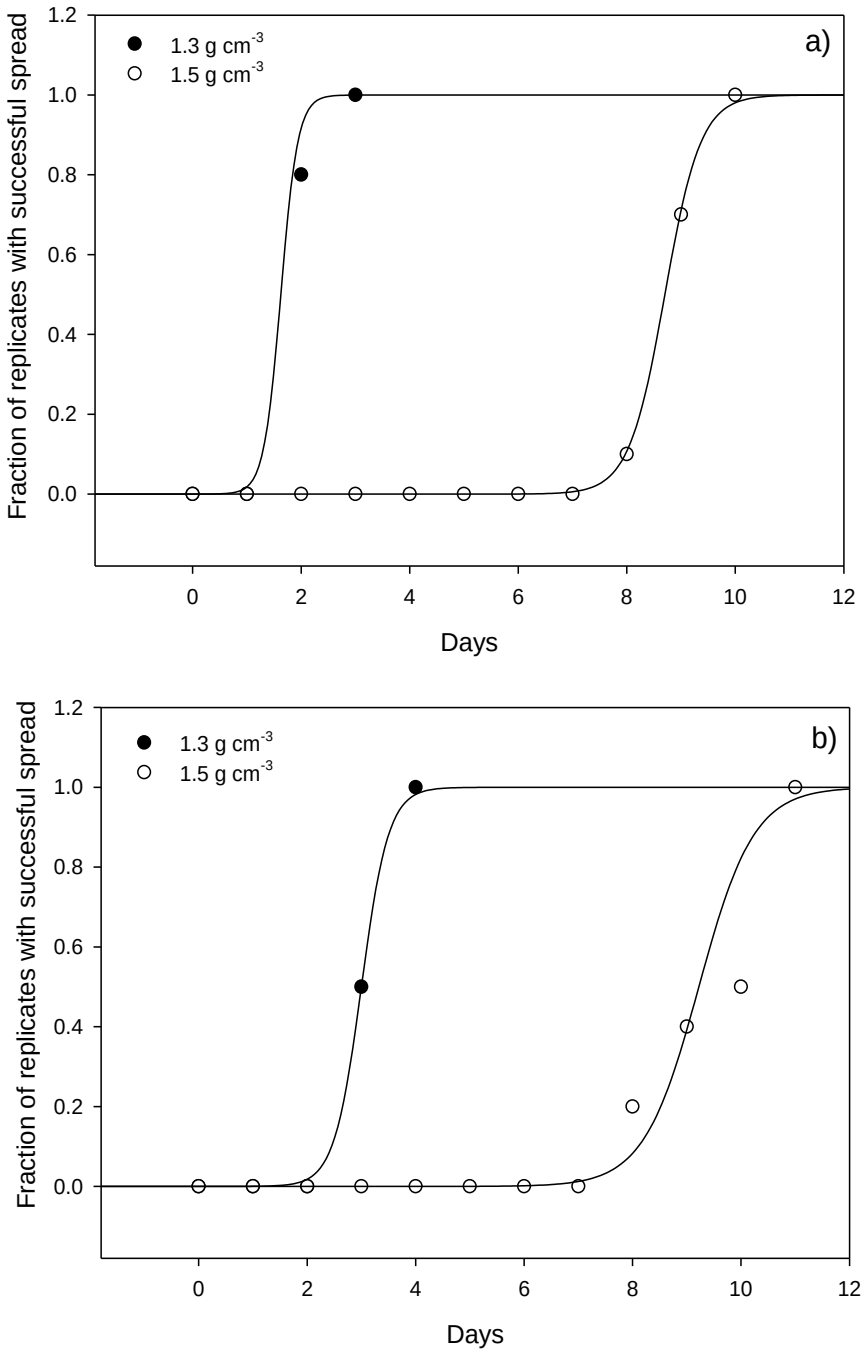

Figure 4.4: Figure 4.4: Number of positive replicates with successful spread of a distance of 1.5 cm through soil with 60% water filled pores wetness packed at 1.3 g cm^{-3} (●) and 1.5 g cm^{-3} (○) for *Bacillus* (a) and *Pseudomonas* (b). The lines are sigmoidal curves. For both treatments successful colonisation was quantified as the number of successful colonisations of a bait placed at a distance from a source of inoculum.

4.3.3 Influence of aggregate size on spread of *Pseudomonas* and *Bacillus* in soil

Irrespective of the aggregate size, all replicates became colonised within 5 days showing rapid spread for all treatments. There was however an effect of aggregate size with a different response to aggregate size for the two bacterial strains (Figure 4.5; Table 4.8). In samples inoculated with *Bacillus*, colonization day was 2.00 days for soil with 0.5-1 mm, 2.55 (se 0.32) days for soil with 1-2 mm and 2.50 (se 0.45) days for soil with 2-4 mm aggregate sizes. The colonization day of *Pseudomonas* inoculated samples was 2.83 (se 0.14) days for soil with 0.5-1 mm, 2.55 days for soil with 1-2 mm and 2.62 (se 0.52) days for soil with 2-4 mm aggregate sizes (Table 4.8). The spread of *Pseudomonas* and *Bacillus* was faster in soil with 1-2 mm compared to 0.5-1 mm aggregate-sizes. The colonization day of *Bacillus* was shorter than *Pseudomonas* in soil with different aggregate size treatment (Figure 4.5). In both treatments no colonization was observed in any of the replicates of control samples.

Table 4.8: Estimated parameters of a sigmoidal curve fitted to the data describing the relationship between the fraction of replicates with successful spread and sampling days for *Pseudomonas* and *Bacillus* inoculated in soil with aggregate sizes 0.5-1 mm; 1-2 mm and 2-4 mm with packed to bulk-density1.3 g cm^{-3}.

Strains	Aggregate size (mm)	r^2	Parameter a	Parameter b	Parameter X_0
Bacillus	0.5-1	0.999	1..0	0.25	2.00
	1-2	0.991	1.0	0.15	1.62
	2-4	0.999	1.0	0.12	2.50
Pseudomonas	0.5-1	0.996	1.0	0.23	2.83
	1-2	0.998	1.0	0.13	2.55
	2-4	0.992	1.0	0.15	2.62

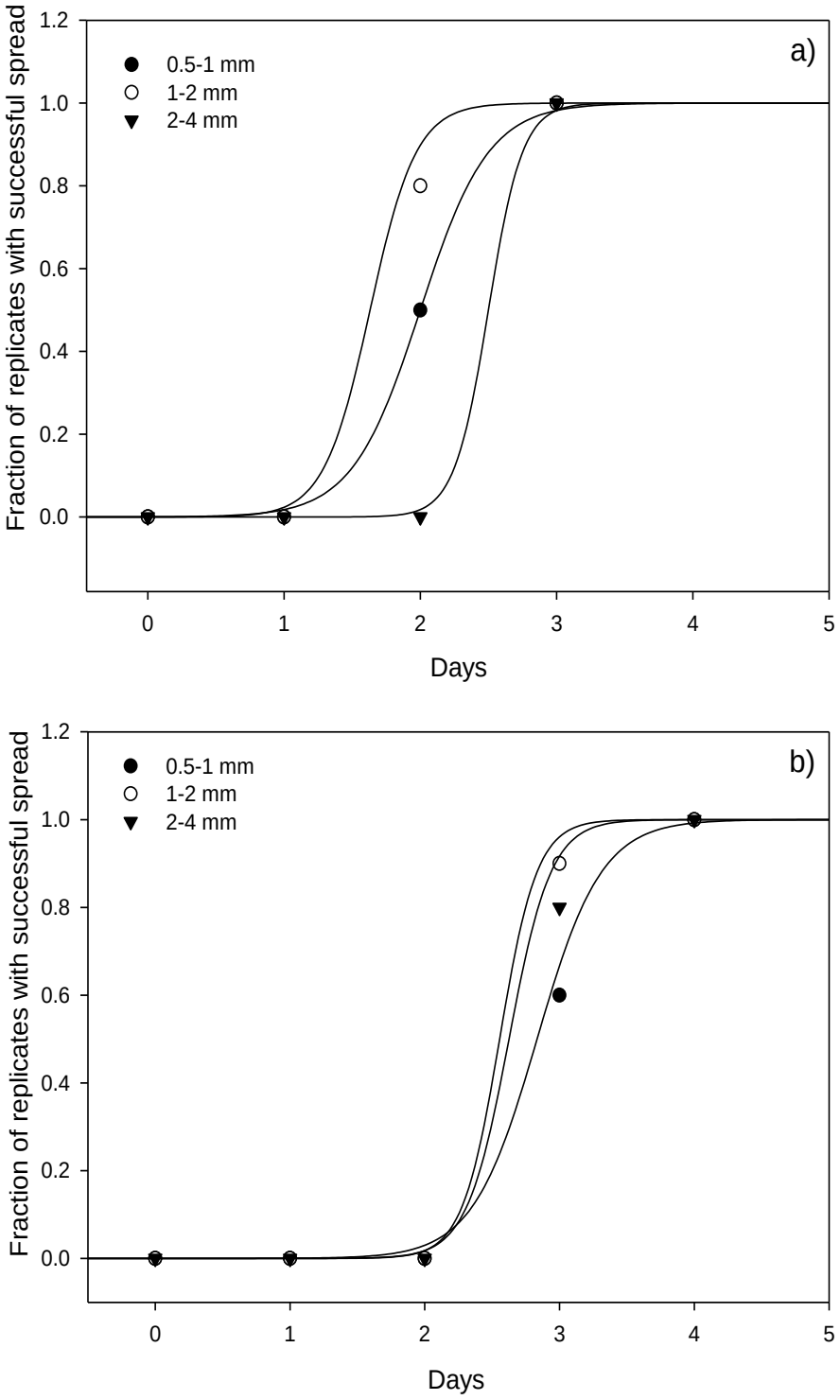

Figure 4.5: Number of positive replicates with successful spread of a distance of 1.5 cm through soil packed at 1.3 g cm^{-3} with aggregate sizes 0.5-1 (●);1-2 (○);2-4 (▼) mm and 60 % water filled pores for *Bacillus* (a) and *Pseudomonas* (b) inoculated treatment. The lines are sigmoidal curves. For both treatments successful colonisation was quantified as the number of successful colonisations of a bait placed at a distance from a source of inoculum.

4.3.4 Influence of distance on spread of *Pseudomonas* in soil

For all distances tested <3 cm, all samples were colonised by day 11. However, none of the samples at greater distances showed any signs of colonisation. For each day the probability of successful colonisation of the target in relation to the distance followed a sigmoidal decline. The value of the inflection point ($X_{0,}$ equivalent to distance at which the fraction of replicates with positive spread equals to 0.5) was used to compare the rate of colonisation at different distances. This is hereafter referred to as colonization distance. Figure 4.6 shows the fraction of replicates with successful spread through soil samples of varying thickness at different samplings days. Spread rate of *Pseudomonas* decreased with increasing thickness of soil samples (Figure 4.6; Table 4.8). As the thickness of samples increased, it took more days for *Pseudomonas* to colonize the bait from the inoculation point (table 4.8). For example, the colonization distance of *Pseudomonas* covered by day 3 was 1.75 cm (se 164.4) and by day 11 was 2.75 cm (se 0.08). In samples with a thickness 3.0 cm and 4.0 cm no colonization of *Pseudomonas* was observed till sampling day 15 (data not shown). The steepness parameter showed that the fraction of replicates with successful spread declined with increasing thickness of samples

Table 4.9: Estimated parameters of a sigmoidal curve fitted to the data describing the relationship between the fraction of replicates with successful spread and thickness of samples for *Pseudomonas* inoculated in soil with 60 % water filled pores packed at bulk-density1.3 g cm^{-3}.

Sampling days	r^2	Parameter a	Parameter b	Parameter X_0
3	0.999	0.3	-0.06	1.75
5	0.993	1.0	-0.10	2.14
7	0.999	1.0	-0.12	2.50
9	0.993	1.0	-0.08	2.68
11	0.999	1.0	-0.06	2.75

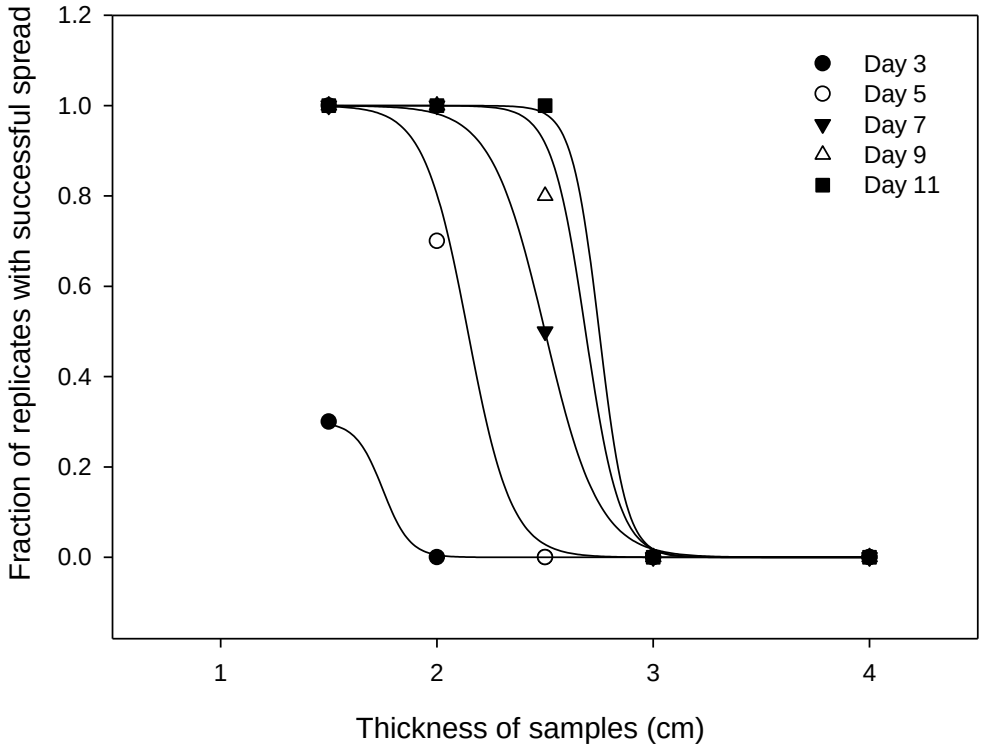

Figure 4.6: Fraction of *Pseudomonas* positive replicates with successful spread through soil in relation to the distance for soil packed at 1.3 g cm^{-3} after 3 (●), 5(○), 7(▼), 9 (Δ) 11(■).The lines are sigmoidal curves. Successful colonisation was quantified as the number of successful colonisations of a bait placed at specified distances from a source of inoculum.

4.4 Discussion

In this chapter, the influence of soil structure on transport of bacteria was studied in repacked soil microcosms. The effect of different soil factors like moisture content, bulk-density and aggregate sizes on bacterial transport was investigated.

In this study the experimental set up was adapted from Otten et al. (2001) and had several advantages for examining the spread of bacteria under different soil conditions. Firstly, use of liquid inoculum (bacterial cell suspension) would have resulted in bacteria moving through the interface between the walls of the column and the soil. This was eliminated by introducing bacteria in the form of a point source inoculum. Secondly, natural soil macropores, formed by burrowing organisms and plant roots through which bacteria would have moved easily, were eliminated by using sieved soil. Lastly, the effect of biological factors like predation or parasitism, which is found in undisturbed soil columns, was eliminated by using autoclaved soil.

The effect of soil moisture content showed a positive effect on the spread of bacteria through soil columns. The spread of *Pseudomonas* and *Bacillus* was faster in higher moisture content soil. This could be due to presence of more water filled pores which facilitates passive and/or active motility of bacteria as they are dependent on water for functioning in soil (Wolf et al., 2013). This results are in agreement with the previous studies that reported that vertical movement of genetically modified *Pseudomonas fluorescens* strains was higher in wetter soil compare to dry soil (van Elsas et al., 1991).

The effect of increasing bulk-density on the movement of bacteria in soil was studied by some researchers (Huysman & Verstraete, 1993; van Elsas et al., 1991; Singh et al., 2002; Trevors et al., 1990). In most of these studies the soil bulk-density ranged between 1.0 -1.3 g cm^{-3}. In this study therefore bulk-density 1.3 and 1.5 g cm^{-3} was taken to investigate spread of bacteria in two very different range of bulk-density. From chapter 3, it was evident that porosity and connectivity of pores is significantly reduced with increasing bulk-density. This suggests that movement of bacteria is reduced due to alteration in the pore geometry of soil.

The results of different aggregate sizes treatment showed no effect on spread of *Pseudomonas* and *Bacillus* in soil. A study by Tan et al. (1991) contradicts the finding of this experiment. In the results reported by that study, movement of bacteria was more in 0.5-1.0 mm aggregate size compared to fine fraction 0-0.5 mm. The reason for the delay in movement of bacteria in fine soil could be due to adsorption or adhesion of bacteria onto the surface of aggregates. Since the 0.5-1 mm aggregate size soil had more surface area this would have led to adsorption of bacteria onto soil surfaces (Tan et al., 1991).

In all the above three treatments between the two bacterial strains, spread of *Bacillus* was faster than *Pseudomonas* in soil. The plausible explanation for this could be difference in size and shape of microorganisms. In a study by Gannon et al. (1991) effect of cell size was observed between 10 different bacterial strains in soil. Bacteria cells of size less than 1 µm showed higher percentage of transport in soil. Also, in my preliminary experiments of growth study rate of

both strains in pure medium showed higher growth rate of *Bacillus* cells was faster than *Pseudomonas* cells bacteria (see section 2.2).

The movement of *Pseudomonas* bacteria was studied in soil packed in different size rings ranged from 1.5 - 4.0 cm height in order to study the transport of bacteria in soil. The hypothesis that movement of bacteria will be slower with increasing distance was supported by *Pseudomonas* movement results. No positive sign of bacterial movement in microcosms of height 3.0 and 4.0 cm was observed. This can be either due to starvation and death of bacteria or due to drying up of soil microcosms. Another reason could be the adsorption of *Pseudomonas* cells on the soil surfaces or the organic matter present in soil. Previous investigations on transport of introduced strains in soil have revealed the effect of organic matter or organic-clay complexes (Guimaraes et al., 1997). Also, since no water was added to the soil column in addition the *Pseudomonas* cells might have mostly desorbed in water and moved. Hence, further work is required to optimize the experimental setup to prevent drying up of soil microcosms and using other types of bacteria as the time taken to reach a particular site can differ between different strains.

4.5 Conclusion

Spread of introduced bacteria in soil was influenced by the soil bulk-density and moisture content of soil. Spread of bacteria was observed to be faster in wetter soil with lower bulk-densities. These findings can be translated into practical applications by managing and possibly altering the soil properties of the target soil (bulk-density and wetness) so that they are favourable for spread of introduced bacteria for bioremediation purposes. One limitation of the findings is how generalizable the results to undisturbed soils which reflect the natural conditions and this needs to further investigated. However, there is no reason why additional heterogeneity cannot be introduced into these microcosm systems (e.g. Otten and Gilligan, 2006), or indeed be conducted with natural undisturbed sample, although these treatments would be expected to substantially enhance variability between replicated samples.

5 Combining techniques to visualise bacteria in relation to their micro-habitat

5.1 Introduction

The capability of soil bacteria to execute a wide range of activities, like promoting plant growth and degrading pollutants have drawn researcher's interest in studying the patterns of bacterial activity and distribution in soil (Dechesne et al., 2005). Soil is heterogeneous at a phenomenal range of spatial scales, and microbes live in small microhabitats where the physical, biological and chemical properties differ in time and space over distances from nanometres to kilometres (Dechesne et al., 2007). Bacteria are located in their habitat as small colonies and biofilms that tend to aggregate to form microbial hotspots. Hotspots are zones in which the biological activity is much faster and intensive compared to average soil conditions (Kuzyakov & Blagodatskaya, 2015). There is, however, little known on what controls the spatial distribution of bacteria in soil. Studying the spatial patterns at microscale could help to determine the factors controlling microbial community and activity. Subsequently this data and knowledge of factors could help in the development of predictive models to further the understanding of bacterial contributions to soil functions. Over the years the spatial distribution of indigenous and introduced bacteria has been studied in undistributed or repacked soil columns (Nunan et al., 2001; Kizungu et al., 2001; Nunan et al., 2003; Dechesne et al., 2003; Pallud et al., 2004; Dechesne et al., 2005). White et al. (1994), introduced pre stained (calcofluor white M2R) *Pseudomonas fluorescens* in soil at specific matric potentials to study their spatial distribution. *P. fluorescens* cells were observed in different pore size classes depending on the matric potential used (White et al., 1994). A review by Li et al. (2004) describes the different type of fluorescent stains that have been used in soil thin sections. The review explains

how different solutions in the impregnation process can have an effect on the external stain used and how the use of general staining makes it difficult to distinguish between bacterial cells and other stained particles with same size distribution (Li et al., 2004). Fluorescent *in situ* hybridisation (FISH) is another alternative to general stains. FISH technique uses 16S rRNA targeted oligonucleotide probes that are labelled with fluorescent dye to detect microbes in soil. Eickhorst et al. (2008) have applied FISH method to undisturbed polished soil sections. Green fluorescent protein (GFP) is another marker which has been used to visualise distribution of bacterial cells in the rhizosphere and on the root surfaces (Jansson et al., 2000; Cao et al., 2011). The major advantages of using this method are it is stable in presence of proteases; does not require any substrates and it can withstand the paraformaldehyde treatment (Errampalli et al., 1999; Zhang & Xing, 2010).

Nunan et al. (2001) developed an image processing and analysis procedure to quantify the number and location of indigenous bacteria by using composite images of soil thin sections. They also applied a combination of image analysis and geostatistical tools to investigate the distribution of bacteria in relation to pores. They observed a difference in the spatial distribution of bacteria in relation to pores at different depths in soil, with bacteria in colonising patches close to pores in subsoil but randomly distributed in the topsoil (Nunan et al., 2003). This technique however was limited to two dimensions, which does not, therefore, provide information of the 3D-physical habitat in which microorganisms operate. Another limitation of this technique was the fluorochromes stain used to visualise bacteria in soil thin sections. With this stain it was not possible to distinguish between different types of bacterial cells

and archaeal cells in soil. To overcome the 2D limitation, a micro-sampling method was developed by Grundmann et al. (2001). They analysed the spatial distribution of nitrifiers (NH_4^+ and NO_2^- oxidizers) at submillimetre scale in undisturbed soil samples. A large number of defined volumes of soil microsamples were randomly sampled and the presence or absence of nitrifiers in each microsample was tested. This experimental data was compared with the theoretical spatial distribution data. The number of theoretical distributions investigated was limited owing to the time requirement to run the simulation (Dechesne et al., 2003). Therefore, Dechense et al. (2003) developed the method by combining a microsampling method with a statistical analysis. The microsampling strategy consisted of simultaneous testing of several different unit volumes for the presence or absence of the targeted microorganisms and the statistical analysis is based on the comparison of experimental sampling data with data from the limited sampling of numerous theoretical spatial distributions. They analysed spatial patterns of NH_4^+ oxidisers and 2, 4-D degraders in repacked soil columns (Dechesne et al., 2003). The analysis showed that the spatial distribution of NH_4^+ oxidisers was significantly ($P \leq 0.025$) different from 2,4-D degraders. In all the studies above, the relationship between the bacterial spatial distribution and 3D soil structure was not considered. Spatial isolation, offered by the complexity of soil air-solid interface, is believed to be one of the factors accounting for the diverse microbial communities in soil. The pore space of soil, which is one of the most important characteristics of soil structure, creates environmental niches for micro-organisms (Crawford and Young, 2004). The properties of pore networks such as the volume available, shape, connectivity of the pore volume, size

distribution of pores, and the tortuosity of pathways within this volume are crucial factors. Such properties of pore networks have a major impact on microbial composition and activity in soil as it regulates the accessibility of organic matter, the diffusion of oxygen through the gaseous phase and the diffusion of dissolved compounds through the water phase, as well as movement of microorganisms in soil. These aforementioned pore characteristics can be measured experimentally or via non-destructive imaging.

Advancements in the application of X-ray micro-tomography has made it possible to visualise and quantify the internal structure of soil in three dimensions at µm resolution without destroying the sample (details in section 1.3). Some recent studies (Kravchenko et al., 2013; Juarez et al., 2013; Wang et al., 2013; Kravchenko et al., 2014; Negassa et al., 2015) have combined X-ray tomography with other analytical methods to investigate the influence of pore structure on distribution (Kravchenko et al., 2013; Wang et al., 2013) composition (Ruamps et al., 2011; Kravchenko et al., 2014) and activity (Ruamps et al., 2013; Juarez et al., 2013) of bacterial communities in soil. For example, Kravchenko et al. (2013) studied the spatial distribution of *E.coli* in intact soil aggregates obtained from soils under different management regimes, and showed that the distribution of *E.coli* in soil was influenced by the intra-aggregates pore size. Another study by Negassa et al. (2015) showed how pore characteristics can influence the structure of microbial communities on the decomposing plant residue in soil. They observed that in samples with both large and small pores a number of bacterial groups known as cellulose decomposers were present on the plant residue, whereas oligotrophic Acidobacteria groups were more abundant on plant residue in samples with

small pores. Thus, the recent study shows how the combination of advanced techniques can help in obtaining experimental evidences on relationships between microbes and physical microscale environment.

Therefore, the aim of this chapter is to develop a protocol that links 2D and 3D techniques to quantify the influence of pore structure on the spatial distribution of bacteria in soil. This will be achieved through the following objectives 1) to test if GFP tagged bacteria and microscopy can be used to visualize and quantify bacterial distribution in 2D thin sections of resin impregnated soil; 2) to use X-ray tomography to quantify in 3D the pore geometry of resin impregnated soil microcosms, packed with different aggregate sizes, and 3) to integrate 2D microscopy with 3D X-ray tomography to determine the effect of soil structure on the spatial distribution of bacteria. Specifically I will quantify how the spatial scale at which we quantify bacterial distribution in 2D affects its association with the pore geometry. This has important implications for developing predictive models, for example those considering biophysical processes to drive C dynamics (e.g. Falconer et al., 2015)

5.1.1 Hypotheses

1) GFP-tagged *Pseudomonas* and *Bacillus* can be used to visualize and quantify bacteria in impregnated samples.
2) Cell density of *Pseudomonas* and *Bacillus* observed in biological thin sections of soil increases with time.
3) Pore characteristics are more variable when characterised at smaller spatial scales relevant to bacteria, showing that aggregate sizes may not be relevant.

4) Pore characteristics influence the distribution of *Pseudomonas* and *Bacillus* distribution in soil.

5.2 Materials and Methods

5.2.1 Preparation of soil microcosms

GFP tagged *Pseudomonas fluorescens* SBW25 and *Bacillus subtilis* NRS1473 (for details see chapter 2) were used in this experiment. As described in section 2.2.2, a cell suspension was prepared of each strain. The cell density of *B. subtilis* was 1.5E+07 cells ml^{-1} and of *P. fluorescens* were 3.6E+07 cells ml^{-1}.

In this experiment, 1-2 mm and 2-4 mm aggregate sizes of a sterilised sandy loam soil were used. The moisture content of soil was adjusted by adding 0.12 cm^3 g^{-1} of sterilised dH_20_{MQ} to acquire 40 % water filled pores for soil packed at a bulk-density of 1.3 g cm^{-3}. The amount of soil required to pack in each steel ring (3.40 cm^3) to attain 1.3 g cm^{-3} bulk-density was weighed out (5.09 g). After weighing the soil was inoculated with 500 µl of the bacterial suspension according to the treatments (Table 5.1). The soil was mixed well to ensure the bacterial inoculum is distributed evenly. The soil was poured in small amounts into the ring and compacted at bulk-density 1.3 g cm^{-3}. Control samples were prepared in a similar way except that sterilised dH_20_{MQ} was used instead of bacteria inoculum. Three replicates per treatment were prepared. In total 24 soil microcosms were prepared and sealed in plastic bags to avoid drying of samples. The samples were incubated at 23°C to allow for bacteria to grow and spread through the soil. The soil microcosms were sampled on day 1 and 5 for resin impregnation.

Table 5.1: A list of treatments used in this chapter where microcosms were packed with aggregates of different size fraction and inoculated without or with a bacterial strain.

Aggregate size (mm)	Bacterial strain
1-2	*P. fluorescens*
1-2	*B. subtilis*
2-4	*P. fluorescens*
1-2	dH_20
2-4	dH_20

5.2.2 Resin impregnation of soil microcosms

For resin impregnation soil microcosms were placed in an upright position onto a wooden plank with holes that are slightly larger than the diameter of rings. Three layers of cotton bandage mesh were laid on the wooden plank to prevent loss of soil during the embedding processes and the soil microcosms were pushed into these holes. The wooden plank was then placed on top of the aluminium gauze stand (Figure 5.1) in a plastic container to enable the various stages required for resin impregnation as described below.

Figure 5.1: Set-up of soil microcosms for resin impregnation. The soil microcosms are kept on top of the cotton mesh layer to prevent loss of soil during exchange of solutions in the impregnation process.

5.2.2.1 Fixation

To preserve the distribution of bacteria within the soil matrix, the samples were fixed using a 2 % formaldehyde (37 % stock solution, Sigma Aldrich) solution (v/v in H_20), the solution was poured down the sides of the container to avoid disturbance of samples and allow exchange of liquids from the bottom to the top. All the samples were completely submerged in the solution and kept overnight for fixation at 4°C. The next day samples were removed from the solution and subsequently transferred to another container. The samples were washed with MQ distilled water by adding it from the side of the container and kept submerged for two hours. Afterwards, water was removed.

5.2.2.2 Dehydration

After washing, the samples were dehydrated with a graded series of acetone (VMR) to remove water from samples, which would otherwise have interfered with the polymerization of resin. Samples were submerged overnight in 50 % (v/v) acetone- water solution at room temperature. The next day a graded series of acetone (70 %, 90 % and 100 % [v/v]) was used for dehydration. Each dehydration step lasted for 2 hours after which the solution was replaced and directly followed by the next acetone concentration. As a last step, the samples were dehydrated three times with 100 % acetone. During the last two 100 % acetone dehydration steps samples were kept under low pressure vacuum (280 mbar) to facilitate dehydration of the pores. Samples were then kept in 100 % acetone solution until resin impregnation.

5.2.2.3 Impregnation

Polyester resin (Oldopol P50-01, Büfa, Germany) was used for impregnation. Two litre volume of impregnation mixture was prepared by mixing 1400 ml of polyester resin with 600 ml of acetone as a thinner. 1300 µl of 1 % Co-accelerator (Oldopal, Büfa, Germany; 0.95 ‰ [v/v] related to resin) and 2600 µl of CHP Catalyst (cyclohexanonperoxide, Akzo Nobel, Germany, 1.9 ‰ [v/v] related to resin) were added to the resin one after the other. The concentration of catalyst and accelerator was set according to the curing time required for a particular resin (Eickhorst and Tippkötter 2008). The resin mixture was kept under low pressure (230-240 mbar) vacuum to remove gas bubbles before adding it onto the samples. The acetone was removed from the container with samples which were then placed into a desiccator. The resin mixture was then added drop-wise from the top of the desiccators into the container to allow the resin to enter the sample from the bottom in order to ensure that the pores of the soil were filled with resin mixture as completely as possible. This step lasted for approximately 30-40 min. Once the resin reached the top surface of samples a controlled low pressure vacuum was applied to ensure most of the pores were filled with resin. Finally the remaining mixture was added to cover the sample completely with resin. Samples were left at room temperature for polymerization of the resin (Figure 5.2).

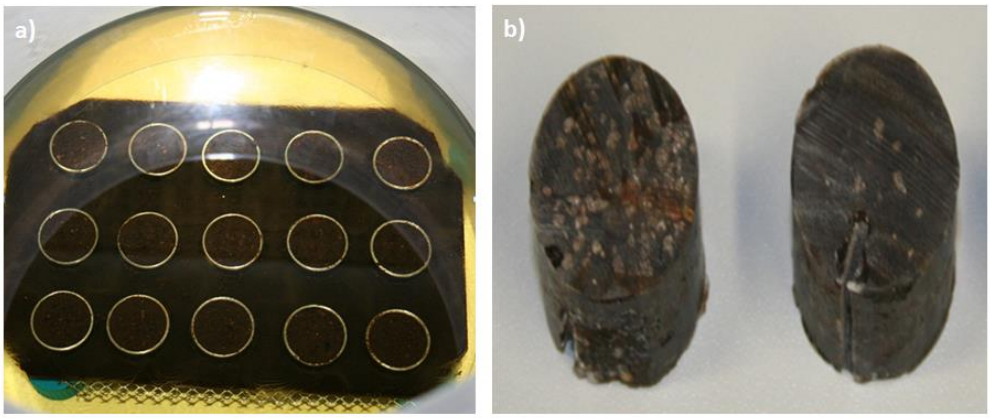

Figure 5.2: Impregnation of soil microcosms with soil samples immersed in resin solution (a), and soil samples after resin polymerization (b).

5.2.2.4 Polymerization

The samples were kept under a fume hood to allow acetone and styrene to evaporate from the samples. After a few days a small steel wire was used to check whether polymerization has begun from the bottom of the sample container. Complete polymerization of samples took 7 weeks. After polymerization, the steel rings were removed from the impregnated samples and excess resin was cut from top and the bottom (Figure 5.2b). Impregnated blocks were then scanned using X-ray tomography.

5.2.3 X-ray CT of resin impregnated samples.

The samples were scanned using a Metris X–Tek HMX CT scanner (details in section 2.5). Samples were scanned at 13.4 µm resolution under energy settings 145 keV and 35 µA and 2000 angular projections. To minimize beam hardening a molybdenum target with a 0.25 mm aluminium filter was used. CT Pro v2.1 software (NIKON metrology, Tring, UK) was used to reconstruct the radiographs into a three dimensional volume. VG Studiomax version 2.2

(Volume graphics, Heidelberg, Germany) software was used to adjust the contrast of reconstructed volumes, which were then exported as image stacks (*bmp format) for further processing.

5.2.4 Preparation of impregnated blocks for cell counting

Bacterial cells were enumerated at three different depths for each impregnated blocks (Figure 5.3). The height of each block was measured using a micrometre (accuracy 2 µm). Then the height for each layer in which bacteria will be quantified was estimated by considering the height 2.5 mm above and below from the centre of the sample. Impregnated blocks were first cut with a diamond saw and then ground down to the estimated height using a grinding machine (MPS 2 120, G & N, Nurnberg, Germany). Paraffin was used as a coolant in the grinding machine. The surface was then hand polished using a grinding paper (silicon carbide, size P1200) to remove the grinding material and make the surface smooth. The blocks were then cleaned with a benzene solution.

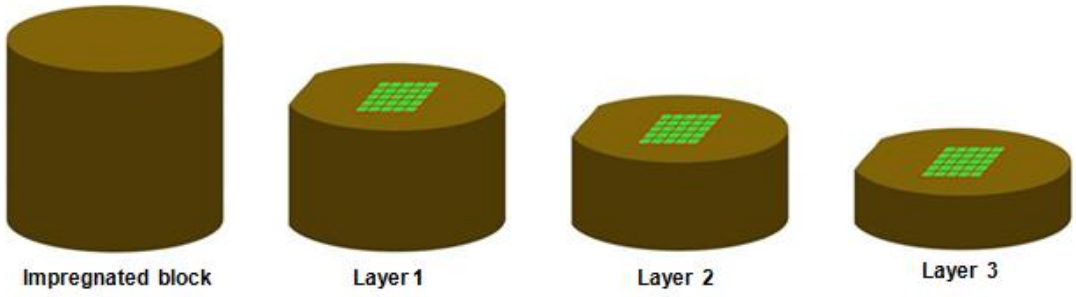

Figure 5.3: Schematic representation of the area quantified for counting bacteria at different layers in a soil sample. The distance between each layer was 2.5 mm. Green frames in the diagram represent the counting area (e.g. 5.2 x 5.2 mm).

5.2.5 Enumeration of bacteria on impregnated blocks

To enumerate bacteria, a drop of approximately 1.5 µg mL^{-1} of Vectashield containing DAPI stain (Vector Laboratories, Burlingame, CA, USA) was applied on top of the polished surface of the block and covered with a cover slip of size 24 × 32 mm (Menzel Glaser, Germany). Bacterial cells were evaluated using a ZEISS Axioscop 2 fluorescence microscope (Carl Zeiss, Jena, Germany) equipped with an HBO 103 W/2 Hg vapour lamp (Osram, Munich, Germany), under 63X objective lens (Plan-Neoflaur, Carl Zeiss, Jena, Germany). GFP signals were detected with double excitation filter (Filter set 24, Carl Zeiss) and total cells were enumerated using a DAPI filter set (F46-000, AHF, Tübingen, Germany). The cells were counted using an ocular with an integrated counting grid (10 × 10, 1.25 mm^2 Carl Zeiss, Germany). The location of starting point for counting in each analysed layer was chosen randomly on the top edge of sample. An area of size 5.2 × 5.2 mm (red frame in Figure 5.4) was selected to counts cells in each layer. In this area, 6 x 6 fields of view (counting spot) were evaluated for cell counting (small green frames in Figure 5.4). The distance between each field of view was set to 1 mm using the xy coordinates on the scale of microscope stage (Figure 5.4). Cell counts were extrapolated to cell density i.e. cell counts/area of field of view.

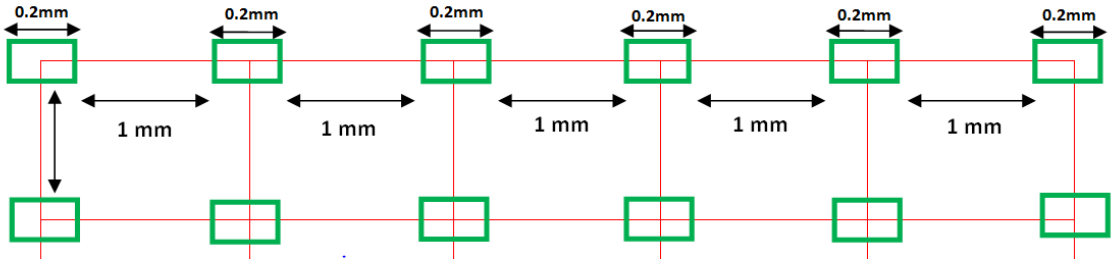

Figure 5.4: Diagrammatic representation of spots where bacteria were counted in the given area of interest (red frame) under microscope. The green frame in the diagram represents each counting spot of size 0.2 x 0.2 mm. The distance between each spot was set to 1 mm.

5.2.6 Alignment of each analysed layer and image processing

A stereomicroscopic image of each layer in which bacteria were counted was taken to help to find the same layer from the stack of CT scanned images. The selection of each layer from the CT image stacks was done by eye matching with the stereomicroscopic image (Figure 5.5). The selected image was then imported in ImageJ to crop the region of interest (area where bacteria was counted). The cropped region of interest was then thresholded using indicator kriging segmentation method (Houston et al., 2013).

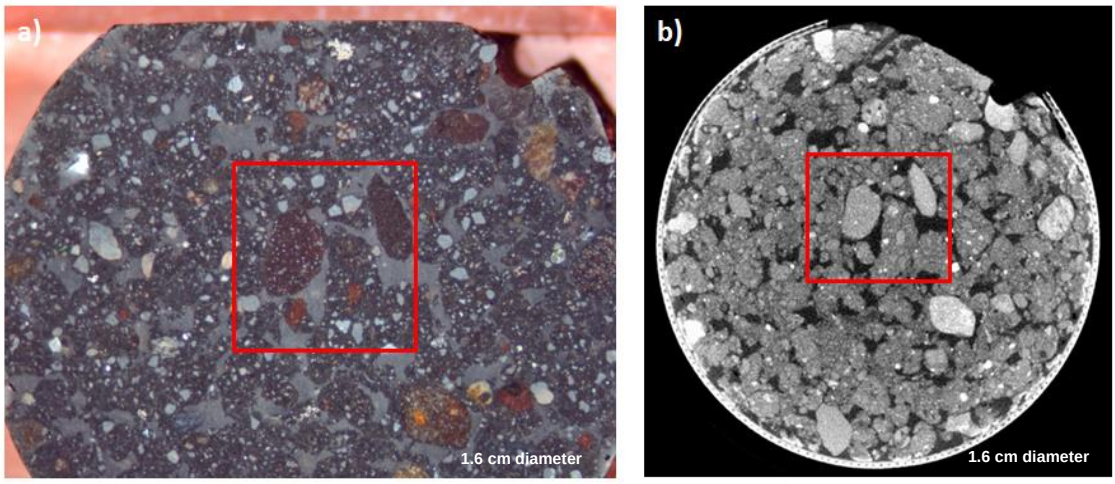

Figure 5.5: Alignment of stereomicroscope image (a) with CT scanned image (b). Red frame represents the area of interest where bacteria were counted.

The pore structure was analysed at two scales: the larger scale representing the region of interest of size 5.2 x 5.2 mm and the smaller scale representing each field of view of size 0.2 x 0.2 mm. For this experiment, the large scale was termed as macroscale and the smaller scale was termed as microscale. In each scale, the pore structure was measured in 2D and 3D.

For the 3D analysis, information pertaining to the third dimension was considered by including information above and below the place a larger area to get broader analysis of relationship between pores and bacteria. For this, the neighbouring 36 slices, above and below the plane, were used to determine the measure of pore structure in 3D. The size of the area analysed at each scale is described in table 5.2. A macro was recorded in ImageJ v1.47 (hhtp://rsbweb.nih.giv/ij/) to crop images at the different scales. For 2D, each slice was 1 voxel thick. In each volume the pore geometry characteristics were quantified. The quantitative measures included porosity, pore connectivity and soil-pore interface.

Table 5.2: Physical dimensions of the region of interest (ROI) analysed for pore structure at macroscale and microscale in at different in 2D and 3D.

Scales	Dimensions	Physical dimension of ROI (mm)
Macroscale	2D	5.2 ×5.2
	3D	6.2 × 6.2 × 6.2
Microscale	2D	0.2 × 0.2
	3D	1 × 1 × 1

5.2.7 Statistical analysis

Statistical analysis was performed using SPSS software version 21. A mixed effect linear model (assuming normal distribution) was applied to investigate differences in soil structure properties for different treatment. To comply with the normality assumption the porosity and connectivity measures were transformed using the probit function. The soil-pore interface area met the normality assumption and therefore they did not require any preliminary transformation.

A generalised mixed effect Poisson model with log link function was used to investigate significant difference in cell numbers between sampling days with day as fixed factor and across different treatments with treatments and days as fixed factors. The effect of soil structure properties such as porosity, connectivity and surface area, on the distribution of bacteria was also determined by Poisson model with day as a fixed factor. The size of the counting spot was introduced as an offset variable in the Poisson model.

5.3 Results

5.3.1 Visualisation and quantification of bacterial distribution in soil

5.3.1.1 Detection of GFP-tagged and DAPI stained bacteria in impregnated soil.

When impregnated samples are observed under a double excitation filter, the black quartz particles were surrounded by clay particles and organic matter. The pore spaces surrounding the soil aggregates were filled with resin and appeared reddish in colour (Figure 5.6). In inoculated samples, GFP tagged

Pseudomonas and *Bacillus* cells were analysed in each layer but no GFP signals were detected (Figure 5.6). However on checking the counterstain (DAPI) on the same layer under UV excitation filter, both *Pseudomonas* and *Bacillus* cells appeared bright blue from which it was concluded that bacteria were present in impregnated samples. Henceforth, DAPI stain was used to quantify both bacterial cells in impregnated soil blocks.

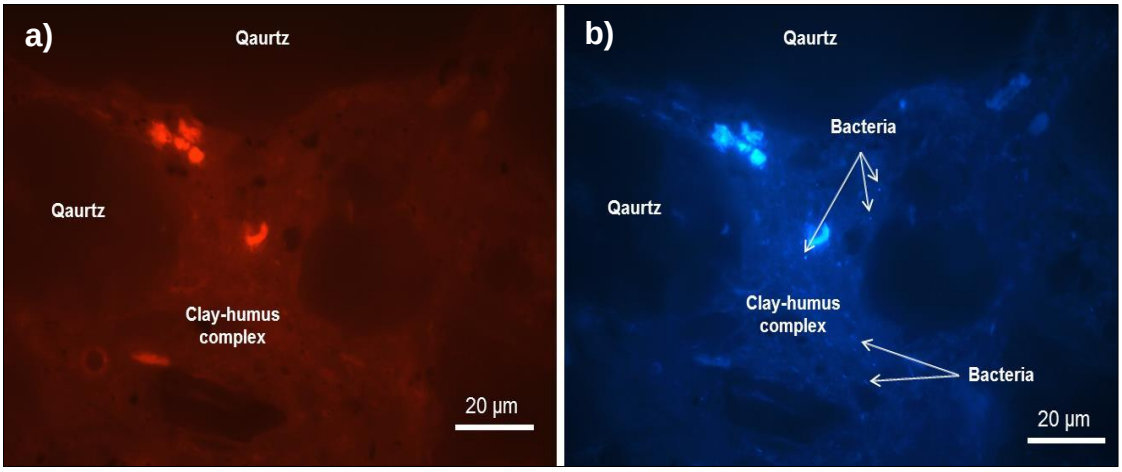

Figure 5.6: Microscopic images of a polished soil section showing that GFP signals of *Pseudomonas* cells were not detectable under double excitation filter (a), but are detectable under a UV excitation filter(b), scale bar: 20 µm

Under UV excitation the soil particles and resin fluoresced blue but both types of bacterial cells were easily distinguishable against the background (Figure 5.7). Both types of bacterial cell appeared on the surface of the clay-humus complex or at soil-pore interfaces. Very few (1-3) cells were observed in a resin filled pore area surrounding the soil particles. No DAPI signals were detected in control samples. Overall the distribution of *Pseudomonas* cells was different from the *Bacillus* cells in soil. DAPI stained *Pseudomonas* cells were observed to be more evenly spread in soil, whereas *Bacillus* cells were observed in small clusters of 8-10 cells throughout the soil (Figure 5.7). In general, the cell

numbers of both bacterial strains differed between different field of view on each analysed layer.

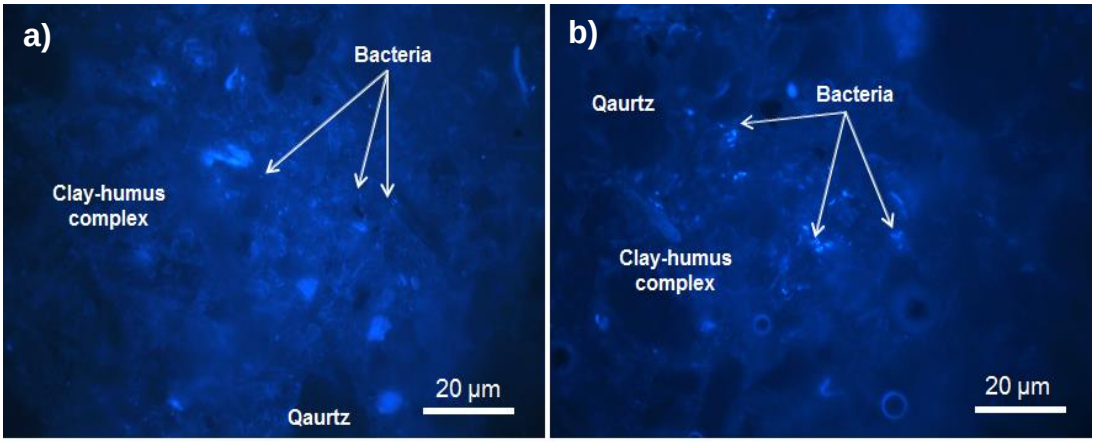

Figure 5.7: DAPI stained inoculated samples in soil polished sections showing the distribution of *Pseudomonas* (a) and *Bacillus* (b) cells, scale bar: 20 µm.

Visual comparison of cell counts in each analysed layer of a treatment was carried out to determine treatment effects (Figure 5.8). In soil with aggregates of a size of 1-2 mm, *Pseudomonas* cell counts ranged from 0 to 30 per field of view on day 1 and 0 to 60 per field of view on day 5. In the case of *Bacillus* inoculated soil with aggregate sizes 1-2 mm, cell counts ranged from 0 to 28 per field of view on day 1 and 0 to 52 per field of view on day 5. For soil with aggregates sized 2-4 mm, *Pseudomonas* cell counts ranged from 0 to 20 per field of view on day 1 and 0 to 35 per field of view on day 5. Therefore, the result showed a variation in the number of cell counts between different treatments.

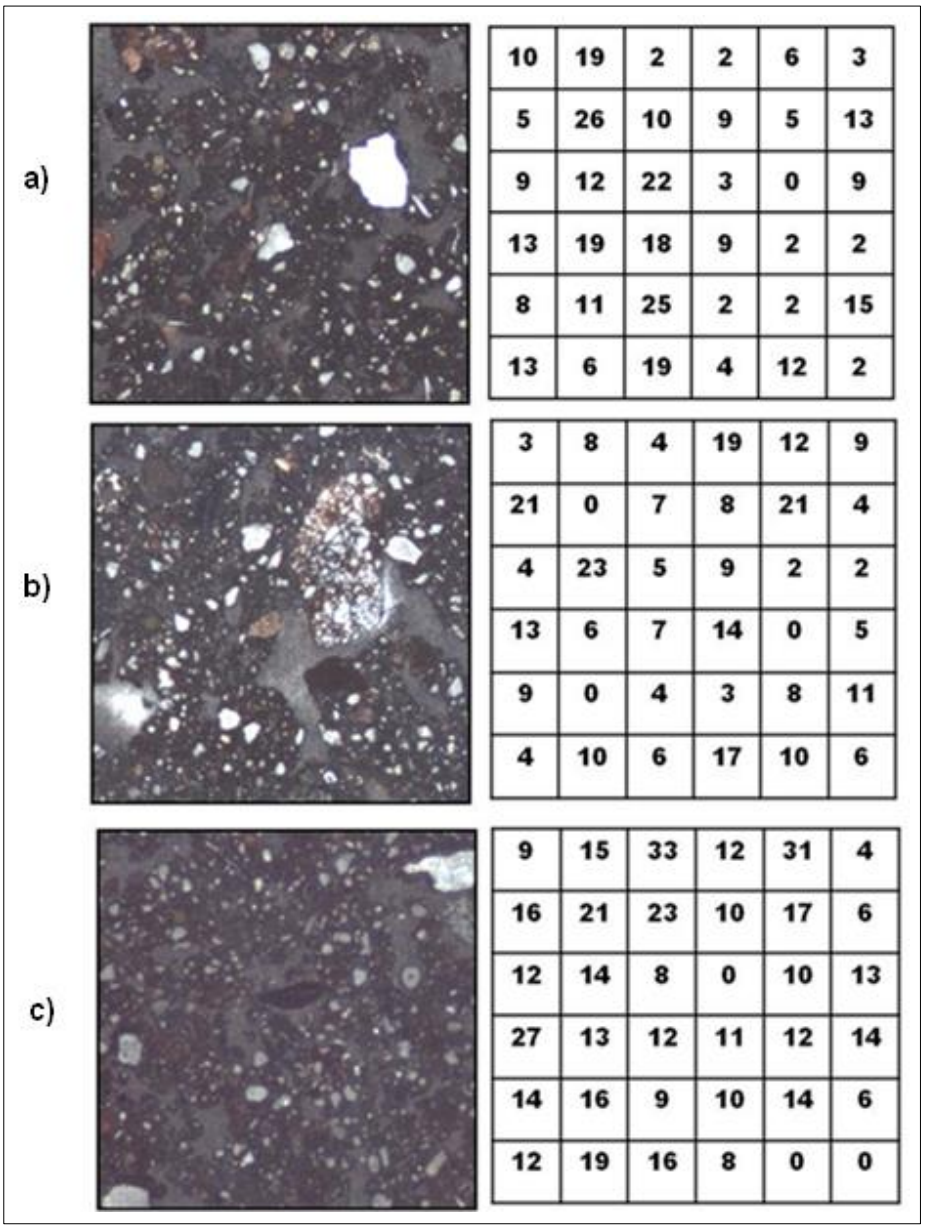

a)

10	19	2	2	6	3
5	26	10	9	5	13
9	12	22	3	0	9
13	19	18	9	2	2
8	11	25	2	2	15
13	6	19	4	12	2

b)

3	8	4	19	12	9
21	0	7	8	21	4
4	23	5	9	2	2
13	6	7	14	0	5
9	0	4	3	8	11
4	10	6	17	10	6

c)

9	15	33	12	31	4
16	21	23	10	17	6
12	14	8	0	10	13
27	13	12	11	12	14
14	16	9	10	14	6
12	19	16	8	0	0

Figure 5.8: Visual comparison of cell counts in each analysed layer in different treatments, with two-dimensional stereomicroscope images (left) and cell counts (right). Treatments are *Pseudomonas* inoculated in 1-2 mm aggregate soil (a), *Bacillus* inoculated in 1-2 mm aggregate soil (b), and *Pseudomonas* inoculated in 2-4 mm aggregate soil (c).

5.3.1.2 Quantification of cell counts in whole microcosm amongst treatments

Mean cell densities (cells mm^{-2}) were calculated on sampling time 1 and 5 for each treatment (Figure 5.9). In *Pseudomonas* inoculated soil with aggregates sized 1-2 mm, no significant difference (p=0.377) in cell density was observed between sampling time, with 252.0 (s.e=10.5) cells mm^{-2} for day 1 and 291.0 (s.e=12.0) cells mm^{-2} for day 5 (Figure 5.8a). Cell density significantly increased (p=0.004) between sampling days in *Bacillus* inoculated soil, with 252.0 (s.e=12.0) cells mm^{-2} counts on day 1 and 308.0 (s.e=13.6) cells mm^{-2} on day 5 (Figure 5.8b). Although the cell density was higher on day 5 than day 1 for *Pseudomonas* inoculated soil with aggregate of size 2-4 mm with 304.0 (s.e=12.7) cells mm^{-2} and 291.0 (s.e=13.2) cells mm^{-2} respectively, the difference was not significant (p=0.757) (Figure 5.9c).

There was no significant difference (p=0.633) between cell densities for *Bacillus* and *Pseudomonas*, with a cell density of 280.0 (s.e=28.2) cells mm^{-2} for *Bacillus* and 271.0 (s.e=19.6) cells mm^{-2} for *Pseudomonas*, (Figure 5.10).

Amongst *Pseudomonas* inoculated in soil with aggregate of sizes 1-2 mm and 2-4 mm, a significant (p= 0.00) difference in the mean cell density was observed, with 271.0 (s.e=19.6) cells mm^{-2} in 1-2 mm and 297.0 (s.e=6.2) cells mm^{-2} in 2-4 mm aggregate soil, (Figure 5.11).

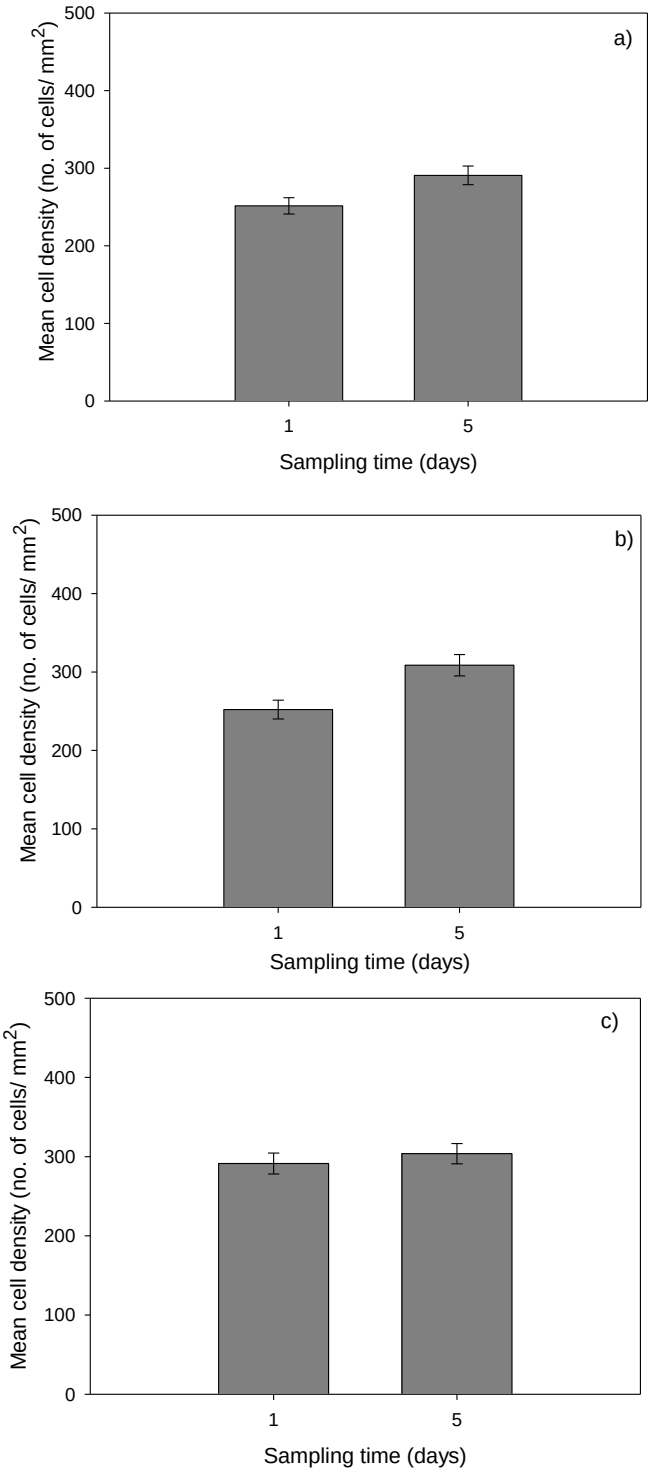

Figure 5.9: Comparison of mean cell density in different treatments between sampling day 1 and 5. Treatments were *Pseudomonas* inoculated soil with aggregate sizes 1-2 mm (a), *Bacillus* inoculated in soil with aggregate sizes 1-2 mm (b) and *Pseudomonas* inoculated in soil with aggregate sizes 2-4 mm (c), Data are means ± SE (n=9).

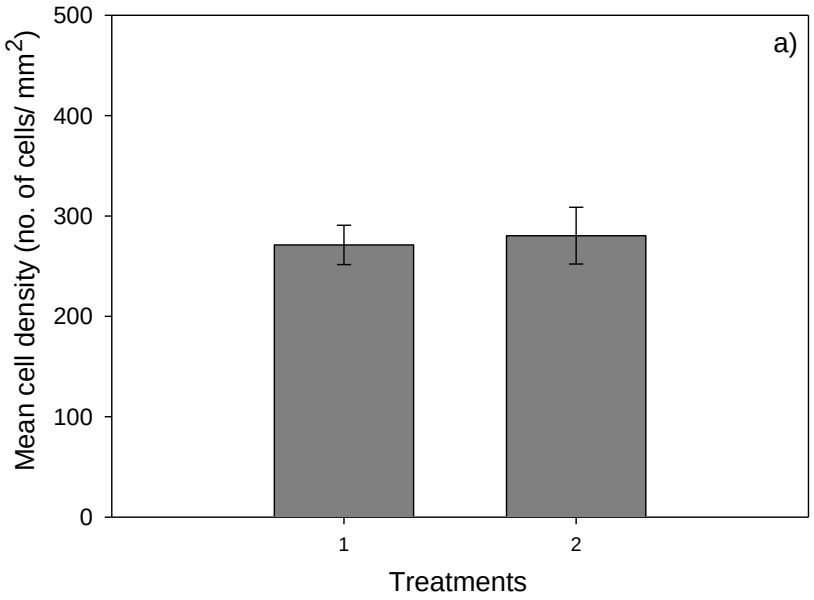

Figure 5.10: Comparison of mean cell density between soils inoculated with different bacterial strain. Treatments were *Pseudomonas* (1) and *Bacillus* (2) inoculated in soil with aggregate sizes 1-2 mm, Data are means ± SE (n=18).

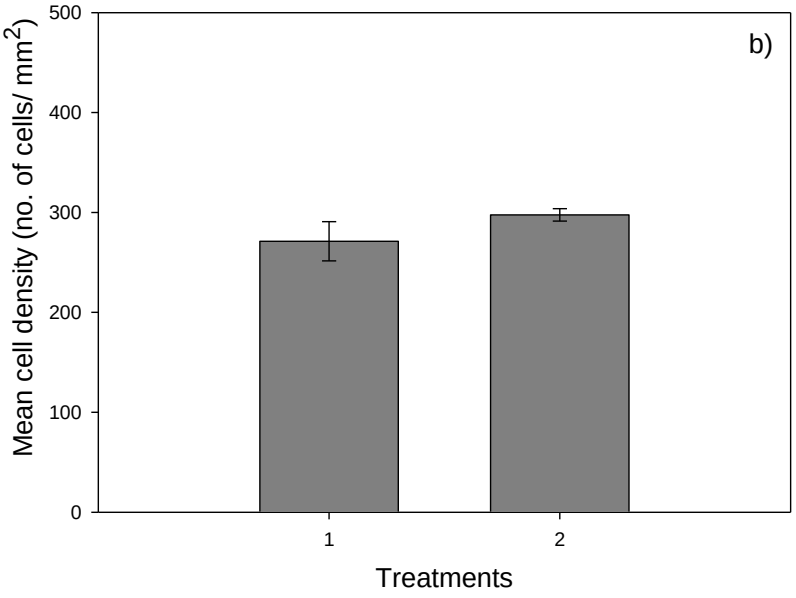

Figure 5.11: Comparison of mean cell density between soils with different size aggregate treatments. Treatments were *Pseudomonas* inoculated in soil with aggregate sizes 1-2 mm (1), and 2-4 mm (2), Data are means ± SE (n=18).

5.3.2 Pore geometry of impregnated soil

Below, the characteristics of the pore geometry are described at 2 spatial scales, the macroscale and the microscale.

5.3.2.1 Macroscale (Image scale/CT scanning scale)

Pore geometry was analysed at macroscale in 2D and 3D. A histogram was plotted to analyse the distribution of porosity, connectivity and soil-pore interface of soil (Figure 5.12-5.13).

In samples analysed at 2D, the porosity of the analysed area ranged from 10-35 % and the soil-pore interface ranged from 2-5 mm^2 for soil with aggregates sized 1-2 mm and 1.5 - 4.5 mm^2 for soil with aggregates sized 2-4 mm (Figure 5.12). Among different aggregate size treatments, soil porosity ($p=0.608$) was not significantly different, with average porosity of 21.6 (s.e=0.86) % in 1-2 mm and 22.7 (s.e=2.04) % in 2-4 mm aggregates sized soil. Also between treatments the average soil-pore interface was not significantly different ($p=0.687$), with 2.77 (s.e=0.05) mm^2 in 1-2 mm and 2.80 (s.e 0.15) mm^2 in 2-4 mm aggregates sized soil.

In samples analysed at the macroscale in 3D, the porosity of the analysed area ranged from 10-40 %, soil connectivity ranged from 88-100 % and the soil-pore interface ranged from 3-4.5 mm^2 for soil with aggregates sized 1-2 mm and 2.5-5.5 mm^2 for soil with aggregates sized 2-4 mm (Figure 5.13). Among different aggregate size treatments, soil porosity ($p=0.412$) was not significantly different, with average porosity of 21.8 (s.e=0.73) % in 1-2 mm and 23.5 (s.e=0.02) % in 2-4 mm aggregates sized soil. Connectivity was also not significantly different

(p=0.604) between treatments, with an average connectivity of 95.8 (s.e=0.45) % in 1-2 mm and 95.1 (s.e=0.01) % in 2-4 mm aggregate sized soil. Also, between different aggregate size treatments the soil-pore interface was not significantly different (p=0.216), with 3.70 (s.e=0.05) mm^2 in 1-2 mm and 3.90 (s.e 0.18) mm^2 in 2-4 mm aggregates sized soil.

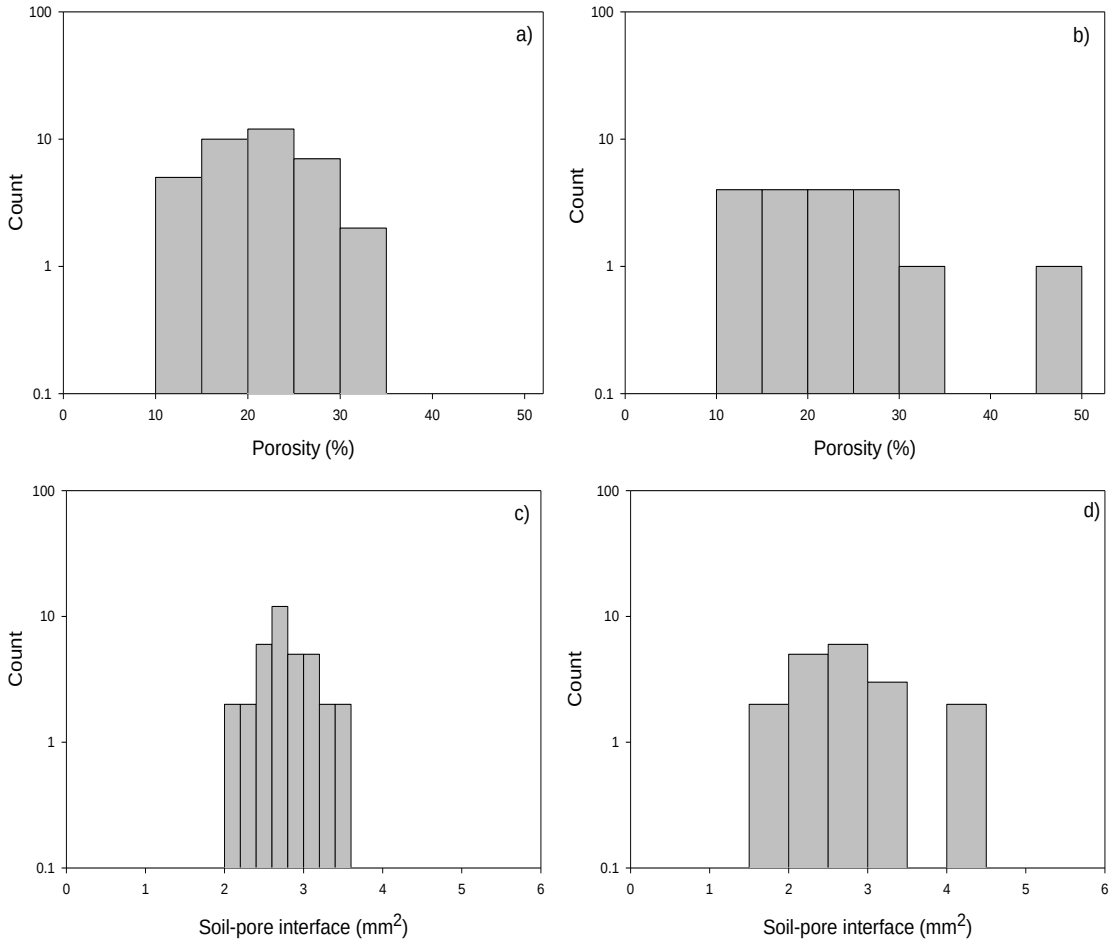

Figure 5.12: Distribution of soil porosity (a, b) and soil-pore interface (c, d) analysed at macroscale in 2D in soil with aggregate sizes 1-2 mm (a, c), and 2-4 mm (b, d) treatment.

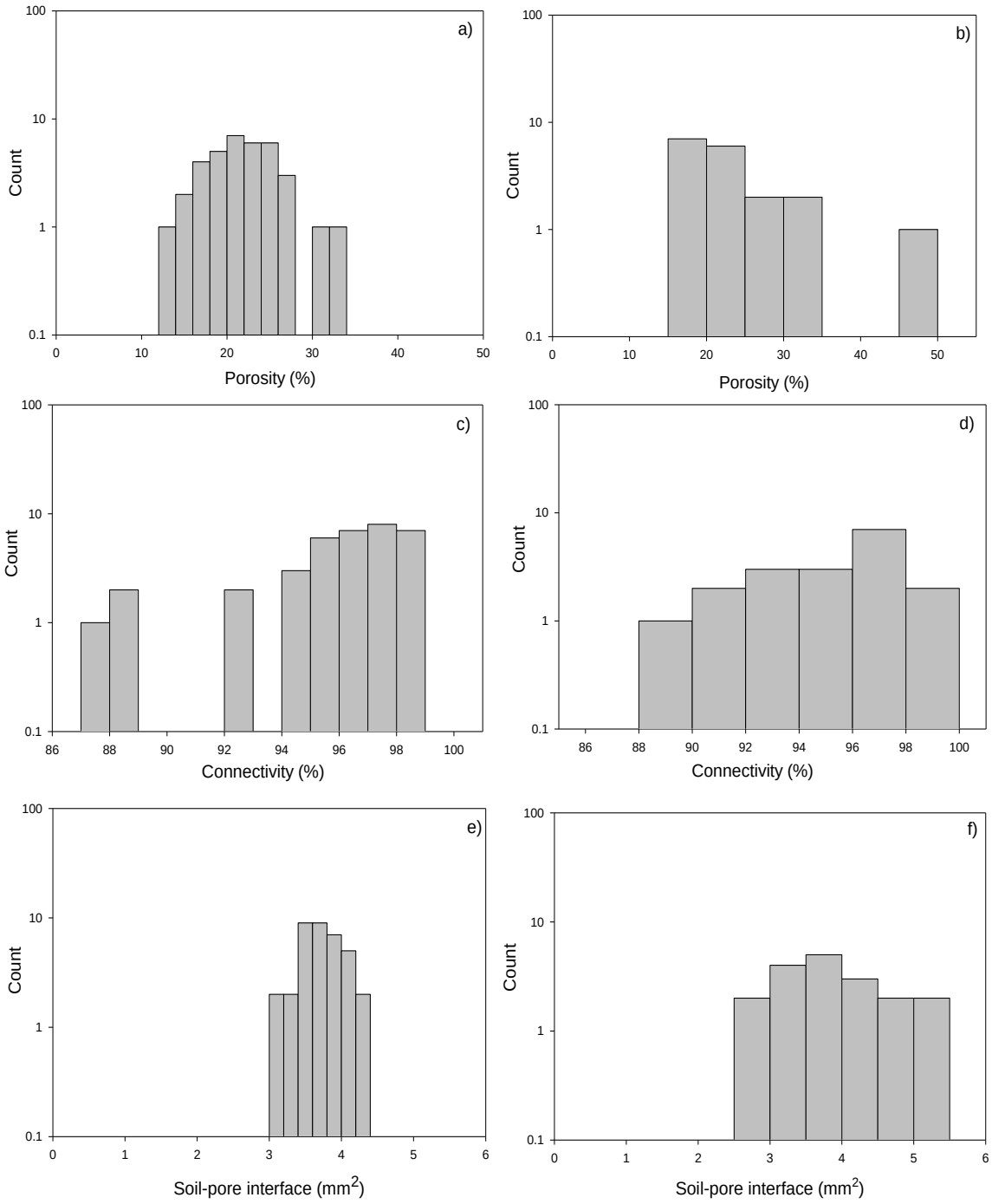

Figure 5.13: Distribution of soil porosity (a, b), connectivity (c, d) and soil-pore interface (e, f) analysed at macroscale in 3D in soil with aggregate sizes 1-2 mm (a, c, e), and 2-4 mm (b, d, f) treatment.

5.3.2.2 Microscale

Pore geometry was analysed at macroscale in 2D and 3D. A histogram was plotted to analyse the distribution of porosity, connectivity and soil-pore interface of soil (Figure 5.14-5.15). There is a substantial difference for all characteristics between the macroscale (Figure 5.12-5.13) and the microscale (Figure 5.14-5.15). In particular, the value range is much broader at the microscale, reflecting greater heterogeneity between replicated fields of view.

In samples analysed in 2D, the porosity of the analysed area ranged from 0-100 % and the soil-pore interface ranged from 0-15 mm^2 in both 1-2 mm and 2-4 mm aggregate sized soil (Figure 5.14). Among different aggregate size treatments, soil porosity ($p=0.750$) was not significantly different, with average porosity of 20.8 (s.e=0.88) % in 1-2 mm and 21.6 (s.e=1.32) % in 2-4 mm aggregates sized soil. Also, the average soil-pore interface between treatments was not significant ($p=0.763$), with 2.79 (s.e=0.10) mm^2 in 1-2 mm and 2.80 (s.e=0.15) mm^2 in 2-4 mm aggregates sized soil.

In samples analysed at microscale in 3D, the porosity of the analysed area ranged from 0-90 %, soil connectivity ranged from 0-100 % and the soil-pore interface ranged from 0-10 mm^2 for soil with aggregates sized 1-2 mm and 0-11 mm^2 for soil with aggregates sized 2-4 mm (Figure 5.15). Among different aggregate size treatments, soil porosity ($p=0.387$) was not significantly different, with average porosity of 21.8 (s.e=0.73) % in 1-2 mm and 23.5 (s.e=0.02) % in 2-4 mm aggregates sized soil. Connectivity of pores between treatments was not significant ($p=0.114$) between treatments, with average connectivity of 95.8 (s.e=0.45) % in 1-2 mm and 95.1 (s.e=0.01) % in 2-4 mm aggregates sized soil.

The difference in soil-pore interface was also not significant (p=0.433), with average soil-pore interface of 2.79 (s.e=0.10) mm^2 in 1-2 mm and 2.87 (s.e=0.16) mm^2 in 2-4 mm aggregates sized soil.

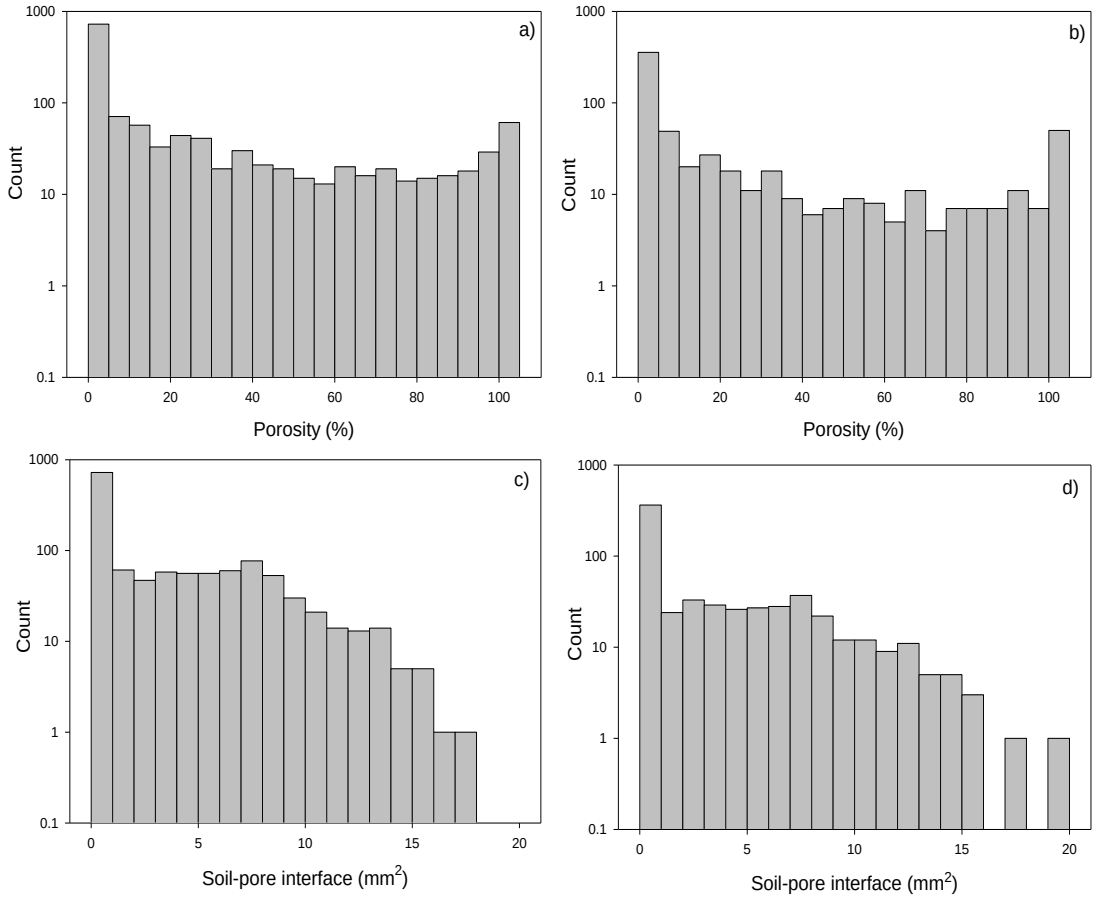

Figure 5.14: Distribution of soil porosity (a, b) and soil-pore interface (c, d) analysed at microscale in 2D in soil with aggregate sizes 1-2 mm (a, c), and 2-4 mm (b, d) treatment.

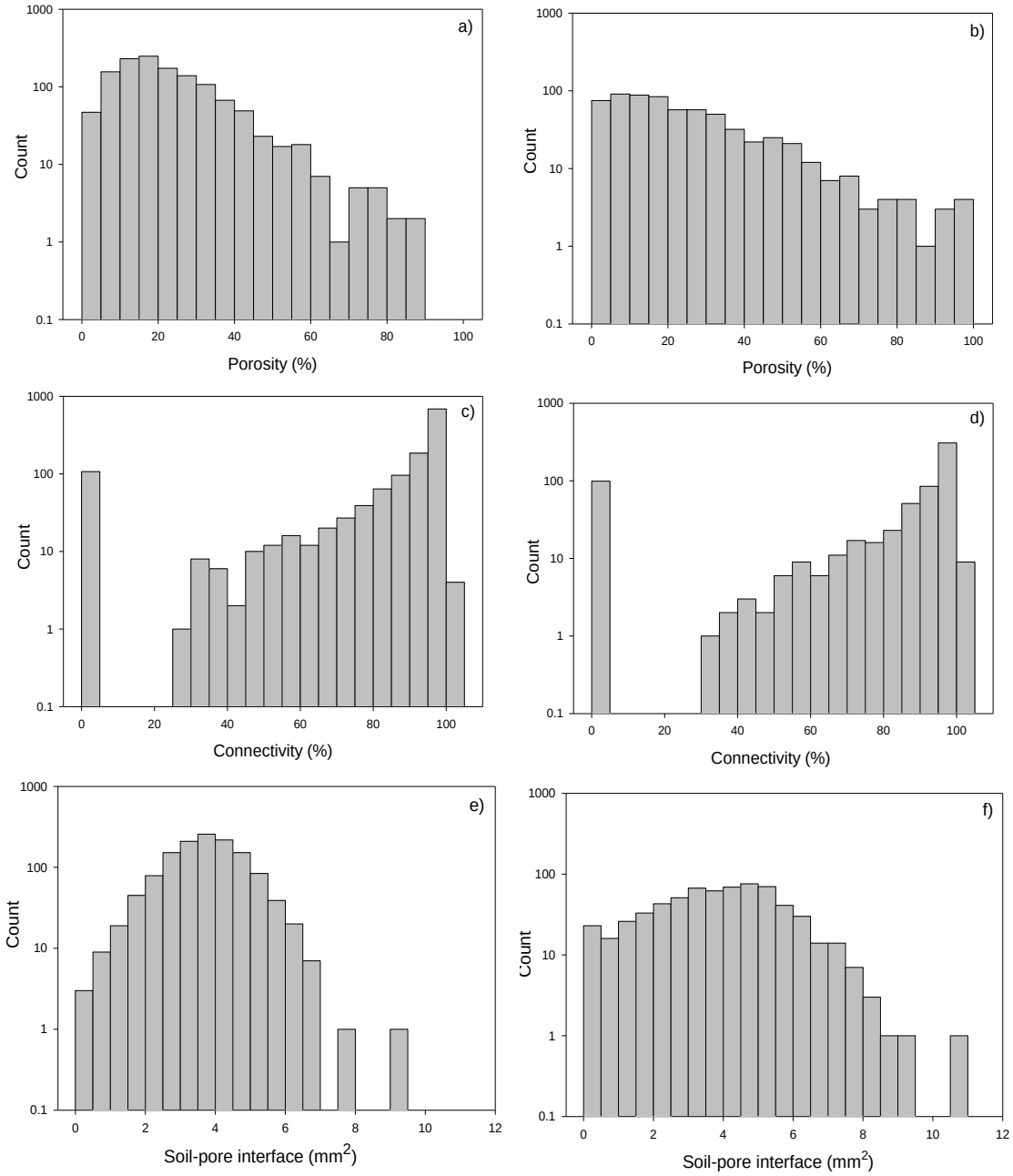

Figure 5.15: Distribution of soil porosity (a, b), connectivity (c, d) and soil-pore interface (e, f) analysed at microscale in 3D in soil with aggregate sizes 1-2 mm (a, c, e), and 2-4 mm (b, d, f) treatment.

5.3.3 Influence of soil pore geometry on bacteria distribution

5.3.3.1 Macroscale

Mean cell densities (no. of cells mm^{-2}) of Pseudomonas and Bacillus in different treatments were plotted against soil porosity, connectivity and soil-pore interface analysed in 2D and 3D (Figure 5.16- 5.21). Mean cell density here refers to the average of cell counts over 36 counting spots in each analysed layer. In samples analysed at 2D, the porosity of the analysed area ranged from 10-46 % with the majority having porosity between 15-25 % (Figure 5.16a-5.18a). The soil-pore interface ranged from 2-5 mm^2 with the majority of the analysed area having a soil-pore interface between 2-3 mm^2 (Figure 5.16-5.18b). The mean cell density ranged between 200-700 cell mm^{-2} (Figure 5.16-5.18). Soil porosity and soil-pore interface significantly ($P<0.05$) related to the distribution of *Pseudomonas* and *Bacillus* in soil with different treatments. The p-value of each treatment is listed in table 5.3.

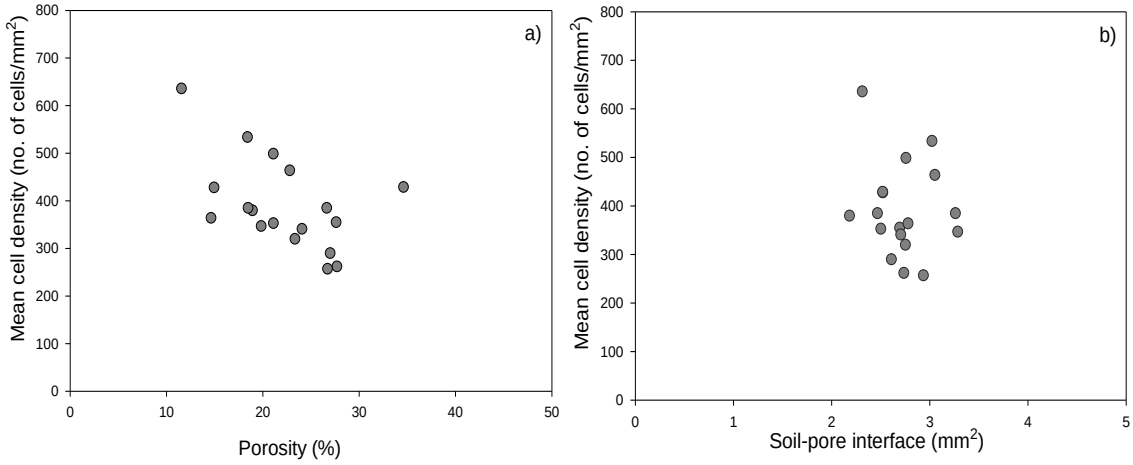

Figure 5.16: Relationship between mean *Pseudomonas* cell density and soil porosity (a) and soil-pore interface (b) analysed at macroscale in 2D in soil with aggregate of sizes 1-2 mm. Data points in the graph represents individual analysed layer of each replicate per treatment.

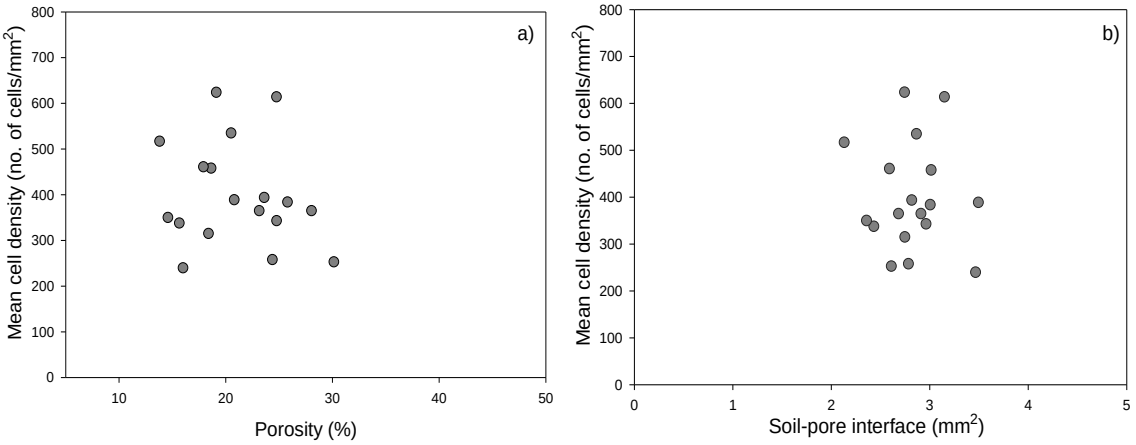

Figure 5.17: Relationship between mean *Bacillus* cell density and soil porosity (a) and soil-pore interface (b) analysed at macroscale in 2D in soil with aggregate of sizes 1-2 mm. Data points in the graph represents individual analysed layer of each replicate per treatment.

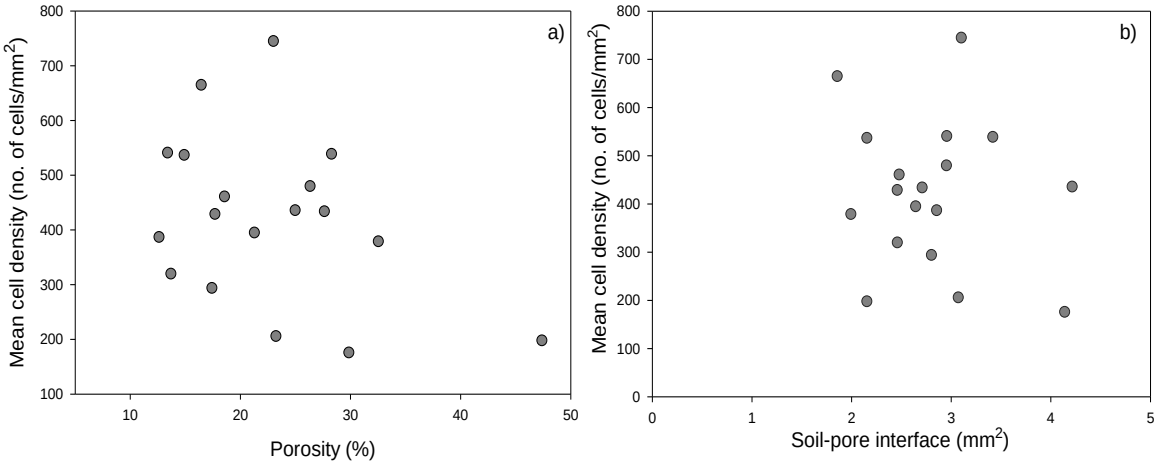

Figure 5.18: Relationship between mean *Pseudomonas* cell density and soil porosity (a) and soil-pore interface (b) analysed at macroscale in 2D in soil with aggregate of sizes 2-4 mm. Data points in the graph represents individual analysed layer of each replicate per treatment.

Table 5.3: Results of the Poisson model analysis on influence of pore structure on distribution of bacteria in different soil at macroscale in 2D and 3D. Numbers reported in the table are the p-values of the analysis.

Scales	Treatments	Porosity (%)	Soil-pore interface (mm^2)	Connectivity (%)
Macroscale 2D	*Pseudomonas* inoculated in soil with aggregate sizes 1-2 mm	0.000	0.001	-
	Bacillus inoculated in soil with aggregate sizes 1-2 mm	0.001	0.007	-
	Pseudomonas inoculated in soil with aggregate sizes 2.4 mm	0.000	0.000	-
Macroscale 3D	*Pseudomonas* inoculated in 1-2 mm aggregate soil	0.000	0.004	0.000
	Bacillus inoculated in 1-2 mm aggregate soil	0.370	0.182	0.707
	Pseudomonas inoculated in 2-4 mm aggregate soil	0.000	0.000	0.000

In samples analysed at macroscale in 3D, the porosity of the analysed area ranged from 10-46 % with majority having porosity between 15-25 %, (Figure 5.19a-5.21a). Connectivity of pores ranged between 95-100 % with the majority having connectivity of between 98-100 % (Figure 5.19b-5.21b). The soil-pore interface ranged from 2.5-6 mm^2 with the majority of the analysed area having a soil-pore interface between 3-4 mm^2 (Figure 5.19c-5.21c). The mean cell density ranged between 200-700 cell mm^{-2} (Figure 5.19-5.21). The influence of soil porosity, connectivity and soil-pore interface on distribution of *Pseudomonas* and *Bacillus* cells varied between treatments (table 5.3). In *Pseudomonas* inoculated soil with aggregates of size 1-2 mm, the distribution of

Pseudomonas cells was significantly influenced by porosity (p=0.000), connectivity (p=0.000) and soil-pore interface (p=0.004) of soil. The distribution of *Bacillus* inoculated in soil with aggregate size 1-2 mm was not significantly influenced by porosity (p=0.370), connectivity (p=0.707) and soil-pore interface (p=0.182) of soil. In the case of *Pseudomonas* inoculated in soil with aggregate sizes 2-4 mm, distribution of *Pseudomonas* cells was significantly influenced by porosity (p=0.000), connectivity (p=0.000) and soil-pore interface (p=0.000) of soil.

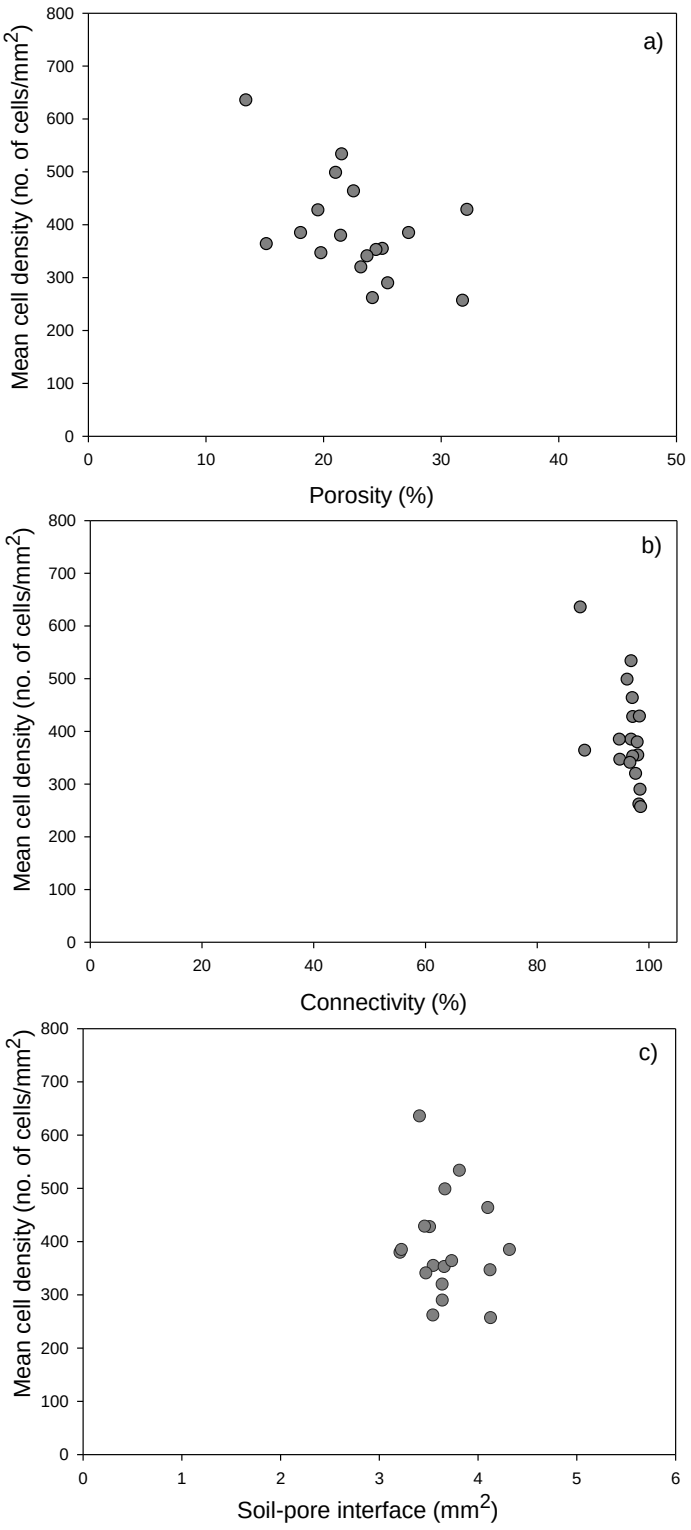

Figure 5.19: Relationship between mean *Pseudomonas* cell density and porosity (a), connectivity (b) and soil-pore interface (c) analysed at macroscale in 3D in soil with aggregate of sizes 1-2 mm. Data points in the graph represents individual analysed layer in each replicate per treatment.

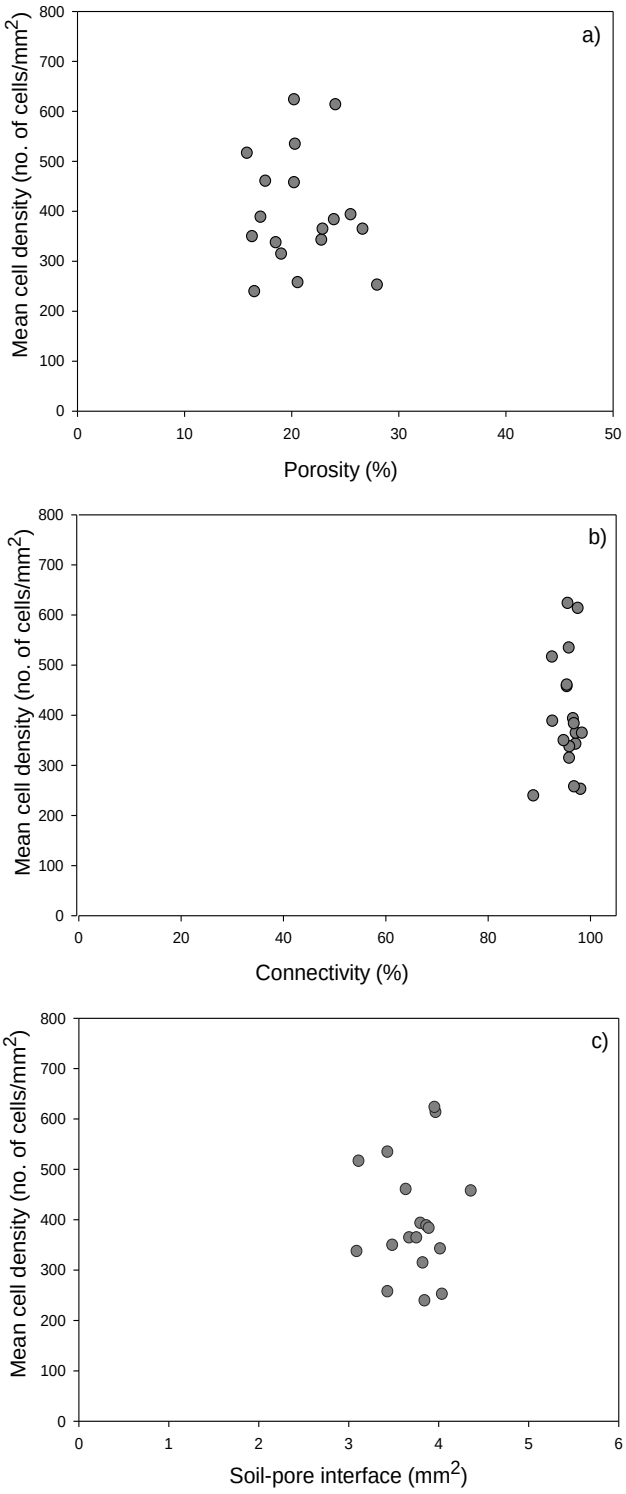

Figure 5.20: Relationship between mean *Bacillus* cell density and porosity (a), connectivity (b) and soil-pore interface (c) analysed at macroscale in 3D in soil with aggregate of sizes 1-2 mm. Data points in the graph represents individual analysed layer in each replicate per treatment.

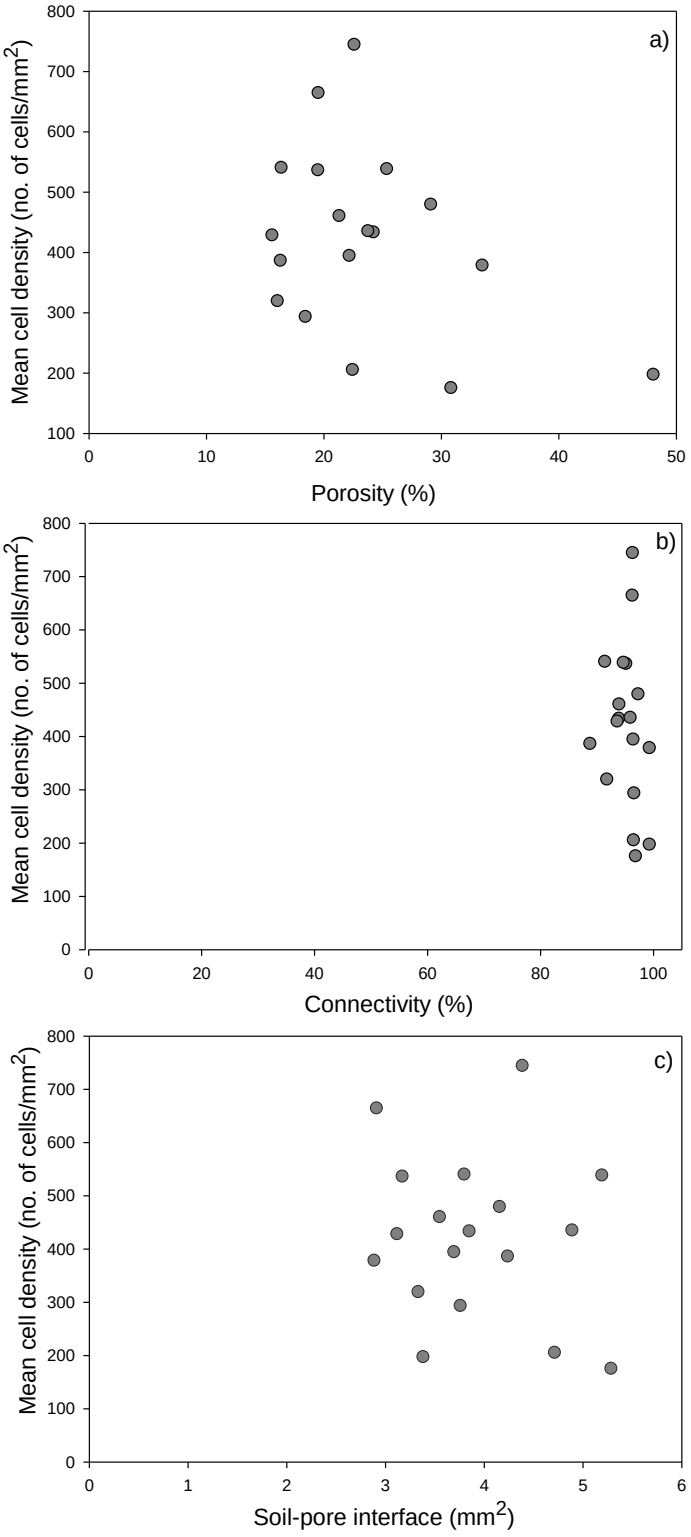

Figure 5.21: Relationship between mean *Pseudomonas* cell density and porosity (a), connectivity (b) and soil-pore interface (c) analysed at macroscale in 3D in soil with aggregate of sizes 2-4 mm. Data points in the graph represents individual analysed layer in each replicate per treatment.

5.3.3.2 Microscale

Cell density (no. of cells mm^{-2}) of *Pseudomonas* and *Bacillus* in different treatments were plotted against soil porosity, connectivity and soil-pore interface analysed at 2D and 3D (Figure 5.22- 5.27).There are more data points in these graph compared to the macroscale graphs (Figure 5.16-5.21) as each data point in the graphs represents analysis of a microscopic field of individual layer in each replicate of a respective treatment and there is a noticeable wider spread in the cell density values.

In samples analysed at the microscale and in 2D, the porosity of the analysed area ranged from 0-100 % with the majority having porosity between 0- 30 %, (Figure 5.22a-5.24a). The soil-pore interface ranged from 0-20 mm^2 with the majority of the analysed area having a soil-pore interface between 0-10 mm^2 (Figure 5.22b-5.24b). The mean cell density ranged between 0-1600 cell mm^{-2} (Figure 5.22-5.24). Again we note the much wider spread of data. The influence of soil porosity and soil-pore interface on distribution of *Pseudomonas* and *Bacillus* cells varied between treatments (table 5.4). In *Pseudomonas* inoculated soil with aggregates of size 1-2 mm, soil porosity ($p=0.736$) and soil-pore interface ($p=0.134$) had no significant influence on the distribution of *Pseudomonas* cells in soil. The distribution of *Bacillus* inoculated in soil with aggregate size 1-2 mm was significantly influenced by porosity ($p=0.000$). Soil-pore interface had no significant influence on *Bacillus* distribution in soil. In *Pseudomonas* inoculated in soil with aggregates sized 2-4 mm treatment, the distribution of *Pseudomonas* cells was significantly influenced only by porosity ($p=0.000$). Soil-pore interface area had no significant ($p=0.270$) influence on the distribution of *Pseudomonas* in soil.

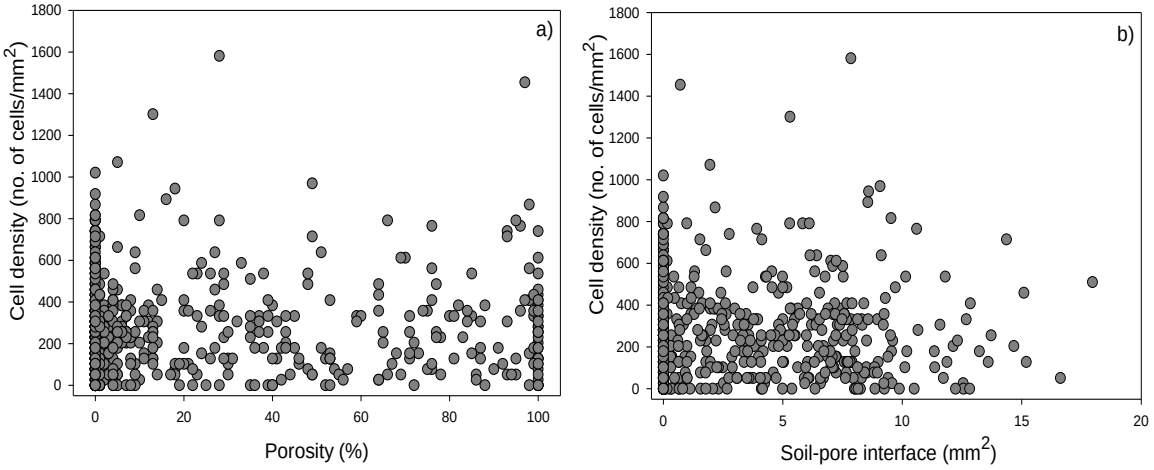

Figure 5.22: Relationship between *Pseudomonas* cell density and soil porosity (a) and soil-pore interface (b) analysed at microscale in 2D in soil with aggregate of sizes 1-2 mm. Data points in the graph represents individual analysed layer of each replicate per treatment.

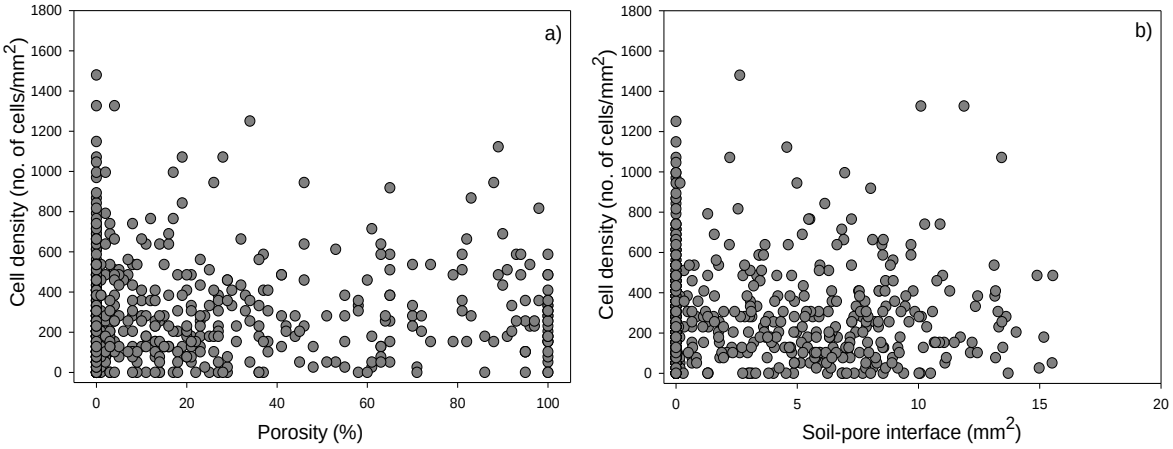

Figure 5.23: Relationship between *Bacillus* cell density and soil porosity (a) and soil-pore interface (b) analysed at microscale in 2D in soil with aggregate of sizes 1-2 mm. Data points in the graph represents individual analysed layer of each replicate per treatment.

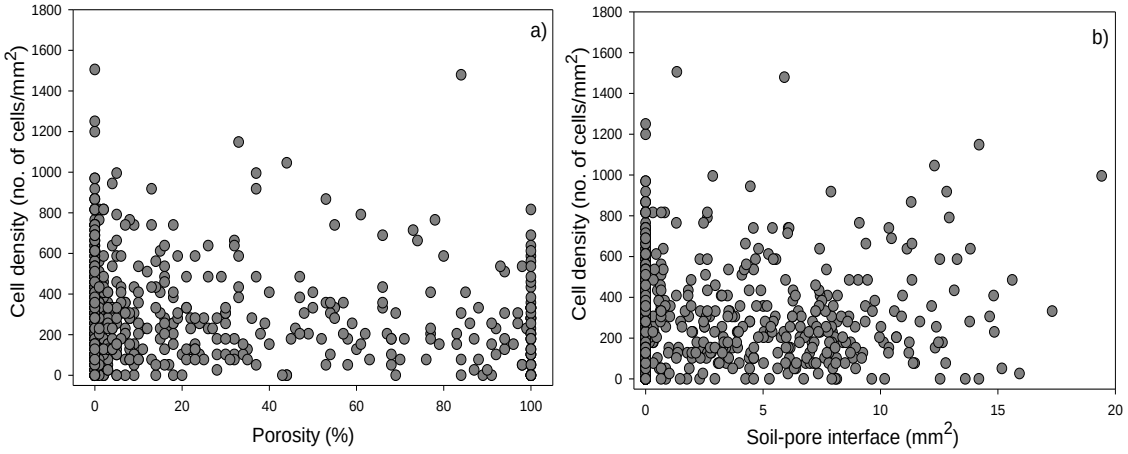

Figure 5.24: Relationship between *Pseudomonas* cell density and soil porosity (a) and soil-pore interface (b) analysed at microscale in 2D in soil with aggregate of sizes 2-4 mm. Data points in the graph represents individual analysed layer of each replicate per treatment.

Table 5.4: Results of the Poisson model analysis on influence of pore structure on distribution of bacteria in different soil at microscale in 2D and 3D. Numbers reported in the table are the p-values of the analysis.

Scales	Treatments	Porosity (%)	Soil-pore interface (mm^2)	Connectivity (%)
Microscale 2D	*Pseudomonas* inoculated in soil with aggregate sizes 1-2 mm	0.736	0.134	-
	Bacillus inoculated in soil with aggregate sizes 1-2 mm	0.000	0.167	-
	Pseudomonas inoculated in soil with aggregate sizes 2.4 mm	0.000	0.270	-
Microscale 3D	*Pseudomonas* inoculated in 1-2 mm aggregate soil	0.274	0.165	0.933
	Bacillus inoculated in 1-2 mm aggregate soil	0.968	0.004	0.605
	Pseudomonas inoculated in 2-4 mm aggregate soil	0.000	0.014	0.000

In samples analysed at the microscale in 3D, the porosity of the analysed area ranged from 0-100 % with the majority having porosity between 0-40 % (Figure 5.25a-5.27a). Connectivity of pores ranged between 95-100 % with majority having connectivity either at 0 % or between 95-100 % (Figure 5.25b-5.27b). The soil-pore interface ranged from 0-11 mm^2 with the majority of the analysed area having a soil-pore interface between 2-5 mm^2, (Figure 5.25c-5.27c). As with the 2D analysis, the mean cell density ranged between 0-1600 cell mm^{-2} (Figure 5.25, 5.26, 5.27). The influence of soil porosity, connectivity and soil-pore interface on distribution of *Pseudomonas* and *Bacillus* cells varied between treatments (table 5.4). In *Pseudomonas* inoculated soil with aggregates of size 1-2 mm, soil porosity (p=0.274), connectivity (p=0.933) and soil-pore interface (p=0.165) had no significant influence on distribution of *Pseudomonas* in soil. Soil porosity (p=0.968) and connectivity (p=0.605) had no significant influence on the distribution of *Bacillus* inoculated soil with aggregates sized 1-2 mm. However, soil-pore interface had a significant (p=0.004) influence on *Bacillus* distribution in soil. In case of *Pseudomonas* inoculated in soil with aggregate sizes 2-4 mm, distribution of *Pseudomonas* cells was significantly influenced by porosity (p=0.000), connectivity (p=0.000) and soil-pore interface (p=0.014) of soil. Therefore, compare to the results at the macroscale it is noted that fewer significant relationships are found between pore characteristics and bacterial distribution at microscale (Table 5.3 versus 5.4).

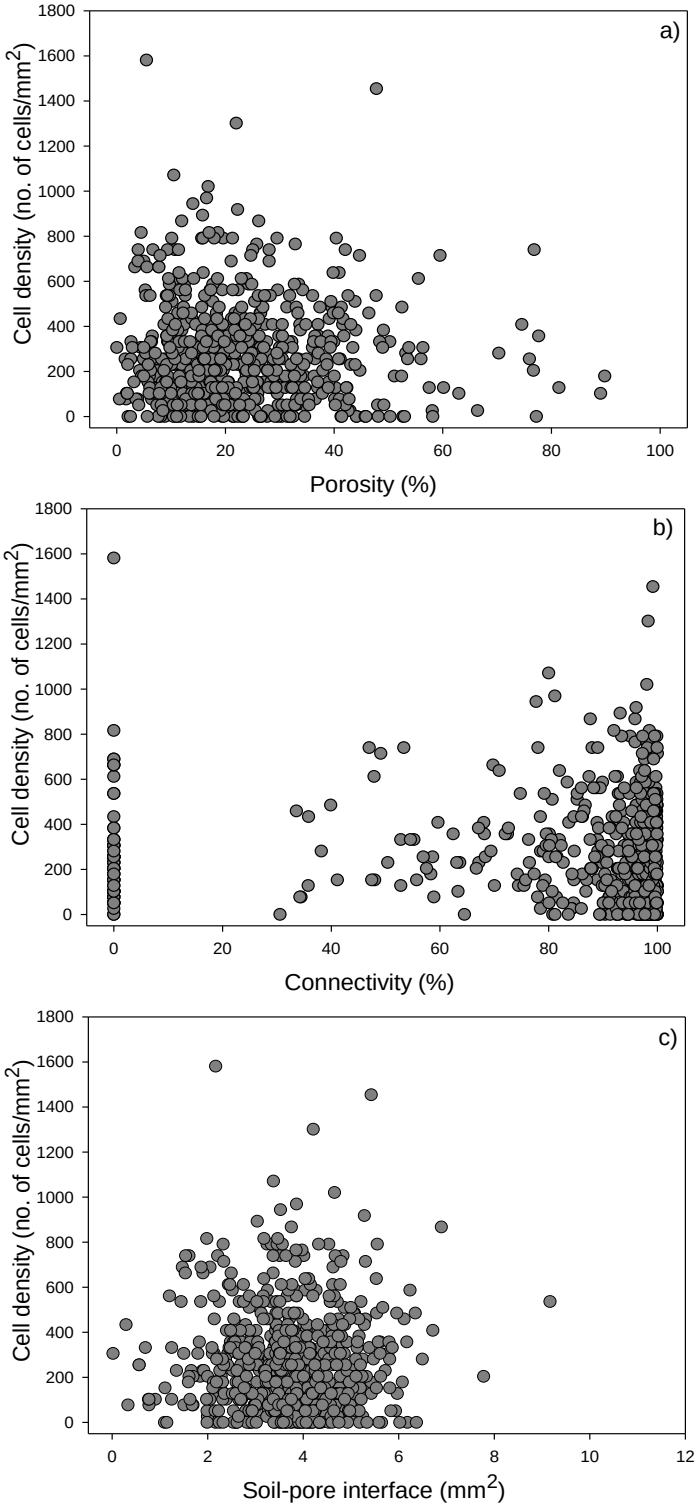

Figure 5.25: Relationship between *Pseudomonas* cell density and porosity (a), connectivity (b) and soil-pore interface (c) analysed at microscale in 3D in soil with aggregate of sizes 1-2 mm. Data points in the graph represents individual analysed layer in each replicate per treatment.

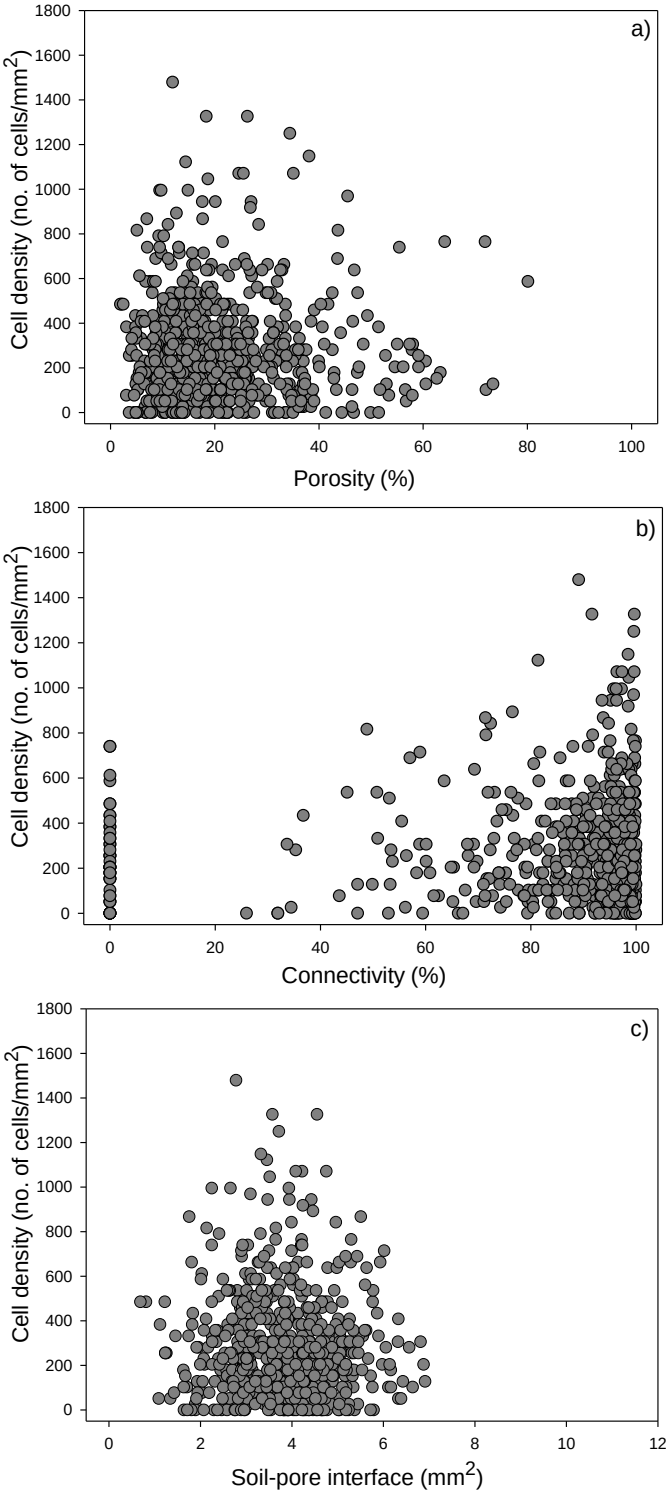

Figure 5.26: Relationship between *Bacillus* cell density and porosity (a), connectivity (b) and soil-pore interface (c) analysed at microscale in 3D in soil with aggregate of sizes 1-2 mm. Data points in the graph represents individual analysed layer in each replicate per treatment.

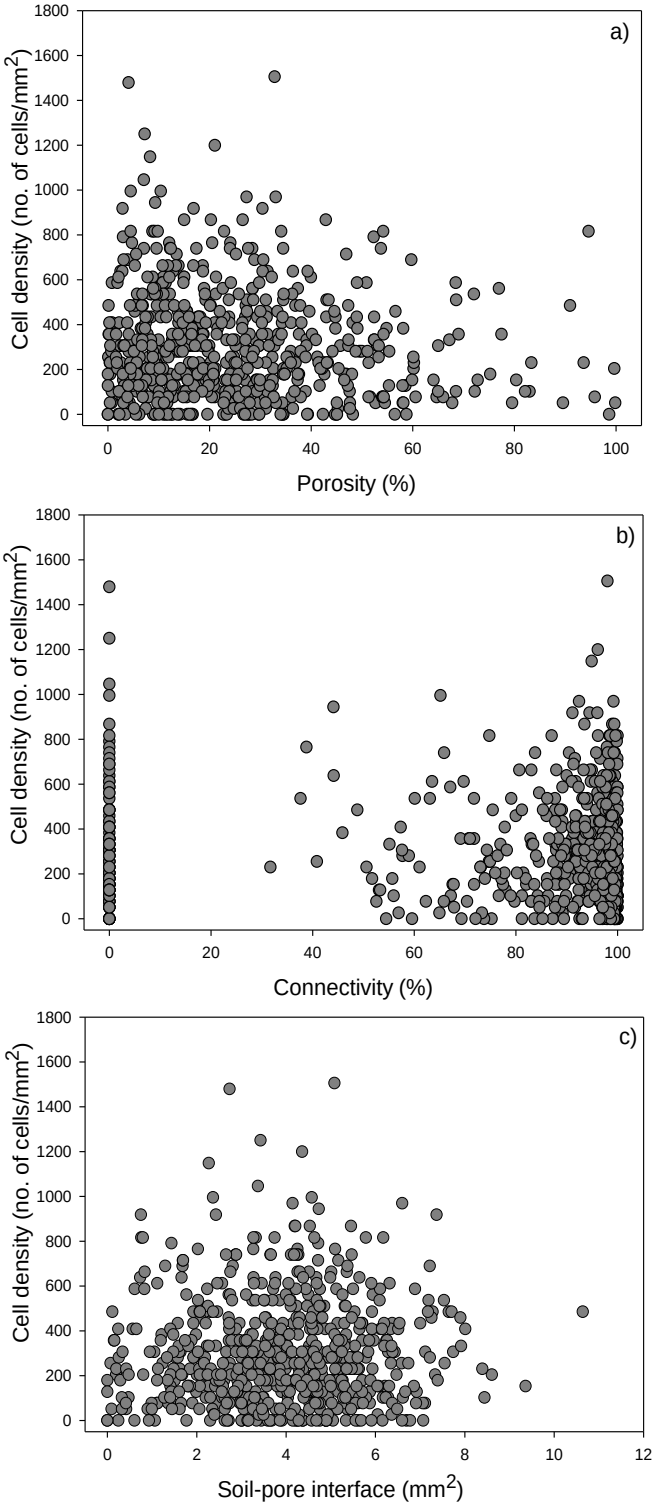

Figure 5.27: Relationship between *Pseudomonas* cell density and porosity (a), connectivity (b) and soil-pore interface (c) analysed at microscale in 3D in soil with aggregate of sizes 2-4 mm. Data points in the graph represents individual analysed layer in each replicate per treatment.

5.4 Discussion

5.4.1 Bacteria distribution in soil

One of the goals of this chapter was to use green fluorescence protein (GFP) marker to visualise bacteria *insitu* in soil. GFP marker was chosen as it possesses excellent features as a reporter protein and has been used previously in plant-microbes interaction studies in soil (Elväng et al., 2001; Zhang et al., 2011). In this study, GFP signals were not detected in the impregnated soil for all treatments. The acetone solution used during the dehydration process is not the reason for the loss of GFP signal as a preliminary test was carried to check the stability of GFP signals in a pure acetone solution. The test showed that GFP was not affected by the solution. The likely reason for a loss of the GFP signal could either be the long polymerization period of the resin or the signal was too weak in the presence of relatively high auto fluorescence of the resin and soil matrix. Similar kind of results were observed by Postma and Altemuller (1990) who examined the different steps of impregnation for successful staining of bacteria *Rhizobium leguminosarm biovartrofolli* in soil thin sections. Combinations of different fluorochromes were tested to see if they withstand mounting in polyester resin and rinsing in acetone. Most of the combinations failed due to adsorption of stain by resin or due to negative influence of acetone on staining effect. The best result was obtained with fluorescent brightener calcoflour white M2R applied before embedding in polyester resin and counterstaining the soil matrix with acridine orange in thin sections (Postma and Altemuller, 1990). An alternative DAPI stain was therefore used for staining bacteria in this study.

DAPI stain has been used before to visualise indigenous bacteria in resin impregnated soil samples (Li et al., 2003; Eickhorst & Tippkötter, 2008). For example, Eickhorst et al. (2008) used DAPI as a counter-stain to visualise indigenous bacteria in undisturbed soil samples.

No DAPI signals were detected in control samples, which confirms that the autoclaving procedure successfully sterilised the soils and that the bacteria which are visualised in inoculated samples are only introduced bacteria in the soil. Both *Pseudomonas* and *Bacillus* cells were observed on the surface of the soil particles or at soil-pore interface. No cells were observed in the pore space. This is no surprise and inherent to the method because if there had been bacterial cells in pores these will have got removed during the exchange of liquids for dehydration procedure. In other studies, however, it was found that only limited cell numbers are washed away during impregnation (Eickhorst, pers. communication) so it is likely that the majority of bacteria are attached to the surfaces. In polished sections, *Pseudomonas* cells were observed to be more evenly spread through the soil matrix. White et al (1994) also observed similar distribution of *Pseudomonas* f*luorescens* stained cells throughout the soil pore network. *Bacillus* cells on the other hand were observed in small clusters. This kind of pattern was observed in indigenous bacteria in the form of small clusters or microcolonies constituted by cells of identical or different morphologies (Nunan et al., 2001; Li et al., 2004; Eickhorst & Tippkotter, 2008), but is shown here to also occur in soil. The difference in the spatial pattern between two different species in soil was a novel finding. Differences in the distribution pattern can be related to how bacteria spread and access nutrient sources in soil. It suggests that a different response between species can be

expected in their relationship with the soil structure. On visual comparison, a heterogeneous distribution in cell counts between different fields of view in each analysed layer was observed. Previous studies have shown a non-random distribution of microorganisms in soil (Nunan et al., 2003; O'Donnell et al., 2007; Young et al., 2008) For example, Nunan et al. (2003) found variation in bacterial numbers per quadrant in different depths of soil samples. They suggested that spatial variability in bacterial numbers was related to nutrients status of soil (Nunan et al., 2003). There will be a complex number of factors influencing the bacterial distribution ranging from physical (pore geometry), to nutritional and biological (differences in motility and attachment). The dominant processes remain to be identified, but the technique developed here offers real opportunities to disentangle these processes.

Both time and physical properties affected the spatial distribution or numbers with differential effects for the two species. *Pseudomonas* inoculated samples showed no significant difference in cell density between sampling irrelevant of the aggregate size of soil. On the other hand, *Bacillus* showed a significant difference between two days. This difference in between two species can be related either to growth rate or spread rate of bacteria in soil. Among different aggregate size treatments, a significant difference in *Pseudomonas* cell density was observed. Soil with 2-4 mm aggregate size had higher cell density compare to soil with 1-2 mm aggregate size. This result is consistent with chapter 3 experiment where effect of aggregate size on growth rate of *Pseudomonas* in soil was determined. Similar kinds of difference in numbers of bacterial populations have been reported by past studies related to different soil particle sizes or aggregate factions (Ranjard and Richaume, 2001; Sessitsch et al.,

2001). Therefore the hypothesis that bacterial cell density increases overtime in biological sections applied only for *Bacillus* strain.

5.4.2 Influence of soil pore geometry on bacteria distribution

The other goal of this chapter was to develop a methodological approach to analyse the effect of pore characteristics on spatial patterns of bacteria at microhabitat scales. The approach was to combine 2D and 3D methods to gain quantitative information on the relationship between pore characteristics and introduced bacteria in soil as it known from previous works that the spatial distribution of bacteria is not random at fine scales and their location in soil is dependent on factors like substrate availability, soil water and pore size distribution (Nunan et al., 2003; Ruamps et al., 2011). A recent study by Hapca et al. (2015) used a similar approach and developed a method combining 2D SEM-EDX data with 3D X-ray tomography images to generate the 3D spatial distribution of chemicals in soil. Progress has been made combining techniques to analyse the relationship between soil pore characteristics and microbial community distribution and their activity in soil (Kravchenko et al., 2013; Wang et al., 2013; Kravchenko et al., 2014; Negassa et al., 2015). For example, Kravchenko et al. (2013) studied the effect of intra-aggregate pore structure on the distribution of *E.coli* in macro-aggregates. They used culture based methods (Colony forming unit method) to enumerate *E.coli* distribution in aggregates and X-ray tomography to quantify pore structure of intact aggregates from different managements. Another study, done by Wang et al. (2013), which was a further development of the Kravchenko et al. (2013) study, used qPCR method instead of CFU method to enumerate *E.coli* in the scanned aggregate sections. They

used qPCR as it generated more reproducible and less variable results (Wang et al., 2013). In our study, microscopy examination of polished sections was used to quantify bacteria in soil. The advantage of the method used in this chapter over the culture and non-culture based method was that impregnated soil samples were used which allowed to characterise the *insitu* relationship between bacteria and soil features without destroying the samples. A study by Nunan et al. (2003) that used soil thin sections was able to show how bacterial density values differed between topsoil and subsoil in relation to distance from pores. Another advantage of this methodology was the use of X-ray CT to quantify pore structure in the same layer. The relationship between pore structure and bacterial cell density was analysed at different scales. This was done in order to understand the effect of pore structure at the scale at which microbes actually live and interact with their surrounding environment and also if the effect is specific to that scale or variable at large scales. This kind of analysis at different scale has been done by others to study spatial pattern of either indigenous bacterial population (Nunan et al. 2002) or microbial activity (Gonod, 2006) from metre to micrometre scales. Nunan et al. (2002) found a large variation in the distribution of bacteria in topsoil and subsoil at different scales. They identified spatial structure of bacterial population at microscale in topsoil and at large and microscale in subsoil. They related this difference in spatial pattern at different depths to transport of nutrients through soil (Nunan et al., 2002). Therefore, it is noted that different significant effects are found depending on the spatial scale of the analysis. This confirms that this is an important aspect to be considered when doing this type of analysis, but it also raises the question what might be causing this and how do we proceed.

Therefore, we need to fully understand the spatial variability of soil microbes at different scales.

In this study, the analysis at each scale was done in 2D and 3D because of two reasons. Firstly in 2D, the connectivity of pores which is an important parameter in relation to transport of nutrients and bacteria cannot be determined in 2D and secondly the degree of tortuosity of the pore space is different in 2D compared to 3D. In this study no significant difference in the pore characteristics in 2D and 3D between different aggregate size treatments was observed, but it should be noted that a part of pore volume was not detected by the X-ray scanner due to limitation of scan resolution. Therefore, the conclusion made here are based on the percent of pores observed (i.e. >13.4 µm resolution). Despite this, the hypothesis that pore characteristics influence *Pseudomonas* and *Bacillus* distribution at different spatial scales (macro- and microscale in this case) was supported by the data. But the effect was quite variable across macro- and microscales analysed over different dimensions in each treatment.

Samples analysed in two dimensions (2D) at macroscale showed a significant effect of porosity and soil-pore interface on *Pseudomonas* and *Bacillus* cell distributions in all treatments but at microscale this was not the case as the soil-pore interface showed no significant effect on the distribution of *Pseudomonas* and *Bacillus* bacteria in all treatments. This difference between the two scales could be due to the size of the sample as the information is constrained at this scale. Therefore, to avoid this constraint of sample size used for pore structure determination, the analysis was done in 3D where a bit of the surrounding area of the 3D soil environment was considered. The results showed that at

macroscale, all three pore characteristics showed a significant effect on the *Pseudomonas* inoculated treatment, but was different in case of *Bacillus* inoculated samples. The reason of this observed difference between two samples with same aggregate size and bulk-density but inoculated with different bacterial strain is unknown. However, at microscale in 3D, the effect of pore characteristics was different compare to microscale in 2D. This difference in analysis between two dimensions could be that in 2D the information of pore characteristics information is constrained to the 2D-single plane from 3-D pore structure. The results show that there was no general relationship/link between pore structure and bacterial counts and this varied with the spatial scale and dimension, therefore measuring and identifying whether a relationship exists is tightly linked to identifying the 'appropriate spatial scale'.

The effort made in this chapter to show the effect of pore characteristics at different scales did not show much noticeable differences in all treatments. But it should be noted this difference is relevant only to the visible pores , so conclusion are made only on pores greater than the scan detection limit. Also, there are other parameters like pore-size distribution and tortuosity of the pore space which need to be considered as it is known from some recent works that the composition of bacterial community differs in large and medium size pores (Negassa et al., 2015).

5.5 Conclusion

In this chapter a methodology was presented to determine the relationship between the effect of pore structure and the distribution of bacteria at a range of spatial scales. The data presented in this chapter suggested that porosity, connectivity and soil-pore interface influences the distribution of bacteria in soil at microscales. The information obtained from this combination of method can be used for developing modelling frameworks to understand the distribution of bacteria in a 3D soil environment. The issue of the scale at which to undertake analysis is a central one and in the absence of any general trends the scale containing the most information, within practical limits, should be selected for further analysis.

6 Effect of C distribution and soil structure on spread of bacteria

6.1 Introduction

In a heterogeneous environment like soil, bacteria can exhibit chemotactic responses towards components. Bacterial chemotaxis is the migration of bacteria under the influence of a chemical gradient (Pandey & Jain, 2002). For example, bacteria colonize the rhizosphere of different types of plants by exhibiting chemotactic response towards components of the root exudates (Bacilio-Jimenez & Aguilar-Flores, 2003; Oku et al., 2012). To enhance plant growth or to degrade organic pollutants in soil, bacteria have been introduced in soil and chemotaxis was reported to be one of the major factors enhancing these processes (Lacal, 2011) by affecting the movement and distribution of bacteria. Neal et al. (2012) demonstrated the colonisation of *Pseudomonas fluorescens* towards a specific benzoxanoids produced by maize roots in soil (Neal et al., 2012). Other studies have also reported chemotactic responses of introduced bacteria towards specific organic compounds in soil (Bacilio-Jimenez & Aguilar-Flores, 2003; Oku et al., 2012; Gupta Sood, 2003). In all these cases this can lead to non-uniform distributions of bacteria in soil and contribute to the formation of so called hot-spots.

Mostly, the emphasis has been on the colonization of the introduced bacteria near the target, and the study of spatial patterning of these bacteria at microscales is still limited. In chapter 5 it was shown that it is essential to study spatial patterns at appropriate scales as different conclusions can be drawn about factors influencing the distribution of bacteria based on the spatial scale of analysis. Some previous studies have shown spatial patterns in the distribution of bacteria at a microhabitat scale (Kizungu et al., 2001; Nunan et

al., 2003; Gonod, 2006). For example, Gonod et al. (2006) reported a heterogeneous pattern in mineralization of 2,4-D (2,4 Dichlorophenoxyacetic acid) with an increase in variability of mineralization from field to microhabitat scale. An explanation is that bacteria are not randomly distributed and are located in different microenvironments (i.e. mainly located in pores of different size and shapes) of soil. However, knowledge about the relationship between bacterial distribution and soil structure is still limited and often based on simplified assumptions about sizes of bacteria and pores. Specifically, the influence of pore geometry (which includes connectivity and pore-solid interface surface areas) on the distribution of bacteria in soil is largely unknown.

In chapter 4, an influence of soil structure on the spread of bacteria towards a target source was studied. The results showed the effect of soil structure on the spread of bacteria in the same type of soil. In chapter 5, an analysis method was developed to study the spatial distribution of bacteria in soil at microscales. In that study, the bacteria were randomly mixed through the soil as part of the method development. This will have had an impact on the spatial distribution that was found and can differ from more natural situations that require bacteria to move either from or towards a source.

In this chapter, the experimental procedures developed in chapters 4 & 5 are used to investigate the spread and patterning of bacteria moving away from or moving towards a nutrient source in soil. The main objectives of this chapter are:

1) To analyse the influence of soil structure on the extent of spread of bacteria in soil **from a single source** of inoculum at microscale (henceforth referred to as agarose experiment).
2) To analyse the influence of soil structure on the extent of spread of bacteria **towards a nutrient source** in soil at microscale (henceforth referred to as compost experiment).

This was investigated by quantifying the spatial distribution of *Pseudomonas* and *Bacillus* following introduction into microcosms with a local C source and controlled structural properties by examining biological thin sections and applying the analyses methods developed in Chapter 5. In the microcosms a localised source of C and bacteria from which spread is initiated into the soil or introduced as a layer of compost (as a C source), which was expected to stimulate colonisation from soil, were introduced.

6.1.1 Hypotheses

1. Agarose experiment: colonising soil from a local source

- An increase in soil bulk-density decreases the spread and colonization of soil by *Pseudomonas*.
- Soil porosity, connectivity and soil-pore interface influence the spread and colonization of soil by *Pseudomonas*.

2 Compost experiment: colonising a local C layer from soil

- Higher cell densities of *Pseudomonas* and *Bacillus* bacteria will develop in close proximity to the compost layer.

- Soil porosity, connectivity and soil-pore interface influence the extent of colonization of soil by *Pseudomonas* and *Bacillus* towards in the proximity of the compost layer.

6.2 Material and methods

This study is divided into two experiments based on the objectives set above. Experiment 1 is the agarose experiment, where bacteria were introduced in the centre of the soil sample and packed at bulk-densities 1.3 g cm^{-3} and 1.5 g cm^{-3}. After 14 days of incubation, thin sections of samples were prepared to analyse the spread of bacteria in the soil. Experiment 2 is referred to as the compost experiment, where bacteria were mixed with autoclaved soil. A layer of fresh sterilised compost was added in the centre of the soil sample. After 14 days of incubation, thin sections of soil samples were prepared to analyse the gradient of bacteria towards the compost layer. Details of the experimental design are given below.

6.2.1 Agarose experiment: colonising soil from a local source

6.2.1.1 Inoculum preparation

The bacterial strain *Pseudomonas fluorescens* (SBW25) was used in this experiment. Agarose pellet was used as a source of inoculum (details in section 4.2.1). Briefly, 1000 µl of *Pseudomonas* cell suspension was mixed with 30 ml of 1.5% LMP agarose solution in a 50 ml centrifuge tube. For control samples, 1000 µl of dH_20 was mixed with the agarose solution (henceforth referred as blank agarose pellet). The mixture was shaken gently to avoid formation of bubbles and 15 ml of the solution was poured onto a petridish. The petridish

was swirled gently for even distribution of agarose solution. Glass beads of size 2.0 mm diameter were placed on the semi-solidified agarose and the remaining agarose solution was then poured on top. The petridish was left under the laminar flow to let the agarose cool down at room temperature and solidify. The solidified agarose was then cut down into small cylindrical shaped pellets using the wide end of a pipette tip. The bead pellets were 3.5 mm in diameter and 5 mm in height (Figure 6.1). Each pellet contained a glass bead in its centre. The glass beads were used to ensure that the location of inoculation could be identified in thin sections as described in sections below.

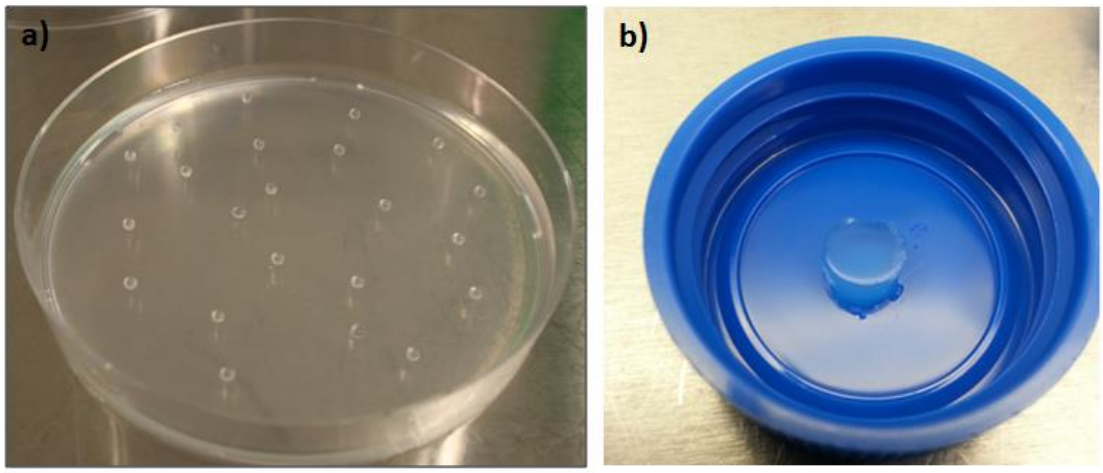

Figure 6.1: Preparation of agarose pellet for inoculation in soil. (a) Glass beads are placed in the agarose and a bacterial suspension mixture poured in the petridish. After cooling the mixture, individual agarose pellets are prepared. (b) Each inoculum pellet contains one glass bead. The size of each pellet is 3.5 mm.

6.2.1.2 Preparation of soil microcosms

The soil used in this experiment is described in Chapter 2 (General material and methods). Sterilised 1-2 mm sieved soil was used for both experiments. The soil was sterilised by autoclaving twice at 121°C and 100 kPa for 20 minutes with a 24hr interval time. Polyethylene rings of size 3.40 cm^3 (diameter 1.70 cm and height 1.5 cm). The bottom sides of the rings were covered with three layers of

cotton gauze to prevent loss of soil during the impregnation procedure. The gauze was fixed with cable ties in different colours indicating the different treatments (Figure 6.2).

Figure 6.2: Arrangements of soil samples for resin imprengation.The soil rings were tied with different color bands in order to easily distinguish between treatment samples after impregnation,here shown for an experiment where red color stands for soil packed at 1.3 g cm^{-3}, black stands for soil packed at 1.5 g cm^{-3} and white color stands for control samples.

Soil was packed at two bulk-densities, 1.3 and 1.5 g cm^{-3} with a moisture content equivalent to 60% of water filled pores. The amount of water added to soil to acquire 60 % water filled pores was 0.224 cm^3 g for bulk-density1.3 g cm^{-3} and 0.1569 cm^3 g for bulk-density 1.5 g cm^{-3}. The amount of soil required to pack in PE rings size 3.40 cm^3 (diameter 1.70 cm and height 1.5 cm) to attain each bulk-density was 5.25 g for 1.3 g cm^{-3} and 5.71 g for 1.5 g cm^{-3}. Soil was poured in rings in two layers, covering half the height each. After packing the first half of soil an agarose pellet was placed on top of the soil layer in its centre and then covered with the second half of soil. Control samples were packed in a similar way but with the blank agarose pellet. Three replicates per treatment

were prepared, producing 12 soil microcosms in total. The microcosms were sealed in plastic bags to avoid drying of the samples and incubated at 23°C in the dark to allow bacteria to grow in soil. The plastic bags were opened and closed every alternate day under a sterile bench to enable air exchange. The soil microcosms were sampled after an incubation period of 14 days.

6.2.1.3 Impregnation of samples

The soil microcosms were impregnated with resin as described in chapter 5 (section 5.3), except for the polymerization time that was reduced to 3 weeks. After polymerization, excess resin and the PE rings of samples were removed to produce a cylindrically shaped resin impregnated soil sample. The bottom part of each sample was removed along with the aluminium gauze and a parallel cut was applied to the top using a diamond saw (Woco 50, Conrad, Germany). The individual samples were labelled afterwards and a straight vertical cut was made to ensure the starting point is the same for all samples while scanning under X-ray CT.

6.2.1.4 Scanning of impregnated microcosms

The impregnated samples were scanned using a Metris X–Tek HMX CT scanner. Samples were scanned at 10.87 µm resolution with energy settings of 200 keV and 56 µA and 2000 angular projections. The straight vertical cut was used as a reference side facing the gun of the CT scanner for each scan to facilitate alignment for image processing described in detail in the following sections. To minimize beam hardening a tungsten target with a 0.25 mm

aluminium filter was applied. CT Pro v2.1 (NIKON metrology, Tring, UK) was used to reconstruct the radiographs into a three dimensional volume.

Reconstruction of radiographs into three dimensional volumes was done using Metris X-Tek software CT Pro v2.1 (NIKON metrology, Tring, UK). VGStudioMAX V2.2 (Volume graphics, Heidelberg, Germany) was used to change contrast in reconstructed volumes and exported into image stacks (*bmp format) for further processing.

6.2.1.5 Preparation of thin sections

To prepare samples for thin sections, the reference side of the soil block was glued onto a petrographic slide of size 27 x 46 mm and thickness 0.15 mm (Beta diamonds Inc, CA, USA) with epoxy resin (Epofix resin, Struers, Denmark). This slide was henceforth referred as reference side (RS).

Two thin sections were prepared parallel to the reference side, one through the centre of the glass bead and other 2.5 mm away from the bead (Figure 6.3). An estimated distance of each thin section from the reference slide was calculated by measuring the distance between the reference side and the glass bead in X-ray CT grey scale images. A cut was made with a diamond saw (Discoplan TS, Struers A/S, Denmark) on the side opposite to the RS to produce a flat plane. This plane cut was made in order to glue the sample on a slide for producing thin sections. After cutting the block was ground using a diamond coated cup-wheel grinder (Discoplan TS, Struers A/S, Denmark) to make the surface of the sample parallel and subsequently hand polished with a wet abrasive paper (P1200, Silicon carbide) on a glass plate in order to remove the grinding

material and make the surface smooth. The thickness of the block was measured with a micrometer 0-25 mm (accuracy 2 µm; Mitutoyo, Japan) and referred to as d3 (i.e. the first section approximately 2.5 mm away from the bead) in Figure 6.3. The distance measurement of the selected section from the reference side was done for later alignment with the CT scan data. A frosted petrographic slide of size 27 × 46 mm (Beta diamonds Inc, CA, USA) was then glued (Eukitt, Struers A/S, Denmark) onto the polished surface of the sample side and then the block was cut with a diamond saw according to the estimated distances to get the first thin section referred to as dIII (Figure 6.3). The dIII slide was further ground to approximately 200 µm and subsequently polished. The thickness of the sections varied a bit after polishing as some sections had to be re-polished to get rid of the grinding material (after checking it under microscope).

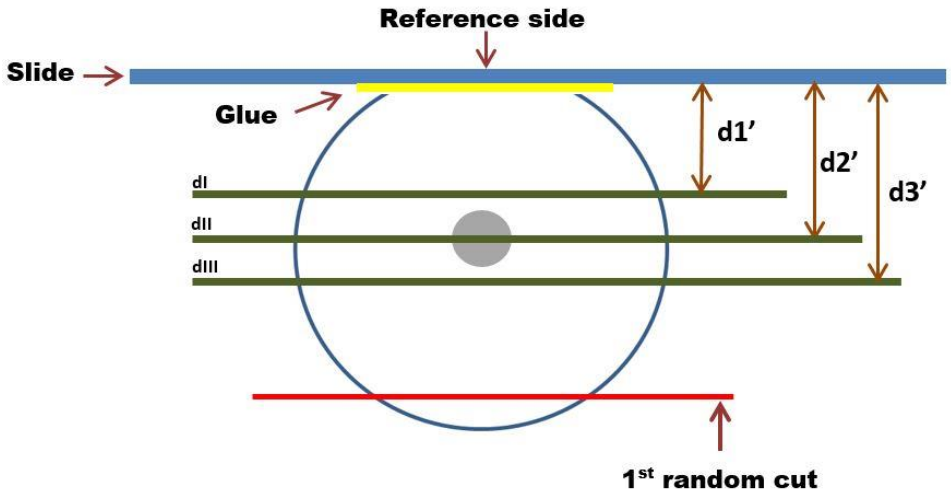

Figure 6.3: Schematic of the thin sections selected in samples of the agarose experiment. Each thin section was at a distance 2.5 mm from the centre of the bead. The green lines represent the area where thin sections were selected.

The final thickness of the thin section was measured considering the thickness of the slide and the amount of glue added. After removing the first thin section (dIII) by cutting, the remaining block was ground again with the cup-wheel grinder and subsequently polished as described above. A new frosted slide was then glued onto the polished block and the same steps were repeated to make another two thin sections. These new thin sections are referred to as dII (through centre of bead) and dI (approximately 2.5 mm away from the bead towards the reference side); the corresponding distance to the reference side was referred to as d2 and d1. The distances d1 and d2 were used to calculate the final distances between the surface on the reference side and the surface of the sample referred to as d1' and d2' respectively (Table 6.1). Due to time constraints only thin section dI and dII were used for further analysis; the third section was kept as a back-up and to test other staining techniques.

Table 6.1: Thickness of thin sections dI and dII per replicate in soil packed at bulk-density of 1.3 or 1.5 g cm^{-3} of agarose experiment: colonising soil from a local source.

Treatments	Replicates	Thickness of thin sections (µm)	
		dI	dII
Inoculated soil packed at bulk-density1.3 g cm^{-3}	1	109	150
	2	163	155
	3	149	148
Inoculated soil packed at bulk-density1.5 g cm^{-3}	1	118	195
	2	160	195
	3	130	119
Soil without inoculum packed at bulk-density1.3 g cm^{-3}	1	112	59
	2	134	90
	3	122	180
Soil without inoculum packed at bulk-density1.5 g cm^{-3}	1	118	184
	2	79	99
	3	71	175

6.2.1.6 Enumeration of bacteria on thin sections

A drop of vectashield mounting medium containing approximately 1.5 µg ml^{-1} of DAPI stain (Vectashield H-1200, Vector Laboratories, CA, USA) was added on top of the thin sections and covered with a cover slip of size 27 × 46 mm (Beta diamonds Inc, CA, USA). Bacterial cells were counted using an Olympus B×61 fluorescence microscope (Olympus, Japan) equipped with an 100 W Hg vapour lamp (HBO 102 W/2, Osram, Germany), using a 100 × objective (UPlanSApo, Olympus, Japan) under UV excitation (filter set U-MWU2, Olympus, Japan). The cells were counted using a 10 × 10 reticule grid (12.5 mm; Spectra Services, NY, USA) in a 10 × eyepiece (WHN 10×, Olympus, Japan).

Thin section slides were placed in a horizontal position on the microscope stage with the bottom side of the sample facing the scale of the microscope stage. The scale of the microscope stage was used to note down the X and Y coordinates (1 & 2 in Figure 6.4) from the bottom of the sample. This was done in order to be able to start, and revisit, from the same spot in each parallel thin section and also be able to align it with the other parallel thin sections and the CT scan images. In each thin section five lines at a distance of 1 mm were counted. The first counting line was based on the centre of the bead and then two lines above and below the first line was counted at a distance of 1mm respectively (Figure 6.4). The first counting spot (i.e. the starting point in Figure 6.4) was 2 mm away from the bottom of the sample. Four fields of view (henceforth referred as a quadrant) of size 250 µm × 250 µm were counted per spot. The distance between each quadrant was 1 mm (Figure 6.5). In total 9 counting spots per line in each thin section were counted. The cell counts were extrapolated to cell density i.e. cell counts / area of the counting spot.

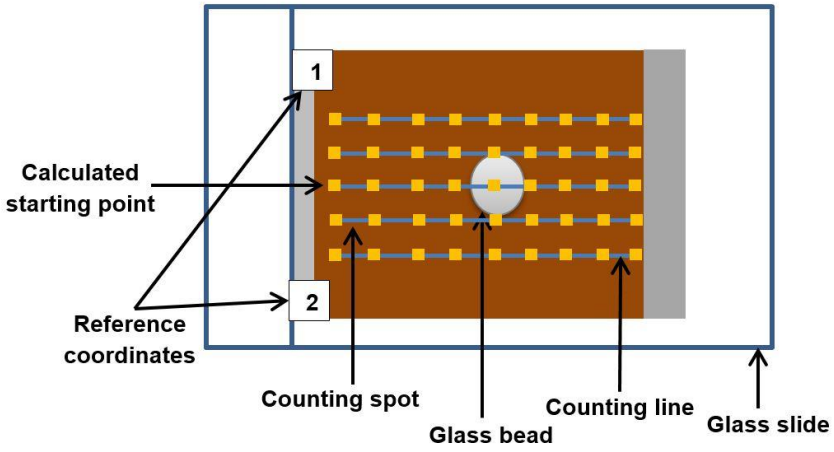

Figure 6.4: Diagrammatic representation of the counting procedure for the agarose experiment. Reference cordinates 1 and 2 were used to estimate the first countling line. The blue lines in the diagrams represents the counting line and yellow boxes in the represents each quadrant (counting spot).

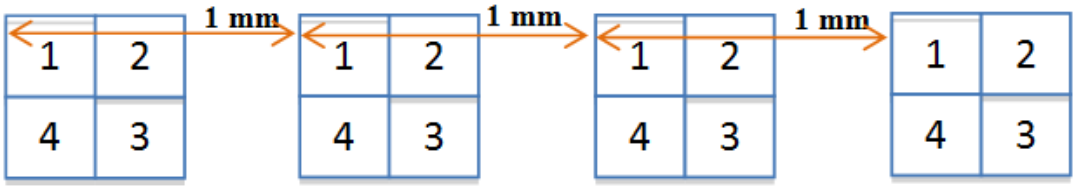

Figure 6.5: Diagrammatic representation of counting spots (250 µm × 250 µm) under the microscope for the agarose or the compost samples. The blue frame represents the microscopic field of view. The number in the box denotes the order in which bacteria was counted under each microscopic field of view.

6.2.1.7 Alignment of thin sections and image processing

To retrieve the same layer from the CT image stacks (thin section) that was used for quantifying bacteria, stereomicroscopic images of each thin section analysed for bacteria were taken. Also, the distance of each thin section from reference side measured earlier (in section 6.2.1.3) was used. The selection of each layer (thin section) from the CT image stacks was done by matching it by eye with the stereomicroscopic image (Figure 6.6).

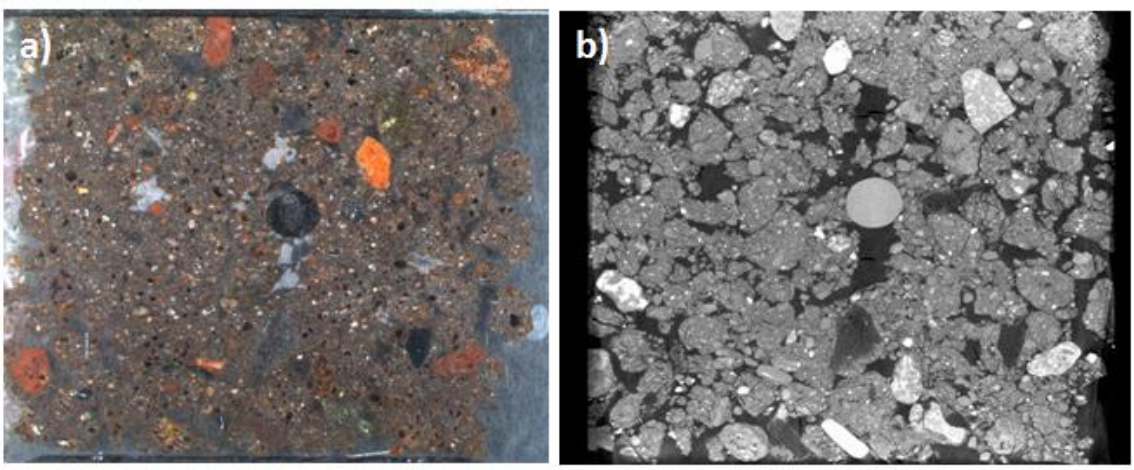

Figure 6.6: An example of alignment of a stereomicroscope images (a) and a CT images (b). The circle in the middle is the glass bead represnting the point of inoculation.

The selected image was then imported into ImageJ to crop the region of interest. The cropped region of interest resembles the same area where counting of bacteria was done in each thin section. Region of interest of each thin section was then thresholded using an in-house developed indicator kriging method (Houston et al.,2013)

To analyse the pore structure in 3D, the surrounding area from all ends for each quadrant (counting spot) was considered. Therefore, each counting spot for structural analysis was 1 mm in size. Since 1 voxel was 10.87 µm, each quadrant was 92 voxels in size. A macro was recorded in ImageJ to crop all the quadrants in each thin section. In-house developed software was used to quantify porosity, connectivity and surface area of the pores (Houston et al., 2013).

6.2.2 Compost experiment: colonising a local nutrient source from soil

6.2.2.1 Bacteria inoculum preparation

The strains used in this experiment were the wild type *Pseudomonas fluorescens* (SBW25) and *Bacillus* subtilis (DSM10). An overnight culture of both strains (details in section 2.3.1) was suspended in 10 ml of sterile PBS solution. This suspension was inoculated in soil as described below. Compost (Kompostierung Nord GmbH, Bremen, Germany) was used as a nutrient source in this experiment. The compost was "fine compost" with 0.90 % N, 0.25 % P, 0.50 % K, pH 6.9, organic matter 24.0 %, total carbon content 14.0 % and total nitrogen 1.05 %. The compost was sterilised twice by autoclaving at 121°C and 100 kPa for 20 minutes with a 24hr interval time.

6.2.2.2 Preparation of soil microcosms

The soil and PE rings used in this experiment were the same as those described for the Agarose experiment (section 6.2.1.2). Soil was packed at a bulk-density1.3 g cm^{-3} with moisture content equivalent to 50 % water filled pores. To obtain 50 % water filled pores, 0.1587 cm^3 of water was added per gram soil. The amount of soil required to pack in PE rings at bulk-density 1.3 g cm^{-3} was 4.22 g. The soil was then inoculated with 500 µl of bacterial suspension, mixed well and divided into two halves for packing. For control samples, soil was inoculated with 500 µl of sterile dH_20 instead of bacteria inoculum. Soil was poured in PE rings in two halves. After packing the first half of soil, 1 g of autoclaved compost layer was added and then remaining soil was added and packed at the desired bulk-density. Control samples were packed the same way. Three replicates per treatment were prepared, producing 9 soil microcosms in total. Microcosms were sealed in plastic bags to avoid drying of samples and incubated at 23°C in the dark. The plastic bags were opened and closed every alternate day for air exchange under a sterile bench. The soil microcosms were sampled after an incubation period of 14 days.

6.2.2.3 Impregnation of samples

Impregnation of samples was done in similar way as for the agarose samples (details in section 6.2.1.3).

6.2.2.4 Scanning of impregnated microcosms

Compost samples were scanned with the same settings as for the agarose samples (details in section 6.2.1.4).

6.2.2.5 Preparation of thin sections

The reference side of the block was glued onto a petrographic slide with epoxy resin as done for agarose samples. The blocks on the reference slides were cut down to 8 mm thickness with a diamond saw (Discoplan TS, Struers A/S, Denmark). The block on the reference slide was ground using a diamond coated cup-wheel grinder (Discoplan TS, Struers A/S, Denmark) to make the surface of the sample parallel and subsequently hand polished with a wet abrasive paper (P1200, Silicon carbide) on a glass plate in order to remove the grinding material and make the surface smooth. The thickness of the block was measured with a micrometer 0-25 mm (accuracy 2 µm; Mitutoyo, Japan) and referred to as d2 (i.e. the first section towards the centre of the block) in the figure 6.7. The distance measurement of the selected section from the reference side was done for later alignment with the CT scan data. A frosted petrographic slide of size 27 × 46 mm (Beta diamonds Inc, CA, USA) was then glued (Eukitt, Struers A/S, Denmark) onto the polished surface of the sample side and then the block was cut as close to the frosted slide as possible to get the first thin section referred to as dII (Figure 6.7). The dII slide was further ground to approximately 200 µm and subsequently polished. The thickness of the sections varied a bit after polishing as some sections had to be re-polished to get rid of the grinding material (after checking it under microscope).

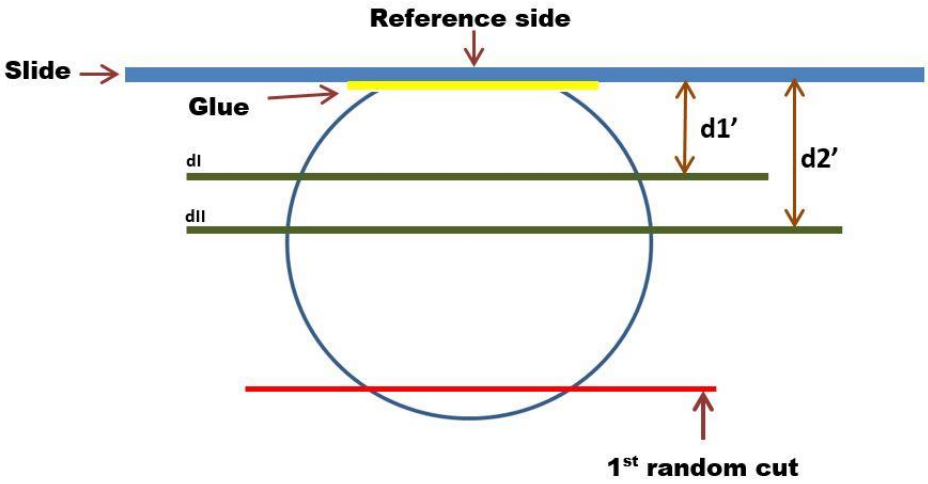

Figure 6.7: Schematic representation of the thin sections selected in samples of the compost experiment. The distance between two thin sections was kept 2.5 mm. The green lines represent the area where thin sections were selected.

The final thickness of the thin section was measured considering the thickness of slide and amount of glue added. After removing the first thin section (dII) by cutting, the remaining block was ground again with the cup-wheel grinder and subsequently polished as describes above. A new frosted slide was then glued onto the polished block and the same steps were repeated to make another thin section. This new thin section was referred to as dI; the corresponding distance to the reference side was referred to as d1. The distances d1 and d2 were used to calculate the final distances between the surface on the reference side and the surface of the sample referred to as d1' and d2', respectively. The thickness of each thin section was measured (table 6.2).

Table 6.2: Thickness of thin sections dI and dII per replicate in soil inoculated with *Pseudomonas* or *Bacillus* in soil packed at a bulk-density1.3 g cm^{-3} the of compost experiment.

Treatments	Replicates	Thickness of thin sections (µm)	
		dI	dII
Soil inoculated with *Pseudomonas fluorescens*	1	112	146
	2	126	167
	3	144	243
Soil inoculated with *Bacillus* subtilis	1	54	141
	2	169	156
	3	147	157
Soil inoculated with dH_20 (Control)	1	160	182
	2	108	191
	3	174	113

6.2.2.6 Enumeration of bacteria on thin sections

The quantification of bacteria in compost samples was done in the same way as the agarose samples except for the selection of first counting line. For compost samples, the first counting line was always from the centre of the section based on the coordinates 1 & 2 (Figure 6.8), perpendicular to the layer of compost. Also, the first counting spot (starting point in Figure 6.4b) was 1 mm away from the bottom of the sample.

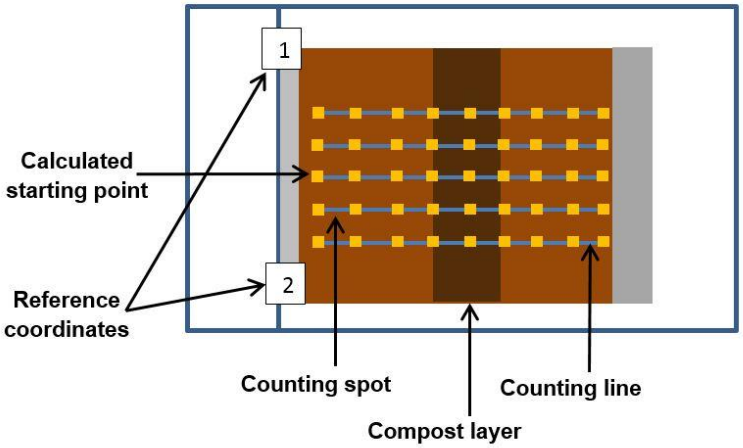

Figure 6.8: Diagrammatic representation of counting procedure for the compost experiment. Reference cordinates 1 and 2 in the diagrams are used to estimate the first countling line. The blue lines in the diagrams represents the counting line and yellow boxes represent the quadrants (counting spots).

6.2.2.7 Alignment of thin sections and image processing

The alignment of thin sections and selection of region of interest was done in a similar manner as for the agarose samples (section 6.2.2.7) (Figure 6.9).

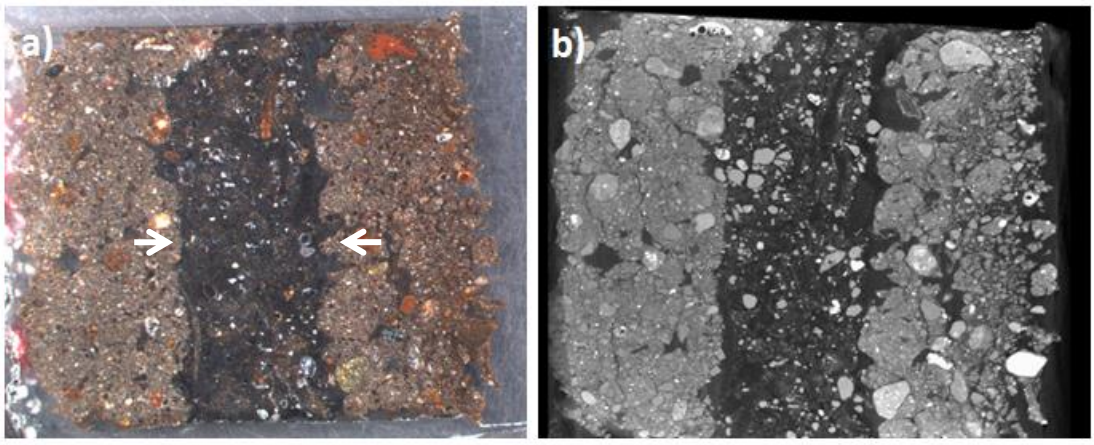

Figure 6.9: An example of alignment of stereomicroscope images (a) and a CT image (b). The dark material in the centre (white arrrow) is the layer of compost.

For the compost experiment, voxels containing compost were excluded from analysis of soil structure, as the grey-scales of compost were distinct from other

solids and inclusion of compost led to wrong identification of solid and pores as the analyses methods have been developed only for 2-phase systems. Since the compost layer was irregularly distributed, some quadrants had a mixture of soil and compost. Spots where the proportion of compost was higher than soil were excluded from the analysis as these would lead to erroneous estimates (Figure 6.10). Each of the remaining quadrants was then cropped to a size 93 x 93 x 93 voxels as for agarose samples.

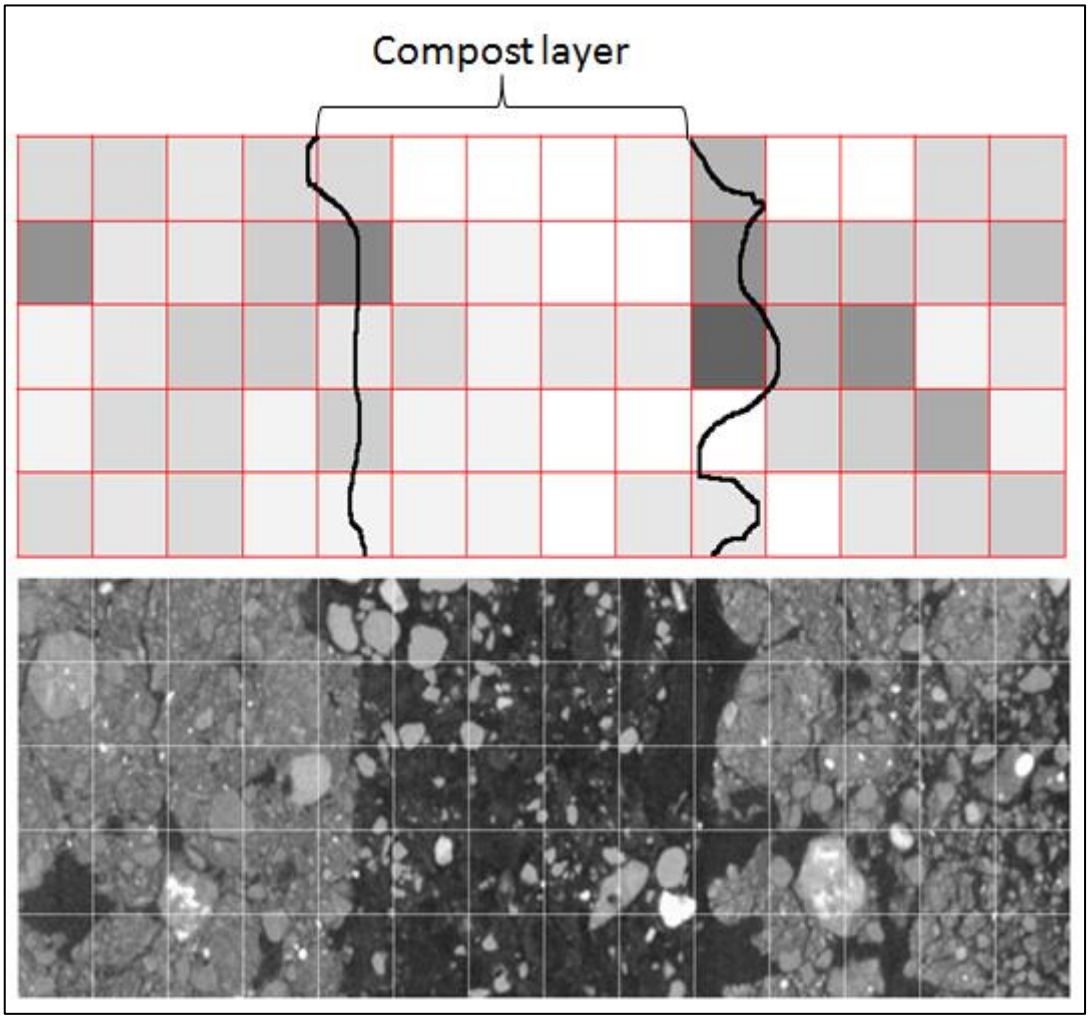

Figure 6.10: An example of how the compost layer is defined in thin sections for pore characteristics analysis. The compost layer was exculded from the pore characteristics analysis.

6.2.3 Statistical analysis

Statistical analysis was performed using SPPS version 22. A mixed effect linear model (assuming normal distribution) was used to investigate differences in soil structure properties for different treatments. To comply with the normality assumption the porosity and connectivity measures were transformed using the probit function. The soil-pore interface measures met the normality assumption; hence they did not require any preliminary transformation. A generalised mixed effect Poisson model with log link function was used to investigate significant difference in bacterial cell density between different treatments with thin sections and treatments as fixed factor. The effect of soil structure properties such as porosity, connectivity and soil-pore interface on the extent of spread of bacteria was also analysed by a Poisson model with thin sections as a fixed factor. The size of each quadrant was introduced as an offset variable in the Poisson model.

6.3 Results

6.3.1 Agarose experiment: colonising soil from a local source

6.3.1.1 Effect of bulk-density on bacterial cell densities in thin sections

6.3.1.1.1 Visualization of *Pseudomonas* cells in soil thin sections

Under UV excitation with the DAPI filter set, black quartz particles were surrounded with clay and organic particles. *Pseudomonas* cells stained with DAPI appeared bright blue in colour against a brown coloured soil background. The black quartz particles surrounded the organic matter and clay particles. The

pore area filled with resin appeared blue in colour under UV excitation. Inoculated *Pseudomonas* cells appeared bright blue in colour and were scattered either on the soil matrix or at soil-pore interface. It was easy to distinguish *Pseudomonas* cells from some of the autofluorescent soil components as they appeared yellowish in colour. *Pseudomonas* was observed as single cell or in small colonies on soil aggregates (Figure 6.11).

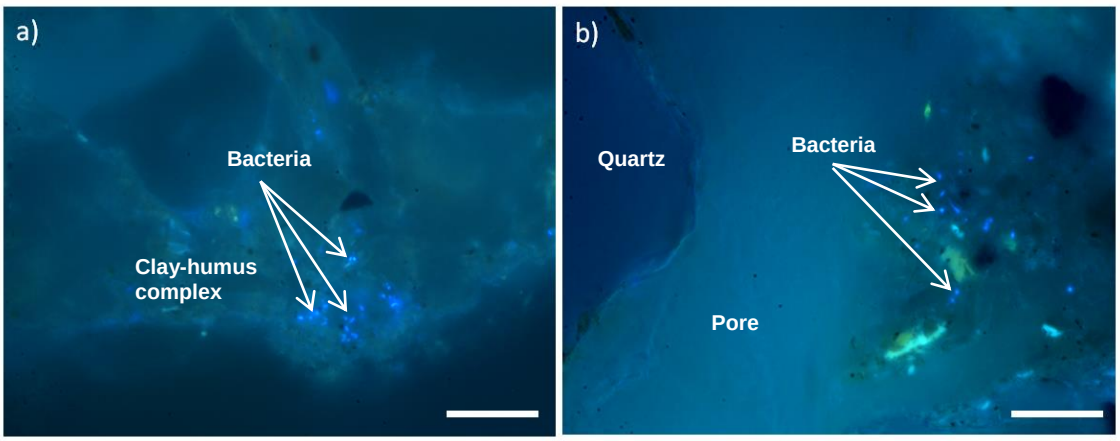

Figure 6.11: DAPI stained *Pseduomonads* cells in lower (a) and higher (b) bulk-density soil thin sections of the agarose experiment. Bacterial cells are bright blue in colour, Scale bar 20 µm.

For a visual comparison of the extent of *Pseudomonas* spread in soil packed at different bulk-densities, spatial maps (definition in M&M) of cells counted at each quadrant of a thin section were prepared (Figure 6.12).The spatial maps showed an effect of bulk-density on the spread of *Pseudomonas* cells. Both soil densities showed a substantial variability at the micro-scale with wide ranging bacterial densities. *Pseudomonas* cells ranged from 0 to 33 cells per quadrant in soil with low bulk-density and from 0 to 23 cells per quadrant in soil with high bulk-density. In control samples, bacterial cells ranged from 0 to 11 in soil with a low bulk-density and 0 to 6 in soil with a high bulk-density. It was evident from

spatial maps that *Pseudomonas* cells spread further from the from the source of inoculum in soil packed at 1.3 g cm^{-3} compare to soil packed at 1.5 g cm^{-3}, as is evidenced by the higher numbers at distances away from the inoculum. Some quadrants were observed to be completely devoid of cells. The proportion of quadrants with empty cells was greater in soil packed at 1.5 g cm^{-3} compare to soil packed at 1.3 g cm^{-3} (Figure 6.12a).

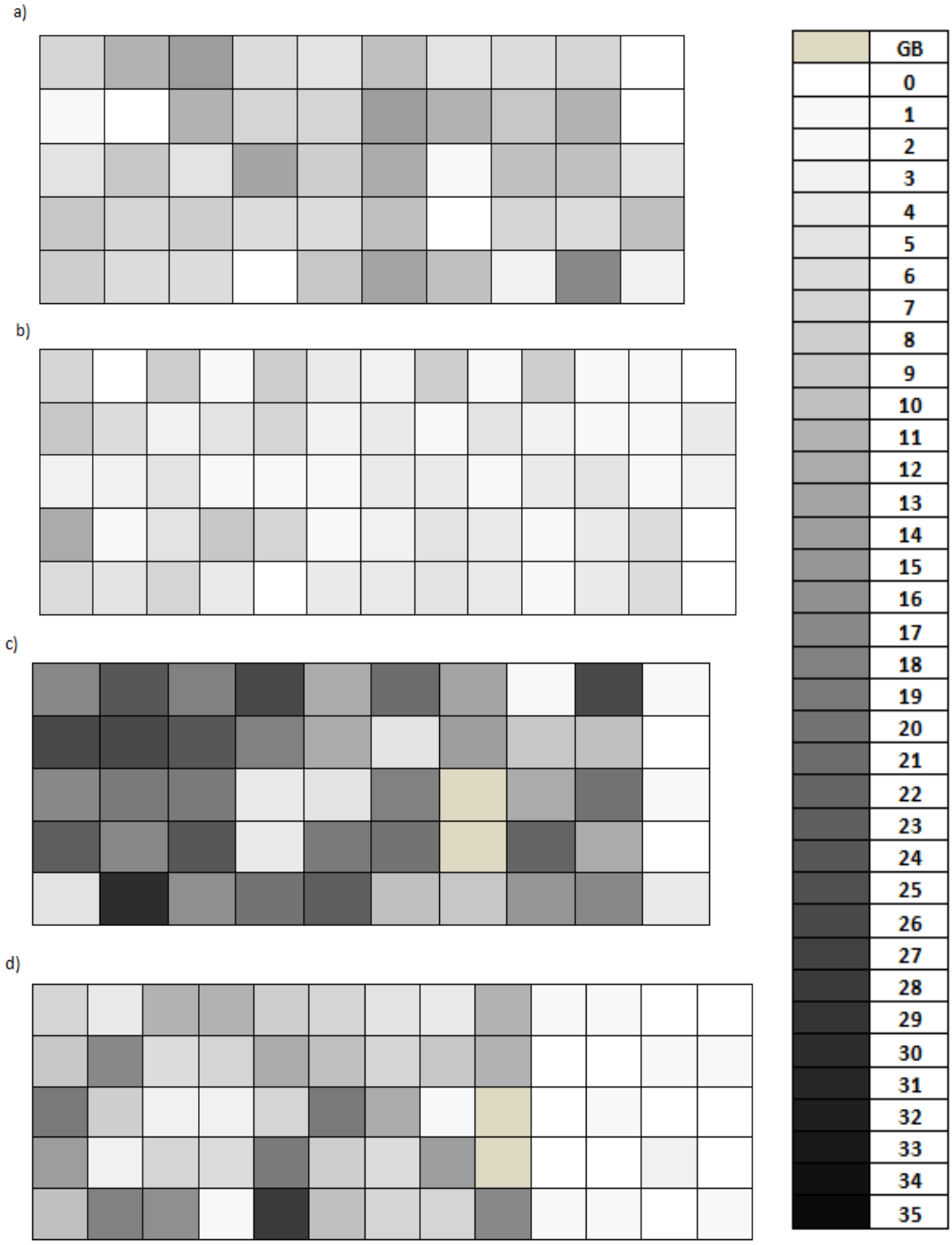

Figure 6.12: Spatial maps of *Pseudomonas* cell counts in soil packed at lower (a, c) and higher (b, d) bulk-density. Examples of cell counts in thin sections dI (a, b) and dII (c, d) of one replicate are presented. Each box represents one quadrant. The grey scale bar represents the range of bacterial cell counts. Scale bar 10-13 mm.

6.3.1.1.2 Quantification of *Pseudomonas* cells in soil thin sections

On average, bacterial cell density was 42 % higher in soil with the lower bulk-density ($P<0.001$) with 174 (s.e 6.3) cells mm^{-2}, compared to soil packed at the higher bulk-density which had a bacterial density of 99 (s.e 4.3) cells mm^{-2} (Figure 6.13). In control samples, bacterial cell density was 26 (s.e 4.3) cells mm^{-2} for soil packed at bulk-density 1.3 g cm^{-3} and 14 (s.e 1.1) cells mm^{-2} for soil packed at bulk-density 1.5 g cm^{-3}. In both treatments, bacterial cell density in control samples was significantly ($P<0.001$) lower than for samples inoculated with *Pseudomonas* bacteria.

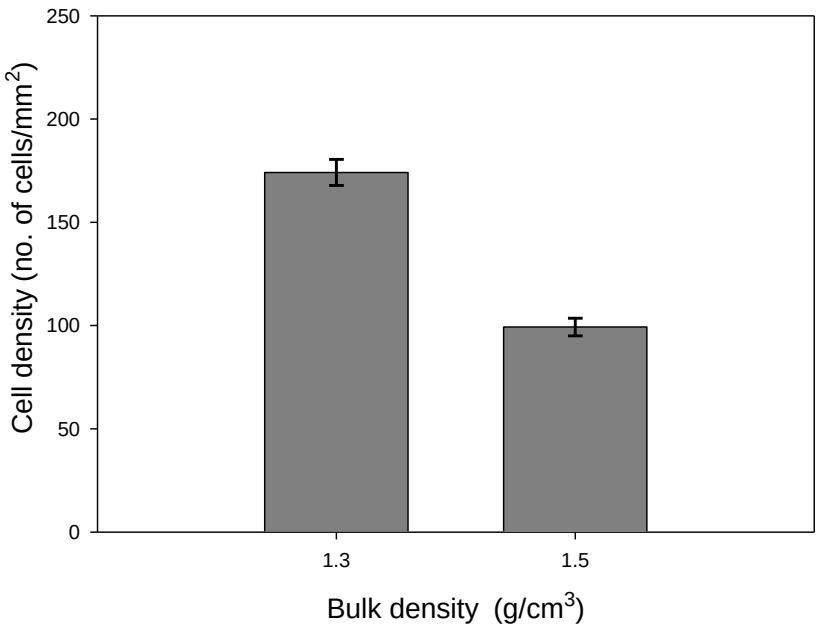

Figure 6.13: Mean bacterial cell density at different distance from the source of inouclum in lower 1.3 g cm^{-3} (a) and higher 1.5 g cm^{-3} (b) bulk-density soil. Data are mean ± SE (n=3).

Mean cell density was significantly ($P<0.001$) higher in thin sections closer to the inoculation point source compared to the other thin sections that were at a further distance (Figure 6.14). On average, bacterial cell density in thin section dII were 212 (s.e 10.0) cells mm^{-2} for soil packed at 1.3 g cm^{-3} and 107 (s.e 5.7)

cells mm^{-2} for soil packed at 1.5 g cm^{-3} compare to thin section dI where it was 136 (s.e 6.2) cells mm^{-2} for soil packed at 1.3 g cm^{-3} and 92 (se 6.3) cells mm^{-2} for soil packed at 1.5 g cm^{-3}. The difference in mean cell density between two thin sections was 36 % in lower bulk-density soil and 14 % for soil packed at bulk-density 1.5 g cm^{-3}. The most likely explanation for this is that section dI is further removed from the inoculum than section dII. Therefore, these results confirm that *Pseudomonas* cells dispersed further from the inoculation point source in soils packed at 1.3 g cm^{-3} compare to soil packed at 1.5 g cm^{-3}.

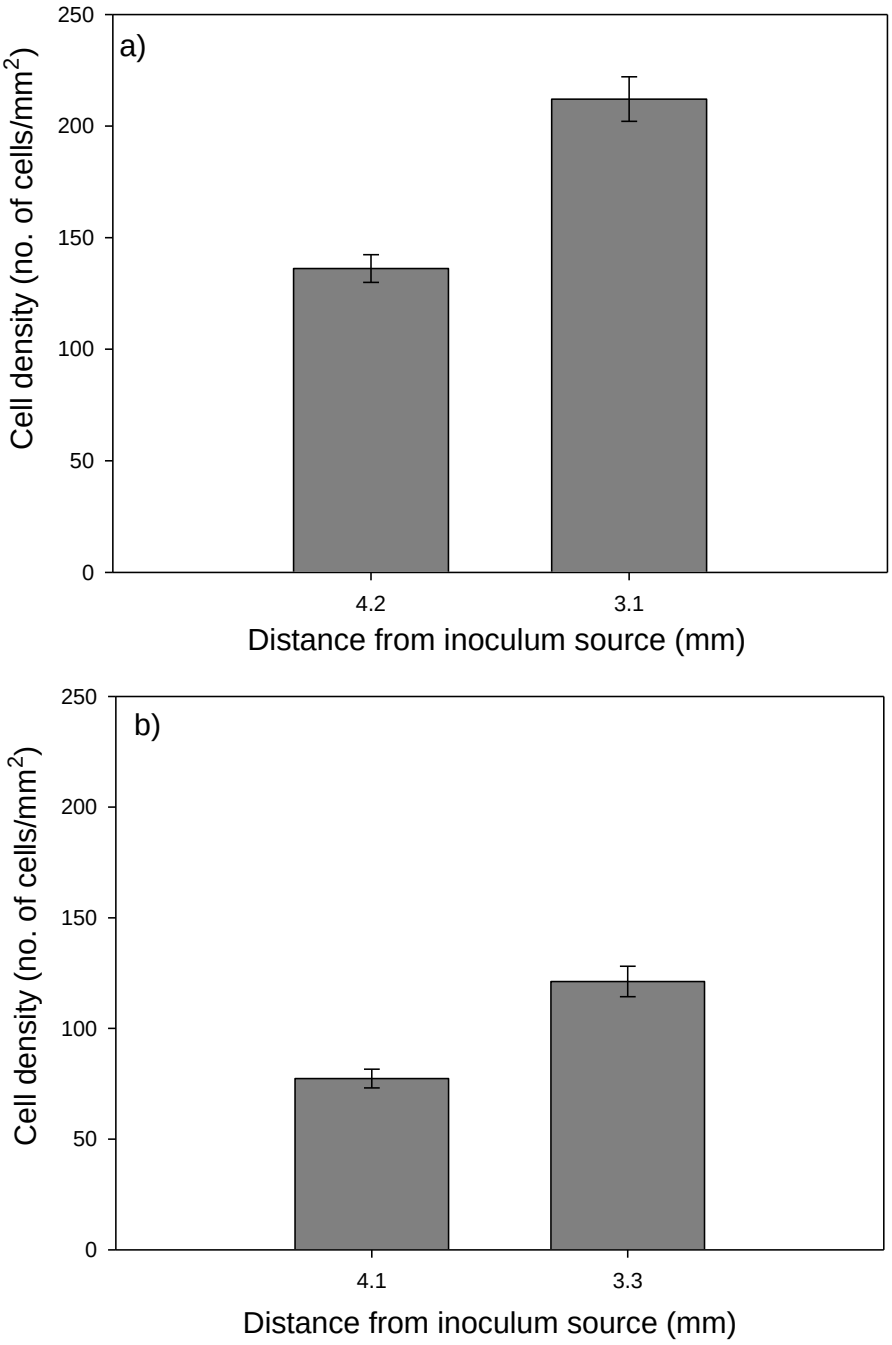

Figure 6.14: Mean bacterial cell density at different distances from the source of inouclum in lower (a) and higher (b) bulk-density soil. Data are mean ± SE (n=3).

6.3.1.2 Effect of bulk-density on pore geometry of soil

Pore geometry of soil packed with different bulk-densities was analysed at the microscale (i.e. each quadrant) in 3D. Porosity of the analysed area ranged from 0-100 %, soil connectivity ranged from 0-100 % and the soil-pore interface ranged from 0-10 mm^2 for soil packed at bulk-density1.3 g cm^{-3} and 0- 7 mm^2 for soil packed at bulk-density 1.5 g cm^{-3} (Figure 6.14 & 6.15). Between different bulk-density treatments, the average porosity of soil packed at bulk-density 1.3 g cm^{-3} was higher with 24 (s.e 0.01) % compare to soil packed at higher bulk-density 1.5 g cm^{-3} with 22 (s.e 0.01) %, the difference was not significant (p= 0.389). The connectivity of pores also showed no significant (p= 0.456) difference between the two treatments, with an average connectivity of 84 (s.e 0.01) % for soil packed at a lower bulk-density and 83 (s.e 0.01) % for soil packed at higher bulk-density. Average soil-pore interface significantly (p= 0.000) declined with increasing bulk-density from 4.86 (s.e 0.09) % in soil packed at lower bulk-density to 3.68 (s.e 0.06) % in soil packed at higher bulk-density.

6.3.1.3 Influence of soil pore geometry on the extent of *Pseudomonas* spread in soil

Cell density of *Pseudomonas* was plotted against soil porosity, connectivity and soil-pore interface of each quadrant for each bulk-density treatment (Figure 6.14 & 6.15). The porosity of the quadrants ranged from 0-100 % with the majority having porosity between 0-40 %. The pore connectivity value ranged from 0-100 % with the majority of the quadrants having a connectivity of either 0 % or a connectivity between >85 %.The soil-pore interface ranged from 0-10 mm^2 with

the majority of the quadrants having a soil-pore interface between 2-7 mm^2 for soil packed at 1.3 g cm^{-3} and 2- 5 mm^2 for soil packed at 1.3 g cm^{-3} (Figure 6.14 &6.15).

Some of the soil pore geometry characteristics showed an effect on the extent of *Pseudomonas* spread in both bulk-density treatments. The p-value of each treatment is listed appendix III. Soil porosity (p=0.001) and soil-pore interface (p= 0.000) significantly affected the spread of *Pseudomonas* in soil packed at the lower bulk-density. Where soil was packed at a higher bulk-density, soil-pore interface (p= 0.001) significantly affected the spread of *Pseudomonas* in soil, but soil porosity didn't (p= 0.264). In both bulk-density treatments, connectivity of pores showed no significant effect (p= 0.565 for 1.3 g cm^{-3} and p= 0.165 for 1.5 g cm^{-3}) on the spread of *Pseudomonas* in soil.

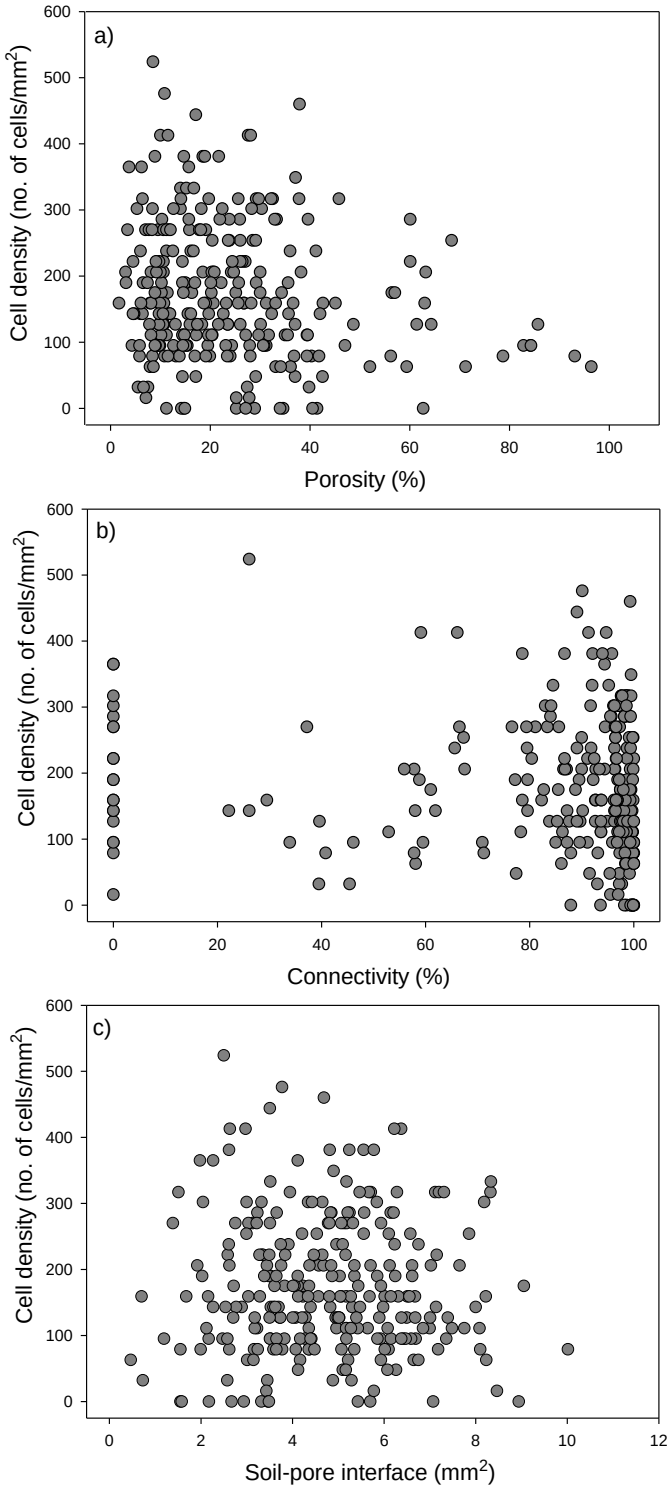

Figure 6.15: Relationship of *Pseudomonas* cell density with soil porosity, connectivity and soil-pore interface in soil thin sections packed at bulk-density1.3 g cm^{-3}. Each data point in the graph represents one quadrant (counting spot) analysed in each replicate of a thin section.

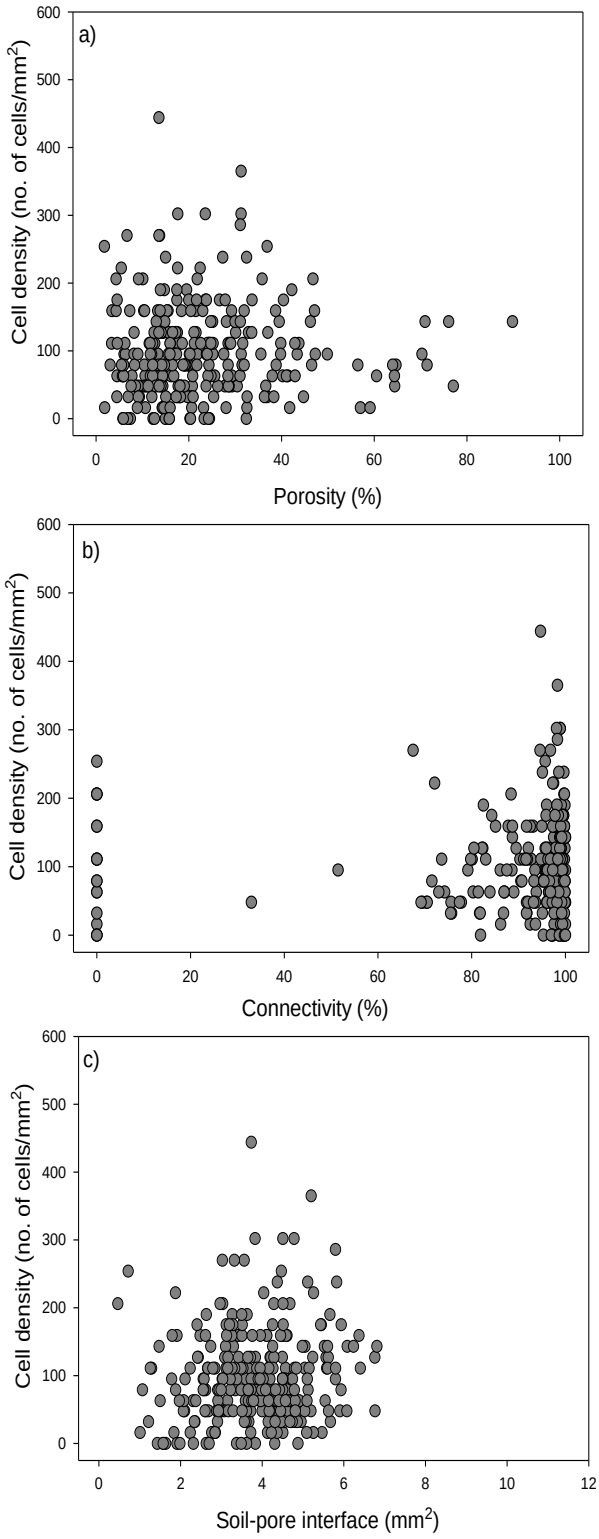

Figure 6.16: Relationship of *Pseudomonas* cell density with soil porosity, connectivity and soil-pore interface in soil thin sections packed at bulk-density1.5 g cm^{-3}. Each data point in the graph represents one quadrant (counting spot) analysed in each replicate of a thin section.

6.3.2 Compost experiment

6.3.2.1 Bacteria cell density gradient in thin sections

6.3.2.1.1 Visualization of bacteria in soil thin sections

Both *Pseudomonas* and *Bacillus* cells in inoculated samples appeared bright blue in colour against the soil and compost background under a UV excitation filter. Figure 6.17 shows an example of the distribution of *Pseudomonas* cells in different regions of compost layer. The compost layer appeared brownish black in colour and some materials in compost exhibited very high autofluorescence (Figure 6.17a). Due to this high autofluorescence it was difficult in some areas to detect bacterial cells in compost layer.

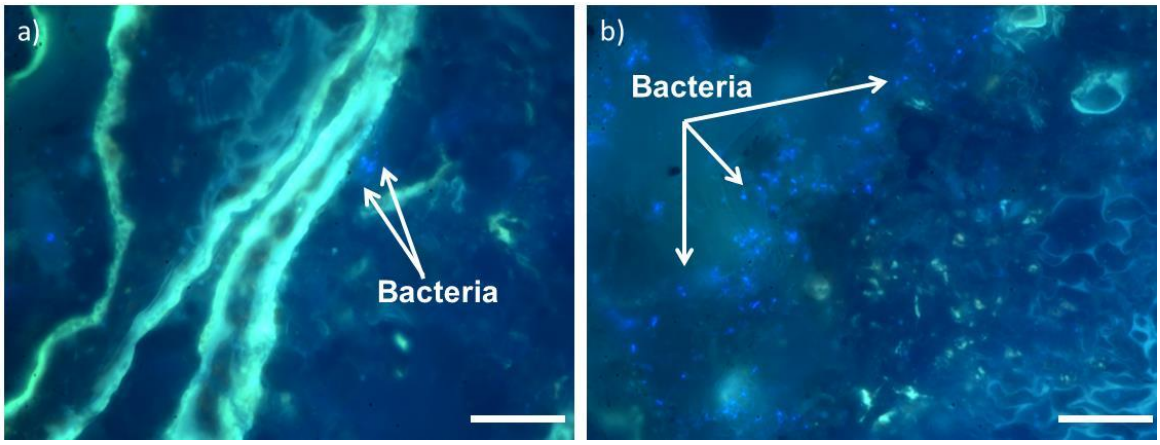

Figure 6.17: DAPI stained *Pseudomonas* cells in compost layer of soil thin sections. Examples of very few (a) to high (b) colonisation of cells in compost layer of soil, scale bar 20 µm. The bright stripes (a) are some materials in the compost layer that exhibit very high autofluorescence.

Figure 6.18 shows spatial maps of *Pseudomonas* and *Bacillus* cells counted at each quadrant for visual comparison of the cell density distribution with respect to the compost layer. In compost layer, cell counts ranged between 0-48 cells per quadrant for *Pseudomonas* and 0-41 cell per quadrant for *Bacillus* bacteria. Some of the quadrants were devoid of cells. From the spatial maps it can be seen that *Pseudomonas* inoculated samples showed more colonization in the compost layer (Figure 6.18a) as compared to *Bacillus* inoculated samples (Figure 6.18b).

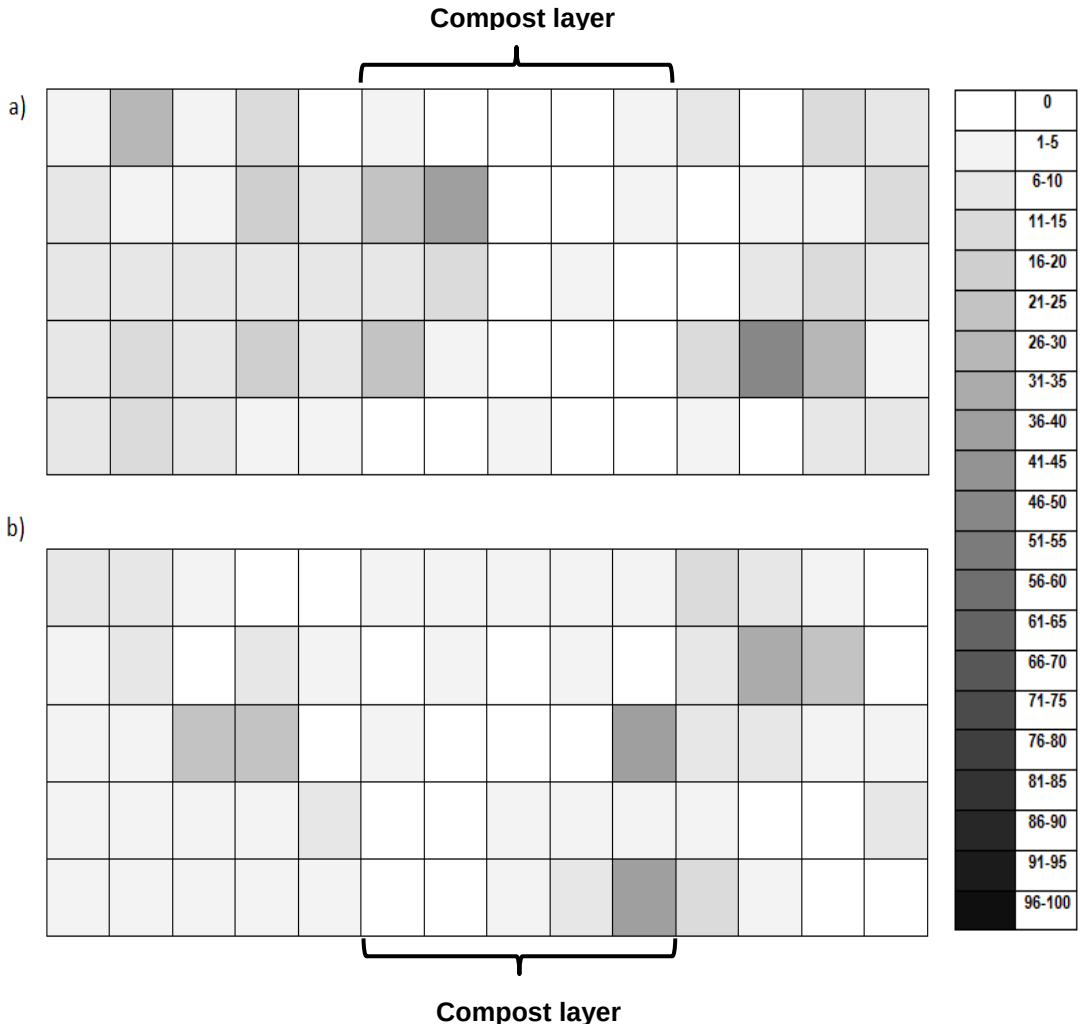

Figure 6.18: Spatial maps of *Pseudomonas* (a) and *Bacillus* cell counts (b) in compost experiment. Examples of cell counts in thin sections dII of one replicate are presented. Each box represents one quadrant. The brace indicates the compost layer in each thin section. The grey scale bar represents the range of bacterial cell counts. Scale bar 14 mm

6.3.2.1.2 Quantification of bacterial cells in soil thin sections

Figure 6.19 shows the mean cell density in the compost and soil layer of *Pseudomonas* or *Bacillus* inoculated samples. Mean cell density of *Pseudomonas* was 71.6 (s.e 9.5) cells mm^{-2} and *Bacillus* was 56.9 (s.e 9.3) cells mm^{-2} in the compost layer. Whereas in soil layer mean cell density of *Pseudomonas* was 194 (s.e 13.5) cells mm^{-2} and *Bacillus* was 85 (s.e 5.4) cells mm^{-2} in soil layer. Although the mean cell density in the compost layer was lower compared to the soil layer in both inoculated treatments, the difference was significant (p= 0.001) only in *Pseudomonas* inoculated samples. In control samples, cell density was 17 (s.e 1.9) cells mm^{-2} in the soil layer and 13 (s.e 1.3) cells mm^{-2} in compost layer. The mean cell density was significantly lower (p= 0.00) in control samples in compost layer compare to the inoculated samples.

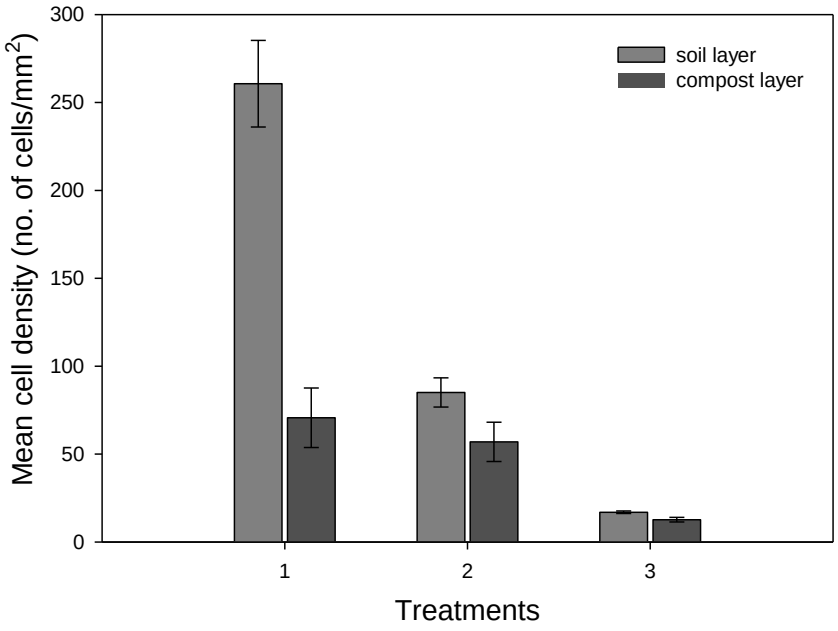

Figure 6.19: Mean bacterial cell density in compost (light grey) and soil (dark grey) inoculated with *Pseudomonas*(1) , *Bacillus* (2) and control soil samples (3). Data are mean ± SE (n=3).

Figure 6.20 shows the cell density gradient of *Pseudomonas* and *Bacillus* at different distances from soil towards the compost layer. The cell density of both inoculated treatments was quite variable at different distances towards the compost layer. For example, at 0 mm *Pseudomonas* cell density was 220 (s.e 41.7) cells mm^{-2} at 0 mm, 194 (s.e 25.0) cells mm^{-2} at 1 mm, 239 (s.e 35.2) cells mm^{-2} at 2 mm and 215 (s.e 36.2) cells mm^{-2} at 3 mm distance from the compost layer. In case of *Bacillus* inoculated treatment , cell density was 95.5 (s.e 14.2) cells mm^{-2} at 0 mm, 113 (s.e 14.7) cells mm^{-2} at 1 mm, 91 (s.e 14.2) cells mm^{-2} at 2 mm, 91 (s.e 12.2) cells mm^{-2} at 3 mm and 103 (s.e 24.4) cells mm^{-2} at 4 mm distance from the compost layer. This difference in the gradient of cell density, however, was not significant in either inoculated treatment. Therefore, within the range of distances investigated no evidence of bacterial cell gradient towards the compost layer was observed.

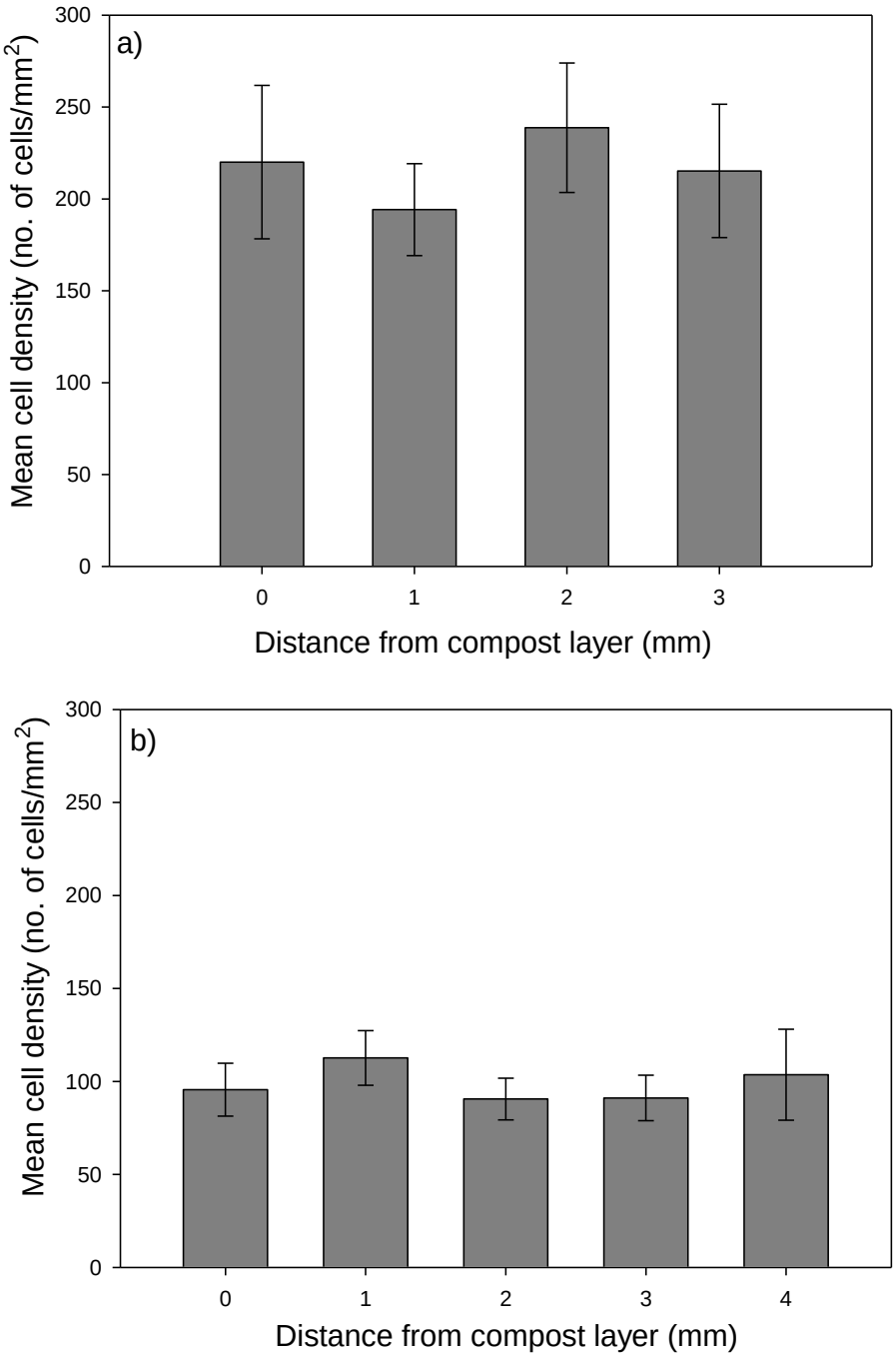

Figure 6.20: Mean bacterial cell density in soil at different distances from the compost layer for *Pseudomonas* (a) or *Bacillus* (b) inoculated soil samples. Data are mean ± SE (n=3).

6.3.2.2 Influence of soil pore geometry on the spread of bacteria compost in soil

Cell density was plotted against soil porosity, connectivity and soil-pore interface of each quadrant for *Pseudomonas* and *Bacillus* inoculated treatment (Figure 6.21 & 6.22). The porosity of the quadrants ranged from 0-90 % with the majority having porosity between 0-30 %. The pore connectivity value ranged from 0-100 % with the majority of the quadrants having a connectivity either at 0 % or between 95-100 % .The soil-pore interface ranged from 0-10 mm^2 with the majority of the quadrants having a soil-pore interface between 1-5 mm^2. Pore characteristics showed significant ($p<0.05$) effect on the spread of towards compost in soil. The p-value of each treatment is listed in appendix III. Soil porosity and connectivity were observed to influence the distribution of *Pseudomonas* (p= 0.000 for porosity, p= 0.000 for connectivity) and *Bacillus* (p= 0.000 for porosity, p= 0.003 for connectivity) in soil. Soil-pore interface significantly influenced the distribution of *Pseudomonas* (p= 0.000) inoculated samples.

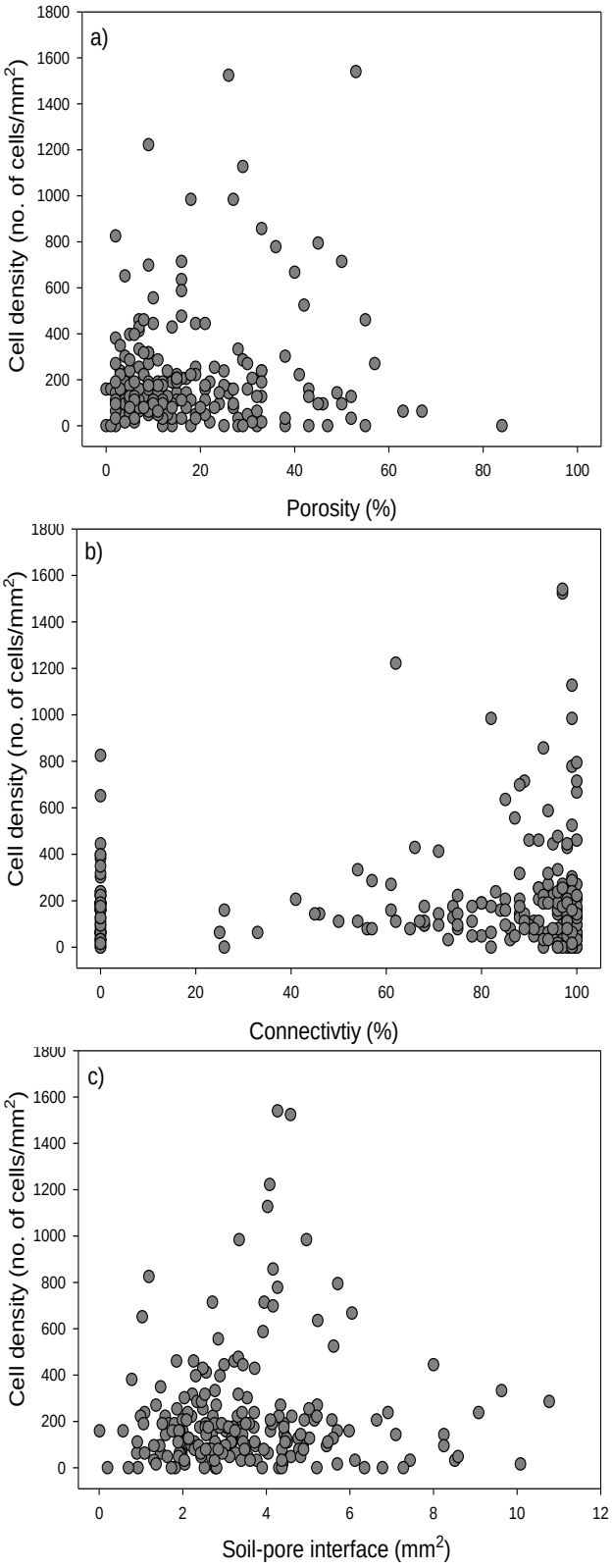

Figure 6.21: Relationship of *Pseudomonas* cell density with porosity, connectivity and soil-pore interface. Each data point in the graph represents one quadrant (counting spot) analysed in each replicate of a thin section.

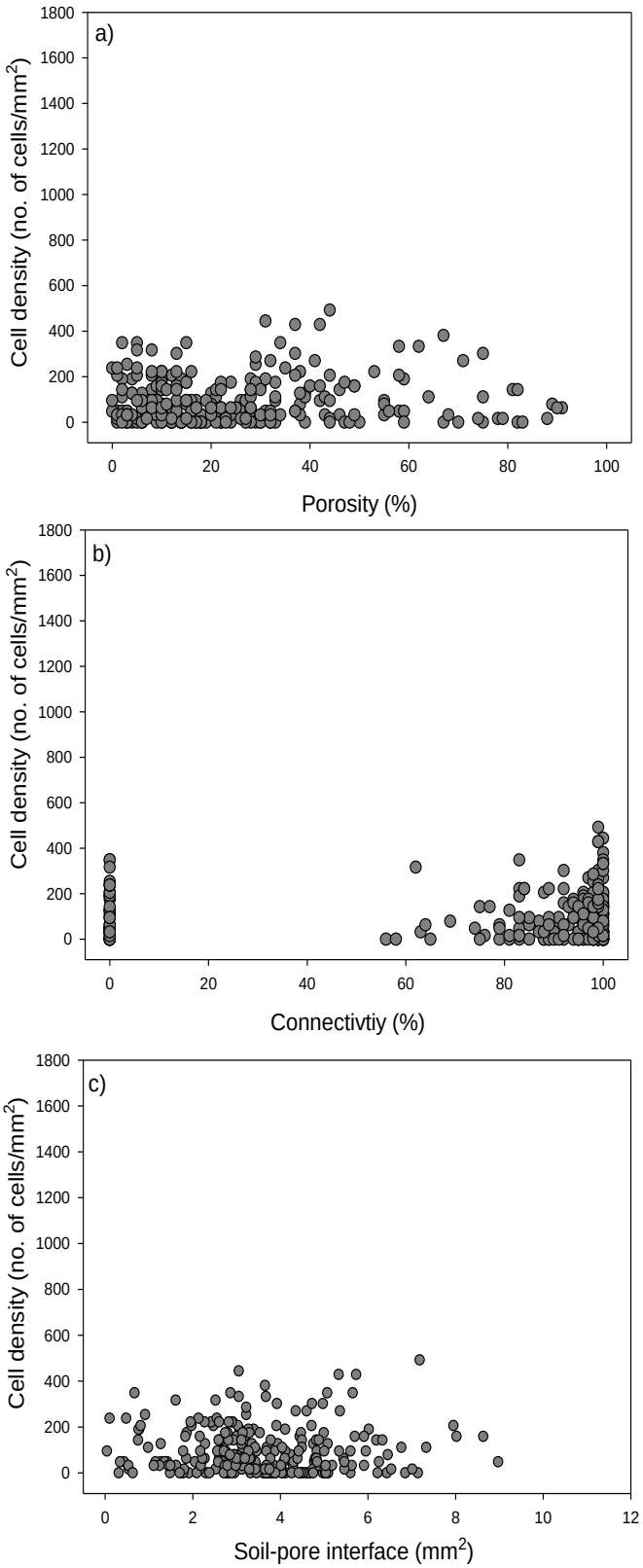

Figure 6.22: Relationship of *Bacillus* cell density with porosity, connectivity and soil-pore interface. Each data point in the graph represents one quadrant (counting spot) analysed in each replicate of a thin section.

6.4 Discussion

In this chapter the influence of soil pore geometry on the spatial spread of bacteria towards and away from localised nutrients in soil was investigated. The experimental set up was different in both the cases but the incubation time and analysis method was the same. Significant colonisation of *Pseudomonas* from a local source into soil was observed. However, no significant colonisation of *Pseudomonas* and *Bacillus* from soil into a compost layer was observed.

6.4.1 Agarose experiment: colonising soil from a local source

In this experiment, the introduction of bacteria in the form of agarose pellet into soil has been proposed as way to introduce bacteria in solid form. Because some amount of water is already present in soil, additional liquid suspension of bacteria inoculum would influence spread of introduced bacteria in soil, as water movement would occur and lead to redistribution of bacteria immediately after introduction. The effect of this was discussed in Chapter 4. The introduction of a localised source of inoculum and nutrients resulted into dispersion of bacteria into the soil. From the spatial maps of both treatments (Figure 6.10) it was evident that *Pseudomonas* cells had colonized the surrounding soil area. A plausible explanation for this is that *Pseudomonas* exhibited chemotactic responses towards the nutrient present in the soil, as the source of inoculation was nutrient poor compared to the soil. The spatial map showed variability in cell counts range at different distances from the inoculation point. This could be due to the concentration of nutrients available in different region of soil, e.g. nutritional heterogeneity at microscopic scales, but it may also reflect different pathways for spread. Sood (2003) showed higher numbers of *Pseudomonas*

fluorescens cells attracted towards substances exuded by vesicular-arbuscular mycorrhizal roots compared to non-vesicular arbuscular mycrorrhizal roots. Higher response of *Pseudomonas fluorescens* WCS365 towards substances from root exudates of tomato was also observed by Weert et al. (2002). They showed *P. fluorescens* was attracted towards some organic acids and amino acids in root exudates of tomato. Another study by Neal et al. (2012) showed similar high chemotactic response of *Pseudomonas putida* towards metabolites from roots exudates of maize roots. A difference in the spread rate of bacteria between two treatments was also observed. This could be due to the pore geometry distribution as the amount of bacteria added in both treatments was the same. A difference in average cell counts between two treatments was also observed in dispersed samples. *Pseudomonas* numbers were also estimated in dispersed samples to determine the proportion being analysed in thin sections (appendix II). The cell counts in the dispersed samples were more than that analysed in thin sections. In soil packed at lower bulk-density cell counts was 7.90E+07 (s.e 9.58E+06) cells per g of soil in dispersed samples and 3.35E+06 (s.e 1.21E+05) cells per g of soil in thin sections and, in soil packed at higher bulk-density cell counts was 4.53E+07 (s.e 5.03E+06) cells per g of soil in dispersed samples and 2.21E+06 (s.e 9.45E+04) cells per g of soil in thin sections. This difference in cell counts in thin sections could be either due to insufficient staining of *Pseudomonas* cells in thin sections or detection of cells would have been harder due to high autofluorescence in soil. Another reason could be that the cells were in highly clustered which made it difficult to differentiate how many cells were present in that region.

Bacterial numbers showed high variability in the distribution of bacteria at different distances from the inoculation point. The number of bacteria was higher in the thin section closer to the inoculation point compared to the other one in both treatments. This may be because the distance to access nutrients in soil was shorter in thin section dII compared to thin section dI. A study by (Nunan et al, 2002) also showed a high degree of aggregation of bacterial cells in surface soil compared to subsoil. Another study by (Dechesne et al., 2005) also found a high variability in distribution of introduced bacteria *Pseudomonas putida* in soil columns. Another reason may also be that by the sampling time, bacteria might have grown and colonised this section more than the other section. Bacterial numbers were estimated (by CARD-FISH) in dispersed samples of both treatments showed an increase in cell counts on day 14 compare to day 1. For example, *Pseudomonas* cell counts increased from 7.33E+07 (s.e 5.11E+06) on day 1 to 1.37E+08 (s.e 2.04E+08) on day 14.

Among the two treatments, the hypothesis that increasing bulk-density would affect the spread rate of bacteria in soil did apply, and a decrease in the spread of bacteria with increasing bulk-density was observed. This result confirms the findings in chapter 3 where a decrease in growth rate of bacteria overtime with increasing bulk-density was observed. As mentioned in chapter 3, this difference could be due to alterations in soil pore geometry which limited the access of bacteria to nutrients in soil. The pore geometry of each quadrant where bacteria were counted was also analysed. Results showed that only connectivity and soil pore interface area of pores was affected with increasing bulk-density. Soil porosity of both bulk-densities was quite similar. This may be

because the pores analysed here were limited to the scanning resolution (i.e. only pores greater than 10.87 µm were analysed here).

To investigate if the pore geometry did influence the spread rate of bacteria in soil, pore characteristics of each quadrant (where bacteria was enumerated) were analysed at microscale (for definition see chapter 5 2.3). Soil porosity showed a significant influence on the extent of *Pseudomonas* spread only in soil packed at lower bulk-density. The exact reason for this difference is unknown as no significant difference in porosity between these two treatments at microscale was observed. One reason could be that pores observed here are just the percent of pores >10.87 µm and there must be more volume of pores in soil packed at lower bulk-density compare to soil back at higher bulk-density. Another reason can be that the pores detected here are air-filled pores whereas majority of bacteria are located in water filled pores. No significant influence of pores connectivity with bacterial cell density was observed in both treatments. This could be explained by the fact that the majority of visible pores analysed here were highly connected. Some bacterial cell density was observed in 0 % connected pores This may appear counterintuitive, as connectivity is required for bacteria to move, but it is possible that these pores are connected through pores below the scanning resolution limitation, but large enough for bacteria to move through. A significant influence of soil-pore interface of pores on bacterial cell spread rate was observed in both lower and higher bulk-density treatment. A plausible explanation for this is that nutrients might have been readily available to bacteria as they are transported through soil and, therefore, bacteria might have colonised near the vicinity of these pores. Therefore, in the present study some of the soil pore characteristics like porosity and soil-pore

interface showed significant influence on the extent of bacteria spread in soil at microscale.

6.4.2 Compost experiment: colonising local nutrient spot from soil

In this experiment, the objective was to study the extent of spread of bacteria towards a higher nutrient (carbon) source in soil. Compost was chosen as a natural form of nutrient source as addition of compost to soil is known to stimulate microbial activity and enhance soil fertility (Pérez-Piqueres et al., 2006; Ros et al., 2006; Bastida et al., 2008). Analysis of sterilised soil and compost used in the present study showed that the amount of total C and Organic matter in compost was 77 % higher than in the soil. This shows that the compost was higher in nutrient source compare to soil and theoretically bacteria should show a sharp gradient towards the higher nutrient source in soil. However, chemotactic response of bacteria could be either towards or away from the organic components present in the compost layer. In this study, two different type of bacterial strain was used to investigate the chemotactic response of individual bacteria towards compost and whether the pore characteristics influenced the spread of these bacteria towards compost in the soil microcosms.

The spatial maps showed colonization of both *Pseudomonas* and *Bacillus* in compost layer. However, the mean cell density of both bacterial strains was higher in the soil layer compare to the compost layer. Also, there was no gradient in cell density of either bacteria towards the compost layer. This was most likely due to sampling time, as bacteria might have spread and colonized the compost layer from chapter 4 it was observed that *Pseudomonas*and

Bacillus spread further within 2-3 days and by the sampling time most of the bacterial cells were dead. This results is opposite to that observed by Gaillard & Chenu (1999), who found high abundance of microorganisms near the wheat straw in soil cores over several millimetres. Chenu et al. (2001) also showed that addition of substrate on surface of aggregate induced a large number of bacteria and fungi in soil aggregates. But the incubation time of their study was much shorter (2 days) compare to the present study where it was 14 days.

Among the two strains, *Bacillus* strains showed no significant difference in cell density between compost and soil layer. The most plausible justification for this result is that there were some organic compounds in the compost layer which either attracted (as in case of *Bacillus*) or prevented the spread of bacteria (as in case of *Pseudomonas*) towards compost. There have been some studies who looked at response of bacterial communities on addition of different type of compost in soil and the results showed that not all type of compost favoured increase in bacterial abundance in soil (Perez-Piqueres et al. , 2006; Bastida et al., 2008).

To see if the soil pore geometry influenced the spread of bacteria towards the compost layer, different pore characteristics like porosity, connectivity and surface area of pores of each counting spot was quantified. Soil porosity and connectivity of pores significantly influenced spread of *Pseudomonas* and *Bacillus* bacteria towards the compost layer. This was because soil was packed at a lower bulk-density; the sample was porous with highly connected pores which allowed further spread of bacteria towards compost layer. An influence of soil porosity and connectivity of pores on decomposition of added substrate was

observed by some studies (Haling et al. 2013; Negassa et al. 2015). For example, Hailing et al. (2013) observed that samples with higher bulk-density (lower porosity) showed slower decomposition of plant roots added to soil. Negassa et al. (2015) also showed that decomposition of added plant residue was affected by pore size distribution and connectivity of pores. One pore characteristic that significantly influenced the spread of *Pseudomonas* bacteria only was soil-pore interface area. Note that in both treatments, soil was packed at the same bulk-density, so there was no difference in the pore characteristics between the two samples. Therefore, this difference of soil-pore interface on spread of bacteria can be related to growth and spread rate difference between *Pseudomonas* and *Bacillus* bacteria.

6.5 Conclusion

In this study, the rate of spread of bacteria towards a nutrient source was determined. In the first part of the study a difference in spread of bacteria from a local source towards nutrient sources inherent in natural soil was revealed in soil packed at different bulk-densities. The rate of spread of bacteria was faster in soil packed at lower bulk-density compare to soil packed at higher bulk-density. Analysis of X-ray images of thin sections of samples packed at lower and higher bulk-density revealed that the rate of spread of bacteria was influenced by the soil-pore interface of pores. The second part of the study revealed no significant difference in bacterial density gradient of *Pseudomonas* and *Bacillus* towards compost (high nutrient source) from soil (low nutrient source). This suggests that not all types of plant growth promoting bacteria are attracted towards compost added in soil.

7 Discussion

7.1 Approaches and Key Findings

The main objective of this thesis was to evaluate the influence of soil structure on growth and spatial distribution of introduced bacteria. Throughout this thesis techniques were integrated e.g. X-ray CT to characterize the 3D soil structure and Fluorescence microscopy to visualize and quantify bacteria in 2D thin sections of soil. Different experimental approaches were also used to inoculate bacteria in soil, either as inoculum suspension (chapter 3 & 5) or as inoculum bead (chapter 4 & 6) in order to assess bacterial growth and spread in soil. Bacteria inoculum was mixed with soil in the first experiment (Chapter 3) to assess the growth rate of *Pseudomonas* and *Bacillus* in soil with different structures. A method was developed (Chapter 5) to determine the spatial distribution of introduced bacteria in soil at different spatial scales. The method developed in chapter 5 was subsequently applied to investigate the effect of pore characteristics on the rate of bacterial spread towards nutrient source at microscale. The effect of different structures on the ability of bacteria to spread towards a nutrient source was then determined using this method.

From the findings of this study I conclude that soil pore geometry is important growth and distribution of bacteria in soil.

A summary of the key findings of this thesis are:

- Increasing bulk-density significantly decreased the porosity, connectivity and soil-pore interface of pores. This means that the pore geometry can be experimentally controlled in soil microcosms.
- Increasing bulk-density decreased the growth and spread of bacteria in soil. A higher rate of growth and spread of bacteria was found in soil that was highly porous with large connected pores volumes.

- Growth rate and spread of bacteria was influenced more by bulk-density than aggregate sizes as increasing bulk-density caused a decline in the number of connected pores and in pore volume.
- The influence of bulk-density and aggregate sizes on growth rate and the extent of spread differed between *Pseudomonas* and *Bacillus*.
- The influence of pore characteristics on the distribution of *Pseudomonas* and *Bacillus* varied between different analysed spatial scales (macroscale and microscale). This shows the need of analysing at an appropriate bacterial habitat scale as the effect of structure on distribution of bacteria is different at macro- and microscale.
- The influence of soil porosity, pore connectivity and soil-pore interface of pores on the spatial on distribution varied between *Pseudomonas* and *Bacillus*. This is because the rate of growth and extent of spread was different between the two selected bacteria. This shows how the distribution can vary between individual bacteria at the pore scale.
- Soil porosity, pore connectivity and soil-pore interface of pores influenced the extent of bacterial spread towards nutrient source in soil. The extent of spread and colonization was further in soil with highly connected pore volumes.

Therefore, the thesis highlights the importance of soil physical conditions in microbial studies. Nevertheless these are hardly ever reported in the literature. Also, the thesis showed how different experimental techniques can be combined to understand microbial distribution in a 3D soil environment. This is the first time such a combination of techniques is used.

7.1.1 Influence of soil structure on pore geometry

X-ray CT was used throughout all experimental work to determine the soil structure non-invasively within intact soil samples. In this thesis, this technique was used to visualize and quantify pores and its characteristics. The characteristics of pores like porosity, connectivity and soil-pore interface were considered to be of particular interest as they control the gas exchange, water and nutrient distribution in soil (Crawford et al. 2005). Chapter 3 investigated the effect of different bulk-density and aggregate size on pore geometry in soil microcosms. Bulk-density and aggregate sizes are used as experiment variables but the way they affect pore geometry was still unknown. The results showed that increasing bulk-density significantly decreased the porosity and connectivity of soil pores. Soil packed at a bulk-density of 1.6 g cm^{-3} had the lowest porosity with 40 % less connected pores compare to soil packed at lower bulk densities. This is because at higher bulk-density soil is more compact which causes reduction in void space by rearrangement of soil aggregates closer to each other. The present results confirm the findings of other researchers that have also shown the effect of compaction on soil pore geometry (Frey et al. 2009; Beylich et al. 2010; Kim et al. 2010). Nawaz et al. 2013 in their review showed how the use of heavy machineries in conventional agricultural practices causes compaction of soil which modifies the structure of soil by increasing the bulk-density, altering the geometry of soil pores and increasing the soil strength. Effect of increasing aggregate size on the pore geometry system was also investigated (chapter 3). It was hypothesized that the soil-pore interface will decrease with increasing size of aggregates. The soil-pore interface of aggregate size 2-4 mm was 8 % lower than that of aggregate

size 1-2 mm, but this difference was not significant. Also for soil packed at different bulk-density the soil-pore interface was not significantly different. This was probably due to the limitation of the scan resolution as the substantial range of pores is not covered (i.e. pores smaller than the resolution of scan are missing). For example, in the bulk-density treatment the total porosity of a sample packed at bulk-density of 1.3 g cm^{-3} is 49 % and of soil packed at bulk-density of 1.6 g cm^{-3} it is 37 %. However, the porosity determined by X-ray CT scanned at a resolution of 24 µm gave only 17 % for soil packed at a bulk-density of 1.3 g cm^{-3} and 8 % for soil packed at bulk-density 1.6 g cm^{-3}. This means that the around 60-70 % of the pores are not detected by the scanner. Therefore, the conclusions made in this study on the pore characteristics are based on the pores greater than the detection limit. This shows that the samples need to be scanned at higher resolution to get the majority of the pores detected. Currently there are technical limitations which prevent this.

7.1.2 Effect of soil structure on growth and spread of bacteria

Chapter 3 highlighted that the growth rate of introduced bacteria was significantly affected by increasing bulk-density and aggregate sizes in soil microcosms, with the effect correlated to pore geometry over the time course of investigation. Both *Pseudomonas* and *Bacillus* showed higher number of cell counts in soil packed with lower bulk-density. With increasing bulk-density the number of cell counts declined by 36-68 % for *Pseudomonas* and 30-60 % for *Bacillus*. These results agree with the findings of Li et al. (2001) who also reported a decline by 26-39 % of total number of bacteria, fungi and actinomycetes in soil packed at bulk-density 1.0-1.6 g cm^{-3}. This is probably

caused by the pore geometry as soil packed at lower bulk-density have relatively higher percentage of porosity and connected pores which allowed rapid transfer of air, water and substrates through soil compare to soil packed at higher percent bulk-density as shown in chapter 3 of this thesis. A significant correlation of all three pore characteristics with cell counts was observed, but connectivity of pores showed the highest impact on growth of *Pseudomonas* and *Bacillus*. However, between the two selected bacterial strains, the growth rate of *Pseudomonas* was 50 to 60 % faster than the *Bacillus* in soil packed at different bulk densities. As bacterial suspension was mixed in soil, this difference in cell counts between two species can be related to either doubling time of each strain or the spread mechanism of bacteria to access nutrients in soil.

To investigate this, the effect of soil factors (moisture content, bulk-density and aggregate size) on the extent of spread of *Pseudomonas* and *Bacillus* was examined in chapter 4, where the bacterial inoculum was introduced as a point source rather than mixing the inoculum as done in chapter 3. The spread of *Pseudomonas* and *Bacillus* was faster in soil with higher moisture content compared to dry soil. This is because bacteria thrive only on part of the pore network that is either water filled or is covered by water films (Vos et al., 2013). This is also the reason why the spread was faster in soil packed at lower bulk-density compared to higher bulk-density as the available pore space was higher in soil with a lower bulk-density. Bacteria can also spread through the air-filled pores by gliding on water films or on fungal hyphae (Nazir et al., 2010). The spread of bacteria would be different in the field to the repacked microcosms

with uniform soil conditions because there will be cracks and biopores present in the field which will provide rapid pathways when water filled.

The bacterial counts measured here are counts per gram of soil, but with this data no information can be obtained whether cells are grouped at a single location or distributed throughout the soil. To estimate the likelihood of encounters among bacteria and between bacteria and substrates knowledge on the spatial distribution of bacteria is important.

7.1.3 Effect of sampling scale on observed impact of soil structure on the distribution of bacteria at different spatial scale of analysis.

Polished sections were used to evaluate the distribution of introduced bacterial cells in bulk soil at microscales. Bacterial cells were observed to be more heterogeneously distributed and the numbers of cell counts were variable between treatments (Chapter 5). Dechesne et al. (2005) also showed that the distribution of introduced bacteria was more heterogeneously distributed than the indigenous one. Some other studies also showed a non-random pattern in spatial distribution of the microbial community (Franklin and Mills, 2003; Nunan et al., 2003; O'Donnell et al., 2007; Young et al., 2008). The variation in bacterial distribution was related to a range of factors like the organic matter, soil water, aggregate size classes and their location within aggregate and pore size class (Franklin and Mills, 2009; Kravchenko et al., 2014; Or et al., 2007; Ruamps et al., 2011).

A method was developed (Chapter 5) to determine the relationship between the pore space, connectivity and soil-pore interface, quantified at different spatial scales and cell densities of introduced bacteria in soil microcosms. The method

developed here was to bridge the gap between scales as bacteria are visualised at µm-scale under a microscope whereas pore geometry that controls diffusion and transport of nutrients in soil operates at –mm and cm- scales. The most appropriate scale to study the spatial distribution of microbes would be the microhabitat scale at which individual bacteria and microbial communities are actually living and interacting. However from the published works the opinion of the range of microscales depends either upon the individual micro-organism under study or the microbial process of interest and also to some extent on the tools available for the studies (Grundmann, 2004). Therefore, the analysis in this study was done at two different scales (macro- and microscale) to investigate the effect scale has on the analysis of the spatial distribution of bacteria. The influence of all three pore characteristics on the distribution of bacteria was found to be different between the two analysed scales. The porosity, connectivity and soil-pore interface showed significant influence on the distribution of *Pseudomonas* bacteria at macroscale; however the effect was insignificant at the microscale. Similar kind of results were obtained by the findings of Nunan et al. (2002) who also showed that the spatial structure (i.e. spatial correlations between bacteria) was only present at the micrometre scale in the topsoil, while in the subsoil there were two distinct spatial scales (micrometre scale and scales ranging over centimetres to metres).

Among different aggregate size treatment, the porosity, connectivity and soil-pore interface showed a significant effect on the distribution of introduced bacteria only in 2-4 mm size aggregate treatment. A plausible reason for this difference between aggregate sizes on distribution of bacteria could be because of pores not detected by the scanner (<13.4 µm) as there was no significant

difference in the pore geometry between the two treatments. But also there can be other pore characteristics that are not analysed here which would have influenced the distribution of bacteria in different aggregate size treatments like pore size distribution and tortuosity of pores. Wang et al. (2013) showed a positive correlation of *E.coli* distribution with porosity, presence of large and medium size pores and tortuosity of pores in aggregates of size 4-6.3 mm. Ruamps et al. (2011) also showed a significant difference in microbial community structure in different pore size classes. Therefore, the present results shows how the effect of pore geometry on microbial distribution can differ when analysed at different scale. From the techniques available so far, the microscale selected in this study is the closest scale one can use to quantify bacteria in their 3D soil environment. The method presented here is a significant step towards understanding how bacterial distribution is affected by the soil structure and raises issues regarding the 'appropriate' spatial scale for analyses. The appropriate scale is needed to help understand the development of the microbial spatial patterns and to determine the factors that regulates and maintains the soil biodiversity and microbial community function in soil.

This method was used to quantify the effect of pore characteristics on the spread and colonization of bacteria towards a nutrient source in soil. At the microscale, soil-pore interface affected the spread and colonisation of bacteria towards nutrients in soil. The reason for this may be that in partially saturated soil, water is retained on the surfaces as thin films to accommodate introduced bacterial cells (Carminati et al., 2008). In addition bacteria tend to grow on surfaces of substrates as can be seen from the thin sections. The consequence of this result is that if pore geometry affects the spread and colonisation of

bacteria at microscale, it will also affect the activity of microbes in soil. This shows that the pore characteristics control the access of nutrients in soil. Strong et al. (2004) showed that the rate of decomposition of organic C depends on the location in the soil pore network. Ruamps et al. (2011) also showed that decomposition of organic C and microbial community structure varies at pores scale in soil.

Thus the method developed in the present study can be used to study how introduced bacteria contact their target through soil to carry out activities like promoting plant growth or mineralization of soil pollutant.

There are several factors which will affect repeatability of my experiments. These factors include soil type and unintended microscopic heterogeneity which cannot be controlled experimentally, as explained below. The growth and spread rate of bacteria will depend on soil type. For example if the sample is taken from a sandy clay soil or from a sandy loam soil, these two samples could have different bulk-densities, particle size distribution and water content. Moreover, if all physical conditions could be replicated, as described in this thesis, they would differ nutritionally which may impact on the results. If this will have an impact on the conclusions is a topic for further investigation.

To understand the effect of soil structure on the temporal and spatial distribution of bacteria, bulk-density, aggregate sizes and water content were controlled. These factors, however, are characteristics of the bulk volume of soil. The advantage is that they can be experimentally controlled and repeated by other researchers. However, each sample will still differ at the microscopic scale. Conditions cannot be controlled experimentally at this scale. For that reason I used X-ray CT to quantify differences at that scale. However, it means that

variability can be expected between microcosms prepared this way at microscopic scales, whilst they are similar at macroscopic scales.

The experiments were performed using minimum three replicates per treatment to increase the reliability of the data produced. Mostly increasing the sample size is given more importance to get reliable data than the repetition of an experiment. But Mobley et al., (2012) in their survey on data reproducibility in cancer research have shown that ~ 50 % of researchers were unable to reproduce the published data, thus highlighting the impact data reproducibility can have on the general application of a technique in a specific field. This highlights the importance of repeating experiments to obtain more reliable conclusions and that unexpected outcomes can sometimes occur in repeated experiments. Therefore, in my thesis, the results of the growth was partially verified in Chapter 6 by confirming bacterial densities at two sampling times coinciding with the sampling times of the thin section preparation (the bacterial densities are given in Appendix II).

7.2 Conclusion and future work

The following key conclusions can be drawn from the research presented in this thesis:

- The use of X-ray CT allowed determining the effect of bulk-density on the soil porosity, connectivity and soil-pore interface. A significant decline in the porosity, connectivity and soil-pore interface with increasing bulk-density was observed. An effect of this on the growth rate of introduced bacteria was observed. Bacterial growth decreased with increasing bulk-density as less amount of pores space with connected pores was

available at higher bulk-density. Increasing aggregate size also showed significant decrease in the number of *Pseudomonas* and *Bacillus* cells. The extent of bacterial spread was faster in soil packed at lower bulk-density (1.3 g cm^{-3}) and higher moisture content soil microcosms.

- Between the two selected strains, the growth rate of *Pseudomonas* was faster than *Bacillus* but the extent of spread was faster for *Bacillus* compared to *Pseudomonas* in soil.
- At microscale analysis, soil porosity, connectivity and soil-pore interface showed significant effect on the distribution of bacteria in samples with aggregate sizes 2-4 mm.
- Application of the method (analysis of spatial distribution of bacteria) showed that the extent of spread of bacteria decreased with increasing bulk-density at the microscale. The extent of spread and colonisation of *Pseudomonas* was significantly further towards nutrient source in soil packed with lower bulk-density and the soil porosity and soil-pore interface significantly influenced the extent of this spread in soil thin sections

7.3 Future Research

In this thesis a combination of techniques was used to quantify the relation between soil structure and bacteria growth and distribution in soil.

- In all the experiments bacteria were inoculated in repacked sieved soil. The next step would be assessment of growth and colonisation of introduced bacteria in different soil types and undisturbed soil cores from field under different management practices.

- In this study the effect of structure was studied for *Pseudomonas* and *Bacillus* sp. as they are known for their plant growth promoting activity. Quantifying the effect of structure on other benefice al bacteria and the interaction between bacteria would be the next step in understanding structural effect on introduced bacteria for successful bioremediation in soil.
- A general stain was used in this study to visualise bacterial distribution in soil thin sections. To differentiate between bacterial strains and bacterial cells form other soil particles of same size distribution, specific stains like FISH technique needs to be applied on thin sections. During this study a preliminary experiment was carried out where TETRA-FISH protocol was optimized and applied on thin sections. The study showed successful application of TETRA-FISH on soil thin sections as it was easy to distinguish bacterial cells against the soil background (Figure 7.1). However the signal intensity was not high enough. The future work could involve optimization of the protocol to improve the signal intensity against the soil background.

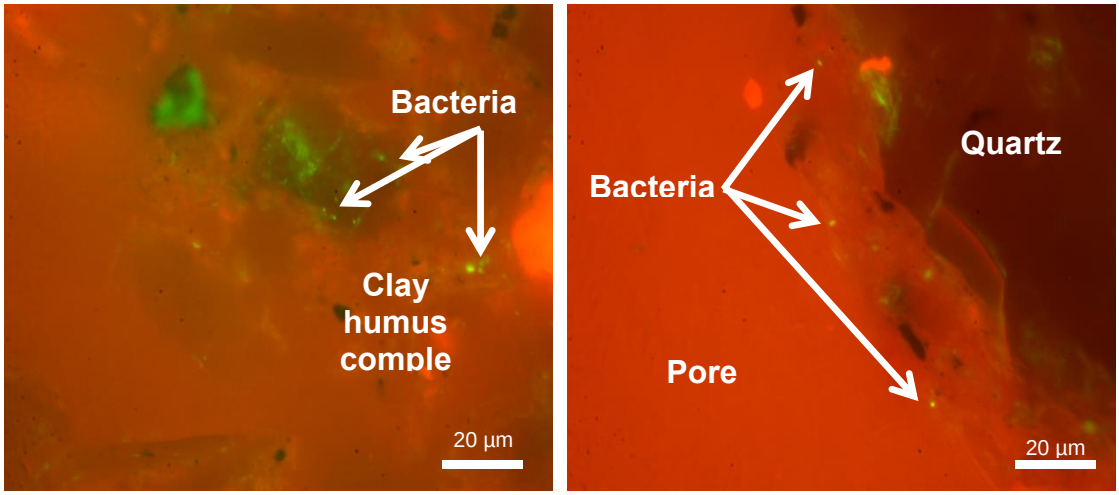

Figure 7.1: Tetra-FISH stained *Pseudomonas fluorescens* cells in soil thin sections under double excitation filter (465-505 and 564-892 nm). Scale bar 20 µm.

- For better understanding of the 3D soil environment, the future work could involve integration of methodologies developed in this thesis along with for e.g. techniques like SEM-EDX to map the biological distribution along with the chemical and physical properties of soil.
- The pore characteristics analysed here were porosity, connectivity and soil-pore interface. But there are other pore characteristics which also affect the distribution and composition of microbial community structure and its function is soil like pores size distribution and tortuosity of pores. Future work could involve quantifying these pore characteristics of soil.
- The method developed in this study could be applied to various problems. For example it could be applied to study the ability of bacteria to colonise Biochars in soil and determine the biochar and soil characteristics that determine the colonisation efficiency. Biochar is a porous, carbon rich material produced through heating of organic material under low oxygen condition, a process referred to as pyrolysis, it is added in soil to improve soil fertility. Specifically, this could quantify for

the first the micro-environments introduced by Biochar in soil are amenable to deliberate and targeted manipulation and modification of habitats suitable for microbial colonisation. This project is currently ongoing funded by DAAD (German Academic Exchange service).

8 References

Abu-Ashour, J. Joy, D.M. Lee, H. Whiteley, H.R. and Zelin, S. 1994. Transport of microorganisms through Soil, Water, Air and Soil Pollution. (519): pp. 141–158.

Adesemoye, A.O. Torbert, H.A. and Kloepper, J.W. 2009. Plant growth-promoting rhizobacteria allow reduced application rates of chemical fertilizers. *Microbial Ecology*. 58(4): pp. 921–9.

Ahemad, M. and Kibret, M. 2014. Mechanisms and applications of plant growth promoting rhizobacteria: Current perspective. J*ournal of King Saud University - Science*. 26(1): pp. 1–20.

Anderson, S.H. Wang, H. Peyton, R.L. and Gantzer, C.J. 2003. Estimation of porosity and hydraulic conductivity from x-ray CT-measured solute breakthrough. *Geological Society, London, Special Publications*. 215(1): pp. 135-149.

Bacilio-Jimenez, M. Aguilar-Flores, S. Ventura-Zapata, E. Pérez-Campos, E. Bouquelet, S. and Zenteno, E. 2003. Chemical characterization of root exudates from rice (Oryza sativa) and their effects on the chemotactic response of endophytic bacteria. *Plant and Soil. 249(2): pp. 271-277*.

Banerjee, M.R. Yesmin, L. Vessey, J.K. and Rai, M.K. 2005. Plant-growth-promoting rhizobacteria as biofertilizers and biopesticides.*Handbook of microbial biofertilizers*. pp. 137-181.

Barrios, E. 2007. Soil biota, ecosystem services and land productivity. *Ecological Economics*. 64(2): pp. 269–285.

Bastida, F. Kandeler, E. Moreno, J.L. Ros, M. Garcia, C. and Hernandez, T. 2008. Application of fresh and composted organic wastes modifies structure, size and activity of soil microbial community under semiarid climate, *Applied Soil Ecology*. 40 (2): pp. 318–329.

Baveye, P. Rogasik, H. Wendroth, O. Onasch, I. and Crawford, J.W. 2002. Effect of sampling volume on the measurement of soil physical properties: simulation with x-ray tomography data. *Measurement Science and Technology*. 13(5): pp. 775–784.

Baveye, P.C. Laba, M. Otten, W. Bouckaert, L. Dello Sterpaio, P. Goswami, R.R. 2010. Observer-dependent variability of the thresholding step in the quantitative analysis of soil images and X-ray microtomography data. *Geoderma*.157: 51–63.

Berthod, M. Kato, Z. Yu, S. and Zerubia, J. 1996. Bayesian image classification using Markov random fields.*Image and Vision Computing*.14(4): pp. 285-295.

Beylich, A. Oberholzer, H-R. Schrader, S. Hoper, H. and Wilke, B-M. 2010. Evaluation of soil compaction effects on soil biota and soil biological processes in soils. *Soil and Tillage Research*. 109(2): pp. 133–143.

Bhattacharyya, P.N. and Jha, D.K. 2012. Plant growth-promoting rhizobacteria (PGPR): Emergence in agriculture. *World journal of microbiology & biotechnology*. 28(4): pp. 1327–50.

Blair, J.M. Falconer, R.E. Milne, A.C. Young, I.M. and Crawford, J.W. 2007. ModelingThree-Dimensional Microstructure in Heterogeneous Media. *Soil Science Society of America Journal*.71(6): pp. 1807-1812.

Bossuyt, H. Denef, K. Six, J. Frey, S.D. Merckx, R. and Paustian, K. 2001. Influence of microbial populations and residue quality on aggregate stability. *Applied Soil Ecology*. 16(3): pp. 195–208.

Bouckaert, L. Sleutel, S. and Loo, D.V. 2013. Carbon mineralisation and pore size classes in undisturbed soil cores. *Soil Research*. (C): pp. 14–22.

Bradford, S.A. Simunek, J. and Walker, S.L. 2006. Transport and straining of E. coli O157:H7 in saturated porous media. *Water Resources Research*. 42(12): p. n/a–n/a.

Bronick, C.J. and Lal, R. 2005, Soil structure and management: a review, *Geoderma*, 124(1-2): pp. 3–22.

Burd, G.I. Dixon, D.G. and Glick, B.R. 2000. Plant growth-promoting bacteria that decrease heavy metal toxicity in plants.*Canadian Journal of Microbiology*. *46*(3): pp. 237-245.

Cambardella, C.A. 2006. Aggregation and organic matter. *Encyclopedia of Soil Science. Taylor and Francis, Boca Raton*, *FL*. pp. 52-55.

Cao, Y. Zhang, Z. Ling, N. Yuan, Y. Zheng, X. Shen, B. and Shen, Q. 2011. *Bacillus* subtilis SQR 9 can control Fusarium wilt in cucumber by colonizing plant roots. *Biology and Fertility of Soils*. 47(5): pp. 495–506.

Capowiez, Y. Pierret, A. Daniel, O. and Monestiez, P. 1998. 3D skeleton reconstruction of natural earthworm burrow systems using CAT scan images of soil cores. *Biology and Fertility of Soils.* 27: pp. 51-59.

Carson, J.K. Gonzalez-Quinones, V. Murphy, D.V. Hinz, C. Shaw, J.A. and Gleeson, D.B. 2010. Low pore connectivity increases bacterial diversity in soil. *Applied and environmental microbiology*. 76(12): pp. 3936–42.

Cassel, D.K. and Nielsen, D.R. 1986. Field capacity and available water capacity. *Methods of Soil Analysis: Part 1—Physical and Mineralogical Methods methodsofsoilan1*. pp. 901-926.

Cnudde, V. and Boone, M.N. 2013. High-resolution X-ray computed tomography in geosciences: A review of the current technology and applications. *Earth-Science Reviews*.123: pp. 1-17.

Crawford, J.W. Deacon, L.J. Grinev, D.V. Harris, J. Ritz, K. Singh, B.K. and Young, I.M. 2011. Microbial diversity affects self-organization of the soil-microbe system with consequences for function. *Journal of The Royal Society*.

Dechesne, A. Pallud, C. Debouzie, D. Flandrois, J.P. Vogel, T.M. Gaudet, J.P. and Grundmann, G.L. 2003. A novel method for characterizing the microscale 3D spatial distribution of bacteria in soil. *Soil Biology and Biochemistry*. 35(12): pp. 1537–1546.

Dechesne, A. Bertolla, F. Grundmann, L. Lyon, C.B. and Icrobiol, APPLE N. M. 2005. Impact of the Microscale Distribution of a *Pseudomonas* Strain Introduced into Soil on Potential Contacts with Indigenous Bacteria. *Applied And Environmental Microbiology*. 71(12): pp. 8123–8131.

Dechesne, A. Pallud, C. and Grundmann, G.L. 2007. Chapter 4 Spatial distribution of bacteria, *The Spatial Distribution of Microbes in the Environment*: pp. 87–107.

de Weert, S. Vermeiren, H. Mulders, I.H. Kuiper, I. Hendrickx, N. Bloemberg, G.V. and Lugtenberg, B.J. 2002. Flagella-driven chemotaxis towards exudate components is an important trait for tomato root colonization by *Pseudomonas* fluorescens. *Molecular Plant-Microbe Interactions*.15(11): pp.1173-1180.

Dıaz-Zorita, M, Perfect, E and Grove, J 2002, Disruptive methods for assessing soil structure, *Soil and Tillage Research*, 64(1):pp.3-22.

Dick, R.P. Rasmussen, P.E. and Kerle, E.A. 1988. Influence of long-term residue management on soil enzyme activities in relation to soil chemical properties of a wheat-fallow system.*Biology and Fertility of Soils*.*6*(2): pp. 159-164.

Downie, H. Holden, N. Otten, W. Spiers, A.J. Valentine, T.A. and Dupuy, L.X. 2012. Transparent soil for imaging the rhizosphere. *Plos one*. 7(9): pp. e44276.

Drazkiewicz, M. 1994. Distribution of microorganisms in soil aggregates: effect of aggregate size.*Folia Microbiologica*.*39*(4): pp. 276-282.

Drees, L.R. Wilding, L.P. Karathanasis, A.D. and Blevins, R.L. 1994. Micromorphological characteristics of long-term no-till and conventionally tilled soils. *Soil Science Society of America*. 58: pp. 508-517.

Drury, C.F. Yang, X.M. Reynolds, W.D. and Tan, C.S. 2004. Influence of crop rotation and aggregate size on carbon dioxide production and denitrification.*Soil and Tillage Research*.*79*(1): pp. 87-100.

Edwards, A.P. and Bremner, J.M. 1967. Microaggregates in soils. *Journal of Soil Science*.*18*(1): pp. 64-73.

Eickhorst, T. and Tippkotter, R. 2008. Detection of microorganisms in undisturbed soil by combining fluorescence in situ hybridization (FISH) and

micropedological methods. *Soil Biology and Biochemistry*. 40(6): pp. 1284–1293.

Eickhorst, T. and Tippkotter, R. 2008. Improved detection of soil microorganisms using fluorescence in situ hybridization (FISH) and catalyzed reporter deposition (CARD-FISH). *Soil Biology and Biochemistry*. 40(7). pp. 1883–1891.

Eilers, K.G. Debenport, S. Anderson, S. and Fierer, N. 2012. Digging deeper to find unique microbial communities: the strong effect of depth on the structure of bacterial and archaeal communities in soil.*Soil Biology and Biochemistry*. *50*: pp. 58-65.

Elsas, J.D. Dijkstra, A.F. Govaert, J.M. and Veen, J.A. 1986. Survival of *Pseudomonas* fluorescens and *Bacillus* subtilis introduced into two soils of different texture in field microplots. *FEMS Microbiology Letters*. 38(3): pp. 151–160.

Elvang, A.M. Westerberg, K. Jernberg, C. and Jansson, J.K. 2001. Use of green fluorescent protein and luciferase biomarkers to monitor survival and activity of Arthrobacter chlorophenolicus A6 cells during degradation of 4-chlorophenol in soil. *Environmental Microbiology*. 3(1): pp. 32–42.

Enwall, K. Throback, I.N. Stenberg, M. Soderstrom, M. and Hallin, S. 2010. Soil resources influence spatial patterns of denitrifying communities at scales compatible with land management. *Applied and Environmental Microbiology*. 76(7): pp. 2243–50.

Errampalli, D. Leung, K. Cassidy, M.B. Kostrzynska, M. Blears, M. Lee, H. and Trevors, J.T. 1999. Applications of the green fluorescent protein as a molecular marker in environmental microorganisms. *Journal of Microbiological Methods*, 35(3): pp. 187–99.

Ettema, C.H. and Wardle, D.A. 2002. Spatial soil ecology. *Trends in Ecology & Evolution.* 17(4): pp. 177–183.

Falconer, R.E. Houston, A.N. Otten, W. and Baveye, P.C. 2012. Emergent behavior of soil fungal dynamics. *Soil Science*. 177(2): pp. 111–119.

Falsone, G. Wilson, C.A. Cloy, J.M. Graham, M. C. & Bonifacio, E. (2014). Relating microfeatures of soil organic matter to C stabilisation: optical microscopy, SEM-EDS, abiotic oxidation.*Biology and fertility of soils*,50(4), 623-632.

Feeney, D.S. Crawford, J.W. Daniell, T. Hallett, P.D. Nunan, N. Ritz, K. Rivers, M. and Young, I.M. 2006. Three-dimensional microorganization of the soil-root-microbe system. *Microbial Ecology*. 52(1): pp. 151–8.

Fierer, N. Bradford, M.A. Jackson, R.B. 2007. Toward an ecological classification of soil bacteria. *Ecology*. 88: pp. 1354–1364.

Fontes, D.E. Mills, A.L. Hornberger, G.M. and Herman, J.S. 1991. Physical and chemical factors influencing transport of microorganisms through porous media.*Applied and Environmental Microbiology*.*57*(9): pp. 2473-2481.

Foster, R. and Rovira, A. 1973. The rhizosphere of wheat roots studied by electron microscopy of ultra-thin sections. *Bulletins of the Ecological Research Committee.* 17: pp. 93–95.

Foster, R. C. 1988. Microenvironments of soil microorganisms. *Biology and Fertility of Soils*.*6*(3): pp.189-203.

Franklin, R.B. and Mills, A.L. 2007, The importance of microbial distribution in space and spatial scale to microbial ecology.In: R.B. Franklin and A.L. Mills, eds. *The Spatial Distribution of Microbes in the Environment*. pp. 1–30.-- to be confirmed

Frey, B. Kremer, J. Rudt, A. Sciacca, S. Matthies, D. and Luscher, P. 2009. Compaction of forest soils with heavy logging machinery affects soil bacterial community structure. *European Journal of Soil Biology*. 45(4): pp. 312–320.

Frey, S.D. 2015. Chapter 8 - The Spatial Distribution of Soil Biota. *Soil Microbiology Ecology and Biochemistry*. 4th ed. Elsevier Inc. pp. 223–244.

Gaillard, V. and Chenu, C. 1999. Carbon, nitrogen and microbial gradients induced by plant residues decomposing in soil. *European Journal of Soil Science*.50(4), 567-578.

Gannon, J.T. Manilal, V.B. and Alexander, M. 1991. Relationship between cell surface properties and transport of bacteria through soil.*Applied and Environmental Microbiology*.*57*(1): pp. 190-193.

Gannon, J.T. Mixgelgrin, U. Alexander, M. and Wagenet, R.J. 1991. Bacterial transport through homogeneous. *Soil Biol. Biochem*. 23(12): pp. 1155-1160.

Gannon, J. T. Mingelgrin, U. Alexander, M. & Wagenet, R. J. (1991). Bacterial transport through homogeneous soil. *Soil Biology and Biochemistry*, *23(12)*: *pp. 1155-1160*.

Gans, J. Wolinsky, M. and Dunbar, J. 2005. Computational improvements reveal great bacterial diversity and high metal toxicity in soil.*Science*. *309*(5739): pp. 1387-1390.

Glick, B.R. Plant growth-promoting bacteria: mechanisms and applications. *Scientifica* 2012., http://dx.doi.org/10.6064/2012/963401, Article ID 963401

Gonod, L.V. 2006. Spatial distribution of microbial 2, 4-dichlorophenoxy acetic acid mineralization from field to microhabitat scales. *Soil Science Society of America Journal. 70(1): pp. 64-71.*

Gray, E.J. and Smith, D.L. 2005. Intracellular and extracellular PGPR: commonalities and distinctions in the plant–bacterium signaling processes.*Soil Biology and Biochemistry*.*37*(3): pp. 395-412.

Gregory, P.J. Hutchison, D.J. Read, D.B. Jenneson, P.M. Gilboy, W.B. and Morton, E.J. 2003. Non-invasive imaging of roots with high resolution X-ray micro-tomography. *In Roots: The Dynamic Interface between Plants and the Earth.*pp. 351-359.

Grundmann, G.L. Dechesne, A. Bartoli, F. Flandrois, J.P. Chasse, J.L. and Kizungu, R. 2001. Spatial modeling of nitrifier microhabitats in soil. *Soil Science Society of America Journal*. 65(6): pp. 1709–1716.

Guimaraes, V.F. Cruz, I.V. Hagler, A.N. Mendon, L.C. and Elsas, J.D.V. 1997. Transport of a genetically modified *Pseudomonas* fluorescens and its parent strain through undisturbed tropical soil cores. *Applied Social Ecology*. 7: pp. 41–50.

Gupta Sood, S. 2003. Chemotactic response of plant-growth-promoting bacteria towards roots of vesicular-arbuscular mycorrhizal tomato plants. *FEMS Microbiology Ecology*, 45(3): pp. 219–27.

Haling, R. E. Tighe, M. K. Flavel, R. J. & Young, I. M. 2013. Application of X-ray computed tomography to quantify fresh root decomposition in situ. *Plant and soil*,372(1-2): pp. 619-627.

Haney, R.L. and Haney, E.B. 2010. Simple and Rapid Laboratory Method for Rewetting Dry Soil for Incubations. *Communications in Soil Science and Plant Analysis*. 41(12): pp. 1493–1501.

Hapca, S.M. Houston, A.N. Otten, W. and Baveye, P.C. 2013. New local thresholding method for soil images by minimizing grayscale intra-class variance.*Vadose Zone Journal*.*12*(3).

Hapca, S.M. Baveye, P.C. Wilson, C. Lark, R.M. Otten, W. 2015. Three-dimensional mapping of soil chemical characteristics at micrometric scale by combining 2D SEM-EDX data and 3D X-ray CT images, submitted to PLOS One

Harris, K. Crabb, D. Young, I.M. Weaver, H. Gilligan, C.A. Otten, W. and Ritz, K. 2002. In situ visualisation of fungi in soil thin sections: problems with crystallisation of the fluorochrome FB 28 (Calcofluor M2R) and improved staining by SCRI Renaissance 2200.*Mycological Research*. *106*(03): pp. 293-297.

Harris, K. Young, I.M. Gilligan, C.A. Otten, W. and Ritz, K. 2003. Effect of bulk density on the spatial organisation of the fungus Rhizoctonia solani in soil. *FEMS Microbiology Ecology*. 44(1): pp. 45–56.

Harshey, R.M. 2003. Bacterial motility on a surface: many ways to a common goal. *Annual review of microbiology*. 57(1): pp. 249–73.

Hayat, R. Ali, S. Amara, U. Khalid, R. and Ahmed, I. 2010. Soil beneficial bacteria and their role in plant growth promotion: a review. *Annals of Microbiology*, 60(4): pp. 579–598.

Heeraman, D.A. Hopmans, J.W. and Clausnitzer, V. 1997. Three dimensional imaging of plant roots in situ with X-ray computed tomography.*Plant and Soil*. *189*(2): pp. 167-179.

Heijnen, C. 1991. A determination of protective microhabitats for bacteria introduced into soil. *FEMS Microbiology Letters*. 85(1): pp. 73–80.

Heijs, A.W. De Lange, J. Schoute, J.T. and Bouma, J. 1995. Computed tomography as a tool for non-destructive analysis of flow patterns in macroporous clay soils.*Geoderma.64*(3): pp. 183-196.

Heijs, A.W. Ritsema, C.J. and Dekker, L.W. 1996. Three-dimensional visualization of preferential flow patterns in two soils. *Geoderma*. *70*(2): pp. 101-116.

Helliwell, J.R. Sturrock, C.J. Grayling, K.M. Tracy, S.R. Flavel, R.J. Young, I.M. Whalley, W.R. and Mooney, S.J. 2013 Applications of X-ray computed tomography for examining biophysical interactions and structural development in soil systems: a review. *European Journal of Soil Science*. 64(3): pp. 279–297.

Houston, A.N. Otten, W. Baveye, P.C. and Hapca, S. 2013. Adaptive-window indicator kriging: A thresholding method for computed tomography images of porous media. *Computers & Geosciences*. 54: pp. 239–248.

Huysman, F. and Verstraete, W. 1993. Water-facilitated transport of bacteria in unsaturated soil columns : influence of cell and soil properties. *Soil Biol. Biochem*. 25(1): pp. 83–90.

Iassonov, P. Gebrenegus, T. and Tuller, M. 2009. Segmentation of X-ray computed tomography images of porous materials: A crucial step for characterization and quantitative analysis of pore structures.*Water Resources Research*. *45*(9).

Jansson, J.K. Bjorklof, K. Elvang, A.M. and Jorgensen, K.S. 2000. Biomarkers for monitoring efficacy of bioremediation by microbial inoculants. *Environmental pollution (Barking, Essex : 1987)*. 107(2): pp. 217–23.

Je´gou, D. Brunotte, J. Rogasik, H. Capowiez, Y. Diestel, H. Schrader, S. and Cluzeau, D. 2002. Impact of soil compaction on earthworm burrow systems using X-ray computed tomo-graphy: preliminary study. *European Journal of Soil Biology.* 38(3): pp. 329-336.

Jones, D. and Griffiths, E. 1964. The use of thin sections for the study of soil microorganisms. *Plant and Soil.* 20(2): pp. 232–240.

Joschko, M. Muller, P.C. Kotzke, K. Dohring, W. and Larink, O. 1993. Earthworm burrow system development assessed by means of X-ray computed tomography. *Geoderma*. 56: pp. 209-221.

Juarez, S. Nunan, N. Duday, A-C. Pouteau, V. Schmidt, S. Hapca, S. Falconer, R. Otten, W. and Chenu, C. 2013. Effects of different soil structures on the

decomposition of native and added organic carbon. *European Journal of Soil Biology*. 58(September 2013): pp. 81–90.

Kalukin, A.R. Van Geet, M. and Swennen, R. 2000. Principal components analysis of multienergy X-ray computed tomography of mineral samples. *IEEE transactions on nuclear science*. *47*(5): pp. 1729-1736.

Kaestner, A. Schneebeli, M. and Graf, F. 2006. Visualizing three-dimensional root networks using computed tomography.*Geoderma*.*136*(1): pp. 459-469.

Kearns, D. 2010. A field guide to bacterial swarming motility. *Nature Reviews Microbiology*. 8(9): pp. 634–644.

Ketcham, R.A. and Carlson, W.D. 2001. Acquisition, optimization and interpretation of X-ray computed tomographic imagery: applications to the geosciences. *Computers & Geosciences*. 27(4): pp. 381–400.

Kieft, T.L. Soroker, E. and Firestone, M.K. 1987. Microbial biomass response to a rapid increase in water potential when dry soil is wetted. *Soil Biology and Biochemistry*. 19(2): pp. 119-126.

Kim, H. Anderson, S.H. Motavalli, P.P. and Gantzer, C.J. 2010. Compaction effects on soil macropore geometry and related parameters for an arable field. *Geoderma*. 160(2): pp. 244–251.

King, E.O. Ward, M.K. and Raney, D.E. 1954. Two simple media for the demonstration of pyocyanin and fluorescin.*The Journal of Laboratory and Clinical Medicine*.*44*(2): pp. 301-307.

Kizungu, R. Grundmann, G.L. Dechesne, A. Bartoli, F. Flandrois, J.P. and Chasse, J.L. 2001. Spatial modeling of nitrifier microhabitats in soil. *Soil Science Society of America Journal*. 1709: pp. 1709–1716.

Kooistra, M.J. Schoonderbeek, D. Boone, F.R. Veen, B.W. and Van Noordwijk, M. 1992. Root-soil contact of maize, as measured by a thin-section technique. *Plant and soil*. *139*(1): pp. 119-129.

Koorevaar, P. Menelik, G. and Dirksen, H. 1983. *Elements of Soil Physics.*

Kravchenko, A. Chun, H-C. Mazer, M. Wang, W. Rose, J.B. Smucker, A. and Rivers, M. 2013. Relationships between intra-aggregate pore structures and distributions of Escherichia coli within soil macro-aggregates. *Applied Soil Ecology*. 63: pp. 134–142.

Kravchenko, A.N. Wang, A.N.W. Smucker, A.J.M. and Rivers, M.L. 2011. Long-term differences in tillage and land use affect intra-aggregate pore heterogeneity. *Soil Science Society of America Journal*. 75(5): p. 1658.

Kravchenko, A. Chun, H-C. Mazer, M. Wang, W. Rose, J.B. Smucker, A. and Rivers, M. 2013. Relationships between intra-aggregate pore structures and distributions of Escherichia coli within soil macro-aggregates. *Applied Soil Ecology*. 63(2013): pp. 134–142.

Kravchenko, A.N. Negassa, W.C. Guber, A.K. Hildebrandt, B. Marsh, T.L. and Rivers, M.L. 2014. Intra-aggregate Pore Structure Influences Phylogenetic Composition of Bacterial Community in Macroaggregates. *Soil Science Society of America Journal*. 78(6): pp. 1924-1939.

Krid, S. Triki, M.A. Gargouri, A. and Rhouma, A. 2011. Biocontrol of olive knot disease by *Bacillus* subtilis isolated from olive leaves. *Annals of Microbiology*. 62(1): pp. 149–154.

Kuzyakov, Y. and Blagodatskaya, E. 2015. Microbial hotspots and hot moments in soil: concept & review. *Soil Biology and Biochemistry*. 83(2015): pp. 184–199.

Lacal, J. Munoz-Martínez, F. Reyes-Darias, J.A. Duque, E. Matilla, M. Segura, A. and Ramos, J.L. 2011. Bacterial chemotaxis towards aromatic hydrocarbons in *Pseudomonas*.*Environmental Microbiology*.*13*(7): pp. 1733-1744.

Lahlou, M. Harms, H. Springael, D. and Ortega-Calvo, J-J. 2000. Influence of Soil Components on the Transport of Polycyclic Aromatic Hydrocarbon-Degrading Bacteria through Saturated Porous Media. *Environmental Science & Technology*. 34(17): pp. 3649–3656.

Langmaack, M. Schrader, S. Rapp-Bernardt, U. and Kotzke, K. 2002. Soil structure rehabilitation of arable soil degraded by compaction. *Geoderma.* 105: pp. 141-152.

Lauber, C.L. Ramirez, K.S. Aanderud, Z. Lennon, J. and Fierer, N. 2013. Temporal variability in soil microbial communities across land-use types. *The ISME Journal*.*7*(8): pp. 1641-1650.

Lavelle, P. 2013. Soil as a Habitat. In: Diana H. Wall, ed. *Soil Ecology and Ecosystem Services*. pp. 7-27.

Li, C.H. Ma, B.L. and Zhang, T.Q. 2002. Soil bulk density effects on soil microbial populations and enzyme activities during the growth of maize (Zea mays L.) planted in large pots under field exposure.*Canadian Journal of Soil Science*.*82*(2): pp. 147-154.

Li, Y. Dick, W.A. and Tuovinen, O.H. 2003. Evaluation of fluorochromes for imaging bacteria in soil. *Soil Biology and Biochemistry*. 35(6): pp. 737–744.

Li, Y. Dick, W.A. and Tuovinen, O.H. 2004. Fluorescence microscopy for visualization of soil microorganisms: a review. *Biology and Fertility of Soils*. 39(5): pp. 301–311.

Lontoc-Roy, M. Dutilleul, P. Prasher, S.O. Han, L. Brouillet, T. and Smith, D.L. 2006. Advances in the acquisition and analysis of CT scan data to isolate a crop root system from the soil medium and quantify root system complexity in 3-D space.*Geoderma*.*137*(1): pp. 231-241.

Lucy, M. Reed, E. and Glick, B.R. 2004. Applications of free living plant growth-promoting rhizobacteria.*Antonie van Leeuwenhoek*. *86*(1): pp. 1-25.

Luo, L. Lin, H. and Li, S. 2010. Quantification of 3-D soil macropore networks in different soil types and land uses using computed tomography. *Journal of Hydrology*. 393:(1-2): pp. 53–64.

Madigan, M.T. Clark, D.P. Stahl, D. and Martinko, J.M. 2010. Brock Biology of Microorganisms . In: Benjamin Cummings, ed. *edition*.

Mailloux, B.J. Fuller, M.E. Onstott, T.C. Hall, J. Dong, H. DeFlaun, M.F. Streger, S.H. Rothmel, R.K. Green, M. Swift, D.J.P. and Radke, J. 2003. The role of physical, chemical, and microbial heterogeneity on the field-scale transport and attachment of bacteria. *Water Resources Research*. 39(6).

Mangalassery, S. Sjogersten, S. Sparkes, D.L. Sturrock, C.J. and Mooney, S.J. 2013. The effect of soil aggregate size on pore structure and its consequence on emission of greenhouse gases. *Soil and Tillage Research.* 132(2013): pp. 39–46.

Mees, F. Swennen, R. Van Geet, M. and Jacobs, P. 2003. Applications of X-ray Computed tomography in the Geosciences. *Geological Society Special Publications, London*.215(1): pp. 1-6

Mooney, S.J. 2002. Three-dimensional visualization and quantification of soil macroporosity and water flow patterns using computed tomography. *Soil Use and Management.* 18: pp. 142–151.

Mooney, S.J. Pridmore, T.P. Helliwell, J. and Bennett, M.J. 2012. Developing X-ray Computed Tomography to non-invasively image 3-D root systems architecture in soil. *Plant and Soil*. 352(1-2): pp. 1–22.

Moran, C.J. Koppi, A.J. Murphy, B.W. and McBratney, A.B. 1988. Comparison of the macropore structure of a sandy loam surface soil horizon subjected to two tillage treatments.*Soil Use and Management*. *4*(3): pp. 96-102.

Nakashima, Y. Mitsuhata, Y. Nishiwaki, J. Kawabe, Y. Utsuzawa, S. and Jinguuji, M. 2011. Non-destructive analysis of oil-contaminated soil core samples by X-ray computed tomography and low-field nuclear magnetic resonance relaxometry: a case study.*Water, Air and Soil Pollution*.*214*(1-4): pp. 681-698.

Nannipieri, P. Ascher, J. Ceccherini, M. Landi, L. Pietramellara, G. and Renella, G. 2003. Microbial diversity and soil functions.*European Journal of Soil Science*.*54*(4): pp. 655-670.

Natsch, A. Keel, C. Troxler, J. Zala, M. Albertini, N.V. Natsch, A. Keel, C. Troxler, J. and Zala, M. 1996. Importance of preferential flow and soil management in vertical transport of a biocontrol strain of *Pseudomonas* fluorescens in structured field soil. *Applied and Environmental Microbiology*. 62(1): pp. 33-40.

Nawaz, M.F. Bourrie, G. and Trolard, F. 2012. Soil compaction impact and modelling. A review. *Agronomy for Sustainable Development*. 33(2): pp. 291–309.

Neal, A.L. Ahmad, S. Gordon-Weeks, R. and Ton, J. 2012. Benzoxazinoids in root exudates of maize attract *Pseudomonas* putida to the rhizosphere. *PloS one*. 7(4): p. e35498.

Negassa, W.C. Guber, A.K. Kravchenko, A.N. Marsh, T.L. Hildebrandt, B. and Rivers, M.L. 2015. Properties of soil pore space regulate pathways of plant residue decomposition and community structure of associated bacteria. *PloS one*. 10(4): p. e0123999.

Nunan, N. Ritz, K. Crabb, D. Harris, K. Wu, K. Crawford, J.W. and Young, I.M. 2001. Quantification of the in situ distribution of soil bacteria by large-scale imaging of thin sections of undisturbed soil. *FEMS Microbiology Ecology*. 36: pp. 67–77.

Nunan, N. Wu, K. Young, I.M. Crawford, J.W. and Ritz, K. 2002. In situ spatial patterns of soil bacterial populations, mapped at multiple scales, in an arable soil. *Microbial Ecology*. 44(4): pp. 296–305.

Nunan, N. Wu, K. Young, I.M. Crawford, J.W. and Ritz, K. 2003. Spatial distribution of bacterial communities and their relationships with the micro-architecture of soil. *FEMS Microbiology Ecology*. 44(2): pp. 203–15.

Nunan, N. Ritz, K. Rivers, M. Feeney, D.S. and Young, I.M. 2006. Investigating microbial micro-habitat structure using X-ray computed tomography. *Geoderma*. 133(3-4): pp. 398–407.

Nunan, N. Young, I.M. Crawford, J.W. and Ritz, K. 2007. Bacterial interactions at the microscale – linking habitat to function in soil. In: R.B. Franklin and A.L. Mills, eds. *The Spatial Distribution of Microbes in the Environment*. pp. 61–85.

O'Donnell, A.G. Young, I.M. Rushton, S.P. Shirley, M.D. and Crawford, J.W. 2007. Visualization, modelling and prediction in soil microbiology. *Nature reviews. Microbiology*, 5(9): pp. 689–99.

Oh, W. and Lindquist, W. 1999. Image thresholding by indicator kriging. *IEEE Transactions on Pattern Analysis and Machine Intelligence.* 21: pp. 590–602.

Oku, S. Komatsu, A. Tajima, T. Nakashimada, Y. and Kato, J. 2012. Identification of Chemotaxis Sensory Proteins for Amino Acids in *Pseudomonas* fluorescens Pf0-1 and Their Involvement in Chemotaxis to Tomato Root Exudate and Root Colonization. *Microbes and Environments*. 27(4): pp. 462–469.

Or, D. Smets, B.F. Wraith, J.M. Dechesne, A. and Friedman, S.P. 2007. Physical constraints affecting bacterial habitats and activity in unsaturated porous media–a review.*Advances in Water Resources*.*30*(6): pp. 1505-1527.

Otten, W. and Gilligan, C.A. 2006. Soil structure and soil-borne diseases: using epidemiological concepts to scale from fungal spread to plant epidemics. *European Journal of Soil Science*.57(1): pp. 26-37.

Otten, W. Hall, D. Harris, K. Ritz, K. Young, I.M. and Gilligan, C.A. 2001. Soil physics, fungal epidemiology and the spread of Rhizoctonia solani.*New Phytologist*.151(2): pp. 459-468.

Otten, W. Bailey, D.J. and Gilligan, C.A. 2004. Empirical evidence of spatial thresholds to control invasion of fungal parasites and saprotrophs.*New Phytologist*.*163*(1): pp. 125-132.

Otten, W. Pajor, R. Schmidt, S. Baveye, P.C. Hague, R. and Falconer, R.E. 2012. Combining X-ray CT and 3D printing technology to produce microcosms with replicable, complex pore geometries.*Soil Biology and Biochemistry*.*51*: pp. 53-55.

Page, A.L. 1982.*Methods of soil analysis. Part 2. Chemical and microbiological properties*. American Society of Agronomy, Soil Science Society of America.

Pagliai, M. Vignozzi, N. and Pellegrini, S. 2004. Soil structure and the effect of management practices.*Soil and Tillage Research*.*79*(2): pp. 131-143.

Pajor, R. 2012. *Quantification of short term interactions between soil and fungi*. PhD thesis. Abertay University.

Pajor, R. Falconer, R. Hapca, S. and Otten, W. 2010. Modelling and quantifying the effect of heterogeneity in soil physical conditions on fungal growth. *Biogeosciences*. 7(11): pp. 3731–3740.

Pallud, C. Dechesne, A. Gaudet, J.P. Debouzie, D. Grundmann, G.L. Lyon, B. Cedex, V. and Lyon, C.B. 2004, Modification of Spatial Distribution of 2 , 4-Dichlorophenoxyacetic Acid Degrader Microhabitats during Growth in Soil Columns. *Applied and Environmental Microbiology*. 70(5): pp. 2709–2716.

Pandey, G. and Jain, R. 2002. Bacterial chemotaxis toward environmental pollutants: role in bioremediation. *Applied and Environmental Microbiology*. 68(12): pp. 5789–5795.

Papadopoulos, A. Bird, N.R.A. Whitmore, A.P. and Mooney, S.J. 2009. Investigating the effects of organic and conventional management on soil aggregate stability using X-ray computed tomography. *European Journal of Soil Science*. 60(3): pp. 360–368.

Patrick, E.A. Mackie, L.A. and Mullins, C.E. 1985. The use of plaster of Paris in the study of soil structure.*Soil Use and Management*.*1*(2): pp. 70-72.

Pereg, L. and McMillan, M. 2015. Scoping the potential uses of beneficial microorganisms for increasing productivity in cotton cropping systems. *Soil Biology and Biochemistry*. 80: pp. 349–358.

Perez-Piqueres, A. Edel-Hermann, V. Alabouvette, C. and Steinberg, C. 2006. Response of soil microbial communities to compost amendments, *Soil Biology and Biochemistry*. 38(3): pp. 460–470.

Perret, J. Prasher, S.O. Kantzas, A. and Langford, C. 1997. 3-D visualization of soil macroporosity using X-ray CAT scanning.*Canadian Agricultural Engineering*.*39*(4): pp. 249-262.

Perret, J.S. Al-Belushi, M.E. and Deadman, M. 2007. Non-destructive visualization and quantification of roots using computed tomography.*Soil Biology and Biochemistry*.*39*(2): pp. 391-399.

Petrovic, A.M. Siebert, J.E. and Rieke, P.E. 1982. Soil bulk density analysis in three dimensions by computed tomographic scanning. *Soil Science Society of America Journal*. 46: pp. 445–450.

Ping, L. Birkenbeil, J. and Monajembashi, S. 2013. Swimming behavior of the monotrichous bacterium *Pseudomonas* fluorescens SBW25. *FEMS Microbiology Ecology*, 86(1): pp. 36–44.

Pires, L.F. Borges, J.A.R. Bacchi, O.O.S. and Reichardt, K. 2010. Twenty- five years of computed tomography in soil physics: a literature review of the Brazilian contribution. *Soil and Tillage Research*, 110: pp. 197–210.

Pohlmeier, A. Vergeldt, F. Gerkema, E. Van As, H. Van Dusschoten, D. and Vereecken, H. 2010. MRI in soils: Determination of water content changes due to root water uptake by means of a multi-slice-multi-echo sequence (MSME).*Open Magnetic Resonance Journal*. *3*: pp. 69-74.

Portillo, M.C. Leff, J.W. Lauber, C.L. and Fierer, N. 2013. Cell size distributions of soil bacterial and archaeal taxa. Applied and Environmental Microbiology. 79(24): pp. 7610–7617.

Postma, J. and Altemuller, H.J. 1990. Bacteria in thin soil sections stained with the fluorescent brightener calcofluor white M2R.*Soil Biology and Biochemistry*.*22*(1): pp. 89-96.

Pupin, B. Freddi, S. and Nahas, E. 2009. Microbial alterations of the soil influenced compaction. 33: pp. 1207–1213.

Ranjard, L. and Richaume, A. 2001. Quantitative and qualitative microscale distribution of bacteria in soil.*Research in Microbiology*.152(8): pp. 707-716.

Redman, J.A. Walker, S.L. and Elimelech, M. 2004. Bacterial Adhesion and Transport in Porous Media : Role of the Secondary Energy Minimum. *Environmental Science & Technology*. 38(6): pp. 1777–1785.

Rogasik, H. Crawford, J.W. Wendroth, O. Young, I.M. Joschko, M. Ritz, K. 1999. Discrimination of soil phases by dual energy X-ray tomography. *Soil Sci Soc Am J.* 63: pp. 741–751.

Ros, M. Pascual, J.A. Garcia, C. Hernandez, M.T. and Insam, H. 2006. Hydrolase activities, microbial biomass and bacterial community in a soil after long-term amendment with different composts. *Soil Biology and Biochemistry*. *38*(12): pp. 3443-3452.

Ruamps, L.S. Nunan, N. and Chenu, C. 2011. Microbial biogeography at the soil pore scale. *Soil Biology and Biochemistry*. 43(2): pp. 280–286.

Ruamps, L.S. Nunan, N. Pouteau, V. Leloup, J. Raynaud, X. Roy, V. and Chenu, C. 2013. Regulation of soil organic C mineralisation at the pore scale. *FEMS Microbiology Ecology*. 86(1): pp. 26–35.

Santoyo, G. Orozco-Mosqueda, M.D.C. and Govindappa, M. 2012. Mechanisms of biocontrol and plant growth-promoting activity in soil bacterial species of *Bacillus* and *Pseudomonas* : a review. *Biocontrol Science and Technology*. 22(8): pp. 855–872.

Schmidt, S. Bengough, A.G. Gregory, P.J. Grinev, D.V. and Otten, W. 2012. Estimating root–soil contact from 3D X-ray microtomographs.*European Journal of Soil Science*.63(6): pp. 776-786.

Sessitsch, A. Weilharter, A. Gerzabek, M.H. Kirchmann, H. and Kandeler, E. 2001. Microbial population structures in soil particle size fractions of a long-term fertilizer field experiment.*Applied and Environmental Microbiology*.67(9): pp. 4215-4224.

Sey, B.K. Manceur, A.M. Whalen, J.K. Gregorich, E.G. and Rochette, P. 2008. Small-scale heterogeneity in carbon dioxide, nitrous oxide and methane production from aggregates of a cultivated sandy-loam soil.*Soil Biology and Biochemistry*.40(9): pp. 2468-2473.

Shein, E.V. and Devin, B.A. 2007. Current problems in the study of colloidal transport in soil. *Eurasian Soil Science*. 40(4): pp. 399–408.

Singh, T. Srivastava, A.K. and Arora, D.K. 2002. Horizontal and vertical movement of *Pseudomonas* fluorescens toward exudate of Macrophomina phaseolina in soil: influence of motility and soil properties. *Microbiological Research*. 157(2): pp. 139–48.

Sivasakthi, S. Usharani, G. and Saranraj, P. 2014. Biocontrol potentiality of plant growth promoting bacteria (PGPR) - *Pseudomonas* fluorescens and *Bacillus* subtilis : A review. *African Journal of Agricultural Research*. 9(16): pp. 1265–1277.

Sleutel, S. Cnudde, V. Masschaele, B. Vlassenbroes, J. Dierick, M. Van Hoorebeke, L. Jacobs, P. De Neve, S. 2008. Comparison of different nono- and micro-focus X-ray computed tomography set-ups for the visualization of the soil microstructure and soil organic matter. *Comp. & Geosci.* 34: pp. 931–938.

Smeltzer, D.L.K. Bergdahl, D.R. and Donnelly, J.R. 1986. Forest ecosystem responses to artificially induced soil compaction. II. Selected soil microorganism populations.*Canadian Journal of Forest Research*.16(4): pp. 870-872.

Stres, B. Danevcic, T. Pal, L. Fuka, M.M. Resman, L. Leskovec, S. Hacin, J. Stopar, D. Mahne, I. and Mandic-Mulec, I. 2008. Influence of temperature and soil water content on bacterial, archaeal and denitrifying microbial communities in drained fen grassland soil microcosms. *FEMS Microbiology Ecology*. 66(1): pp. 110–22.

Strong, D.T. Wever, H.D. Merckx, R. and Recous, S. 2004. Spatial location of carbon decomposition in the soil pore system.*European Journal of Soil Science*.*55*(4): pp. 739-750.

Taina, I.A. Heck, R.J. and Elliot, T.R. 2008. Application of X-ray computed tomography to soil science : A literature review.C*anadian Journal of Soil Science*,*88*(1): pp. 1-19.

Tan, X. and Chang, S.X. 2007. Soil compaction and forest litter amendment affect carbon and net nitrogen mineralization in a boreal forest soil. *Soil and Tillage Research*. 93(1): pp. 77–86.

Tan, Y. Bond, W.J. Rovira, A.D. and Brisbane, P.G. 1991. Movement through soil of a biological control agent, psuedomonas fluorescens. *Soil Biology and Biochemistry* . 23(9): pp. 821–825.

Tan, X. Chang, S.X. and Kabzems, R. 2008. Soil compaction and forest floor removal reduced microbial biomass and enzyme activities in a boreal aspen forest soil.*Biology and Fertility of Soils*.*44*(3): pp. 471-479.

Tippkotter, R. and Ritz, K. 1996. Evaluation of polyester, epoxy and acrylic resins for suitability in preparation of soil thin sections for in situ biological studies.*Geoderma*.*69*(1): pp. 31-57.

Tippkotter, R. Eickhorst, T. Taubner, H. Gredner, B. and Rademaker, G. 2009. Detection of soil water in macropores of undisturbed soil using microfocus X-ray tube computerized tomography (µCT). *Soil and Tillage Research*. *105*(1): pp. 12-20.

Tisdall, J.M. and Oades, J. 1982. Organic matter and water-stable aggregates in soils.*Journal of Soil Science*.*33*(2): pp. 141-163.

Tombolini, R. and Jansson, J.K. 1998. Monitoring of GFP-tagged bacterial cells. *Methods in molecular biology*. 102: pp. 285–98.

Torbert, H.A. and Wood, C.W. 1992. Effects of soil compaction and water-filled pore space on soil microbial activity and N losses.*Communications in Soil Science & Plant Analysis*.*23*(11-12): pp. 1321-1331.

Torsvik, V. Goksoyr, J. and Daae, F.L. 1990. High diversity in DNA of soil bacteria.*Applied and Environmental Microbiology*.*56*(3): pp. 782-787.

Tracy, S.R. Colin, R. Black, J.A. Roberts, A.M. Davidson, R. Tester, M. Samec, M. Korosak, D. Sturrock, C. and Sacha, J.M. Quantifying the effect of soil compaction on three varieties of wheat (Triticum aestivum L.) using X-ray Micro Computed Tomography (CT).*Plant and Soil.*353(1-2): pp.195-208.

Trevors, J. Kuikman, P. and Elsas, J.V. 1994. Release of bacteria into soil: cell numbers and distribution. *Journal of Microbiological Methods*. 19: pp. 247–259.

Trevors, J.T. 1996. Sterilization and inhibition of microbial activity in soil. *Journal of Microbiological Methods* . 26: pp. 53–59.

Trevors, J.T. Elsas, J. Overbeek, L. and Starodub, M. 1990. Transport of a genetically engineered *Pseudomonas* fluorescens strain through a soil microcosm. *Applied and Environmental Microbiology*. 56(2): pp. 401–408.

Uhlirova, E. Elhottova, D. Triska, J. and Santruckova, H. 2005. Physiology and microbial community structure in soil at extreme water content. *Folia microbiologica*. 50(2): pp. 161–166.

van Elsas, J.D. Trevors, J.T. and van Overbeek, L.S. 1991. Influence of soil properties on the vertical movement of genetically-marked *Pseudomonas* fluorescens through large soil microcosms. *Biology and Fertility of Soils*. 10(4): pp. 249–255.

Van Veen, J.A. van Overbeek, L.S. and van Elsas, J.D. 1997. Fate and activity of microorganisms introduced into soil. *Microbiology and Molecular Biology Reviews*. 61(2): pp. 121–35.

Voroney, R.P. and Heck, R.J. 2015. Chapter 2 - The Soil Habitat. *Soil Microbiology Ecology and Biochemistry*. 4th ed, Elsevier Inc., pp. 15–39.

Vos, M. Wolf, A.B. Jennings, S.J. and Kowalchuk, G.A. 2013. Micro-scale determinants of bacterial diversity in soil. *FEMS Microbiology Reviews*. 37(6): pp. 936–54.

Wang, W. Kravchenko, A.N. Smucker, A.J.M. and Rivers, M.L. 2011. Comparison of image segmentation methods in simulated 2D and 3D microtomographic images of soil aggregates. *Geoderma.* 162: pp. 231–241.

Wang, W. Kravchenko, A.N. Johnson, T. Srinivasan, S. Ananyeva, K.A. Smucker, A. J.M. Rose, J.B. and Rivers, M.L. 2013. Intra-Aggregate Pore Structures and Distribution by Water Flow within and Movement Out of Soil Macroaggregates. *Vadose Zone Journal*. 12(4).

Wang, W. Kravchenko, A.N. Smucker, A.J.M. Liang, W. and Rivers, M.L. 2012. Intra-aggregate pore characteristics: X-ray computed microtomography analysis. *Soil Science Society of America Journal*, 76(4): p. 1159.

Wang, Y. Bradford, S.A. and Simunek, J. 2013. Transport and fate of microorganisms in soils with preferential flow under different solution chemistry conditions. *Water Resources Research*. 49(5): pp. 2424–2436.

White, D. Fitzpatrick, E.A. and Killham, K. 1994. Use of stained bacterial inocula to assess spatial distribution after introduction into soil. *Geoderma*. 63(3-4): pp. 245–254.

Wildenschild, D. Hopmans, J.W. Vaz, C.M.P. Rivers, M.L. and Rikard, D. 2002. Using X-ray computed tomography in hydrology : systems, resolutions, and limitations. *Journal of Hydrology*. 267: pp. 285–297.

Wolf, A.B. Vos, M. de Boer, W. and Kowalchuk, G.A. 2013. Impact of matric potential and pore size distribution on growth dynamics of filamentous and non-filamentous soil bacteria. *PloS One*. 8(12): p. e83661.

Wu, T. Chellemi, D.O. Graham, J.H. Martin, K.J. Rosskopf, E.N. 2008. Comparison of soil bacterial communities under diverse agricultural land management and crop production practices. *Microb Ecol.* 55: pp. 293–310.

Young, I.M. Crawford, J.W. and Rappoldt, C. 2001. New methods and models for characterising structural heterogeneity of soil. *Soil and Tillage Research*. 61(1-2): pp. 33–45.

Young, I.M. and Crawford, J.W. 2004. Interactions and self-organization in the soil-microbe complex.*Science*.*304*(5677): pp. 1634-1637.

Young, I. and Ritz, K. 2005. The habitat of soil microbes. Biological Diversity *and Function in Soils*: pp. 31–43.

Young, I. Crawford, J. and Nunan, N. 2008. Microbial distribution in soils: physics and scaling. *Advances in Agronomy*. 100: pp. 81-121.

Zaidi, A. Khan, M. Ahemad, M. and Oves, M. 2009. Plant growth promotion by phosphate solubilizing bacteria. *Acta microbiologica et immunologica Hungarica. 56*(3): pp. 263-284.

Zhang, C. and Xing, X. 2010. Fluorescent proteins as a visible molecular signal for rapid quantification of bioprocesses: potential and challenges. *Chinese Journal of Chemical Engineering*. 18(5): pp. 863–869.

Zhang, N. Wu, K. He, X. Li, S. Zhang, Z. Shen, B. Yang, X. Zhang, R. Huang, Q. and Shen, Q. 2011. A new bioorganic fertilizer can effectively control banana wilt by strong colonization with *Bacillus* subtilis N11. *Plant and Soil*. 344(1-2): pp. 87–97.

Zhuang, X. Chen, J. Shim, H. and Bai, Z. 2007. New advances in plant growth-promoting rhizobacteria for bioremediation.*Environment International*. 33(3): pp. 406-413.

9 Appendix

9.1 Appendix I

Experimental design: Optimization of inoculum volume and target for quantification of bacterial spread in soil.

To get an optimized set up for the movement experiment different combinations of soil moisture content and inoculum volume were tested. Also, to quantify bacteria different targets were tested. For the set up trials, *Pseudomonas* bacteria was used and soil of aggregate size 1-2 mm with 40 % water filled pore space was packed at bulk density 1.3 g cm^{-3}. Ten replicates per setup were prepared. For every setup, inoculum source was introduced in soil by placing the soil core on top of the inoculum source. The samples were then incubated at 23°C. To assess the vertical movement of bacteria in soil from bottom to top a target was placed on top of the soil core. On sampling day, the target was removed from the top of soil core and replaced with a fresh target. The target was placed on media plates and incubated at 28°C for 48hrs. After 48hrs the plates were checked for the presence/colonization of bacteria around the targets. The sampling of soil microcosms was done every day until the all the replicates showed positive results.

Trail 1:

In first set up, 500 µl of washed cells was used as inoculum source and a pellet of agar media as target. All replicates showed positive colonization on day 1. The reason for such fast movement of bacteria was thought to be either due to high concentration of bacteria inoculum or due to inclination of bacteria towards high nutrient agar pellet and also inoculum was sucked up the sides of the cylinder – so not a natural movement. Therefore this set up was not considered.

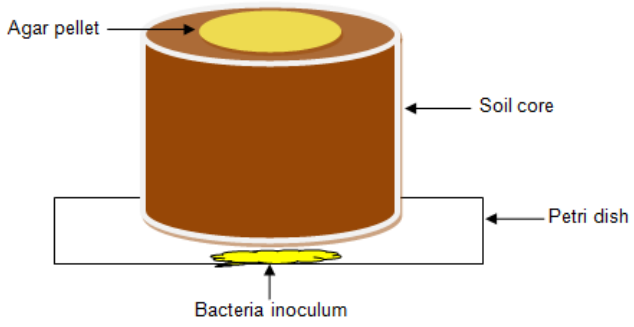

Figure I.a: Diagrammatic representation of the trial experiment setup to quantify bacterial spread in soil. Bacterial suspension was used as a source. It was placed at

the bottom of the soil sample. A single nutrient agar pellet was used as a bait to quantify successful colonisation of the soil. The bait was placed on the top of the sample.

Trail 2:

In this setup three different concentrations (500 µl 250 µl 125 µl) and two different targets (agar pellet and a 2-4 mm aggregate) were tested. In 500 µl inoculum concentration, on day 1 all replicates showed 100% positive colonization on both the targets. With 250µl inoculum concentration, samples showed 100 % colonization of agar pellets and 10 % colonization of aggregate target on day 1. The remaining samples with aggregate target showed 100 % positive on day 2. Soil inoculated with 125 µl on day 1 showed 20 % positive colonization on agar pellet and 0 % positive on aggregate target. By day 2 samples showed 100 % positive colonization on both targets. Since a difference in two targets were observed at lower inoculum volumes and also aggregate was less in nutrients compare to agar pellet henceforth , one aggregate of size 2-4 mm was chosen.

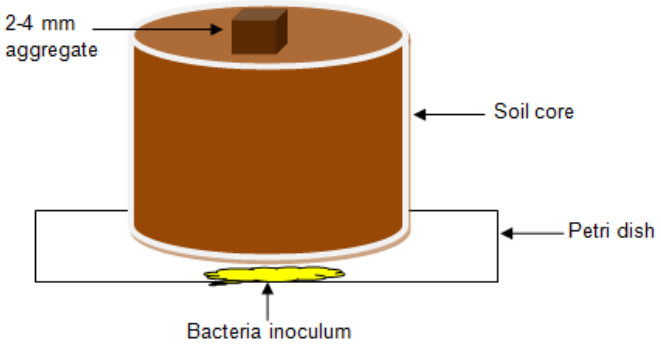

Figure I.b: Diagrammatic representation of the trial experiment setup to quantify bacterial spread in soil. Bacterial suspension was used as a source. It was placed at the bottom of the soil sample. A single 2-4 mm aggregate size pellet was used as a bait to quantify successful colonisation of the soil. The bait was placed on the top of the sample

Trail 3:

To optimise the inoculum volume, another experiment was carried out where the total amount of water (including the inoculum volume) added in soil was kept 1.50 ml. This volume of was chosen at it has been used in experiment of previous chapters. So at 500 µl (i.e. 0.5 ml) inoculum concentration only 1.00 ml of water was added in soil. Similarly, at 250 µl (i.e. 0.25 ml) inoculum 1.25 ml and at 125 µl (i.e. 0.125 ml) inoculum 1.38 ml of water was added in soil. At 500 µl concentrations samples showed 100 % positive colonization on day 1. But

samples inoculated with 250 µl and 125 µl inoculum concentrations showed no positive results until day 5. Samples started drying up because of which experiment was discarded.

From the above trails it was concluded that the high concentration of inoculum volume was increasing the moisture content which influenced faster movement of bacteria towards soil.

Therefore, a solid inoculum source was considered which does not increase the moisture content of soil and has less concentration of nutrients. Also the source structure is porous so that bacteria can move in soil.

Trail 4:

A low melting point agarose (Fisher bioreagents, UK) was selected as it can remain in melting state at 35°C which serves as an advantage as bacterial cells can survive at this temperature. To optimize the amount of inoculum introduce in agarose, three different concentrations of inoculum 500 µl, 750 µl, 1000 µl was tested. To prepare an agarose bead, selected inoculum volume of washed cells were mixed with 30 ml of 1.5 % LMP agarose solution. The mixture was shaken gently to avoid any bubbles formation and poured into a petri dish. The petri dish was left under the laminar flow to let the agarose cool down and solidify. The solidify agarose was then cut down into small circular beads using the circular end of a pipette tip. The beads were of size 2.5 mm in diameter and 5 mm in height. One agarose pellet per soil core was taken. The soil core was placed on top of the agarose pellet as shown in figure 4.2. The target was one aggregate of size 2-4 mm as optimized from earlier trials. Sampling was done in similar ways as the previous trials (for setup see figure 4.1). All three concentrations showed similar positive colonization of targets on day 4. Since no difference between different concentrations was observed 1000 µl inoculum was selected to prepare agarose pellet for further experiments.

9.2 Appendix II

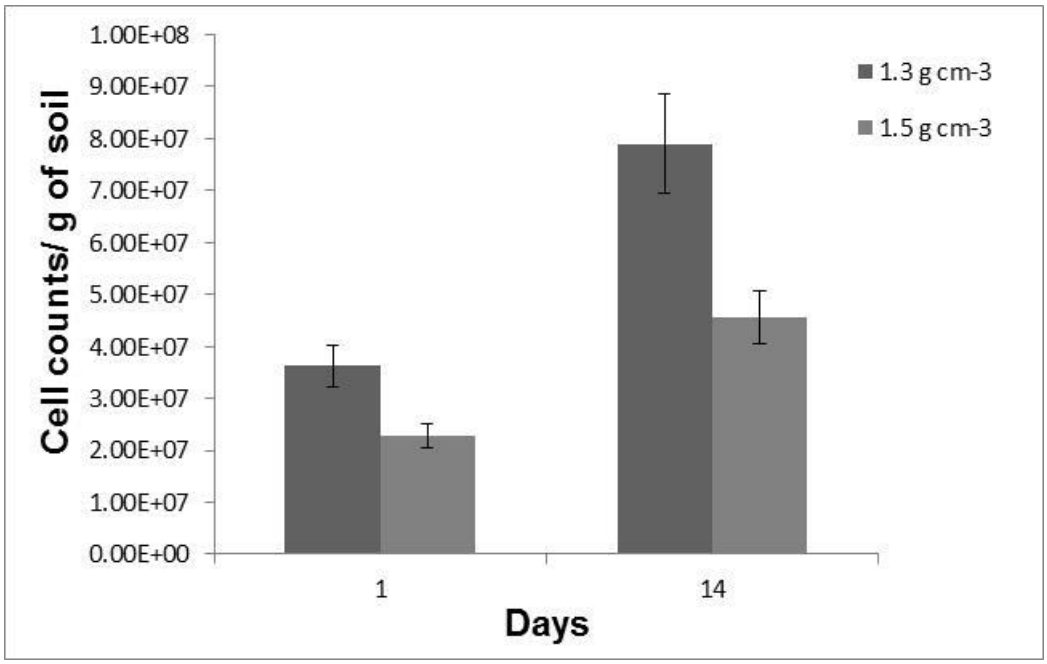

Figure II.a: Average number of CARD-FISH stained *Pseudomonas* cells per gram of soil at different sampling times in agarose samples packed at bulk-densities 1.3 g cm^{-3} (dark grey and 1.5 g cm^{-3}(grey). Data are means ±SE (n=3).

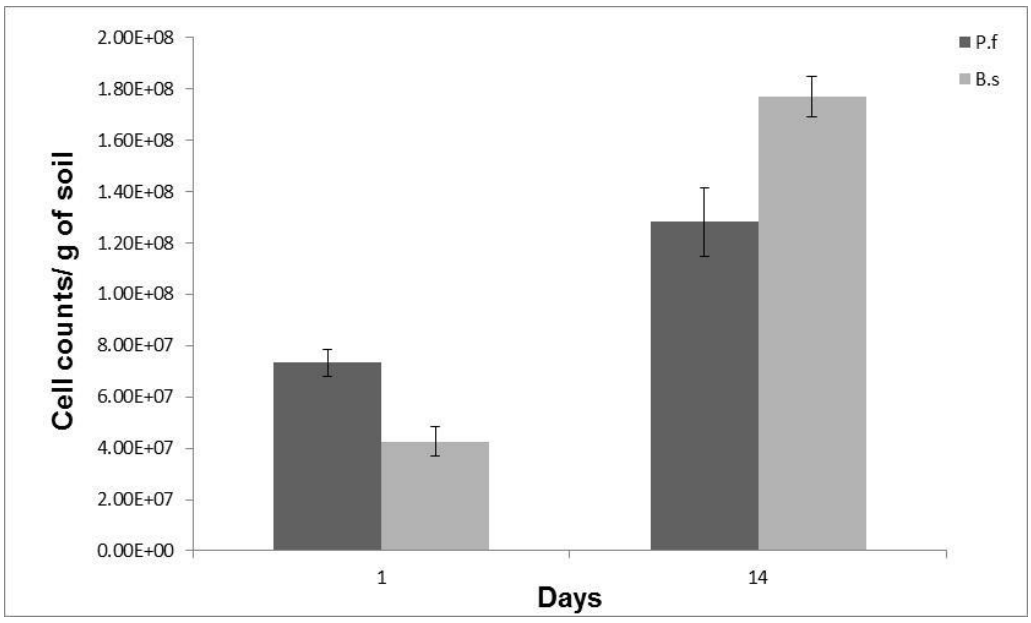

Figure II.b: Average number of CARD-FISH stained *Pseudomonas* (grey) *and Bacillus* (light grey) cells per gram of soil at different sampling times in compost samples packed at bulk-densities 1.3 g cm^{-3}. Data are means ±SE (n=3).

9.3 Appendix III

Table III.a: Results of the Poisson model analysis on influence of pore structure on spread of bacteria in agarose and compost experiment.

Scales	Treatments	Porosity (%)	Soil-pore interface (mm^2)	Connectivity (%)
Agarose experiment	*Pseudomonas* inoculated in soil packed at bulk-density 1.3 g cm^{-3}	0.000	0.565	0.000
	Pseudomonas inoculated in soil packed at bulk-density 1.5 g cm^{-3}	0.264	0.165	0.001
Compost experiment	*Pseudomonas* inoculated in soil packed at bulk-density 1.3 g cm^{-3}	0.000	0.000	0.000
	Bacillus inoculated in soil packed at bulk-density 1.3 g cm^{-3}	0.000	0.003	0.327